LOW-THRUST PERTURBATION GUIDANCE

Thesis by

Thomas Patrick Bauer

In Partial Fulfillment of the Requirements

for the Degree of

Doctor of Philosophy

California Institute of Technology

Pasadena, California

1982

(Submitted May 25, 1982)

ACKNOWLEDGMENTS

ABSTRACT

Low-thrust perturbation guidance, as applied to the minimum time problem of an Earth to Mars rendezvous, has been reexamined and shown to perform orders of magnitude better, as measured by the terminal state error, than previous studies indicated. The orbits of Earth and Mars were assumed to be inclined and elliptical. The only forces considered were the Sun's gravity and that of the constant thrust rocket engine.

First order necessary conditions of the calculus of variations were developed for the nominal trajectory. The resulting nonlinear two-point boundary value problem was solved with the Backward Sweep Method. Feedback gain related and trajectory information is stored on a file during the optimization of the nominal trajectory to be retrieved later in the guidance programs by a high order interpolator.

Two guidance schemes, Time-To-Go Guidance and Minimum Distance Guidance, were investigated for several initial perturbations in velocity and position. The performance of the two schemes was found to be clearly acceptable although not quite as good as reoptimization. The two schemes are equivalent in performance. Moreover, a simplified version of the schemes, Current Time Guidance, was found to be comparable in performance to the more elaborate guidance schemes.

A comparison of the current results with those of previous studies was made showing that terminal state errors can be reduced 100 to 10,000 times more than found earlier. This apparent improvement may possibly be explained by the use of a high fidelity integrator and other enhancements implemented in the software, although algorithm and programming mistakes in the earlier studies are suspected.

A similar minimum time problem, that of a two-dimensional Earth to Mars orbit transfer using a solar sail, was also reexamined. The optimized trajectory was found to be very similar to those obtained by most earlier studies. A recent report which prompted the study was found to have an error in a transversality condition causing anomalous results.

TABLE OF CONTENTS

TABLE OF CONTENTS (cont.)

TABLE OF CONTENTS (cont.)

viii

LIST OF FIGURES

LIST OF TABLES

I. INTRODUCTION

Researchers seeking more efficient methods of finding a new optimal trajectory after the occurrence of a state perturbation have considered many techniques. One group of techniques, referred to collectively as perturbation guidance, promises simple algorithms and modest computing costs. While trajectory reoptimization would probably be used in a real mission for a perturbed trajectory because of its greater accuracy, in a time critical case or for an autonomous spacecraft with limited computational capability, a perturbation guidance technique with sufficient accuracy might be preferred. Also, in premission studies, tens or hundreds of trajectories might need to be completed, in which case a perturbation guidance scheme would save considerable computational effort, especially in a covariance analysis. Since computer costs keep declining rapidly, there may not seem to be a big difference in cost between the perturbation guidance schemes and reoptimization. However, in solving a real problem, instead of the simple one examined in this study, the additional complexities involved may introduce a significant difference in the costs of the two techniques. Therefore, the perturbation guidance schemes should not be summarily dismissed.

The main purpose of this study is to show that two perturbation guidance schemes, Time-To-Go Guidance and Minimum Distance Guidance, examined previously by Hart[1], Lattimore[2], and Stoker[3], perform adequately and, in fact, much better than the earlier studies indicate. Another purpose of the study is to compare the guidance schemes with each other and to determine whether one is clearly superior. Hart[1] claims that Minimum Distance Guidance is the better of the pair, and Stoker[3] counters

with a claim of approximate parity of the two schemes. Since both

authors obtained but marginally acceptable performance (as measured by

terminal error), if not divergence, in many cases, any comparisons were

of dubious value. An incidental byproduct of this study is the comparison

of the computer costs of the perturbation guidance schemes and trajec-

tory reoptimization. But as mentioned above, any real mission would be

fairly complex, and it is only in that context that computer costs can

be realistically compared. Therefore, computer cost comparison is not a

major purpose of this study.

For purposes of comparison, the problem studied is the same as that

of Hart[1], Lattimore[2], and Stoker[3]. This problem is the Earth to Mars

rendezvous of a spacecraft with a constant low-thrust rocket engine.

The gravity fields of Earth and Mars are neglected, as are all other

forces except the Sun's gravity field and the rocket thrust. Propellant

consumption is minimized with thrust constrained to be constant, so that

time is also minimized. The initial spacecraft state (position and

velocity) is that of the Earth at the initial time and is identical to

that given in the earlier studies. Since a rendezvous is required in

this problem, the spacecraft state is constrained to match the Martian

state at the final time.

While an Earth to Mars rendezvous using a constant thrust (i.e.,

nuclear powered) engine is an unlikely mission, it serves as a good

test problem for perturbation guidance schemes. These low-thrust pertur-

bation guidance schemes could be easily adapted to missions to other

planets or missions with solar electric or solar sail propulsion. In fact,

perturbation guidance schemes could be applied to a large number of

aerospace problems. Any problem that has continuously changing controls, such as launch into orbit, orbit transfer, reentry, fuel minimization for aircraft, etc., could potentially be solved using perturbation guidance techniques.

Perturbation guidance schemes, which calculate a change in control as a linear function of a change in state, require feedback gain information derived from the nominal trajectory. So first, the nominal trajectory is found or optimized using a Backward Sweep Algorithm (BSA) which utilizes a set of necessary conditions of variational calculus. Once the nominal trajectory is found, stored by-products of the BSA (feedback gains) may be used in the guidance schemes to calculate "optimal" perturbed trajectories rather than reoptimizing the perturbed trajectory from scratch. This report reflects this two-stage process, in that Chapters 2 and 3 describe the development and results of the nominal trajectory optimization, and Chapters 4 and 5 describe the development and results of the perturbation guidance schemes.

Standard notational conventions are used. All vectors are column vectors, and are denoted by underlined lower case letters, e.g., $\underline{x}$, $\underline{\lambda}$. Matrices are denoted by capital letters, e.g., A, S. Scalars may be either upper or lower case, e.g., r, H, Ω, β. A superscript T denotes a transpose of a matrix or vector, e.g., R^T, $\underline{\lambda}^T$. A superscript $^{-1}$ denotes inverse of a square matrix, e.g., Q^{-1}. The first partial derivative of a scalar with respect to a vector is a vector, e.g.,

$$\frac{\partial H}{\partial \underline{x}} = H_{\underline{x}} = \left(\frac{\partial H}{\partial x_1} \quad \frac{\partial H}{\partial x_2} \quad \cdots \quad \frac{\partial H}{\partial x_n} \right)$$

Likewise second partial derivatives of scalars with respect to vectors are matrices, e.g.,

$$\frac{\partial^2 H}{\partial \underline{u} \partial \underline{x}} = \frac{\partial}{\partial \underline{u}} \left(\frac{\partial H}{\partial \underline{x}} \right)^T = H_{\underline{xu}} = \begin{bmatrix} H_{x_1 u_1} \cdots H_{x_1 u_m} \\ \vdots \\ H_{x_n u_1} \cdots H_{x_n u_m} \end{bmatrix}$$

First partial derivatives of vectors with respect to vectors are matrices, e.g.,

$$\frac{\partial \underline{f}}{\partial \underline{x}} = \underline{f}_{\underline{x}} = \begin{bmatrix} \frac{\partial f_1}{\partial x_1} \cdots \frac{\partial f_1}{\partial x_n} \\ \vdots \qquad \vdots \\ \frac{\partial f_n}{\partial x_1} \cdots \frac{\partial f_n}{\partial x_n} \end{bmatrix}$$

The variation (time held fixed) of, e.g., $\underline{x}$, is denoted by $\delta \underline{x}$. The differential (allowing a change in time, dt) of, e.g., $\underline{x}$, is denoted by $d\underline{x}$. Derivatives with respect to time are denoted by raised dots, e.g., $\dot{x} = \frac{dx}{dt}$, $\ddot{x} = \frac{d^2 x}{dt^2}$. $\frac{d}{dt}$ indicates a total derivative, e.g., $\frac{d\psi}{dt} = \frac{\partial \psi}{\partial t} + \frac{\partial \psi}{\partial \underline{x}} \dot{\underline{x}}$. To conserve space in the tables, values are represented in a modified scientific notation where the " x 10" is omitted and the exponent lowered, e.g., $-.543 - 8 = -5.43 \times 10^{-9}$. The equations are numbered by section, e.g., Equation (2.3.14) is the fourteenth equation in Section 2.3, which is the third section in Chapter 2.

2. DETERMINATION OF THE OPTIMAL TRAJECTORY

In order to compare the guidance results of this study with those of the previous works of Hart[1], Lattimore[2], and Stoker[3], the same Earth to Mars rendezvous problem is examined. This rendezvous problems is a generalization of the two-dimensional Earth to Mars orbit transfer studied by Wood[4] and others[5-14, 31-32], in that the planetary orbits are eccentric and inclined — not circular and coplanar. The former rendezvous problem is more realistic in that rendezvous with Mars is required, whereas for the orbit transfer problem (of Refs. 4-14,31-32), rendezvous is effected only along the nominal trajectory and only if the departure date is timed to coincide with the proper Mars heliocentric angle. In other words, a rendezvous is not effected for nearly all perturbed trajectories. This makes the rendezvous problem more constraining, since a degree of freedom is lost.

The coordinate system, initial conditions, and vehicle and planetary constants are those of References 1-3. The gravity fields of Earth and Mars are ignored. The only forces acting on the spacecraft are the central force field of the Sun and that of the constant low-thrust rocket engine. These simplifications remove complexity from the problem, but do not alter the relative performance of the guidance algorithms.

2.1 THE EARTH TO MARS RENDEZVOUS PROBLEM (EMRP)

As mentioned previously, the problem is that of References 1-3. Therefore, the coordinate system, spacecraft equations of motion, initial conditions, terminal constraints, and performance index given below are identical to those of the previous works.

2.1.1 Coordinate System

The coordinate system is depicted in Figure 1. It has the following features:

Heliocentric - origin is Sun's center

Rectangular - x_4, x_5, x_6 are coordinates along orthogonal axes:

x_4 - in direction of ascending note of Mars

x_5 - in ecliptic plane

x_6 - parallel to Earth orbit angular momentum vector

Inertial - nonrotating

2.1.2 Spacecraft Equations of Motion

The spacecraft equations of motion are:

$$\dot{x}_1 = \frac{-\mu\, x_4}{r^3} + \frac{T}{m} \cos u_1 \cos u_2 \tag{2.1.1}$$

$$\dot{x}_2 = \frac{-\mu\, x_5}{r^3} + \frac{T}{m} \cos u_1 \sin u_2 \tag{2.1.2}$$

$$\dot{x}_3 = \frac{-\mu\, x_6}{r^3} + \frac{T}{m} \sin u_1 \tag{2.1.3}$$

$$\dot{x}_4 = x_1 \tag{2.1.4}$$

$$\dot{x}_5 = x_2 \tag{2.1.5}$$

$$\dot{x}_6 = x_3 \tag{2.1.6}$$

where

$$r = \sqrt{x_4{}^2 + x_5{}^2 + x_6{}^2} \tag{2.1.7}$$

$$T = \beta\, v_{ex} \tag{2.1.8}$$

$$m = m_o - \beta t \tag{2.1.9}$$
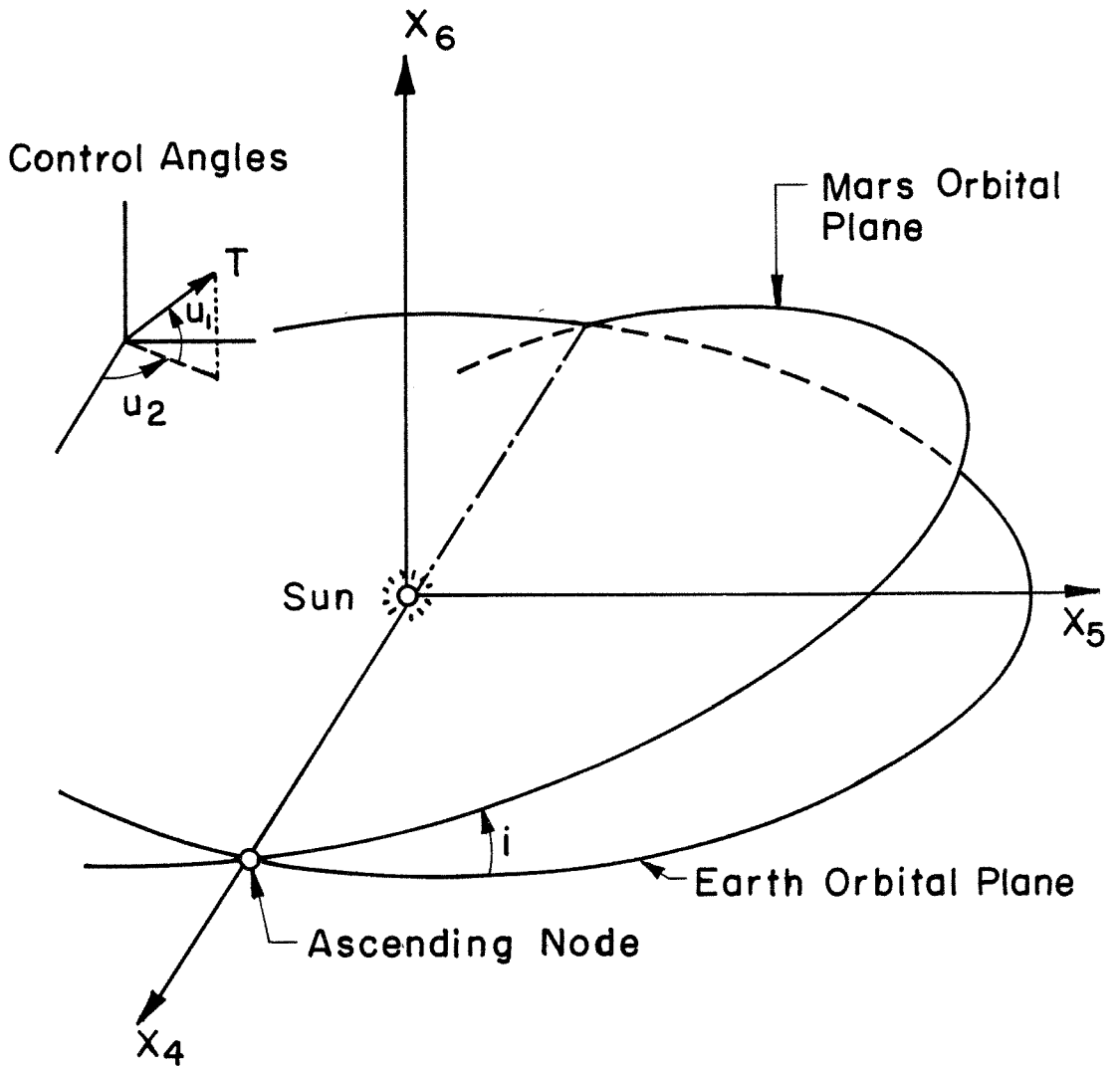
FIG. I COORDINATE SYSTEM

and

x_4, x_5, x_6 — heliocentric position coordinates

x_1, x_2, x_3 — heliocentric velocity components

μ — gravitational parameter of the Sun

T   — thrust of spacecraft rocket

m   — spacecraft mass

u_1, u_2 — inertial thrust vector control angles (Fig. 1)

β — mass flow rate (constant)

v_{ex} — rocket exhaust velocity

m_o — initial spacecraft gross mass

t   — time

2.1.3 Initial conditions

As previously mentioned, for purposes of comparison the initial conditions used in this study are the same as those used in previous works[1-3]. These initial conditions are meant to correspond to Earth's state on the hypothetical launch date, 1200 January 9, 1982.

$$x_1(t_o) = x_{o_1} \equiv -1.4835073 \times 10^{-2} \text{ AU/day} \tag{2.1.10}$$

$$x_2(t_o) = x_{o_2} \equiv 9.2714508 \times 10^{-3} \text{ AU/day} \tag{2.1.11}$$

$$x_3(t_o) = x_{o_3} \equiv 0 \qquad\qquad \text{AU/day} \tag{2.1.12}$$

$$x_4(t_o) = x_{o_4} \equiv 5.199345 \times 10^{-1} \text{ AU} \tag{2.1.13}$$

$$x_5(t_o) = x_{o_5} \equiv 8.3463802 \times 10^{-1} \text{ AU} \tag{2.1.14}$$

$$x_6(t_o) = x_{o_6} \equiv 0 \qquad\qquad \text{AU} \tag{2.1.15}$$

$$t = 0 \text{ at launch or } t_o = 0 \tag{2.1.16}$$

(No attempt was made to verify that the above launch date was indeed the optimal launch date from the set of optimal rendezvous trajectories for

1981-2. Also, the Earth state for the launch date was not verified.)

2.1.4 Terminal Constraints

Since a rendezvous with Mars is desired, the spacecraft state must equal the Martian state at the final time, t_f. The fact that the spacecraft position at the initial time corresponds to Earth's center and at the final time corresponds to Mars' center again is just a simplification that does not alter the relative performance of the guidance algorithms.

$x_{M_4}(t_f)$, $x_{M_5}(t_f)$, $x_{M_6}(t_f)$ – Mars' heliocentric position coordinates at the final time

$x_{M_1}(t_f)$, $x_{M_2}(t_f)$, $x_{M_3}(t_f)$ – Mars' heliocentric velocity components at the final time

$$x_1(t_f) = x_{M_1}(t_f) \tag{2.1.17}$$

$$x_2(t_f) = x_{M_2}(t_f) \tag{2.1.18}$$

$$x_3(t_f) = x_{M_3}(t_f) \tag{2.1.19}$$

$$x_4(t_f) = x_{M_4}(t_f) \tag{2.1.20}$$

$$x_5(t_f) = x_{M_5}(t_f) \tag{2.1.21}$$

$$x_6(t_f) = x_{M_6}(t_f) \tag{2.1.22}$$

To find $x_{M_i}(t)$, the eccentric anomaly and Kepler's equation are introduced. See Figure 2.

$E(t)$ – eccentric anomaly

E_o – eccentric anomaly at t_o

$\gamma(t)$ – true anomaly

e   - eccentricity

a   - semi-major axis

r(t) - radial distance

From Reference 15, the radial distance is

$$r = a (1-e \cos E) \tag{2.1.23}$$

When compared with the polar equation of the ellipse

$$r = \frac{a(1-e^2)}{1+e \cos \gamma} \tag{2.1.24}$$

the following relationships are established:

$$\cos \gamma = \frac{\cos E - e}{1 - e \cos E} \tag{2.1.25}$$

$$\sin \gamma = \frac{\sqrt{1-e^2} \sin E}{1 - e \cos E} \tag{2.1.26}$$

Therefore, in the orbit plane coordinates, x', y', and z', shown in Figure 2, the position of Mars (M subscript - Mars) is:

$$x_M' = r_M \cos \gamma_M = r_M \frac{\cos E_M - e_M}{1 - e_M \cos E_M}$$

$$= a_M(1 - e_M \cos E_M) \frac{\cos E_M - e_M}{1 - e_M \cos E_M} = a_M(\cos E_M - e_M) \tag{2.1.27}$$

$$y_M' = r_M \sin \gamma_M$$

$$= a_M (1 - e_M \cos E_M) \frac{\sqrt{1-e_M^2} \sin E_M}{1 - e_M \cos E_M} = a_M \sqrt{1-e_M^2} \sin E_M \tag{2.1.28}$$

$$z_M' = 0 \tag{2.1.29}$$
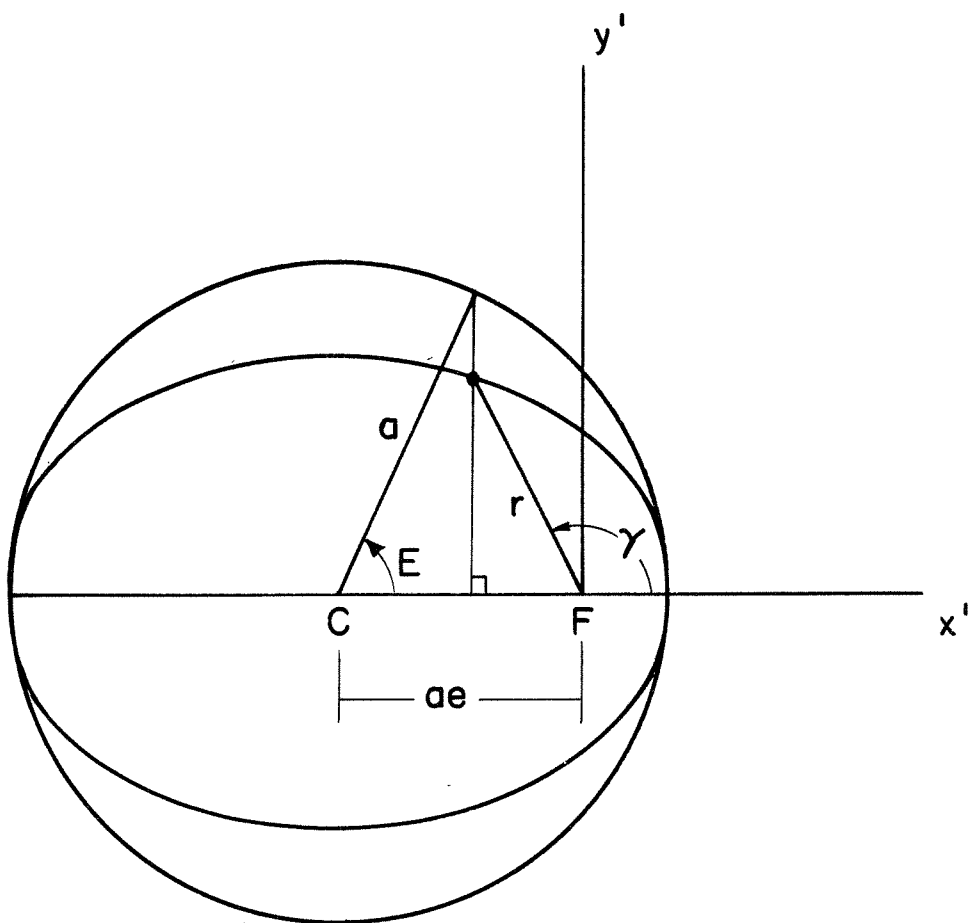
FIG. 2 ORBITAL ANOMALIES FOR ELLIPTIC
MOTION

The transformation between the primed system in Mars' orbit plane and the study coordinate system is defined with the Eulerian angles[15]:

i_M — inclination of Mars' orbit to the ecliptic

ω_M — argument of perihelion of Mars

Ω_M — longitude of Mars' ascending node

The transformation in general is:

$$\begin{bmatrix} x \\ y \\ z \end{bmatrix} = \begin{bmatrix} \ell_1 & \ell_2 & \ell_3 \\ m_1 & m_2 & m_3 \\ n_1 & n_2 & n_3 \end{bmatrix} \begin{bmatrix} x' \\ y' \\ z' \end{bmatrix}$$

(2.1.30)

(2.1.31)

(2.1.32)

where

$$\ell_1 = \cos \Omega \cos \omega - \sin \Omega \sin \omega \cos i \qquad (2.1.33)$$

$$\ell_2 = - \cos \Omega \sin \omega - \sin \Omega \cos \omega \cos i \qquad (2.1.34)$$

$$\ell_3 = \sin \Omega \sin i \qquad (2.1.35)$$

$$m_1 = \sin \Omega \cos \omega + \cos \Omega \sin \omega \cos i \qquad (2.1.36)$$

$$m_2 = - \sin \Omega \sin \omega + \cos \Omega \cos \omega \cos i \qquad (2.1.37)$$

$$m_3 = - \cos \Omega \sin i \qquad (2.1.38)$$

$$n_1 = \sin \omega \sin i \qquad (2.1.39)$$

$$n_2 = \cos \omega \sin i \qquad (2.1.40)$$

$$n_3 = \cos i \qquad (2.1.41)$$

In this study, $\Omega_M = 0$, so that the transformation (2.1.30-41) becomes

$$\begin{bmatrix} x_{M_4} \\ x_{M_5} \\ x_{M_6} \end{bmatrix} = \begin{bmatrix} \cos \omega_M & - \sin \omega_M & 0 \\ \sin \omega_M \cos i_M & \cos \omega_M \cos i_M & -\sin i_M \\ \sin \omega_M \sin i_M & \cos \omega_M \sin i_M & \cos i_M \end{bmatrix} \begin{bmatrix} x'_M \\ y'_M \\ z'_M \end{bmatrix}$$

(2.1.42)

(2.1.43)

(2.1.44)

Substituting Equations (2.1.27-29) into Equations (2.1.42-44) yields

$$x_{M_4}(t) = \cos \omega_M \, a_M \, [\cos E_M(t) - e_M] \tag{2.1.45}$$

$$- \sin \omega_M \, a_M \, \sqrt{1-e_M^2} \, \sin E_M(t)$$

$$x_{M_5}(t) = \sin \omega_M \cos i_M \, a_M \, [\cos E_M(t) - e_M] \tag{2.1.46}$$

$$+ \cos \omega_M \cos i_M \, a_M \, \sqrt{1-e_M^2} \, \sin E_M(t)$$

$$x_{M_6}(t) = \sin \omega_M \sin i_M \, a_M \, [\cos E_M(t) - e_M] \tag{2.1.47}$$

$$+ \cos \omega_M \sin i_M \, a_M \, \sqrt{1-e_M^2} \, \sin E_M(t)$$

where $E_M(t)$ is given by Kepler's equation:

$$E_M(t) - e_M \sin E_M(t) = t \sqrt{\frac{\mu}{a_M^3}} + E_{M_0} - e_M \sin E_{M_0} \tag{2.1.48}$$

Mars' velocity components are given by

$$x_{M_1}(t) = \dot{x}_{M_4}(t) = \cos \omega_M \, [-a_M \, \dot{E}_M(t) \, \sin E_M(t)] \tag{2.1.49}$$

$$- \sin \omega_M \, a_M \, \dot{E}_M(t) \, \sqrt{1-e_M^2} \, \cos E_M(t)$$

$$x_{M_2}(t) = \dot{x}_{M_5}(t) = \sin \omega_M \cos i_M \, [-a_M \, \dot{E}_M(t) \, \sin E_M(t)] \tag{2.1.50}$$

$$+ \cos \omega_M \cos i_M \, a_M \, \dot{E}_M(t) \, \sqrt{1-e_M^2} \, \cos E_M(t)$$

$$x_{M_3}(t) = \dot{x}_{M_6}(t) = \sin \omega_M \sin i_M \, [-a_M \, \dot{E}_M(t) \, \sin E_M(t)] \tag{2.1.51}$$

$$+ \cos \omega_M \sin i_M \, a_M \, \dot{E}_M(t) \, \sqrt{1-e_M^2} \, \cos E_M(t)$$

where from Equation (2.1.48)

$$\dot{E}_M(t) = \frac{\sqrt{\dfrac{\mu}{a_M^3}}}{1 - e_M \cos E_M(t)} \tag{2.1.52}$$

2.1.5 Performance Index

Final mass is to be maximized for this problem. This is the same as minimizing propellant consumption, assuming a fixed initial mass. Therefore, the performance index is

$$J = \int_{t_{o=0}}^{t_f} \beta dt \tag{2.1.53}$$

Since β is constrained to be a constant, minimizing the expression in Equation (2.1.53) is equivalent to minimizing final time.

$$J_{eq} = \int_{o}^{t_f} dt = t_f \quad . \tag{2.1.54}$$

2.2 NECESSARY CONDITIONS FOR THE TWO POINT BOUNDARY VALUE PROBLEM (TPBVP)

Necessary conditions of optimality for a general problem of the type just outlined will be presented. These necessary conditions will then be applied to the problem at hand, the Earth to Mars Rendezvous Problem (EMRP).

2.2.1 Necessary Conditions in General

Reference 16 contains the necessary conditions of optimality for the type of problem described in the last section, namely, for the problem of continuous systems with functions of the state variables specified at an unspecified terminal time. In general, then, the problem may be described as follows:

$\underline{x}$ – state vector $\qquad$ (n x 1)

$\underline{u}$ – control vector $\qquad$ (m x 1)

t – independent variable

The differential equations are

$$\dot{\underline{x}} = \underline{f} \left[\underline{x}(t), \underline{u}(t), t \right] \tag{2.2.1}$$

The initial conditions are given by

$$\underline{x}(t_o) = \underline{x}_o \; ; \qquad t_o \text{ given} \tag{2.2.2}$$

The constraint equations are

$$\underline{\psi} \left[\underline{x}(t_f), t_f \right] = 0 \, , \qquad \underline{\psi} - q \, (\leq n) \text{ vector} \tag{2.2.3}$$

The performance index to be minimized is

$$J = \phi \left[\underline{x}(t_f), t_f \right] + \int_{t_o}^{t_f} L \left[\underline{x}(t), \underline{u}(t), t \right] dt \tag{2.2.4}$$

If Equations (2.2.1) and (2.2.2) are adjoined to Equation (2.2.4) with Lagrange multipliers $\underline{\lambda}(t)$ and $\underline{v}$, Equation (2.2.4) becomes

$$\overline{J} = [\phi + \underline{\nu}^T \underline{\psi}]_{t=t_f} + \int_{t_o}^{t_f} \left\{ L (\underline{x}, \underline{u}, t) + \underline{\lambda}^T [\underline{f} (\underline{x}, \underline{u}, t) - \underline{\dot{x}}] \right\} dt$$

(2.2.5)

The Hamiltonian is defined as

$$H = L (\underline{x}, \underline{u}, t) + \underline{\lambda}^T (t) \, f(\underline{x}, \underline{u}, t)$$

(2.2.6)

The first variation of Equation (2.2.5) is then

$$d\overline{J} = \left[\left(\frac{\partial \Phi}{\partial t} + L \right) dt + \frac{\partial \Phi}{\partial \underline{x}} \, d\underline{x} \right]_{t=t_f}$$

(2.2.7)

$$+ \int_{t_o}^{t_f} \left(\frac{\partial H}{\partial \underline{x}} \, \delta\underline{x} + \frac{\partial H}{\partial \underline{u}} \, \delta\underline{u} - \underline{\lambda}^T \, \delta\underline{\dot{x}} \right) dt - L \Big|_{t=t_o} \, dt_o$$

where

  $\delta\underline{x}$ and $\delta\underline{u}$ are the variations in $\underline{x}$ and $\underline{u}$ for time held fixed

  $d\underline{x}$ is the total differential of $\underline{x}$

  $$\Phi = \phi + \underline{\nu}^T \underline{\psi}$$

(2.2.8)

Integrating by parts and noting that to first order

$$\delta\underline{x} = d\underline{x} - \underline{\dot{x}} \, dt$$

(2.2.9)

gives

$$d\overline{J} = \left[\frac{\partial \Phi}{\partial t} + L + \underline{\lambda}^T \underline{\dot{x}} \right]_{t=t_f} dt_f + \left[\left(\frac{\partial \Phi}{\partial \underline{x}} - \underline{\lambda}^T \right) d\underline{x} \right]_{t=t_f}$$

(2.2.10)

$$+ [\underline{\lambda}^T \delta\underline{x}]_{t=t_o} + \int_{t_o}^{t_f} \left[\left(\frac{\partial H}{\partial \underline{x}} + \underline{\dot{\lambda}}^T \right) \delta\underline{x} + \frac{\partial H}{\partial \underline{u}} \, \delta\underline{u} \right] dt$$

$$- L \Big|_{t=t_o} dt_o$$

If we now choose $\underline{\lambda}(t)$ and one component of $\underline{\nu}$ to make the coefficients of

$\delta\underline{x}(t)$, $d\underline{x}(t_f)$, and dt_f vanish, i.e.,

$$\underline{\dot{\lambda}}^{T} = - \frac{\partial H}{\partial \underline{x}} = - \underline{\lambda}^{T} \frac{\partial \underline{f}}{\partial \underline{x}} - \frac{\partial L}{\partial \underline{x}} \qquad (2.2.11)$$

$$\underline{\lambda}^{T} (t_{f}) = \left[\frac{\partial \Phi}{\partial \underline{x}} \right]_{t=t_{f}} = \left[\frac{\partial \phi}{\partial \underline{x}} + \underline{\nu}^{T} \frac{\partial \underline{\psi}}{\partial \underline{x}} \right]_{t=t_{f}} \qquad (2.2.12)$$

$$\left[\frac{\partial \Phi}{\partial t} + L + \underline{\lambda}^{T} \underline{\dot{x}} \right]_{t=t_{f}} = \left[\frac{d\Phi}{dt} + L \right]_{t=t_{f}} = 0 = \Omega \qquad (2.2.13)$$

where

$$\frac{d\Phi}{dt} \overset{\Delta}{=} \frac{\partial \Phi}{\partial t} + \frac{\partial \Phi}{\partial \underline{x}} \underline{\dot{x}} \qquad (2.2.14)$$

Equation (2.2.10) becomes

$$dJ = \int_{t_{o}}^{t_{f}} \frac{\partial H}{\partial \underline{u}} \delta \underline{u} \, dt + \underline{\lambda}^{T} (t_{o}) \, d\underline{x}(t_{o}) - H(t_{o}) dt_{o} \qquad (2.2.15)$$

Since $\underline{x}(t_{o})$ and t_{o} are given, the second and third terms vanish. For a stationary value of J the coefficient of $\delta \underline{u}$ must also vanish (see Ref. 16).

$$\frac{\partial H}{\partial \underline{u}} = \underline{\lambda}^{T} \frac{\partial \underline{f}}{\partial \underline{u}} + \frac{\partial L}{\partial \underline{u}} = 0 \qquad (2.2.16)$$

In summary then, the necessary conditions are given by Equations (2.2.1-3), Equations (2.2.11-13), and Equations (2.2.16) and form a Two Point Boundary Value Problem (TPBVP).

2.2.2 Necessary Conditions for the EMRP

For the problem at hand, the differential equations (2.2.1) are given by Equations (2.1.1-6) plus Equations (2.1.7-9). The initial conditions (2.2.2) are given by Equations (2.1.10-15) [and Equation (2.1.16)]. The terminal constraint equations (2.2.3) are deduced by rewriting equations (2.1.17-22):

$$\psi_1 \left[\underline{x}(t_f), \ t_f \right] = x_1(t_f) - x_{M_1}(t_f) = 0 \tag{2.2.17}$$

$$\psi_2 \left[\underline{x}(t_f), \ t_f \right] = x_2(t_f) - x_{M_2}(t_f) = 0 \tag{2.2.18}$$

$$\psi_3 \left[\underline{x}(t_f), \ t_f \right] = x_3(t_f) - x_{M_3}(t_f) = 0 \tag{2.2.19}$$

$$\psi_4 \left[\underline{x}(t_f), \ t_f \right] = x_4(t_f) - x_{M_4}(t_f) = 0 \tag{2.2.20}$$

$$\psi_5 \left[\underline{x}(t_f), \ t_f \right] = x_5(t_f) - x_{M_5}(t_f) = 0 \tag{2.2.21}$$

$$\psi_6 \left[\underline{x}(t_f), \ t_f \right] = x_6(t_f) - x_{M_6}(t_f) = 0 \tag{2.2.22}$$

where $x_{M_{1-6}}(t_f)$ are given by Equations (2.1.45-52). The performance index (2.2.4) is given by Equation (2.1.53). The Hamiltonian is, therefore

$$H = \beta + \lambda_1 \left(\frac{-\mu x_4}{r^3} + \frac{T}{m} \cos u_1 \ \cos u_2 \right) \tag{2.2.23}$$

$$+ \lambda_2 \left(\frac{-\mu x_5}{r^3} + \frac{T}{m} \cos u_1 \ \sin u_2 \right)$$

$$+ \lambda_3 \left(-\frac{\mu x_6}{r^3} + \frac{T}{m} \sin u_1 \right) + \lambda_4 x_1 + \lambda_5 x_2 + \lambda_6 x_3$$

Equation (2.2.8) becomes, since $\phi = 0$,

$$\Phi = \nu_1 \left[x_1(t_f) - x_{M_1}(t_f) \right] + \nu_2 \left[x_2(t_f) - x_{M_2}(t_f) \right] \tag{2.2.24}$$

$$+ \nu_3 \left[x_3(t_f) - x_{M_3}(t_f) \right] + \nu_4 \left[x_4(t_f) - x_{M_4}(t_f) \right]$$

$$+ \nu_5 \left[x_5(t_f) - x_{M_5}(t_f) \right] + \nu_6 \left[x_6(t_f) - x_{M_6}(t_f) \right]$$

Using Equation (2.2.3), the Euler-Lagrange equations (2.2.11) are

$$\dot{\lambda}_1 = - \lambda_4 \tag{2.2.25}$$

$$\dot{\lambda}_2 = - \lambda_5 \tag{2.2.26}$$

$$\dot{\lambda}_3 = - \lambda_6 \tag{2.2.27}$$

$$\dot{\lambda}_4 = \lambda_1 \frac{\mu}{r^3} - \frac{3\mu x_4}{r^5} (\lambda_1 x_4 + \lambda_2 x_5 + \lambda_3 x_6) \tag{2.2.28}$$

$$\dot{\lambda}_5 = \lambda_2 \frac{\mu}{r^3} - \frac{3\mu x_5}{r^5} (\lambda_1 x_4 + \lambda_2 x_5 + \lambda_3 x_6) \tag{2.2.29}$$

$$\dot{\lambda}_6 = \lambda_3 \frac{\mu}{r^3} - \frac{3\mu x_6}{r^5} (\lambda_1 x_4 + \lambda_2 x_5 + \lambda_3 x_6) \tag{2.2.30}$$

The transversality conditions (2.2.12) are, from Equation (2.2.24),

$$\lambda_1 (t_f) = \nu_1 \tag{2.2.31}$$

$$\lambda_2 (t_f) = \nu_2 \tag{2.2.32}$$

$$\lambda_3 (t_f) = \nu_3 \tag{2.2.33}$$

$$\lambda_4 (t_f) = \nu_4 \tag{2.2.34}$$

$$\lambda_5 (t_f) = \nu_5 \tag{2.2.35}$$

$$\lambda_6 (t_f) = \nu_6 \tag{2.2.36}$$

The remaining transversality condition (2.2.13) is

$$\Omega = \beta + \nu_1 \left[\dot{x}_1(t_f) - \dot{x}_{M_1}(t_f) \right] + \nu_2 \left[\dot{x}_2(t_f) - \dot{x}_{M_2}(t_f) \right] \tag{2.2.37}$$

$$+ \nu_3 \left[\dot{x}_3(t_f) - \dot{x}_{M_3}(t_f) \right] + \nu_4 \left[\dot{x}_4(t_f) - \dot{x}_{M_4}(t_f) \right]$$

$$+ \nu_5 \left[\dot{x}_5(t_f) - \dot{x}_{M_5}(t_f) \right] + \nu_6 \left[\dot{x}_6(t_f) - \dot{x}_{M_6}(t_f) \right] = 0$$

whereupon differentiating Equations (2.2.45-47) and (2.1.49-52):

$$\dot{x}_{M_1}(t_f) = - a_M \ddot{E}_M(t_f) \left[\cos \omega_M \sin E_M(t_f) \right. \tag{2.2.38}$$

$$+ \sqrt{1-e_M^2} \sin \omega_M \cos E_M(t_f) \bigg] - a_M \left[\dot{E}_M(t_f) \right]^2$$

$$\cdot \left[\cos \omega_M \cos E_M(t_f) - \sqrt{1-e_M^2} \sin \omega_M \sin E_M(t_f) \right]$$

$$\dot{x}_{M_2}(t_f) = a_M \ddot{E}_M(t_f) \cos i_M \left[- \sin \omega_M \sin E_M(t_f)\right. \qquad (2.2.39)$$

$$\left. + \sqrt{1-e_M^2} \cos \omega_M \cos E_M(t_f)\right] - a_M \left[\dot{E}_M(t_f)\right]^2 \cos i_M$$

$$\cdot \left[\sin \omega_M \cos E_M(t_f) + \sqrt{1-e^2} \cos \omega_M \sin E_M(t_f)\right]$$

$$\dot{x}_{M_3}(t_f) = a_M \ddot{E}_M(t_f) \sin i_M \left[- \sin \omega_M \sin E_M(t_f)\right. \qquad (2.2.40)$$

$$\left. + \sqrt{1-e_M^2} \cos \omega_M \cos E_M(t_f)\right] - a_M \left[\dot{E}_M(t_f)\right]^2 \sin i_M$$

$$\cdot \left[\sin \omega_M \cos E_M(t_f) + \sqrt{1-e_M^2} \cos \omega_M \sin E_M(t_f)\right]$$

$$\dot{x}_{M_4}(t_f) = x_{M_1}(t_f) \qquad (2.2.41)$$

$$\dot{x}_{M_5}(t_f) = x_{M_2}(t_f) \qquad (2.2.42)$$

$$\dot{x}_{M_6}(t_f) = x_{M_3}(t_f) \qquad (2.2.43)$$

and

$$\ddot{E}_M(t_f) = \frac{-e_M \sin E_M(t_f) \left[\dot{E}_M(t_f)\right]^2}{1-e_M \cos E_M(t_f)} \qquad (2.2.44)$$

With regard to Equation (2.2.16),

$$\frac{\partial L}{\partial \underline{u}} = 0 \qquad (2.2.45)$$

In matrix notation the vector $\underline{f}$, given by Equation (2.2.1) and Equations (2.1.1-6), differentiated by the vector

$$\underline{u} = \begin{bmatrix} u_1 \\ u_2 \end{bmatrix} \qquad (2.2.46)$$

is

$$\frac{\partial f}{\partial \underline{u}} = \underline{f}_{\underline{u}} = \frac{T}{m} \begin{bmatrix} -\sin u_1 \cos u_2 & -\cos u_1 \sin u_2 \\ -\sin u_1 \sin u_2 & \cos u_1 \cos u_2 \\ \cos u_1 & 0 \\ 0 & 0 \\ 0 & 0 \\ 0 & 0 \end{bmatrix} \qquad (2.2.47)$$

Hence, Equation (2.2.16) becomes

$$\frac{\partial H}{\partial u_1} = -\lambda_1 \frac{T}{m} \sin u_1 \cos u_2 - \lambda_2 \frac{T}{m} \sin u_1 \sin u_2 \qquad (2.2.48)$$

$$+ \lambda_3 \frac{T}{m} \cos u_1 = 0$$

$$\frac{\partial H}{\partial u_2} = -\lambda_1 \frac{T}{m} \cos u_1 \sin u_2 + \lambda_2 \frac{T}{m} \cos u_1 \cos u_2 = 0 \qquad (2.2.49)$$

2.3 SOLUTION OF THE TPBVP BY THE BACKWARD SWEEP METHOD

The Backward Sweep Method in general is presented followed by the

general Backward Sweep Algorithm. The Backward Sweep Method and

Algorithm as applied to the EMRP are then presented.

2.3.1 The Backward Sweep Method in General

The Backward Sweep Method is in the class of iterative techniques

for solving a TPBVP known as Neighboring Extremal Algorithms. These

algorithms, as their name implies, solve the TPBVP by driving the initial

state and terminal constraints to their specified values by integration

of successive perturbations of end conditions starting with a guess of,

for instance, final time, state and multipliers. For each iteration,

the necessary conditions hold (except for the boundary conditions);

therefore, each perturbation leads to a neighboring extremal with dif-

ferent end states.

The Backward Sweep Method "sweeps" the known boundary conditions

from the final time to the initial time by the integration of sweep

matrices, as shown below[16].

The objective is to find the control, $\underline{u}(t)$, such that the perfor-

mance index, J, is minimized. To do this requires that necessary

conditions (2.2.1-3), (2.2.11-13), and (2.2.16) hold. Consider pertur-

bations in the necessary conditions. The perturbation of Equation (2.2.2)

can be chosen

$$\delta\underline{x}(t_o) = \delta\underline{x}_o \qquad\qquad (2.3.1)$$

Linearizing Equations (2.2.1), (2.2.11), (2.2.16), (2.2.12), (2.2.3),

and (2.2.13) gives[16]

$$\delta \underline{\dot{x}} = f_{\underline{x}} \ \delta \underline{x} + \underline{f}_{\underline{u}} \ \delta \underline{u} \tag{2.3.2}$$

$$\delta \underline{\dot{\lambda}} = - H_{\underline{xx}} \ \delta \underline{x} - \underline{f}_{\underline{x}}^{T} \ \delta \underline{\lambda} - H_{\underline{xu}} \ \delta \underline{u} \tag{2.3.3}$$

$$0 = H_{\underline{ux}} \ \delta \underline{x} + \underline{f}_{\underline{u}}^{T} \ \delta \underline{\lambda} + H_{\underline{uu}} \ \delta \underline{u} \tag{2.3.4}$$

$$d\underline{\lambda}(t_f) = \left[\frac{\partial^2 \phi}{\partial \underline{x}^2} \ d\underline{x} + \left(\frac{\partial \underline{\psi}}{\partial \underline{x}} \right)^{T} \ d\underline{\nu} + \frac{\partial^2 \phi}{\partial t \partial \underline{x}} \ dt_f \right]_{t=t_f} \tag{2.3.5}$$

$$d\underline{\psi} = \left[\frac{\partial \underline{\psi}}{\partial \underline{x}} \ d\underline{x} + \frac{\partial \underline{\psi}}{\partial t} \ dt_f \right]_{t=t_f} \tag{2.3.6}$$

$$d\Omega = \left[\frac{\partial \Omega}{\partial \underline{x}} \ d\underline{x} + d\underline{\nu}^{T} \ \frac{d\underline{\psi}}{dt} + \frac{\partial \Omega}{\partial t} \ dt_f \right]_{t=t_f} \tag{2.3.7}$$

where $\quad \dfrac{\partial \Omega}{\partial \underline{u}} = H_{\underline{u}} = 0 \tag{2.3.8}$

Using the linear approximations

$$d\underline{\lambda}(t_f) = \delta\underline{\lambda}(t_f) + \underline{\dot{\lambda}}(t_f)dt_f \tag{2.3.9}$$

$$d\underline{x}(t_f) = \delta\underline{x}(t_f) + \underline{\dot{x}}(t_f) \ dt_f \tag{2.3.10}$$

the expression for $\delta\underline{\lambda}(t_f)$ is, from Equation (2.3.5)

$$\delta\underline{\lambda}(t_f) = \left\{ \frac{\partial^2 \phi}{\partial \underline{x}^2} \ \delta\underline{x} + \left(\frac{\partial \underline{\psi}}{\partial \underline{x}} \right)^{T} \ d\underline{\nu} + \left[\frac{d}{dt} \left(\frac{\partial \phi}{\partial \underline{x}} \right)^{T} - \underline{\dot{\lambda}} \right] dt_f \right\}_{t=t_f} \tag{2.3.11}$$

Define

$$A(t) = \underline{f}_{\underline{x}} - \underline{f}_{\underline{u}} \ H_{\underline{uu}}^{-1} \ H_{\underline{ux}} \tag{2.3.12}$$

$$B(t) = \underline{f}_{\underline{u}} \ H_{\underline{uu}}^{-1} \ \underline{f}_{\underline{u}}^{T} \tag{2.3.13}$$

$$C(t) = H_{\underline{xx}} - H_{\underline{xu}} \ H_{\underline{uu}}^{-1} \ H_{\underline{ux}} \tag{2.3.14}$$

Then Equations (2.3.2-4) become

$$\delta \dot{\underline{x}} = A \ \delta \underline{x} - B \ \delta \underline{\lambda} \tag{2.3.15}$$

$$\delta \dot{\underline{\lambda}} = - C \ \delta \underline{x} - A^T \ \delta \underline{\lambda} \tag{2.3.16}$$

$$\delta \underline{u} = - H_{\underline{uu}}^{-1} \ (H_{\underline{ux}} \ \delta \underline{x} + \underline{f}_{\underline{u}}^T \ \delta \underline{\lambda}) \tag{2.3.17}$$

From Equations (2.2.13-14), (2.2.11), and (2.2.12)

$$\left(\frac{\partial \Omega}{\partial \underline{x}} \right)^T = \left[\frac{\partial}{\partial \underline{x}} \left(\frac{\partial \Phi}{\partial t} + \frac{\partial \Phi}{\partial \underline{x}} \ \dot{\underline{x}} + L \right) \right]^T \tag{2.3.18}$$

$$= \left(\frac{\partial^2 \Phi}{\partial \underline{x} \partial t} + \dot{\underline{x}}^T \frac{\partial^2 \Phi}{\partial \underline{x}^2} + \frac{\partial \Phi}{\partial \underline{x}} \frac{\partial \underline{f}}{\partial \underline{x}} + \frac{\partial L}{\partial \underline{x}} \right)^T$$

$$= \frac{\partial^2 \Phi}{\partial t \partial \underline{x}} + \frac{\partial^2 \Phi}{\partial \underline{x}^2} \ \dot{\underline{x}} + \left(\underline{\lambda}^T \frac{\partial \underline{f}}{\partial \underline{x}} + \frac{\partial L}{\partial \underline{x}} \right)^T$$

$$= \frac{d}{dt} \left(\frac{\partial \Phi}{\partial \underline{x}} \right)^T - \dot{\underline{\lambda}}$$

Thus, using Equation (2.3.10), Equations (2.3.11) and (2.3.6-7) are, in matrix form,

$$\begin{bmatrix} \delta \underline{\lambda}(t_f) \\ \\ d \underline{\psi} \\ \\ d \Omega \end{bmatrix}^{\cdot} = \begin{bmatrix} \dfrac{\partial^2 \Phi}{\partial \underline{x}^2} & \left(\dfrac{\partial \underline{\psi}}{\partial \underline{x}} \right)^T & \left(\dfrac{\partial \Omega}{\partial \underline{x}} \right)^T \\ \\ \dfrac{\partial \underline{\psi}}{\partial \underline{x}} & 0 & \dfrac{d \underline{\psi}}{dt} \\ \\ \dfrac{\partial \Omega}{\partial \underline{x}} & \left(\dfrac{d \underline{\psi}}{dt} \right)^T & \dfrac{d \Omega}{dt} \end{bmatrix}_{t=t_f} \begin{bmatrix} \delta \underline{x}(t_f) \\ \\ d \underline{\nu} \\ \\ dt_f \end{bmatrix} \tag{2.3.19}$$

Equations (2.3.1-4) and (2.3.19) form a linear TPBVP for a neighboring extremal with perturbations in initial conditions, $\delta \underline{x}(t_o)$, and terminal constraints, $d \underline{\psi}$. This linear TPBVP is readily solved, and thus the original nonlinear TPBVP is solved by driving towards the specified end conditions by solving successive linear TPBVP's.

To solve the linear TPBVP, a solution of Equations (2.3.3) and (2.3.6-7) is assumed[16]:

$$
\begin{bmatrix} \delta\underline{\lambda}(t) \\ d\underline{\psi} \\ d\Omega \end{bmatrix} = \begin{bmatrix} S(t) & R(t) & \underline{m}(t) \\ R^T(t) & Q(t) & \underline{n}(t) \\ \underline{m}^T(t) & \underline{n}^T(t) & \alpha(t) \end{bmatrix} \begin{bmatrix} \delta\underline{x}(t) \\ d\underline{\nu} \\ dt_f \end{bmatrix} \qquad (2.3.20)
$$

Differentiating Equation (2.3.20) and noting that $d\underline{\psi}$, $d\underline{\nu}$, and dt_f are constants and that along an extremal

$$
d\Omega = 0 \qquad (2.3.21)
$$

we obtain

$$
\begin{bmatrix} \delta\dot{\underline{\lambda}} \\ \underline{0} \\ 0 \end{bmatrix} = \begin{bmatrix} \dot{S} & \dot{R} & \dot{\underline{m}} \\ \dot{R}^T & \dot{Q} & \dot{\underline{n}} \\ \dot{\underline{m}}^T & \dot{\underline{n}}^T & \dot{\alpha} \end{bmatrix} \begin{bmatrix} \delta\underline{x} \\ d\underline{\nu} \\ dt_f \end{bmatrix} + \begin{bmatrix} S \\ R^T \\ \underline{m}^T \end{bmatrix} \delta\dot{\underline{x}} \qquad (2.3.22)
$$

Substituting Equations (2.3.15-16) in Equation (2.3.22) and using Equation (2.3.20a) yields

$$
\begin{bmatrix} 0 \\ 0 \\ 0 \end{bmatrix} = \begin{bmatrix} \dot{S} + SA + A^T S - SBS + C & \dot{R} + (A^T - SB)R & \dot{\underline{m}} + (A^T - SB)\underline{m} \\ \dot{R}^T + R^T(A - BS) & \dot{Q} - R^T BR & \dot{\underline{n}} - R^T B\underline{m} \\ \dot{\underline{m}}^T + \underline{m}^T(A - BS) & \dot{\underline{n}}^T - \underline{m}^T BR & \dot{\alpha} - \underline{m}^T B\underline{m} \end{bmatrix} \begin{bmatrix} \delta\underline{x}(t) \\ d\underline{\nu} \\ dt_f \end{bmatrix}
$$

$$(2.3.23)$$

Equation (2.3.23) is satisfied for all possible nontrivial $\delta\underline{x}(t)$, $d\underline{\nu}$, dt_f if

$$
\dot{S} = - SA - A^T S + SBS - C \qquad (2.3.24)
$$

$$
\dot{R} = - (A^T - SB) R \qquad (2.3.25)
$$

$$
\dot{Q} = R^T BR \qquad (2.3.26)
$$

$$
\dot{\underline{m}} = - (A^T - SB) \underline{m} \qquad (2.3.27)
$$

$$\dot{\underline{n}} = R^T B\underline{m} \qquad\qquad (2.3.28)$$

$$\dot{\alpha} = m^T B\underline{m} \qquad\qquad (2.3.29)$$

Evaluation of Equation (2.3.20) at $t = t_f$ and comparison with Equation (2.3.19) yields

$$S(t_f) = \frac{\partial^2 \Phi}{\partial \underline{x}^2}\Big|_{t=t_f} \qquad\qquad (2.3.30)$$

$$R(t_f) = \left(\frac{\partial \underline{\psi}}{\partial \underline{x}}\right)^T_{t=t_f} \qquad\qquad (2.3.31)$$

$$Q(t_f) = 0 \qquad\qquad (2.3.32)$$

$$\underline{m}(t_f) = \left(\frac{\partial \Omega}{\partial \underline{x}}\right)^T_{t=t_f} \qquad\qquad (2.3.33)$$

$$\underline{n}(t_f) = \frac{d\underline{\psi}}{dt}\Big|_{t=t_f} \qquad\qquad (2.3.34)$$

$$\alpha(t_f) = \frac{d\Omega}{dt}\Big|_{t=t_f} \qquad\qquad (2.3.35)$$

Writing Equation (2.3.20) in more compact form yields

$$\begin{bmatrix} \delta\underline{\lambda}(t) \\ d\,\overline{\underline{\psi}} \end{bmatrix} = \begin{bmatrix} \underset{\sim}{S}(t) & \underset{\sim}{R}(t) \\ \underset{\sim}{R}^T(t) & \underset{\sim}{Q}(t) \end{bmatrix} \begin{bmatrix} \delta\underline{x}(t) \\ d\overline{\underline{v}} \end{bmatrix} \qquad (2.3.36)$$

where, using Equation (2.3.21)

$$\underset{\sim}{S}(t) = S(t) \qquad\qquad (2.3.37$$

$$\underset{\sim}{R}(t) = \begin{bmatrix} R(t) & \underline{m}(t) \end{bmatrix} \qquad\qquad (2.3.38)$$

$$\underset{\sim}{Q}(t) = \begin{bmatrix} Q(t) & \underline{n}(t) \\ \underline{n}^T(t) & \alpha(t) \end{bmatrix} \qquad\qquad (2.3.39)$$

$$d\overline{\underline{\psi}} = \begin{bmatrix} d\underline{\psi} \\ \\ 0 \end{bmatrix} \qquad\qquad (2.3.40)$$

$$d\overline{\underline{\nu}} = \begin{bmatrix} d\underline{\nu} \\ \\ dt_f \end{bmatrix} \qquad\qquad (2.3.41)$$

Equation (2.3.36) can be rewritten

$$\begin{bmatrix} \delta\underline{\lambda}(t) \\ \\ -d\overline{\underline{\nu}} \end{bmatrix} = \begin{bmatrix} \underset{\sim}{S}_*(t) & \underset{\sim}{R}_*(t) \\ \\ \underset{\sim}{R}_*^T(t) & \underset{\sim}{Q}_*(t) \end{bmatrix} \cdot \begin{bmatrix} \delta\underline{x}(t) \\ \\ d\overline{\underline{\psi}} \end{bmatrix} \qquad (2.3.42)$$

where

$$\underset{\sim}{S}_* = \underset{\sim}{S} - \underset{\sim}{R} \; \underset{\sim}{Q}^{-1} \; \underset{\sim}{R}^T \qquad\qquad (2.3.43)$$

$$\underset{\sim}{R}_* = \underset{\sim}{R} \; \underset{\sim}{Q}^{-1} \qquad\qquad (2.3.44)$$

$$\underset{\sim}{Q}_* = - \; \underset{\sim}{Q}^{-1} \qquad\qquad (2.3.45)$$

Note that $\{\underset{\sim}{S}, \underset{\sim}{R}, \underset{\sim}{Q}\}$ and $\{\underset{\sim}{S}_*, \underset{\sim}{R}_*, \underset{\sim}{Q}_*\}$ satisfy Equations (2.3.24-26), but the starred matrices satisfy different boundary conditions. Equation (2.3.42) yields $\delta\underline{\lambda}(t_o)$, $d\underline{\nu}$, and dt_f at $t=t_o$.

2.3.2   The Backward Sweep Algorithm in General

The backward sweep algorithm employed here consists of the following steps[16]:

1.   Guess t_f, $\underline{x}(t_f)$, $\underline{\nu}$.

2.   Evaluate $\underline{\psi}\left[\underline{x}(t_f), t_f\right]$, $\underline{\lambda}(t_f)$, and Ω from Equations (2.2.3), (2.2.12) and (2.2.13).

3.   Integrate $\dot{\underline{x}}$, $\dot{\underline{\lambda}}$, $\dot{\underset{\sim}{S}}$, $\dot{\underset{\sim}{R}}$, $\dot{\underset{\sim}{Q}}$ backward to t_o, using Equations (2.2.1), (2.2.11), (2.2.16), (2.2.24-29) and boundary conditions (2.3.30-35),

where the partitioning in Equations (2.3.37-41) has been employed. The

transformation (2.3.43-45) is made at some t_1, $t_o \leq t_1 < t_f$.

4. At t_o, set
$$\begin{bmatrix} \delta\underline{x}(t_o) \\ d\underline{\psi} \\ d\Omega \end{bmatrix} = -\ \varepsilon \begin{bmatrix} \underline{x}(t_o) - \underline{x}_o \\ \underline{\psi}\ [\underline{x}(t_f),\ t_f] \\ \Omega \end{bmatrix}$$

$$(2.3.46)$$
$$(2.3.47)$$
$$(2.3.48)$$

where $0 < \varepsilon \leq 1$, and find $d\underline{\nu}$, dt_f, and $\delta\underline{\lambda}(t_o)$ from Equations (2.3.42)

[and Equations (2.3.40-41)].

5. Integrate $\delta\dot{\underline{x}}$, $\delta\dot{\underline{\lambda}}$, $\dot{\underline{x}}$, and $\dot{\underline{\lambda}}$ forward to t_f using Equations

(2.3.12-16), (2.2.1), (2.2.11), (2.2.16).

6. Using Equation (2.3.10) update $\underline{x}(t_f)$, $\underline{\nu}$, and t_f with

$$\begin{bmatrix} \underline{x}(t_f) \\ \underline{\nu} \\ t_f \end{bmatrix}_{new} = \begin{bmatrix} \underline{x}(t_f) \\ \underline{\nu} \\ t_f \end{bmatrix}_{old} + \begin{bmatrix} d\underline{x}(t_f) \\ d\underline{\nu} \\ dt_f \end{bmatrix}$$

$$(2.3.49)$$
$$(2.3.50)$$
$$(2.3.51)$$

7. Iterate <u>Steps 2-6</u> to desired accuracy of $\underline{x}(t_o)$, $\underline{\psi}[\underline{x}(t_f),\ t_f]$,

and Ω.

2.3.3 <u>The Backward Sweep Method and Algorithm as Applied to the EMRP</u>

<u>Step 1</u> is straightforward.

<u>Step 2</u> requires the use of Equations (2.2.17-22), (2.2.31-36), and

(2.2.37) [and Equations (2.1.1-9), (2.2.48-49), (2.2.38-44), and

(2.1.45-52)]. The controls u_1 and u_2 are found from Equations (2.2.48-49);

Equation (2.2.49) reduces to

$$-\ \lambda_1 \sin u_2 + \lambda_2 \cos u_2 = 0 \qquad\qquad (2.3.52)$$

or
$$\tan u_2 = \frac{\lambda_2}{\lambda_1} \qquad\qquad (2.3.53)$$

Thus
$$\sin u_2 = \frac{\pm\ \lambda_2}{\sqrt{\lambda_1^2 + \lambda_2^2}} \qquad\qquad (2.3.54)$$

and $\qquad \cos u_2 = \pm \dfrac{\lambda_1}{\sqrt{\lambda_1^2 + \lambda_2^2}}$ $\qquad\qquad$ (2.3.55)

Substituting Equations (2.3.54-55) into Equations (2.2.48) yields

$$\lambda_1 \sin u_1 \left(\pm \frac{\lambda_1}{\sqrt{\lambda_1^2 + \lambda_2^2}}\right) + \lambda_2 \sin u_1 \left(\pm \frac{\lambda_2}{\sqrt{\lambda_1^2 + \lambda_2^2}}\right)$$

$$- \lambda^3 \cos u_1 = 0 \qquad\qquad (2.3.56)$$

or $\quad \pm \sin u_1 \sqrt{\lambda_1^2 + \lambda_2^2} = \lambda_3 \cos u_1$ $\qquad\qquad$ (2.3.57)

or $\qquad \tan u_1 = \dfrac{\pm \lambda_3}{\sqrt{\lambda_1^2 + \lambda_2^2}}$ $\qquad\qquad$ (2.3.58)

thus $\quad \sin u_1 = \begin{cases} \pm \dfrac{\lambda_3}{\sqrt{\lambda_1^2 + \lambda_2^2 + \lambda_3^2}} & \text{sign in Equation (2.3.58) positive} \\[3mm] \mp \dfrac{\lambda_3}{\sqrt{\lambda_1^2 + \lambda_2^2 + \lambda_3^2}} & \text{sign in Equation (2.3.58) negative} \end{cases}$

$\qquad\qquad$ (2.3.59)

and $\qquad \cos u_1 = \pm \dfrac{\sqrt{\lambda_1^2 + \lambda_2^2}}{\sqrt{\lambda_1^2 + \lambda_2^2 + \lambda_3^2}}$ $\qquad\qquad$ (2.3.60)

To determine the proper signs of Equations (2.3.54-55) and Equations (2.3.59-60), the following element of a set of sufficient conditions for a weak relative minimum must be employed:

$$H_{\underline{uu}} > 0 \qquad\qquad (2.3.61)$$

Equation (2.3.61) can be broken down by components:

$$H_{u_1 u_1} = \frac{T}{m} \left(- \lambda_1 \cos u_1 \cos u_2 - \lambda_2 \cos u_1 \sin u_2 \right. \qquad (2.3.62)$$

$$\left. - \lambda_3 \sin u_1 \right)$$

$$H_{u_1 u_2} = \frac{T}{m} \left(\lambda_1 \sin u_1 \sin u_2 - \lambda_2 \sin u_1 \cos u_2\right) \qquad (2.3.63)$$

$$H_{u_2 u_1} = \frac{T}{m} \left(\lambda_1 \sin u_1 \sin u_2 - \lambda_2 \sin u_1 \cos u_2\right) \qquad (2.3.64)$$

$$H_{u_2 u_2} = \frac{T}{m} \left(- \lambda_1 \cos u_1 \cos u_2 - \lambda_2 \cos u_1 \sin u_2\right) \qquad (2.3.65)$$

There are four possible cases:

Case I   Signs in Equations (2.3.54-55), (2.3.59), and (2.3.60) all positive

Case II   Signs in Equations (2.3.54-55) positive; signs in Equations (2.3.59) and (2.3.60) negative

Case III   Signs in Equations (2.3.54-55) negative; sign in Equation (2.3.59) negative; sign in Equation (2.3.60) positive.

Case IV   Signs in Equations (2.3.54-55) negative; sign in Equation (2.3.59) positive; sign in Equation (2.3.60) negative.

For H_{uu} to be positive definite the principal minors of H_{uu} must be positive, i.e.,

$$\Delta_1 = H_{u_1 u_1} > 0 \tag{2.3.66}$$

$$\Delta_2 = \begin{vmatrix} H_{u_1 u_1} & H_{u_1 u_2} \\ H_{u_2 u_1} & H_{u_2 u_2} \end{vmatrix} > 0 \tag{2.3.67}$$

For all cases $\quad H_{u_2 u_1} = H_{u_2 u_1} = 0$ $\qquad$ (2.3.68)

For Case I

$$\Delta_1 = \left(\frac{T}{m}\right) \frac{1}{\sqrt{\lambda_1^2 + \lambda_2^2 + \lambda_3^2}} \left(- \lambda_1^2 - \lambda_2^2 + \lambda_3^2\right) \tag{2.3.69}$$

$$\Delta_2 = \Delta_1 \left(\frac{T}{m}\right) \frac{1}{\sqrt{\lambda_1^2 + \lambda_2^2 + \lambda_3^2}} \left(-\lambda_1^2 - \lambda_2^2\right) \tag{2.3.70}$$

Since in this case Δ_2 has a sign opposite to that of Δ_1, this case fails the sufficiency condition.

For Case II

$$\Delta_1 = \left(\frac{T}{m}\right)\frac{1}{\sqrt{\lambda_1{}^2 + \lambda_2{}^2 + \lambda_3{}^2}} \quad (\lambda_1{}^2 + \lambda_2{}^2 - \lambda_3{}^2) \qquad (2.3.71)$$

$$\Delta_2 = \Delta_1\left(\frac{T}{m}\right)\frac{1}{\sqrt{\lambda_1{}^2 + \lambda_2{}^2 + \lambda_3{}^2}} \quad (\lambda_1{}^2 + \lambda_2{}^2) \qquad (2.3.72)$$

Case II satisfies the sufficiency condition only when

$$\lambda_3{}^2 < \lambda_1{}^2 + \lambda_2{}^2 \qquad (2.3.73)$$

For Case III

$$\Delta_1 = \left(\frac{T}{m}\right)\frac{1}{\sqrt{\lambda_1{}^2 + \lambda_2{}^2 + \lambda_3{}^2}} \quad (\lambda_1{}^2 + \lambda_2{}^2 + \lambda_3{}^2) \qquad (2.3.74)$$

$$\Delta_2 = \Delta_1\left(\frac{T}{m}\right)\frac{1}{\sqrt{\lambda_1{}^2 + \lambda_2{}^2 + \lambda_3{}^2}} \quad (\lambda_1{}^2 + \lambda_2{}^2) \qquad (2.3.75)$$

Case III satisfies the sufficiency condition always since $\Delta_1 > 0$ and $\Delta_2 > 0$ for all $\underline{\lambda} \neq 0$.

For Case IV

$$\Delta_1 = \left(\frac{T}{m}\right)\frac{1}{\sqrt{\lambda_1{}^2 + \lambda_2{}^2 + \lambda_3{}^2}} \quad (- \lambda_1{}^2 - \lambda_2{}^2 - \lambda_3{}^2) \qquad (2.3.76)$$

$$\Delta_2 = \Delta_1\left(\frac{T}{m}\right)\frac{1}{\sqrt{\lambda_1{}^2 + \lambda_2{}^2 + \lambda_3{}^2}} \quad (-\lambda_1{}^2 - \lambda_2{}^2) \qquad (2.3.77)$$

Since $\Delta_1 < 0$ always for Case IV, it fails the sufficiency condition.

Inspection of Equations (2.3.66-68) reveals that $H_{u_2 u_2}$ must be positive. From Figure 1 it can be seen that $\cos u_i$ must be nonnegative. When Equations (2.3.54-55) are substituted into Equation (2.3.65), these requirements on $H_{u_2 u_2}$ and $\cos u_1$ rule out Case II. Therefore, Case III is the proper choice of signs. The control equations (2.3.54-55) and

(2.3.59-60) become

$$\sin u_1 = \frac{-\lambda_3}{\sqrt{\lambda_1{}^2 + \lambda_2{}^2 + \lambda_3{}^2}} \tag{2.3.78}$$

$$\cos u_1 = \frac{\sqrt{\lambda_1{}^2 + \lambda_2{}^2}}{\sqrt{\lambda_1{}^2 + \lambda_2{}^2 + \lambda_3{}^2}} \tag{2.3.79}$$

$$\sin u_2 = \frac{-\lambda_2}{\sqrt{\lambda_1{}^2 + \lambda_2{}^2}} \tag{2.3.80}$$

$$\cos u_2 = \frac{-\lambda_1}{\sqrt{\lambda_1{}^2 + \lambda_2{}^2}} \tag{2.3.81}$$

Returning to the Backward Sweep Method:

Step 3 is the integration of Equations (2.1.1-6), (2.2.25-30) and (2.3.24-29) [using Equations (2.1.7-9), (2.3.78-81), and (2.3.12-14)] backward using $\underline{x}(t_f)$ from Step 1 (or 6), $\underline{\lambda}(t_f)$ from Step 2, with $\underset{\sim}{S}(t_f)$, $\underset{\sim}{R}(t_f)$, and $\underset{\sim}{Q}(t_f)$ given below, where the partitioning in Equations (2.3.37-39) has been employed.

The various derivatives in Equation (2.3.12-14) for this TPBVP are from Equations (2.2.1) and (2.1.1-9)

$$\underline{f}_{\underline{x}} = \tag{2.3.82}$$

$$
\begin{bmatrix}
0 & 0 & 0 & \dfrac{3\mu x_4{}^2}{r^5} - \dfrac{\mu}{r^3} & \dfrac{3\mu x_4 x_5}{r^5} & \dfrac{3\mu x_4 x_6}{r^5} \\[3ex]
0 & 0 & 0 & \dfrac{3\mu x_5 x_4}{r^5} & \dfrac{3\mu x_5{}^2}{r^5} - \dfrac{\mu}{r^3} & \dfrac{3\mu x_5 x_6}{r^5} \\[3ex]
0 & 0 & 0 & \dfrac{3\mu x_6 x_4}{r^5} & \dfrac{3\mu x_6 x_5}{r^5} & \dfrac{3\mu x_6{}^2}{r^5} - \dfrac{\mu}{r^3} \\[3ex]
1 & 0 & 0 & 0 & 0 & 0 \\[2ex]
0 & 1 & 0 & 0 & 0 & 0 \\[2ex]
0 & 0 & 1 & 0 & 0 & 0
\end{bmatrix}
$$

$$
\underline{f}_{\underline{u}} = \frac{T}{m}
\begin{bmatrix}
-\sin u_1 \cos u_2 & -\cos u_1 \sin u_2 \\[1ex]
-\sin u_1 \sin u_2 & \cos u_1 \cos u_2 \\[1ex]
\cos u_1 & 0 \\[1ex]
0 & 0 \\[1ex]
0 & 0 \\[1ex]
0 & 0
\end{bmatrix}
\tag{2.3.83}
$$

From Equations (2.3.62), (2.3.65), (2.3.78-81), and (2.3.68)

$$
\underline{H}_{\underline{uu}} =
\begin{bmatrix}
\dfrac{T}{m}\sqrt{\lambda_1{}^2 + \lambda_2{}^2 + \lambda_3{}^2} & 0 \\[3ex]
0 & \dfrac{T}{m}\dfrac{\lambda_1{}^2 + \lambda_2{}^2}{\sqrt{\lambda_1{}^2 + \lambda_2{}^2 + \lambda_3{}^2}}
\end{bmatrix}
\tag{2.3.84}
$$

Since $H_{\underline{uu}}$ is diagonal,

$$H_{\underline{uu}}^{-1} = \begin{bmatrix} \dfrac{1}{\dfrac{T}{m}\sqrt{\lambda_1{}^2 + \lambda_2{}^2 + \lambda_3{}^2}} & 0 \\[4ex] 0 & \dfrac{\sqrt{\lambda_1{}^2 + \lambda_2{}^2 + \lambda_3{}^2}}{\dfrac{T}{m}(\lambda_1{}^2 + \lambda_2{}^2)} \end{bmatrix} \qquad (2.3.85)$$

From Equations (2.2.48-49)

$$H_{\underline{ux}} = H_{\underline{xu}}{}^T = \begin{bmatrix} 0 & 0 & 0 & 0 & 0 & 0 \\ 0 & 0 & 0 & 0 & 0 & 0 \end{bmatrix} \qquad (2.3.86)$$

From Equations (2.2.11), (2.2.25-30), and (2.1.7)

$$H_{\underline{xx}} = \begin{bmatrix} 0 & 0 & 0 & 0 & 0 & 0 \\ 0 & 0 & 0 & 0 & 0 & 0 \\ 0 & 0 & 0 & 0 & 0 & 0 \\ 0 & 0 & 0 & H_{x_4 x_4} & H_{x_4 x_5} & H_{x_4 x_6} \\ 0 & 0 & 0 & H_{x_5 x_4} & H_{x_5 x_5} & H_{x_5 x_6} \\ 0 & 0 & 0 & H_{x_6 x_4} & H_{x_6 x_5} & H_{x_6 x_6} \end{bmatrix} \qquad (2.3.87)$$

where

$$H_{x_4 x_4} = \frac{3\mu}{r^5}(3\,\lambda_1\,x_4 + \lambda_2\,x_5 + \lambda_3\,x_6) \qquad (2.3.88)$$

$$- \frac{15\mu}{r^7}\,x_4{}^2\,(\lambda_1\,x_4 + \lambda_2\,x_5 + \lambda_3\,x_6)$$

$$H_{x_4 x_5} = \frac{3\mu}{r^5}(\lambda_1\,x_4 + \lambda_2\,x_4) \qquad (2.3.89)$$

$$- \frac{15\mu}{r^7}\,x_4 x_5(\lambda_1\,x_4 + \lambda_2\,x_5 + \lambda_3\,x_6)$$

$$H_{x_4 x_6} = \frac{3\mu}{r^5} (\lambda_1 \, x_6 + \lambda_3 \, x_4) \tag{2.3.90}$$

$$- \frac{15\mu}{r^7} x_4 x_6 (\lambda_1 \, x_4 + \lambda_2 \, x_5 + \lambda_3 \, x_6)$$

$$H_{x_5 x_4} = H_{x_4 x_5} \tag{2.3.91}$$

$$H_{x_5 x_5} = \frac{3\mu}{r^5} (\lambda_1 \, x_4 + 3\lambda_2 \, x_5 + \lambda_3 \, x_6) \tag{2.3.92}$$

$$- \frac{15}{r^7} x_5{}^2 (\lambda_1 \, x_4 + \lambda_2 \, x_5 + \lambda_3 \, x_6)$$

$$H_{x_5 x_6} = \frac{3\mu}{r^5} (\lambda_2 \, x_6 + \lambda_3 \, x_5) \tag{2.3.93}$$

$$- \frac{15\mu}{r^7} x_5 x_6 (\lambda_1 \, x_4 + \lambda_2 \, x_5 + \lambda_3 \, x_6)$$

$$H_{x_6 x_4} = H_{x_4 x_6} \tag{2.3.94}$$

$$H_{x_6 x_5} = H_{x_5 x_6} \tag{2.3.95}$$

$$H_{x_6 x_6} = \frac{3\mu}{r^5} (\lambda_1 \, x_4 + \lambda_2 \, x_5 + 3 \, \lambda_3 \, x_6) \tag{2.3.96}$$

$$- \frac{15\mu}{r^7} x_6{}^2 (\lambda_1 \, x_4 + \lambda_2 \, x_5 + \lambda_3 \, x_6)$$

The terminal values $\underset{\sim}{S}(t_f)$, $\underset{\sim}{R}(t_f)$, and $\underset{\sim}{Q}(t_f)$ are determined as follows: From Equations (2.3.22), (2.3.30), and (2.2.24)

$$\underset{\sim}{S}(t_f) = \begin{bmatrix} 0 & 0 & 0 & 0 & 0 & 0 \\ 0 & 0 & 0 & 0 & 0 & 0 \\ 0 & 0 & 0 & 0 & 0 & 0 \\ 0 & 0 & 0 & 0 & 0 & 0 \\ 0 & 0 & 0 & 0 & 0 & 0 \\ 0 & 0 & 0 & 0 & 0 & 0 \end{bmatrix} \tag{2.3.97}$$

From Equations (2.3.31) and (2.2.17-22)

$$R(t_f) = \left(\frac{\partial \underline{\psi}}{\partial \underline{x}}\right)^T_{t=t_f} = I \quad [6 \times 6] \tag{2.3.98}$$

and from Equations (2.3.33), (2.2.37), and (2.1.1-9)

$$\underline{m}(t_f) = \left(\frac{\partial \Omega}{\partial \underline{x}}\right)^T_{t=t_f} = \left(\underline{\nu}^T \underline{f}_{\underline{x}}\right)^T_{t-t_f} = \left(\underline{f}_{\underline{x}}^T \underline{\nu}\right)_{t=t_f} \tag{2.3.99}$$

where $\underline{f}_{\underline{x}}$ is given by Equation (2.3.82), and therefore, from Equations (2.3.38), (2.3.97), and (2.3.98)

$$\underset{\sim}{R}(t_f) = \left[I \; \vdots \; \left(\underline{f}_{\underline{x}}^T \underline{\nu}\right)_{t=t_f} \right] \quad [7 \times 6] \tag{2.3.100}$$

From Equations (2.3.34) and (2.2.17-22)

$$\underline{n}(t_f) = \frac{d\underline{\psi}}{dt} \Big|_{t=t_f} = \left(\underline{\dot{x}} - \underline{\dot{x}}_M\right)_{t=t_f} \tag{2.3.101}$$

and from Equations (2.3.35) and (2.2.37)

$$\alpha(t_f) = \frac{d\Omega}{dt} \Big|_{t=t_f} = \left[\underline{\nu}^T \left(\underline{\ddot{x}} - \underline{\ddot{x}}_M\right)\right]_{t=t_f} \tag{2.3.102}$$

Therefore, from Equations (2.3.24), (2.3.32), (2.3.101-102)

$$\underset{\sim}{Q}(t_f) = \begin{bmatrix} 0 \; [6 \times 6] & \vdots & (\underline{\dot{x}} - \underline{\dot{x}}_M) \\ - - - - - - - & + & - - - - \\ (\underline{\dot{x}} - \underline{\dot{x}}_M)^T & \vdots & \underline{\nu}^T (\underline{\ddot{x}} - \underline{\ddot{x}}_M) \end{bmatrix}_{t=t_f} [7 \times 7] \tag{2.3.103}$$

where $\underline{\dot{x}}, \underline{\dot{x}}_M$ are given by Equations (2.1.1-9) and Equations (2.2.38-43) [and Equations (2.1.48) and (2.1.52)], and from Equations (2.1.1-9) $\underline{\ddot{x}}$ is

$$\ddot{x}_1 = -\frac{\mu \dot{x}_4}{r^3} + \frac{3\mu x_4}{r^5}(x_4 \dot{x}_4 + x_5 \dot{x}_5 + x_6 \dot{x}_6) \tag{2.3.104}$$

$$- \frac{T}{m}\left(\frac{-\beta}{m}\cos u_1 \cos u_2 + \sin u_1 \cos u_2 \dot{u}_1 + \cos u_1 \sin u_2 \dot{u}_2\right)$$

$$\ddot{x}_2 = -\frac{\mu \dot{x}_5}{r^3} + \frac{3\mu x_5}{r^5}(x_4 \dot{x}_4 + x_5 \dot{x}_5 + x_6 \dot{x}_6) \tag{2.3.105}$$

$$- \frac{T}{m}\left(\frac{-\beta}{m}\cos u_1 \sin u_2 + \sin u_1 \sin u_2 \dot{u}_1 - \cos u_1 \cos u_2 \dot{u}_2\right)$$

$$\ddot{x}_3 = \frac{-\mu \dot{x}_6}{r^3} + \frac{3\mu x_6}{r^5}(x_4 \dot{x}_4 + x_5 \dot{x}_5 + x_6 \dot{x}_6) \tag{2.3.106}$$

$$+ \frac{T}{m}\left(\frac{\beta}{m}\sin u_1 + \cos u_1 \dot{u}_1\right)$$

$$\ddot{x}_4 = \dot{x}_1 \tag{2.3.107}$$

$$\ddot{x}_5 = \dot{x}_2 \tag{2.3.108}$$

$$\ddot{x}_6 = \dot{x}_3 \tag{2.3.109}$$

To get $\dot{u}_1$, differentiate Equation (2.3.78):

$$\cos u_1 \dot{u}_1 = \left[-\sqrt{\lambda_1^2 + \lambda_2^2 + \lambda_3^2}\ \dot{\lambda}_3\right. \tag{2.3.110}$$

$$\left. + \frac{\lambda_3}{\sqrt{\lambda_1^2 + \lambda_2^2 + \lambda_3^2}}(\lambda_1 \dot{\lambda}_1 + \lambda_2 \dot{\lambda}_2 + \lambda_3 \dot{\lambda}_3)\right]$$

$$/ (\lambda_1^2 + \lambda_2^2 + \lambda_3^2)$$

Substituting Equations (2.3.79) and (2.2.25-57) in Equation (2.3.110) gives

$$\dot{u}_1 = \frac{\lambda_6}{\sqrt{\lambda_1^2 + \lambda_2^2}} - \frac{\lambda_3 (\lambda_1 \lambda_4 + \lambda_2 \lambda_5 + \lambda_3 \lambda_6)}{\sqrt{\lambda_1^2 + \lambda_2^2}\ (\lambda_1^2 + \lambda_2^2 + \lambda_3^2)} \tag{2.3.111}$$

To get $\dot{u}_2$, differentiate Equation (2.3.80):

$$\cos u_2 \; \dot{u}_2 = \left[- \sqrt{\lambda_1{}^2 + \lambda_2{}^2} \; \dot{\lambda}_2 + \frac{\lambda_2}{\sqrt{\lambda_1{}^2 + \lambda_2{}^2}} \; (\lambda_1 \; \dot{\lambda}_1 + \lambda_2 \; \dot{\lambda}_2)\right] \qquad (2.3.112)$$

$$/ \; (\lambda_1{}^2 + \lambda_2{}^2)$$

Substituting Equations (2.3.81) and (2.2.25-26) in Equation (2.3.112)

gives

$$\dot{u}_2 = \frac{- (\lambda_1{}^2 + \lambda_2{}^2)(-\lambda_5) + \lambda_2 \; (- \lambda_1 \; \lambda_4 - \lambda_2 \; \lambda_5)}{- \lambda_1 \; (\lambda_1{}^2 + \lambda_2{}^2)} = \frac{-\lambda_1 \; \lambda_5 + \lambda_2 \; \lambda_4}{\lambda_1{}^2 + \lambda_2{}^2}$$

$$\qquad (2.3.113)$$

From Equations (2.2.38-43) [and Equations (2.1.48) and (2.1.52)], $\dddot{x}_M(t_f)$ is

$$\ddot{x}_{M_1}(t_f) = a_M \left\{[\dot{E}_M(t_f)]^3 - \dddot{E}_M(t_f)\right\} \qquad (2.3.114)$$

$$\cdot \left[\cos \omega_M \sin E_M(t_f) + \sqrt{1-e_M{}^2} \; \sin \omega_M \cos E_M(t_f)\right]$$

$$- 3 \; a_M \; \dot{E}_M(t_f) \; \ddot{E}_M(t_f)$$

$$\cdot \left[\cos \omega_M \cos E_M(t_f) - \sqrt{1-e_M{}^2} \; \sin \omega_M \sin E_M(t_f)\right]$$

$$\ddot{x}_{M_2}(t_f) = a_M \left\{\dddot{E}_M(t_f) - [\dot{E}_M(t_f)]^3\right\} \cos i_M \qquad (2.3.115)$$

$$\cdot \left[- \sin \omega_M \sin E_M(t_f) + \sqrt{1-e_M{}^2} \; \cos \omega_M \cos E_M(t_f)\right]$$

$$- 3 \; a_M \; \ddot{E}_M(t_f) \; \dot{E}_M(t_f) \cos i_M$$

$$\cdot \left[\sin \omega_M \cos E_M(t_f) + \sqrt{1-e_M{}^2} \; \cos \omega_M \sin E_M(t_f)\right]$$

$$\ddot{x}_{M_3}(t_f) = a_M \left\{ \dddot{E}_M(t_f) - [\dot{E}_M(t_f)]^3 \right\} \sin i_M \qquad (2.3.116)$$

$$\cdot \left[-\sin \omega_M \sin E_M(t_f) + \sqrt{1-e_M^2} \cos \omega_M \cos E_M(t_f) \right]$$

$$- 3 a_M \ddot{E}_M(t_f) \dot{E}_M(t_f) \sin i_M$$

$$\cdot \left[\sin \omega_M \cos E_M(t_f) + \sqrt{1-e_M^2} \cos \omega_M \sin E_M(t_f) \right]$$

where from Equation (2.2.44)

$$\dddot{E}_M(t_f) = \Bigg([1-e_M \cos E_M(t_f)] \qquad (2.3.117)$$

$$\cdot \left\{ -e_M \cos E_M(t_f)[\dot{E}_M(t_f)]^3 - 2 e_M \sin E_M(t_f) \dot{E}_M(t_f) \ddot{E}_M(t_f) \right\}$$

$$+ e_M^2 [\sin E_M(t_f)]^2 [\dot{E}_M(t_f)]^3 \Bigg) \Big/ [1-e_M \cos E_M(t_f)]^2$$

$$= - \frac{e_M \cos E_M(t_f)[\dot{E}_M(t_f)]^3}{1-e_M \cos E_M(t_f)}$$

$$- \frac{2 e_M \sin E_M(t_f) \dot{E}_M(t_f) \ddot{E}_M(t_f)}{1-e_M \cos E_M(t_f)} + \frac{[\ddot{E}_M(t_f)]^2}{\dot{E}_M(t_f)}$$

$$= \ddot{E}_M(t_f) \cot E_M(t_f) \dot{E}_M(t_f) + 3 \frac{[\ddot{E}_M(t_f)]^2}{\dot{E}_M(t_f)}$$

Returning to the Backward Sweep Method, <u>Step 3</u>: The transformation
(2.3.43-45) is made at t_1, $t_o \leq t_1 < t_f$.

<u>Step 4</u> is self-explanatory.

<u>Step 5</u> is the forward integration of Equations (2.3.15-16) [using
Equations (2.3.12-14), (2.3.82-83) (2.3.85-96)] and Equations (2.1.1-6)
and (2.2.25-30) [using Equations (2.1.7-9) and (2.3.78-81)] from t_o to t_f,
where $\delta \underline{x}(t_o)$ and $\delta \underline{\lambda}(t_o)$ are from <u>Step 4</u>.

For Step 6, Equation (2.3.10) is used, where $\delta\underline{x}(t_f)$ is from Step 5, $\underline{\dot{x}}(t_f)$ is obtained from Equations (2.1.1-6) [with Equations (2.1.7-9)], and $d\underline{\nu}$ and dt_f are from Step 4.

Step 7 is self-explanatory.

2.4 SUFFICIENT CONDITIONS

Reference 17 contains the derivation of sufficient conditions for a weak minimum for the type of problem at hand. They are:

a) there exists a time t_1 such that $S_*(t)$ is finite for $\quad$ (2.4.1)

$\quad$ $t_o \leq t \leq t_1$ and $S(t)$ is finite for $t_1 \leq t \leq t_f$

b) $H_{uu}(t)$ is positive definite, $\quad$ $t_o \leq t \leq t_f$ $\qquad$ (2.4.2)

These conditions assume that $\underline{x}(t)$ and $\underline{u}(t)$ are continuous and unbounded, that $\underline{f}$, L, $\underline{\psi}$, and ϕ are twice continuously differentiable, and that the nontangency condition in the case of the EMRP.

$$\frac{d\underline{\psi}}{dt_f} \neq 0 \qquad (2.4.3)$$

is satisfied. The assumptions hold in the EMRP. Thus Equations (2.4.1-2) are sufficient conditions.

3. RESULTS OF THE NUMERICAL TRAJECTORY OPTIMIZATION

As in any research, especially when computer programming is involved, a fair measure of "trial and error" experience is necessary. Rather than trying to present the somewhat tedious incremental steps involved in developing a smoothly running, productive program, only the highlights of development and the final results will be presented.

In order to solve the EMRP by implementing the Backward Sweep Algorithm discussed in Subsection 2.3.3, a Fortran V computer program that incorporates a high fidelity integrator was written for use on the Jet Propulsion Laboratory's (JPL) Univac 1100/80 computer system. Double precision is used throughout the program. (A Univac word is 36 bits in length.) Segmenting or overlaying of major portions of the program is used to save core space. Thus, while the total number of words is 42,000, the maximum core used is 30,100 words. Some JPL program library routines, in addition to the integrator, are used, such as an input routine, routines that perform matrix inversion, matrix multiplication, and eigenvalue determination, and a routine that solves Kepler's equation.

In driving toward a solution of the EMRP, parameters of the different subroutines, such as the integrator error tolerance, the transformation time, t_1 , in Step 3, and the change rates and bounds of the Backward Sweep Algorithm ε convergence factor were varied. Also, some special techniques were employed to enhance the accuracy or speed of the program such as the grouping of equations, the writing of the gain file by the integrator, and the use of vector convergence criteria.

The final solution obtained for the EMRP, perhaps due to some of

the effort mentioned above, is shown to satisfy the terminal constraints, i.e., rendezvous with Mars, orders of magnitude better than the solutions of previous studies.

3.1 SPECIFICATION OF PROGRAM PARAMETERS AND TECHNIQUES EMPLOYED IN THE OPTIMIZATION

The specification of the various parameters of the problem and the techniques employed in the optimization can have an important bearing on the accuracy of the results, the speed of convergence, and indeed even the apparent existence of a sensible solution.

3.1.1 The DODE Integrator

The selection of an integrator may have been the most important decision in composing the program to solve the EMRP program. The one chosen, DODE, (an abbreviation for Double precision Ordinary Differential Equations), has been found to be of high quality and accuracy and to possess many useful special features. DODE was written by Fred Krogh[18-20] of JPL in 1975 and is used extensively in JPL's spacecraft and celestial body orbit determination and trajectory propagation software systems.

DODE is a variable order, variable step-size Adams method integrator using modified divided differences to change the step sizes and generalized to accommodate higher order differential equations. An important distinction is that when the step size is changed, the interpolating polynomial passes through the actual past derivative values instead of through coefficients of a representative polynominal of past derivative values.

The many special features of DODE include the ability to handle output and derivative subroutines written by the user, both incremental and specified output calls, restart capability, the saving of the solution

on a file, complete diagnostics, debug output, stepsize control, user-defined error control, equation grouping for a multi-stage corrector, and function zero finding. The features named were used in the EMRP program and, after a period of initiation on the part of the user, were found to enable a precise solution of the problem in a relatively straightforward fashion.

3.1.1.1 Relative Error Tolerance for Each Equation, Step Size

The coupled nature of the state equations (2.2.1) and the Euler-Lagrange equations (2.2.11-12, 2.2.16) requires that the integration be done precisely. Otherwise even small errors in an early integration step can cause the computed trajectory to be grossly inaccurate. Moreover, the integration of the $\dot{\underset{\sim}{S}}$, $\dot{\underset{\sim}{R}}$, and $\dot{\underset{\sim}{Q}}$ equations (2.3.24-29) produces $\underset{\sim}{S}$, $\underset{\sim}{R}$, and $\underset{\sim}{Q}$ components which vary by several orders of magnitude.

At first, a blanket absolute error tolerance of 10^{-7} was tried for all equations. This and other uniformly applied absolute error tolerances did not work. Because of the disparate magnitudes of the various $\underset{\sim}{S}$, $\underset{\sim}{R}$, and $\underset{\sim}{Q}$ components, it was decided to assign a separate error tolerance for each equation. (The EMRP state (2.1.1-6) and Lagrange multiplier (2.2.25-30) equations retain an absolute error tolerance of 10^{-10}.) Also, because of the growth by orders of magnitude in the $\underset{\sim}{S}$, $\underset{\sim}{R}$, and $\underset{\sim}{Q}$ components, a relative error tolerance was chosen. In addition, the transformation (2.3.43-45) in Step 3 necessitates a resetting of the relative error tolerances of the $\underset{\sim*}{S}$, $\underset{\sim*}{R}$ and $\underset{\sim*}{Q}$ components at time t_1, when the integration is restarted.

The relative error tolerance is defined by two parts – the base tolerance and the relative error factor. The relative error factor is determined by the user's setting it equal to the maximum absolute change of the integrated variable in a single step over the first few steps. The base tolerance was chosen to be 10^{-6}. The local error tolerance used is then equal to the product of the base tolerance and the relative error factor. The actual error maintained by the integrator is a tenth of this product.

The relative error factor is set equal to the following expression at each integration step:

$$\max \; \{f_e \; , \; |h| \sum_{j = \hat{I}_k}^{I_k} |F(j)|/(I_k - \hat{I}_k + 1)\} \cdot \rho_{(|L_K| - 1)} \qquad (3.1.1)$$

where f_e = the current relative error factor

h = stepsize

$\hat{I}_k, I_k$ = lowest and highest equation numbers of
  each group (here $\hat{I}_k = I_k$)

$F(j)$ = derivative of jth equation

$\rho_1 = 1 \quad (L_k = -2)$

$\rho_2 = 15/16 \; (L_k = -3)$

L_k was chosen to be -3 for the $\dot{\underset{\sim}{S}}$, $\dot{\underset{\sim}{R}}$, and $\dot{\underset{\sim}{Q}}$ component equations for the backward integration from t_f to t_1 . However, for the restarted integration from t_1 to t_o , the last row of $\underset{\sim}{Q}_*$ requires that L_k be set equal to -2. These 7 equations are relatively stiff and thus necessitate the less constricting error tolerance.

The forward integration error tolerances are specified in a similar manner. The EMRP state (2.1.1-6) and Lagrange multiplier (2.2.25-30) equations use a blanket absolute error tolerance of 10^{-10}. The state perturbation (2.3.15) and Lagrange multiplier perturbation (2.3.16) equations have relative error tolerances for each equation. Again, the base error tolerance was chosen to be 10^{-6} and L_k to be -3.

Step size limits, which are related to error tolerances, were specified. A maximum step size of 2 days was specified to ensure a reasonable density of data points, especially for those quantitites not integrated by the integrator. A minimum step size of 10^{-4} days was specified in conjunction with the error tolerances to preclude prohibitive costs, especially during the program development stage. The integrator stops if the required step size (to meet error tolerances) is less than the minimum. Step size for the integration of a converged optimal solution (of $\dot{x}$ and $\dot{\lambda}$ only) is shown in Figure 3.

3.1.1.2 Multi-Stage Corrector Equation Groups

Because the right-hand sides of the EMRP Lagrange multiplier equations (2.2.25-30) are functions of the state determined by integration of the state equations (2.1.1-6), and the right-hand sides of the $\dot{S}$, $\dot{R}$, and $\dot{Q}$ equations (2.3.24-29) are functions of both the state and Lagrange multipliers, a simple prediction-correction integration of all the equations is not as accurate for a given step as a more elaborate integration where the three groups of equations are corrected in sequence.
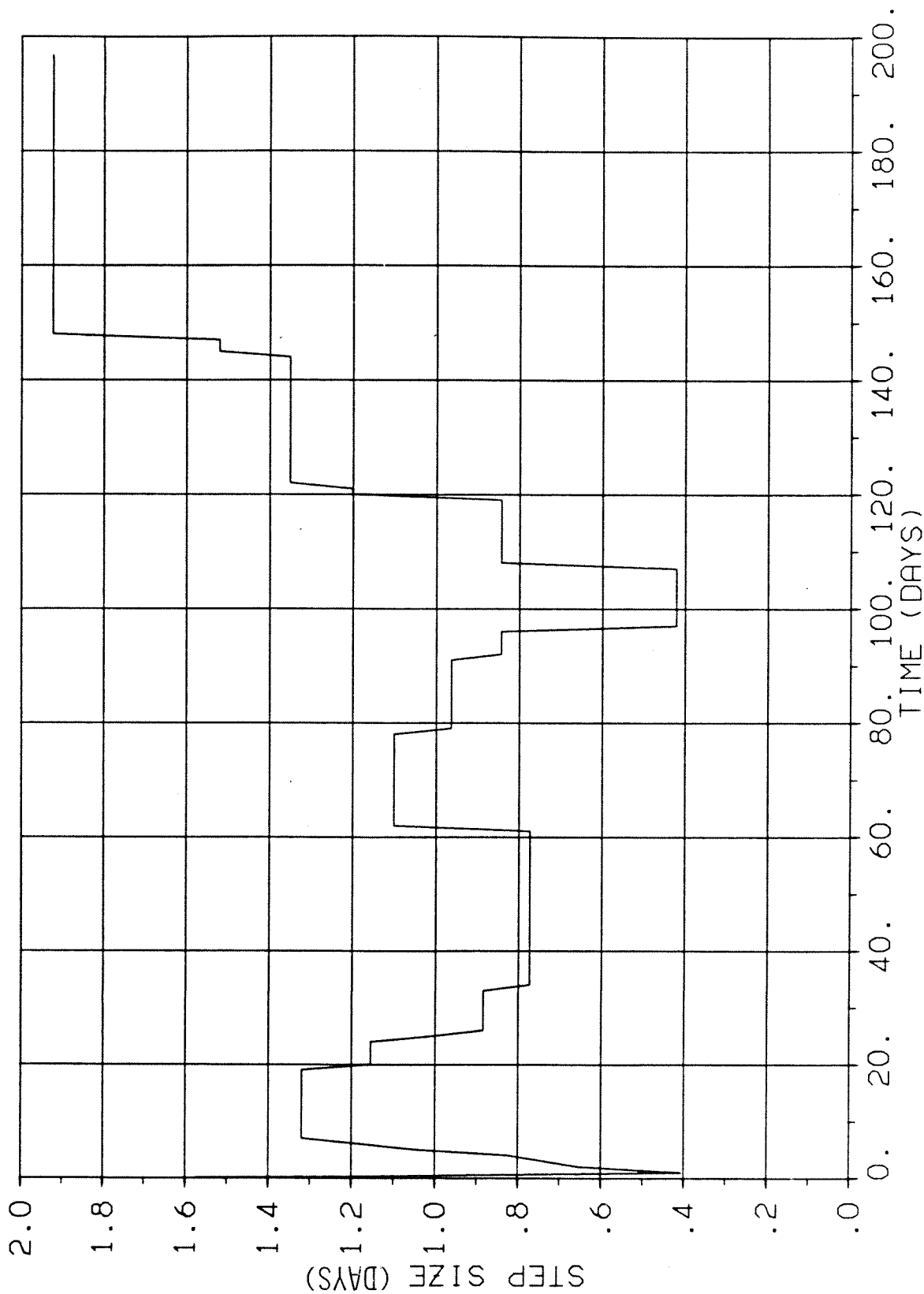
FIGURE 3. STEP SIZE FOR THE INTEGRATION OF A CONVERGED NOMINAL SOLUTION

Therefore, the equation grouping capability of DODE for a multi-stage

corrector step was employed.

For the backward integration, the state equations were placed in

the first group, the Lagrange multiplier equations in the second, and

the $\dot{S}$, $\dot{R}$, and $\dot{Q}$ equations in the third. Thus, predicted derivatives

for the Lagrange multipliers were computed only after the corrected

values of the state were obtained, and predicted derivatives for the

$\dot{S}$, $\dot{R}$, and $\dot{Q}$ equations were computed only after the corrected values

of the Lagrange multipliers (and, therefore, the state) were obtained.

A similar grouping was employed for the forward integration. Again,

the state equations were placed in the first group and the Lagrange

multipliers were placed in the second group. The state perturbation

(2.3.15) and the Lagrange multiplier perturbation (2.3.16) equations were

placed in the third group.

3.1.1.3 Gain File

The purpose of computing the solution of the nominal trajectory is

to provide information for a guidance scheme. The guidance schemes require

such data as the state, the state derivatives, and the gain matrix as

functions of time. One way of providing these data to the guidance schemes

is, when the final solution is obtained, to write these data on a file

(or cards) and interpolate between data points in the guidance scheme.

However, since the DODE integrator has a high-order interpolation capa-

bility, an alternative, more accurate method for providing these data to

the guidance scheme is to write the file for the integrator's interpolator,

and then to interpolate from this file in the guidance scheme with the integrator.

The DODE integrator has the capability to make a call to write an increment of a solution file. When a solution file is written, the integrated values, the derivatives, the difference tables, and other integrator parameters are written at intervals determined by the integrator. In the guidance scheme, the required data is obtained by calling the integrator to interpolate from the nominal trajectory solution file it has previously "written." The main drawback to this approach is that the gain matrix (to be discussed in Subsection 4.2.1) is not integrated but is a function of $\underline{x}, \underline{\lambda}$, and $\underset{\sim}{S}_*$. Moreover, $\underset{\sim}{S}_*$ is not computed for $t_f \geq t \geq t_1$ and is a function of $\underset{\sim}{S}$, $\underset{\sim}{R}$, and $\underset{\sim}{Q}$. Therefore, since the gain matrix is not computed by the integrator, it can't be interpolated by the integrator. Thus, the gain must be computed in the guidance scheme from interpolated values of $\underset{\sim}{S}_*$, $\underline{x}$, and $\underline{\lambda}$. $\underset{\sim}{S}_*$ itself must be computed from $\underset{\sim}{S}$, $\underset{\sim}{R}$, and $\underset{\sim}{Q}$ for $t_f \geq t > t_i$. Consequently, information from the integrator related to $\underline{x}$, $\underline{\lambda}$, $\underset{\sim}{S}$, $\underset{\sim}{R}$ and $\underset{\sim}{Q}$ is written on the solution file from t_f to t_1 and information related to $\underline{x}$, $\underline{\lambda}$, and $\underset{\sim}{S}_*$ is written from t_1 to t_o. This drawback and the complexity of using the integrator's interpolation feature, nevertheless, are more than compensated for by the improved precision of interpolation. (See also Sub-subsection 4.2.2.4.) The size of the gain file written is about 75,000 words.

3.1.1.4 Optimization Intermediate Plot File

For plotting purposes (see Subsection 5.2.1) two other features of the DODE integrator were used. The integrator output interval was set not only for printed output but for an intermediate plot file containing state and control related data. Output could also be generated at a set of discrete times, to be printed and plotted.

The output to the intermediate plot file consisted of t, $\underline{u}$, $\underline{x}$, $\underline{x}_M$, $\underline{\psi}$, $|\underline{\psi}_{1-3}|$, $|\underline{\psi}_{4-6}|$, and stepsize. These variables as functions of time can then be transferred directly to a final plot file or differenced with their counterparts from the guidance intermediate plot files to be discussed later.

3.1.2 Choice of t_1

From Section 2.4, the choice of t_1, the time of transformation (2.3.43-45), is not rigidly specified. It should be far enough from t_f such that $\underline{S}_*$ is well behaved but not so far that $\underline{S}$ does not exist or is poorly behaved. Stoker[3] claims that $t_1 \approx 126$ days is best. This choice seems suitable and is the one used. Other values of t_1 may affect the results and merit further investigation.

3.1.3 Convergence Behavior

The Backward Sweep Algorithm, as applied to the EMRP described in Subsection 2.3.3, requires a method for choosing the convergence factor, ε, in Step 4. Also, in Step 1 a philosophy of letting

$$\underline{x}(t_f) = \underline{x}_M(t_f) \tag{3.1.2}$$

instead of actually guessing $\underline{x}(t_f)$ can affect the convergence.

3.1.3.1 ε Change Bounds

Step 4 mentions only that $0<\varepsilon\leq1$. In Reference 16 it is suggested

that ε start out small, and then be increased towards 1 as the solution

converges. It is further suggested that if actual changes and desired

changes in $\underline{x}(t_o)$, ψ , and Ω differ by more than 10% to 20%, ε should

be reduced and the iteration repeated. Otherwise the algorithm may not

converge.

The simplest way of doing this is to manually check the changes after

each iteration and input a new ε . The less tedious method actually

implemented was to input two tolerances and two multiplicative factors

and to adjust ε automatically after each iteration. If the differences

between the actual change and the desired change in one of the components

of $\underline{x}(t_o)$, ψ, or Ω was more than the maximum tolerance, ε was reduced

by the first multiplicative factor. Conversely, if all the difference

were less than the minimum tolerance, ε was increased by the second

multiplicative factor to at most unity. When all the differences were

within both tolerances ε was left unchanged. The tolerances normally

used were .20 and .05, and the multiplicative factors were .5 and 2

respectively.

For initial convergence, the solutions from References 1-3 were used

for the guess in Step 1 (see Subsection 3.2.1). Since these solutions are

close to the optimal solution, an initial value of unity for ε was

input into the program. For this case, then, the above ε adjustment

technique left ε unchanged. However, in further testing of the program,

a less accurate guess was made with a low initial value of ε , and the

adjustment technique was utilized.

3.1.3.2 Vector Criteria, Accuracy Required

Since the orbits of Earth and Mars are nearly coplanar, the expected

optimal trajectory should not deviate substantially from either of these

planes. Hence, out-of-plane components of $\underline{x}(t_o)$ and $\underline{\psi}$ should be

small relative to in-plane components. Also, because a Cartesian

coordinate system is used, the in-plane components can be different in

magnitude. These imbalances can delay convergence or even produce

divergence. This can happen because the ε adjustment technique treats

all components with equal weight. Thus linearity errors or integration

errors in the small components denigrate the convergence.

The ε adjustment technique was modified to alleviate this difficulty.

Instead of comparing differences between actual and desired changes in

components of $\underline{x}(t_o)$ and $\underline{\psi}$ to the desired changes in the respective

components, vectors of velocity and position differences were compared to

the respective vectors of desired change. This is illustrated below.

By components:

If
$$\left| \frac{\delta x_i^A (t_o) - \delta x_i^D (t_o)}{\delta x_i^D (t_o)} \right| > \varepsilon_{T_1}$$

or
$$\left| \frac{d\psi_i^A [\underline{x}(t_f), t_f] - d\psi_i^D [\underline{x}(t_f), t_f]}{d\psi_i^D [\underline{x}(t_f), t_f]} \right| > \varepsilon_{T_1}$$

or $\left| \dfrac{d\Omega^A - d\Omega^D}{d\Omega^D} \right| > \varepsilon_{T_1}$

for any i, i = 1, 2, ..., 6   (3.1.3)

then $\varepsilon_{new} = \varepsilon_{T_3} \cdot \varepsilon_{OLD}$ (3.1.4)

If <u>all</u> of the above quotients $\leq \varepsilon_{T_2}$ (3.1.5)

then $\varepsilon_{new} = \varepsilon_{T_4} \cdot \varepsilon_{OLD}$ (3.1.6)

where

$(\quad)^A$ = actual value

$(\quad)^D$ = desired value

ε_{T_1} = maximum tolerance for ε

ε_{T_2} = maximum tolerance for ε

ε_{T_3} = multiplicative reduction factor for ε

ε_{T_4} = multiplicative increase factor for ε

<u>By vectors</u>:

If $\dfrac{\sqrt{\sum\limits_{i=1}^{3} [\delta x_{i+j}^{A}(t_o) - \delta x_{i+j}^{D}(t_o)]^2}}{\sqrt{\sum\limits_{i=1}^{3} [\delta x_{i+j}^{D}(t_o)]^2}} > \varepsilon_{T_1}$

or $\dfrac{\sqrt{\sum\limits_{i=1}^{3} \{d\psi_{i+j}^{A}[\underline{x}(t_f),t_f] - d\psi_{i+j}^{D}[\underline{x}(t_f),t_f]\}^2}}{\sqrt{\sum\limits_{i=1}^{3} \{d\psi_{i+j}^{D}[\underline{x}(t_f),t_f]\}^2}} > \varepsilon_{T_1}$

or $\quad \left| \dfrac{d\Omega^A - d\Omega^D}{d\Omega^D} \right| > \varepsilon_{T_1}$

for $\quad j = 0$ or 3 $\hfill (3.1.7)$

then $\varepsilon_{new} = \varepsilon_{T_3} \cdot \varepsilon_{OLD}$ $\hfill (3.1.8)$

If __all__ of the above quotients are $e \leq \varepsilon_{T_2}$ $\hfill (3.1.9)$

then $\varepsilon_{new} = \varepsilon_{T_4} \cdot \varepsilon_{OLD}$ $\hfill (3.1.10)$

The vector method was the one adopted; however, the component method capability has been retained in the software.

The convergence accuracy can be specified by input. This accuracy specification implies the following:

$$\left| \frac{x_i(t_o) - x_{o_i}}{\sqrt{\sum\limits_{j=1}^{3} x_{o_{j+k}}^2}} \right| < a$$

$$\left| \frac{\psi_i [\underline{x}(t_f), t_f]}{\sqrt{\sum\limits_{j=1}^{3} x_{M_{j+k}}^2 (t_f)}} \right| = \left| \frac{x_i(t_f) - x_{M_i}(t_f)}{\sqrt{\sum\limits_{j=1}^{3} x_{M_{j+k}}^2 (t_f)}} \right| < a$$

$$\left. \begin{aligned} \end{aligned} \right\} \quad i = 1, 2, \ldots, 6$$

$$k = \begin{cases} 0 \;, & i \leq 3 \\ 3 \;, & i \geq 4 \end{cases} \qquad (3.1.11)$$

$$|\Omega| < a$$

where

$\quad \underline{x}(t_o) = $ computed initial state

$\quad \underline{x}_o \quad = $ given initial state[Eqs. (2.1.10-15)]

$\quad a \quad = $ specified accuracy

$\underline{\psi}[\underline{x}(t_f), t_f]$ = terminal constraint [Eqs.(2.2.17-22)]

$\underline{x}(t_f)$ = computed final state

$\underline{x}_M(t_f)$ = Mars state at final time

Ω = as defined in Eq. (2.2.37)

The level of accuracy chosen was 10^{-9}, which corresponds to .15 kilometers in position and 2.6 m/day in velocity for $\underline{x}(t_o)$. The actual accuracy obtained was somewhat better than 10^{-9}.

3.1.3.3 Initial $\underline{x}(t_f)$ - To Match Mars' State or Guess?

For the reasons discussed in Sub-subsection 3.1.3.2, if the state of Mars at t_f, $\underline{x}_M(t_f)$, is used as the guess for $\underline{x}(t_f)$ in Step 1 (i.e., a perfect guess), the second set of quotients in both Equation 3.1.3 and Equation 3.1.7 are liable to be greater than the maximum tolerance. Here the use of vectors does not work, unless one were to consider some sort of "combination of the vectors." Alternatively, if $d\underline{\psi}^D[\underline{x}(t_f), t_f]$ were below some threshold, the second set of checks in Equation 3.1.7 could be omitted. This "perfect guess" problem has not been corrected in the program, but is mitigated by guessing $\underline{x}(t_f)$ (hopefully to be other than $\underline{x}_M(t_f)$) or by specifying a factor not equal to unity with which to multiply $\underline{x}_M(t_f)$.

For reoptimization of a perturbed trajectory (see Sub-subsection 4.1.2.1), the nominal solution, except for the perturbed component(s) of $\underline{x}_o$, is used as the initial guess. Therefore, in addition to the problem just mentioned, a similar impediment to convergence arises in the non-perturbed components of $\underline{x}_o$. The entire situation is mitigated in these reoptimizations by suppressing the entire ε adjustment technique by setting the maximum tolerance at a very high level.

3.2 THE OPTIMAL TRAJECTORY

The Backward Sweep Algorithm requires guessing t_f, $\underline{x}(t_f)$, and $\underline{\nu}$ in Step 1. Rather than actually guessing these values at random, $\underline{x}(t_f)$ and $\underline{\nu}$ were obtained by integrating the values of $\underline{x}_o$ and $\underline{\lambda}(t_o)$ given by Hart[1] (and Lattimore[2] and Stoker[3]) to t_f (also given by Hart[1] and Lattimore[2]) and using Equations (2.2.31-36). The solutions given by References 1-3 presumably are close to the optimal solution. These earlier solutions are presented below and compared with the current solution.

3.2.1 The Solution

The initial conditions (2.1.10-16) are given, and $\underline{x}_o$ and t_o are the same as those of References 1-3. The initial conditions together with the converged values of $\underline{\lambda}(t_o)$ and t_f determined by the program uniquely define the solution and are presented in Table 1. The computed initial state $\underline{x}(t_o)$ lies well within the space defined by the convergence accuracy, 10^{-9} in each component, and so is the same as $\underline{x}_o$ to the 8 significant figures shown in Table 1.

Another way of describing the solution is with a time history of the state, $\underline{x}(t)$, and the control, $\underline{u}(t)$, which are shown in Figures 4 and 5.

The final state, $\underline{x}(t_f)$, and Lagrange multipliers, $\underline{\lambda}(t_f)$, and the final time, t_f, are presented in Table 2 along with the terminal error, $\underline{\psi}[\underline{x}(t_f),t_f]$. As expected, the terminal constraint components are nearly zero, and $\underline{x}_M(t_f)$ equals $\underline{x}(t_f)$ to the digits shown. Recall from Equations (2.2.31-36) that the Lagrange multipliers at the final time correspond to the constants, $\underline{\nu}$, that are guessed in Step 1. The accuracy comparison quotients in Equation (3.1.11) are given in Table 3 and reflect normalizing with the appropriate position or velocity vector

TABLE 1. NOMINAL SOLUTION $(\underline{x}_o, \underline{\lambda}(t_o), t_f)$, CURRENT AND PREVIOUS RESULTS

CURRENT			HART[1], LATTIMORE[2], STOKER[3]	
x_{o_1}	$= -.14835073 - 1$	AU/day	$-.14835073 - 1$	AU/day
x_{o_2}	$= .92714508 - 2$	AU/day	$.92714508 - 2$	AU/day
x_{o_3}	$= 0$	AU/day	0	AU/day
x_{o_4}	$= .5199345 + 0$	AU	$.5199345 + 0$	AU
x_{o_5}	$= .83463802 + 0$	AU	$.83463802 + 0$	AU
x_{o_6}	$= 0$	AU	0	AU
$\lambda_1(t_o) =$	$.10054113 + 2$		$.10068717029 + 2$	
$\lambda_2(t_o) =$	$-.21274357 + 2$		$-.21350450338 + 2$	
$\lambda_3(t_o) =$	$-.66937814 + 0$		$-.67014133502 + 0$	
$\lambda_4(t_o) =$	$-.51348615 - 1$		$-.51681265185 - 1$	
$\lambda_5(t_o) =$	$-.43117069 + 0$		$-.43276807729 + 0$	
$\lambda_6(t_o) =$	$-.13308119 - 2$		$-.13232925942 - 2$	
t_f	$= 196.75020696$	days	196.76594763	days

FIGURE 5. TIME HISTORY OF THE STATE, NOMINAL TRAJECTORY

58
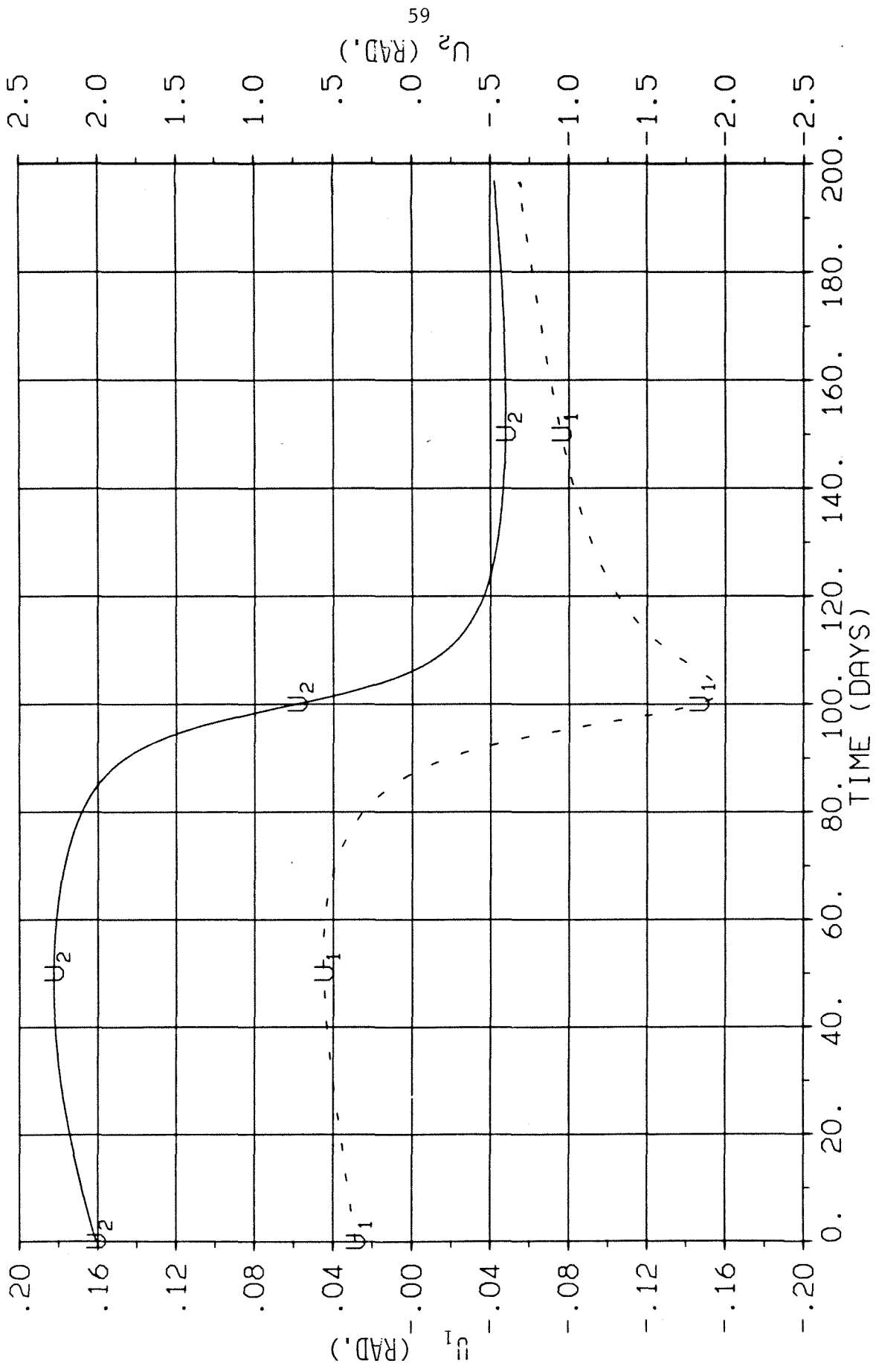
FIGURE 4. TIME HISTORY OF THE STATE, NOMINAL TRAJECTORY

TABLE 2. FINAL STATE, LAGRANGE MULTIPLIERS, AND TIME AND TERMINAL ERROR,
NOMINAL TRAJECTORY

$x_1(t_f) = .54495701 - 2$ AU/day

$x_2(t_f) = -.12987735 - 1$ AU/day

$x_3(t_f) = .41948104 - 3$ AU/day

$x_4(t_f) = -.14378744 + 1$ AU/

$x_5(t_f) = -.45118278 + 0$ AU

$x_6(t_f) = -.14572411 - 1$ AU

$\psi_1[\underline{x}(t_f), t_f] = .36 - 13$ AU/day

$\psi_2[\underline{x}(t_f), t_f] = -.11 - 12$ AU/day

$\psi_3[\underline{x}(t_f), t_f] = -.12 - 13$ AU/day

$\psi_4[\underline{x}(t_f), t_f] = -.24 - 10$ AU

$\psi_5[\underline{x}(t_f), t_f] = -.61 - 11$ AU

$\psi_6[\underline{x}(t_f), t_f] = -.16 - 11$ AU

$\lambda_1(t_f) = .10054113 + 2$

$\lambda_2(t_f) = -.21274358 + 2$

$\lambda_3(t_f) = -.66937814 + 0$

$\lambda_4(t_f) = -.51348615 - 1$

$\lambda_5(t_f) = -.43117069 + 0$

$\lambda_6(t_f) = -.13308119 - 2$

$t_f = 196.750206956$ days

TABLE 3. CONVERGENCE ACCURACY OBTAINED IN OPTIMIZATION OF
NOMINAL TRAJECTORY

i	k	$\left\lvert \dfrac{x_i(t_o) - x_{o_i}}{\sqrt{\sum\limits_{j=1}^{3} x_{o_{j+k}}^2}} \right\rvert$	$\left\lvert \dfrac{x_i(t_f) - x_{M_i}(t_f)}{\sqrt{\sum\limits_{j=1}^{3} x_{M_{j+k}}^2(t_f)}} \right\rvert$
1	0	.39–10	.25–11
2	0	.13–9	.78–11
3	0	.92–11	.86–12
4	3	.32–9	.16–10
5	3	.26–10	.41–11
6	3	.91–11	.11–11

$$|\Omega| = .12\text{–}10$$

magnitude. The various constants that describe the EMRP model are the same as those of Hart[1] and are repeated in Table 4.

3.2.2 Comparison of the Solution with Those of Hart, Lattimore, and Stoker

Stoker mentions in Reference 3 that his solution "agrees to within 1%" with that of Hart[1]; yet his published values of $\underline{\lambda}(t_o)$, together with the given $\underline{x}_o$ and t_f from the solution, are identical to those of Hart (and Lattimore[2]). Stoker implies that there were significant differences (about 1%) in the solution, but nevertheless fails to show them. Stoker does not present the final time, t_f, so perhaps a different final time accounts for the solution differences. The solutions of Stoker, Hart, and Lattimore are presented in Table 1. Since they are identical, except that Stoker carried the Lagrange multipliers, $\underline{\lambda}(t_o)$, to only seven digits and omitted the final time, there is but one presentation.

In comparing the previous solutions with the current solution in Table 1 it can be seen that the current final time, t_f, is slightly less, by .0157 days or about 23 minutes or .008%. Also, the current components of $\underline{\lambda}(t_o)$ agree "to within 1%" with those of the previous solutions.

If the previous solution given in Table 1 is integrated forward to t_f and compared with the state of Mars given by Equations (2.1.45-52), the resulting terminal error is 690 km/day (8 m/sec) in velocity and 75,000 km in position, as shown in Table 5. In contrast, the terminal errors for the current solution are less than 2×10^{-5} km/day in velocity and .004 km in position. Since the actual terminal errors are not

TABLE 4. CONSTANTS OF THE EMRP MODEL

EARTH ORBITAL DATA

Semi-major axis, a_E	1.0 AU
Eccentricity, e_E	0.016726
Argument of perihelion, ω_E	0.0°
Angle of inclination, i_E	0.0°
Argument of ascending node, Ω_E	0.0°
Time of perihelion	Jan 3.022307069, 1950
Period	365.198084 days

MARS ORBITAL DATA

Semi-major axis, a_M	1.523691 AU
Eccentricity, e_M	0.093393
Argument of perihelion, ω_M	286.07366°
Angle of inclination, i_m	1.84991°
Argument of ascending node, Ω_M	0.0°
Time of perihelion	March 17.490627, 1950
Period	686.868886 days
Eccentric anomaly at t_o, E_o	178.995341°

OTHER CONSTANTS

Mass flow rate, β	0.00108 m_o/day
Initial spacecraft mass, m_o	1.0
Exhaust velocity, v_{ex}	0.045365 AU/day
Solar gravitational constant, μ	$2.96007536 \times 10^{-4}$ AU^3/day^2

TABLE 5. HART AND STOKER SOLUTION INTEGRATED FORWARD TO t_f

$x_1(t_f) =$ .54470947-2 AU/day $x_{M_1}(t_f) =$ .54515274-2 AU/day

$x_2(t_f) =$ -.12988510-1 AU/day $x_{M_2}(t_f) =$ -.12987121-1 AU/day

$x_3(t_f) =$ -.41953188-3 AU/day $x_{M_3}(t_f) =$ -.41946120-3 AU/day

$x_4(t_f) =$ -.14379830+1 AU $x_{M_4}(t_f) =$ -.14377887+1 AU

$x_5(t_f) =$ -.45092430+0 AU $x_{M_5}(t_f) =$ -.45138721+0 AU

$x_6(t_f) =$ -.14564962-1 AU $x_{M_6}(t_f) =$ -.14579014-1 AU

$\psi_1[\underline{x}(t_f),t_f] =$ -.44-5 AU/day = -.66+3 km/day

$\psi_2[\underline{x}(t_f),t_f] =$ -.14-5 AU/day = -.21+3 km/day

$\psi_3[\underline{x}(t_f),t_f] =$ -.71-7 AU/day = -.11+2 km/day

$\psi_4[\underline{x}(t_f),t_f] =$ -.19-3 AU = -.29+5 km

$\psi_5[\underline{x}(t_f),t_f] =$ .46-3 AU = .69+5 km

$\psi_6[\underline{x}(t_f),t_f] =$ .14-4 AU = .21+4 km

$t_f = 196.76594763$ days

stated in the previous studies, but are instead computed here as mentioned, the comparison is possibly unfair in that the constants published in the earlier studies may have been truncated versions of those actually used. Another possible source of these large computed errors may lie in the fact that a different integrator and a different routine for solving Kepler's equation were, of course, used in the other studies, obscuring the possibility that the earlier studies themselves, in fact, computed a much smaller terminal error.

A subsequent "coarse" backward integration from the Table 5 value of t_f to t_o of $\dot{\underline{x}}$ from the $\underline{x}(t_f)$ in Table 5 and of the corresponding multipliers was made to check the accuracy of the forward integration. The vector difference of $\underline{x}(t_o)$ before and after the two integrations was .023 km/day in velocity and 12 km in position — a level well below the apparent terminal error given in Table 5. A "coarse" integration here means that only the 11 most significant digits (out of a possible 18) of $\underline{x}(t_f)$, $\underline{\lambda}(t_f)$, and t_f were input to the integration.

4. PERTURBATION GUIDANCE SCHEMES

In preflight mission analysis, the need for a trajectory perturbed slightly off of the nominal trajectory often arises. Such studies as launch window duration determination, launch vehicle injection error tolerance definition, operational and payload margin planning, and navigation covariance analysis may be simplified by and be made less expensive through the use of trajectories derived using linear perturbation guidance techniques. Rather than finding a field of optimal trajectories by using the complex and expensive BSA, perturbation guidance schemes may be invoked with a substantial savings in computer time, since only one nominal trajectory need be computed with the BSA, while the remainder are found with the much simpler perturbation guidance scheme.

For autonomous low-thrust spacecraft navigation and guidance systems, perturbation guidance schemes may be a key element of feasibility in that the relatively modest computational demands of the schemes may enable the use of existing flight-qualified data processing equipment. The nominal trajectory and feedback gains could be loaded on-board prior to launch or uplinked at infrequent intervals.

The above motivations give rise to the search for a perturbation guidance scheme of simplicity and brevity, yet at the same time, acceptable performance. This chapter describes the concepts of perturbation guidance and time indexing, discusses the rationale behind the various proposed schemes, and details the enhancements made here to the schemes to improve performance.

4.1 THE GUIDANCE PROBLEM

The guidance problem may be loosely defined as the determination of how to get from the current state (in general not on the nominal trajectory) to the target state (in general not constant and, therefore, also not on the nominal trajectory for a non-nominal current state) while satisfying certain constraints and perhaps optimizing some criterion. Since the current state is in general not on the nominal trajectory, the concept of a perturbation, a small offset, arises. In a free final time problem, the final time on the perturbed trajectory will not be, in general, the same as the nominal final time. (In our problem, this time difference also implies that the target states will be different.) Thus, the idea of "indexing" the guidance gains also arises.

The various procedures for solving the guidance problem run the gamut from no guidance--the use of nominal control--through current time linear guidance (no indexing) to linear guidance with indexing, such as Time-to-Go[21] Guidance and Minimum Distance[22] Guidance. Reoptimization is the most accurate form of guidance in that the guidance problem is completely resolved from scratch as if it were a new problem.

4.1.1 The Concepts of Perturbation and Indexing

In the course of a flight, perturbations from the nominal trajectory spring from launch delays, insertion errors, thrust system mismodeling, venting, mismodeled solar pressure, planetary ephemeris refinements, and other sources. While the example problem examined in this study assumes freedom from errors continuous in time such as mismodeling, the "discrete" error types--launch delays, insertion errors, and perhaps venting--cause

well-defined, almost impulsive perturbations in the state that are not
continuous in time and are therefore readily amenable to linear perturba-
tion guidance. Other errors similar to the abovementioned discrete errors
are the errors "discovered" by a navigation or ephemeris update, in other
words, the apparent perturbation due to a refinement of the state. It is
obvious that the perturbations due to errors continuous in time compli-
cate the guidance scheme because the system parameters are misrepresented
in this case and thus invalidate the equations of motion and also any
prestored set of gains. Hence, reoptimization might be necessary for
perturbations due to errors continuous in time.

A perturbation as defined in this study is then, the discovery of
the spacecraft's being off of the nominal trajectory, for whatever reason,
with the spacecraft system parameters assumed constant. The perturbation
may be discovered at the initial time or at any intermediate time in the
flight. It is a goal of this study to compare the performance of the
various guidance schemes for perturbations of different sizes and in
different components of the state. Intuitively, one assumes that at some
point the perturbation becomes so large that the linear guidance schemes
break down and diverge. In this case, reoptimization or some other,
perhaps nonlinear, guidance must be resorted to. The determination of
the range of perturbations accommodated by the linear guidance schemes
defines the practicality of those schemes.

In discussing linear guidance schemes in subsequent sections, the
problem of "running out of gains" comes up. As mentioned previously, the
final time on a perturbed trajectory, in general, will be different than
the nominal final time. If the perturbed final time is later than the

nominal final time, the use of current time guidance could break down at times later than the nominal final time if current time gains are required. This predicament has led to the notion of "indexing." Indexing is a method of determining the appropriate nominal time from which gain information should be used, in order to calculate the control change at the current time. This appropriate nominal time is called the index time. The correspondence between nominal time and current time along the entire perturbed trajectory is only approximately one-to-one since the nominal and perturbed trajectories are of different durations. Thus, index time may "compress" or "expand" or omit or duplicate portions of the nominal time interval in the application of gains to the perturbed trajectory.

4.1.2   The Various Guidance Schemes

One of the purposes of this study is to compare the various guidance schemes to each other. The various schemes considered are Nominal Control Guidance, Current Time Guidance, Manual Time-To-Go Guidance, Time-To-Go Guidance, and Minimum Distance Guidance. Reoptimization is used as the basis for all the comparisons.

4.1.2.1   Reoptimization

Strictly speaking, reoptimization is a form of guidance as defined in this study, though it amounts to completely resolving a two-point boundary value problem. Since reoptimization by its very nature is the most accurate form of guidance, it is used as the reference for all other forms of guidance. Therefore, in this study, for each perturbation evaluated by the various schemes, a complete BSA (see Chapter 2) reoptimization is made to establish the truly optimal solution. While very accurate,

reoptimization is complex and computationally expensive; hence, one of
the purposes of this study is the assessment of the accuracy of the
simpler and less costly linear guidance schemes.

4.1.2.2 Nominal Control Guidance

The simplest form of guidance is to make no corrections to the
nominal control history. Although nominal control is not of interest as
a practical method of guidance, it does form the worst case limit of
performance for all sensible guidance schemes. Nominal control guidance
for this study, then, is the use of nominal control on the perturbed
trajectory (index time equals current time) until the nominal final time
or the final time on the perturbed trajectory, whichever comes first.
If the perturbed final time is later than the nominal final time, then for
that portion of the perturbed trajectory later than the nominal final
time, nominal control at the nominal final time is used. Final time on
the perturbed trajectory is defined as that time when the terminal con-
straint has the minimum magnitude in a nondimensionalized summed magnitude
of vectors sense.

$$\underline{u}\,(t) = \underline{u}_N\,(t_I) \tag{4.1.1}$$

$$t_I = \begin{cases} t & t \le t_{f_N} \\ \\ t_{f_N} & t > t_{f_N} \end{cases} \tag{4.1.2}$$

$$ \tag{4.1.3}$$

$$t_f = t \text{ such that } \frac{\sqrt{\sum_{i=1}^{3} [x_i(t) - x_{M_i}(t)]^2}}{\sqrt{\sum_{i=1}^{3} x^2_{o_i}}} + \frac{\sqrt{\sum_{i=4}^{6} [x_i(t) - x_{M_i}(t)]^2}}{\sqrt{\sum_{i=4}^{6} x^2_{o_i}}}$$

is a minimum where

$\underline{u}$ = control on perturbed trajectory

t = time on perturbed trajectory (current time)

$\underline{u}_N$ = control on nominal trajectory

t_I = index time or time on nominal trajectory

t_{f_N} = final time on nominal trajectory

t_f = final time on perturbed trajectory

$\underline{x}(t)$ = spacecraft state on perturbed trajectory

$\underline{x}_o$ = initial state of nominal trajectory (Earth state)

$\underline{x}_M(t)$ = Mars state

4.1.2.3 Current Time Guidance

The most straightforward type of linear perturbation guidance is Current Time Guidance. This kind of guidance is simply the addition to the nominal control of a variation in control based on gain information associated with the nominal trajectory at the current time. As in the last Sub-subsection

$$\underline{u}(t) = \underline{u}_N(t_I) + \delta\underline{u}(t) \qquad (4.1.4)$$

$$t_I = t \qquad (4.1.5)$$

$$\delta\underline{u}(t) = C_1 \, \delta\underline{x}(t) \qquad (4.1.6)$$

$$C_1 = C_1[\underline{u}_N(t_I), \, \underline{\lambda}_N(t_I), \, \underset{\sim}{S}_*(t_I)] \qquad (4.1.7)$$

$$\delta\underline{x}(t) = \underline{x}(t) - \underline{x}_N(t) \qquad (4.1.8)$$

where

C_1 = gain matrix

$\underline{\lambda}_N$ = nominal trajectory Lagrange multipliers

$\underset{\sim}{S}_*$ = transformed sweep matrix associated with nominal trajectory

$\underline{x}_N$ = spacecraft state on nominal trajectory

As in the Nominal Control Guidance used in this study, for cases in which the perturbed trajectory final time [Eq. (4.1.3)] is later than the nominal trajectory final time, the control variation is computed based on gain information associated with the nominal trajectory at the nominal final time.

If $t > t_{f_N}$

$$t_I = t_{f_N} \qquad (4.1.9)$$

$$\delta\underline{x}(t) = \underline{x}(t) - \underline{x}_N(t_{f_N}) - \dot{\underline{x}}_N(t_{f_N})(t-t_I) \qquad (4.1.10)$$

Current Time Guidance will be developed beyond this introduction in Section 4.2.

4.1.2.4 Manual Time-To-Go Guidance

Manual Time-To-Go Guidance is a simplified version of Time-To-Go Guidance introduced below. Indexing of the gain information is done through a constant input value of dt. In spirit this input value of dt' should be roughly equal to the "average" value of dt along the majority of the perturbed trajectory as determined by the Time-To-Go Guidance scheme. In principle dt can be any input value. As in preceding sub-subsections:

$$\underline{u}(t) = \underline{u}_N(t_I) + d\underline{u} \qquad (4.1.11)$$

$$t_I = t - dt \qquad (4.1.12)$$

$$d\underline{u} = \delta\underline{u}(t_I) + \dot{\underline{u}}_N(t_I) \, dt \qquad (4.1.13)$$

where

dt = input value of current time/index time difference

$\dot{\underline{u}}$ = derivative of the control

If zero is input for dt, Manual Time-To-Go Guidance degenerates into Current Time Guidance.

As in Current Time Guidance, if the perturbed trajectory final time [Eq. (4.1.3)] is later than the nominal final time, Equations (4.1.9-10) hold. Similarly, since t_I cannot be negative, if dt is positive, t_I is set equal to 0 for that portion of the trajectory on which t − dt is negative:

If t − dt < 0,

$$t_I = 0 \tag{4.1.14}$$

$$\delta\underline{x}(t) = \underline{x}(t) - \underline{x}_N(0) - \dot{\underline{x}}_N(0)(t-t_I) \tag{4.1.15}$$

Manual Time-To-Go Guidance is also developed beyond this introductory description in Section 4.2.

4.1.2.5 Time-To-Go Guidance

Time-To-Go Guidance is based on the idea[21] that performance should be much improved, as compared with current time guidance, if the gain information is taken from the nominal trajectory at an index time such that the time-to-go on the nominal trajectory is the same as the time-to-go on the perturbed trajectory. Time-to-go is the time remaining in the flight, or the amount of time until the final time is reached. In other words,

$$t_f - t = t_{f_N} - t_I = time\text{-}to\text{-}go \tag{4.1.16}$$

Since t_f is not known a priori, Equation (4.1.15) is not solved directly,
but rather a related expression to be discussed in Section 4.2 is solved
by iteration. In general, this calculated value of t_f, and hence, dt
will change slightly over the course of the trajectory integration,
where

$$dt = t - t_I \tag{4.1.17}$$

As in Equations (4.1.11) and (4.1.13) and as in preceding sub-subsections:

$$\underline{u}(t) = \underline{u}_N(t_I) + d\underline{u} \tag{4.1.18}$$

$$d\underline{u} = \delta\underline{u}(t_I) + \underline{\dot{u}}_N(t_I) \, dt \tag{4.1.19}$$

As in Manual Time-To-Go Guidance, if the computed value of t_I is
negative, t_I is reset to zero. However, there is no corresponding
problem at t_f, since ideally in Time-To-Go Guidance Equation (4.1.16)
holds.

If the computed $t_I < 0$,

$$t_I = 0 \tag{4.1.20}$$

$$\delta\underline{x}(t) = \underline{x}(t) - \underline{x}_N(0) - \underline{\dot{x}}_N(0)(t-t_I) \tag{4.1.21}$$

Time-To-Go Guidance is fully developed in the next section.

4.1.2.6 Minimum Distance Guidance

Minimum Distance Guidance is also based on the idea[22] that improved
performance should be obtained with indexing of the gain information.
In contrast to Time-To-Go Guidance, the index time is that of the state
of the nominal trajectory with the "minimum distance" to the current
state on the perturbed trajectory. "Minimum distance" means the minimi-
zation of a component weighted metric involving the state variable
difference and time difference:

t_I is chosen to minimize

$$\rho = \sqrt{\sum_{i=1}^{6} a_i \left[x_i(t) - x_{N_i}(t_I) \right]^2 + a_0 (t - t_i)^2} \qquad (4.1.22)$$

where

$a_i (i = 0,6)$ = positive weighting factors

As in Equations (4.1.17-19) and as before:

$$\underline{u}(t) = \underline{u}_N(t) + d\underline{u} \qquad (4.1.23)$$

$$d\underline{u} = \hat{c}\underline{u} + \dot{\underline{u}}_N(t_I) \, dt \qquad (4.1.24)$$

$$dt = t - t_I$$

As in Time-To-Go Guidance, if the computed value of t_I is negative, t_I is reset to zero, and there is no problem at t_f because of the nature of the metric in Equation (4.1.22). Equations (4.1.20-21) apply here.

Minimum Distance Guidance is developed fully in Section 4.3.

4.2 DEVELOPMENT OF TIME-TO-GO GUIDANCE

In this section, Time-To-Go Guidance is developed in detail for the free final time problem. The variations of Time-To-Go Guidance introduced in the last section are also presented in detail. Enhancements of Time-To-Go Guidance that improve accuracy are shown. Finally, the application of Time-To-Go Guidance and its variations to the EMRP is given.

4.2.1 <u>Time-To-Go Guidance In General</u>

As was mentioned previously, the object of Time-To-Go Guidance is to compute the control correction based on gain information from a point on the nominal trajectory such that the time-to-go or time remaining on the nominal trajectory is the same as the time-to-go on the perturbed trajectory. (See Fig. 6).

$$T = t_f - t = t_{f_N} - t_I = \text{time-to-go} \tag{4.2.1}$$

Now

$$\underline{u}(t) = \underline{u}_N(t_I) + d\underline{u} \tag{4.2.2}$$

$$\underline{x}(t) = \underline{x}_N(t_I) + d\underline{x} \tag{4.2.3}$$

$$t = t_I + dt \tag{4.2.4}$$

$$\underline{y} = \underline{y}_N + d\underline{y} \tag{4.2.5}$$

and to first order for any time τ

$$d\underline{x} = \delta\underline{x}(\tau) + \dot{\underline{x}}_N(\tau) \, d\tau \tag{4.2.6}$$

$$d\underline{u} = \delta\underline{u}(\tau) + \dot{\underline{u}}_N(\tau) \, d\tau \tag{4.2.7}$$

where

T = time-to-go

t_f = final time on perturbed trajectory
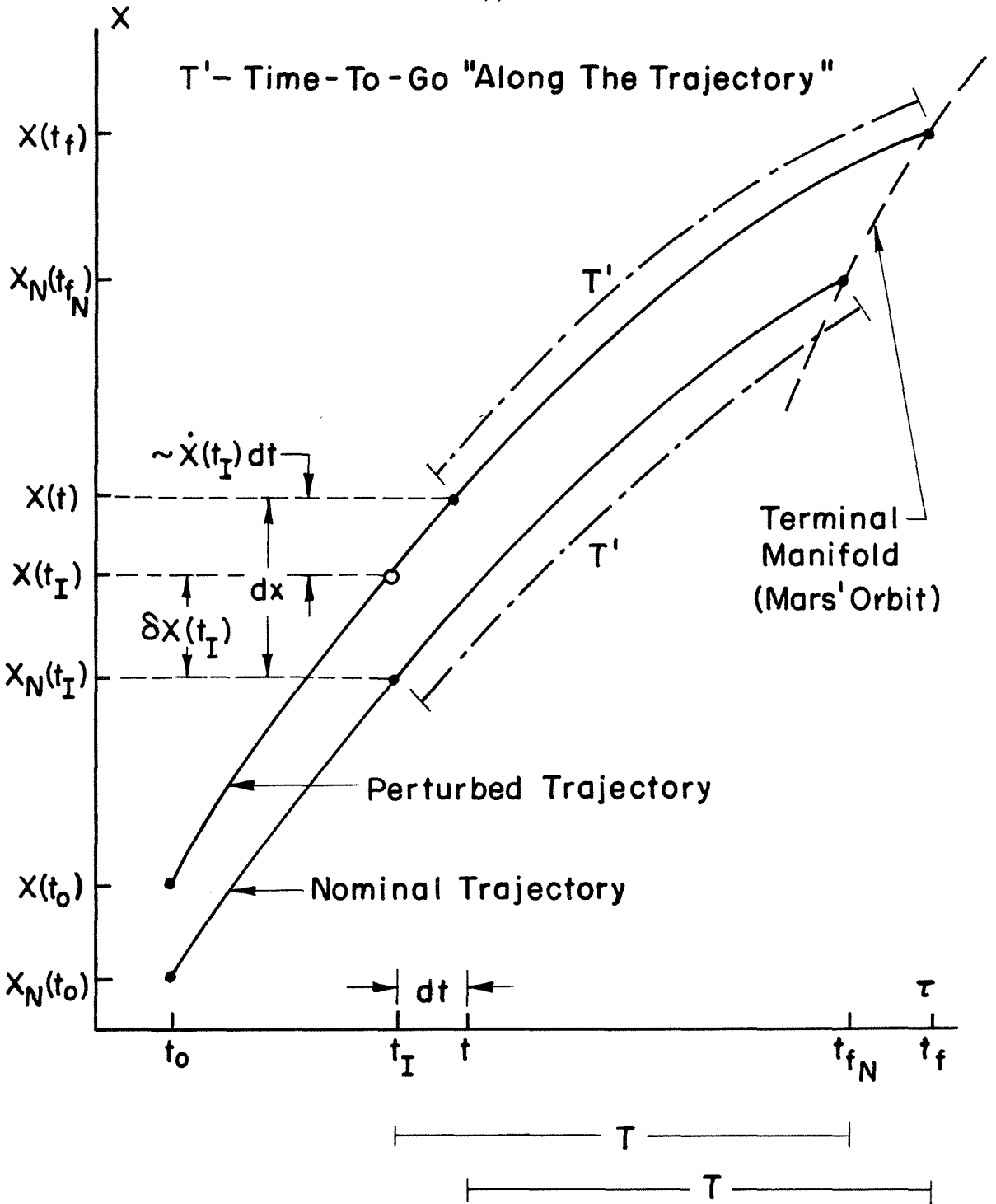
FIG. 6 ONE STATE COMPONENT REPRESENTATION
OF TIME - TO - GO

t = time on perturbed trajectory (current time)

t_{f_N} = final time on nominal trajectory

$t_I (=t_N)$ = index time (time on nominal trajectory)

$\underline{u}(t)$ = control on perturbed trajectory at current time

$\underline{u}_N(t_I)$ = control on nominal trajectory at index time

$d\underline{u}$ = differential of control

$\underline{x}(t)$ = state on perturbed trajectory at current time

$\underline{x}_N(t_I)$ = state on nominal trajectory at index time

$d\underline{x}$ = differential of state

dt = differential of time

$\underline{y}$ = terminal constraint levels on perturbed trajectory

$\underline{y}_N$ = terminal constraint levels on nominal trajectory

$d\underline{y}$ = differential of terminal constraint levels

$\delta\underline{x}(\tau)$ = variation of state (time held fixed)

$\delta\underline{u}(\tau)$ = variation of control (time held fixed)

$\dot{\underline{x}}_N(\tau)$ = time derivative of nominal state

$\dot{\underline{u}}_N(\tau)$ = time derivative of nominal control

By definition

$$\delta\underline{x}(\tau) = \underline{x}(\tau) - \underline{x}_N(\tau) \tag{4.2.8}$$

$$\delta\underline{u}(\tau) = \underline{u}(\tau) - \underline{u}_N(\tau) \tag{4.2.9}$$

Changes in terminal time are[23], from Equations (2.3.40-42):

$$d\tau_f = -\underline{m}_*^T(\tau)\delta\underline{x}(\tau) - \underline{n}_*^T(\tau)d\underline{y} \tag{4.2.10}$$

where $\underset{\sim}{R}_*$ and $\underset{\sim}{Q}_*$ are partitioned as follows

$$\underset{\sim}{R}_* = [\overline{R}_* \quad \underline{m}_*] \tag{4.2.11}$$

$$\underset{\sim}{Q}_* = \begin{bmatrix} \overline{Q}_* & \underline{n}_* \\ \underline{n}_*^T & \alpha_* \end{bmatrix} \tag{4.2.12}$$

and from Equation (4.2.5)

$$d\underline{y} = \underline{y} - \underline{y}_N = d\underline{\psi} \tag{4.2.13}$$

Subtracting $d\tau$ and using Equations (4.2.6) and (2.2.1), Equation (4.2.10) becomes[23]

$$d(\tau_f - \tau) = -\underline{m}_*^T (\tau) d\underline{x}(\tau) - [1 - \underline{m}_*^T (\tau)\underline{f}(\tau)] \, d\tau \tag{4.2.14}$$
$$-\underline{n}_*^T (\tau) d\underline{y}$$

The index time, t_I, is chosen to be that value of τ in Equation (4.2.14) such that $d(\tau_f - \tau) = 0$. This a restatement of Equation (4.2.1).

Using Equations (2.3.42) and (4.2.13), Equation (2.3.17) becomes

$$\delta\underline{u} = -H_{\underline{u} \, \underline{u}}^{-1}[(H_{\underline{u} \, \underline{x}} + \underline{f}_{\underline{u}}^T \underset{\sim}{S}_*) \, \delta\underline{x} + \underline{f}_{\underline{u}}^T \underset{\sim}{R}_* \, d\underline{y}] \tag{4.2.15}$$

Defining

$$C_1 (\tau) = -H_{\underline{u} \, \underline{u}}^{-1} (H_{\underline{u} \, \underline{x}} + \underline{f}_{\underline{u}}^T \underset{\sim}{S}_*) \tag{4.2.16}$$

$$D(\tau) = -H_{\underline{u} \, \underline{u}}^{-1} \underline{f}_{\underline{u}}^T \underset{\sim}{R}_* \tag{4.2.17}$$

Equation (4.2.15) becomes

$$\delta\underline{u} = C_1 \, \delta\underline{x} + D d\underline{y} \tag{4.2.18}$$

Substituting Equation (4.2.18) into Equation (4.2.7) using Equations (4.2.6) and (2.2.1) yields[23]

$$d\underline{u} = C_1(t_I) d\underline{x} + [\underline{\dot{u}}_N(t_I) - C_1(t_I) \, \underline{f}_N(t_I)] \, dt + D(t_I) d\underline{y} \tag{4.2.19}$$

This value of $d\underline{u}$ is then used in Equation (4.2.2) to obtain the control on the perturbed trajectory.

It can be seen from this development that the quantities $\underline{x}$, $\underline{m}_*$, $\underline{f}$, $\underline{n}_*$, C_1, $\underline{\dot{u}} - C_1\underline{f}$, and D need to be stored as functions of time during computation of the nominal trajectory for use in Time-To-Go Guidance. However, the need for saving $\underline{m}_*$ and $\underline{n}_*$ can be obviated with the following consideration:

Assume for the moment that Equations (2.2.1-2), (2.2.11-13), and (2.2.16) hold and that Equation (2.2.3) is replaced by the more general constraint

$$\underline{\psi} \, [\underline{x}(\tau_f),\tau_f] - \underline{y} = 0 \qquad\qquad (4.2.20)$$

Then from Equation (2.2.5), the first variation of the augmented performance index, allowing changes $d\underline{\psi}$, is

$$\delta J = \underline{\lambda}^T (\tau_o) \, \delta\underline{x} \, (\tau_o) - \underline{\nu}^T \, d\underline{y} \qquad\qquad (4.2.21)$$

Since any time τ, $\tau_o \leq \tau < \tau_f$, is an acceptable initial time, comparison of Equation (4.2.21) with Equation (4.2.10), recalling that $J = t_f$, yields[23]

$$\underline{m}_* (\tau) = - \underline{\lambda}(\tau) \qquad\qquad (4.2.22)$$

$$\underline{n}_* (\tau) = \underline{\nu} = \text{constant} \qquad\qquad (4.2.23)$$

Thus $\underline{\lambda}(\tau)$ and $\underline{\nu}$ can be stored in lieu of $\underline{m}_*$ and $\underline{n}_*$.

The Time-To-Go Guidance Algorithm (TTGGA) can be summarized as follows[3,4]:

During the integration of Equations (2.1.1-6) and (2.2.25-30) from t_o to t_f

1. Guess the index time t_I. A good guess is the current time, t.

2. Find $d\underline{x}$, dt and $d\underline{y}$ from Equations (4.2.3-5) and evaluate $d(t_f - t)$ from Equation (4.2.14) [and Equations (4.2.22-23)], using stored values of $\underline{x}_N (\tau)$, $\underline{\lambda}_N (\tau)$, $\underline{f}_N (\tau)$ (and $\underline{\nu}_N$ and $\underline{y}_N$), linearly interpolated to t_I.

3. If $d(t_f - t) > 0$ choose a smaller value for t_I . If $d(t_f - t)$ < 0 choose a larger value for t_I . One might choose for instance, the index time that coincides with the next data point. Using the new value of nominal state and time repeat Step 2. Continue this process until $d(t_f - t)$ changes sign or until either end of the nominal trajectory is reached.

4. If $d(t_f - t)$ has changed sign, estimate the nominal state, control, feedback gains, and index time by linear interpolation between the last two data points. If either endpoint has been reached, use the values at that endpoint.

5. Evaluate $d\underline{x}$, dt , and $d\underline{y}$, from Equations (4.2.3-5), evaluate $d\underline{u}$ from Equation (4.2.19), then find the control on the perturbed trajectory from Equation (4.2.2).

4.2.2 Variations and Enhancements of Time-To-Go Guidance

The different variations of Time-To-Go Guidance were introduced in the last section and are more fully developed here. Enhancements made to the algorithm that increase accuracy are presented.

4.2.2.1 Current Time Guidance

As indicated previously, Current Time Guidance is simply the addition of nominal control and a variation in control based on gain information from the current time, as in Equations (4.1.4-8). Time-To-Go Guidance degenerates into Current Time Guidance when Equation (4.1.5) holds or

$$t_I = t \tag{4.2.24}$$

In this case from Equations (4.2.4-6)

$$dt = 0 \tag{4.2.25}$$

$$d\underline{x}(t) = \delta\underline{x}(t) \tag{4.2.26}$$

$$d\underline{u}\ (t) = \delta\underline{u}\ (t) \tag{4.2.27}$$

and from Equation (4.2.18)

$$d\underline{u}\ (t) = C_1(t)\ \delta\underline{x}\ (t) + Dd\underline{y} \tag{4.2.28}$$

The algorithm used then is the TTGGA except that Step 2, Step 3, and the reference to $d(t_f - t)$ in Step 4 are eliminated and in Step 5, since dt = 0, Equation (4.2.28) may be used instead of Equation (4.2.19).

4.2.2.2 Manual Time-To-Go Guidance

As mentioned previously, Manual Time-To-Go Guidance is a simplified version of Time-To-Go Guidance in that a constant value of dt is manually input into the algorithm.

$$dt = (dt)_{input} = constant \tag{4.2.29}$$

Equation (4.1.12) holds:

$$t_I = t - dt \tag{4.2.30}$$

In this case, then, the algorithm used is the TTGGA except that Equations (4.2.29-30) replace Step 1, and Step 2, Step 3, and the reference to $d(t_f - t)$ in Step 4 are eliminated.

4.2.2.3 Time-To-Go Guidance

Time-To-Go Guidance is the generic guidance developed in Subsection 4.2.1.

4.2.2.4 High Order Indexed Gain Interpolation

Stoker[3] recognized the imprecision of the linear interpolation of $\underline{u}_N(t_I)$ in Step 4 of the TTGGA. He used a second order interpolation instead. However, he evaluated the nominal control at $t_I + t'$, where

$$0 \le t' \le H \tag{4.2.31}$$

and H is the current step size. Instead of Equation (4.2.2) then, he used

$$\underline{u}(t) = d\underline{u} + \underline{u}_N\ (t_I + t') \tag{4.2.32}$$

While he assumes that $d\underline{u}$ stays constant over the step size, H, it is unclear why this displaced evaluation is made for $\underline{u}_N$. Also, why the gain information inherent in $d\underline{u}$ is evaluated at t_I instead of at $t_I + t'$ [corresponding to $\underline{u}_N (t_I + t')$] is not explained. Moreover, the linear interpolations in Step 2 and the other interpolations in Step 4 are retained.

In striving for greater accuracy, therefore, the use of higher order interpolation for evaluating the gains and other quantities from the stored nominal trajectory solution was entertained. While a high order difference or Lagrangian interpolation is feasible for all the required quantities, the process of determining the appropriate order of interpolation and the suitable density of stored data points for each quantity was deemed to be more trouble than it was worth.

Fortunately the DODE integrator used in the integration of the nominal trajectory provides an answer. The EMRP integrated variables and their derivatives can be reconstructed (interpolated) at any time by the DODE interpolator if the proper DODE related quantities are saved. As mentioned in Sub-subsection 3.1.1.3 however, the required gain matrix, $C_1(t_I)$, is not a set of integrated variables--it is a function of integrated variables $\underline{x}$, $\underline{\lambda}$, $\underset{\sim}{S}_*$. Moreover, $\underset{\sim}{S}_*$ is not a set of integrated variables for $t_{f_N} \geq t_I > t_1$ but is a function of $\underset{\sim}{S}$, $\underset{\sim}{R}$, and $\underset{\sim}{Q}$, which are. These circumstances preclude the straightforward interpolation of the gain matrix from the nominal trajectory and, instead, necessitate the DODE interpolation of nominal integrated variables $\underline{x}$, $\underline{\lambda}$, and $\underset{\sim}{S}_*$ (or $\underset{\sim}{S}$, $\underset{\sim}{R}$, $\underset{\sim}{Q}$) with subsequent conversion to $C_1(t_I)$ in the guidance software.

While the DODE interpolation adds complexity to the guidance scheme, the accuracy obtained is essentially that of the nominal trajectory integration. Were the guidance scheme to be evaluated for simplicity, for say an on-board application, the above-mentioned high order interpolation should be implemented to conserve computer costs while retaining accuracy. Since the more expedient method of DODE interpolation is available and the primary purpose of this study is to investigate the performance (accuracy) of the various schemes, the added computational burden is dismissed with the aforementioned caveat.

The foregoing discussion manifests itself in modifications to the general TTGGA. The linear interpolations in Step 2 are replaced with the high order DODE interpolation. The linear interpolations of $\underline{x}_N (t_I)$,

$\underline{u}_N (t_I)$, $C_1 (t_I)$, $[\underline{\dot{u}}_N (t_I) - C_1 (t_I) \underline{f}_N (t_I)]$, and $D(t_I)$ in Step 4

are replaced with the following:

If $0 \leq t_I \leq t_1$, $\underline{x}_N (t_I)$, $\underline{f}_N (t_I)$, $\underline{\lambda} (t_I)$, and $\underset{\sim}{S}_* (t_I)$ are

obtained with the DODE interpolator. $\underline{u}_N (t_I)$ is determined from

Equation (2.2.16), $C_1 (t_I)$ from Equation (4.2.16), $\underline{\dot{u}}_N (t_I)$ from Equations

(2.3.111) and (2.3.113) and $\underline{\dot{u}}_N - C_1 (t_I) \underline{f}_N (t_I)$ by matrix algebra.

If $t_1 < t_I \leq t_f$, the procedure is the same except that $\underset{\sim}{S} (t_I)$,

$\underset{\sim}{R} (t_I)$, and $\underset{\sim}{Q} (t_I)$ are obtained with the DODE interpolator and $\underset{\sim}{S}_* (t_I)$

is determined from Equations (2.3.43-45).

In principle $D(t_I)$ could be obtained in a like manner, but as will be

discussed in Subsection 4.2.3, in the cases investigated here,

$$d\underline{y} = 0 \qquad\qquad (4.2.33)$$

eliminating the need for $D(t_I)$.

4.2.2.5 Second Order Control Variation

One ad hoc means of improving accuracy is computing the variation $\delta\underline{x}$

and, hence, $\delta\underline{u}$ to second order in dt. From Equation (4.2.6)

$$d\underline{x} = \delta\underline{x}\ (\tau) + \dot{\underline{x}}\ (\tau)\ d\tau\ + [\underline{f}_{\underline{x}}\ (\tau)\ \delta\underline{x}\ (\tau) \qquad\qquad (4.2.34)$$

$$+ \underline{f}_{\underline{u}}\ (\tau)\ \delta\underline{u}\ (\tau)]\ d\tau + \tfrac{1}{2}\ \ddot{\underline{x}}\ (\tau)\ d\tau^2$$

Using Equation (4.2.18) [and Equation (4.2.33)] and rearranging,

Equation (4.2.34) becomes

$$\delta\underline{x}\ (\tau) = (I + \underline{f}_{\underline{x}}\ d\tau + \underline{f}_{\underline{u}}\ C_1\ d\tau)^{-1} \qquad\qquad (4.2.35)$$

$$\cdot\ [d\underline{x} - \dot{\underline{x}}\ d\tau - \tfrac{1}{2}\ \ddot{\underline{x}}\ (d\tau)^2]$$

If the inverse exists, Equation (4.2.18) is then

$$\delta\underline{u}(\tau) = C_1(\tau)\ (I + \underline{f}_{\underline{x}}(\tau)\ d\tau + \underline{f}_{\underline{u}}\ (\tau)\ C_1(\tau)\ d\tau)^{-1} \qquad (4.2.36)$$

$$\cdot\ [d\underline{x} - \dot{\underline{x}}(\tau)\ d\tau - \tfrac{1}{2}\ \ddot{\underline{x}}(\tau)(d\tau)^2]$$

Equation (4.2.36) is then used in Equation (4.2.7).

4.2.2.6 Terminal $d\underline{\nu}$ Compensation

As discussed in Section 2.4, one element of a set of conditions for

a weak minimum in the nominal problem is that $\underline{\underset{\sim}{S}}_*\ (\tau)$ be finite for

$t_o \leq \tau \leq t_1$ where $t_1 < t_{f_N}$. However, Equation (4.2.15) requires the

use of $\underline{\underset{\sim}{S}}_*$ for $t_o \leq \tau < t_{f_N}$.

$$\delta\underline{u} = -\ H_{\underline{u}\ \underline{u}}^{-1}\ [(H_{\underline{u}\ \underline{x}} + \underline{f}_{\underline{u}}^{T}\ \underset{\sim}{S}_*)\ \delta\underline{x} + \underline{f}_{\underline{u}}^{T}\ \underset{\sim}{R}_*\ d\underline{y}] \qquad (4.2.37)$$

where $\underset{\sim}{S}_*$ and $\underset{\sim}{R}_*$ are constructed through Equations (2.3.43-45). Inspec-

tion of Equations (2.3.32), (2.3.39), and (2.3.43) shows that $\underset{\sim}{S}_*\ (t_{f_N})$

does not exist because $\underset{\sim}{Q}(t_{f_N})$ is singular. In other words, Equation

(4.2.37) does not make sense at t_{f_N} ; that is, infinite gains are required at the final time. Correspondingly, the gains begin to diverge shortly before the final time.

In the less constrained two-dimensional orbit transfer problem[4-14,31-32], this gain divergence is partially compensated for by the fact that

$$\delta \underline{x} (\tau) \rightarrow 0 \qquad \text{as} \quad \tau \rightarrow t_{f_N} \qquad (4.2.38)$$

In the more constrained three-dimensional problem at hand, because of the time variance of the terminal constraint, $\delta \underline{x} (\tau)$ does not go to zero as τ goes to t_{f_N} . Because the gains must be reasonably accurate for use in a guidance program, the following open loop substitution is made instead of just limiting $\delta \underline{u} (\tau)$ as τ approaches t_{f_N} .

Recall Equation (2.3.17):

$$\delta \underline{u} = -H_{\underline{u} \, \underline{u}}^{-1} (H_{\underline{u} \, \underline{x}} \; \delta \underline{x} + \underline{f}_{\underline{u}}^{T} \delta \underline{\lambda}) \qquad (4.2.39)$$

Note in passing that from Equation (2.3.42), using Equation (4.2.20),

$$- d\underline{\overline{\nu}} = R_{\underline{*}}^{T} \delta \underline{x} + Q_{\underline{*}} \; d\underline{y} \qquad (4.2.40)$$

or using Equation (4.2.33)

$$- d\underline{\overline{\nu}} = R_{\underline{*}}^{T} \delta \underline{x} \qquad (4.2.41)$$

Recall from Equation (2.3.36)

$$\delta \underline{\lambda} = S \delta \underline{x} + R d\underline{\overline{\nu}} \qquad (4.2.42)$$

Substitution of Equation (4.2.42) into Equation (4.2.39) yields

$$\delta \underline{u} = -H_{\underline{u} \, \underline{u}}^{-1} [H_{\underline{u} \, \underline{x}} \; \delta \underline{x} + \underline{f}_{\underline{u}}^{T} (S \; \delta \underline{x} + R d\underline{\overline{\nu}})] \qquad (4.2.43)$$

Collecting terms in Equation (4.2.43) yields

$$\delta \underline{u} = -H_{\underline{u}\,\underline{u}}^{-1} \left[(H_{\underline{u}\,x} + \underline{f}_{\underline{u}}^{\ T}\, S)\, \delta \underline{x} + \underline{f}_{\underline{u}}^{\ T}\, R d\overline{\underline{\nu}} \right] \qquad (4.2.44)$$

The time, $t_{\overline{\underline{\nu}}}$, for which Equation (4.2.40) is evaluated and used

in Equation (4.2.44) as described above, is then introduced into the

scheme as an imput parameter. This time should be as close as possible

to t_{f_N} , so as to not prematurely mask the proper evolution of the

closed loop feedback gain process with an open loop process, but not so

close so that round-off errors, because of gain divergence, corrupt the com-

putation of the gains. Equation (4.2.44) is used instead of Equation

(4.2.15); thus Equation (4.2.19) in Step 5 is replaced with (for $t_I > t_{\overline{\underline{\nu}}}$)

$$d\underline{u} = -H_{\underline{u}\,\underline{u}}^{-1}\, \underline{f}_{\underline{u}}^{\ T}\, (S d\underline{x} + R d\overline{\underline{\nu}}\,) + (\dot{\underline{u}} + H_{\underline{u}\,\underline{u}}^{-1}\, \underline{f}_{\underline{u}}^{\ T}\, S \underline{f}) dt \qquad (4.2.45)$$

where Equations (4.2.6) and (4.2.33) have been used and the argument t_I

suppressed.

4.2.2.7 Iterative Index Time Interpolation

The index time obtained in Step 4 of the TTGGA is determined by

linear interpolation between the last two data points, with t_I ideally

corresponding to that time where $d(t_f - t)$ equals zero. This is the

same as requiring Equation (4.2.1) to hold. Equation (4.2.1) may be

rewritten as

$$g(t, t_I) = d(t_f - t) = (t_f - t) - (t_{f_N} - t_I) = 0 \qquad (4.2.46)$$

where t_{f_N} is fixed and t_f is a function of t and t_I . At a given current

time, t, the slope of $g(t, t_I)$ with respect to index time is

$$\frac{\partial g}{\partial t_I} = 1 + \frac{\partial t_f}{\partial t_I} \qquad (4.2.47)$$

Assuming that changes in t_f due to changes in t_I at a given time t are

small, Equation (4.2.47) indicates that $d(t_f - t)$ should have a slope of about unity with respect to t_I .

This fact causes the linear interpolation for t_I to be fairly accurate if the data points are close enough. However, since the structure of $\frac{\partial t_f}{\partial t_I}$ has not been determined, the more accurate method of determining t_I by iteration ensures that slight errors in determining t_I will not be amplified in the calculation of $d\underline{u}$ because of the nonconstancy of the indexed quantities. The simplest way of determining the zero crossing of $d(t_f - t)$, taking into account starting and endpoint considerations, is by successive linear interpolations of t_I and evaluations of $d(t_f - t)$ until $\left| d(t_f - t) \right|$ is less than an input tolerance.

$$t_I^{(i+1)} = \begin{cases} t_I^{(i)} + \dfrac{d(t_f - t)_{neg}}{d(t_f-t)_{neg}-g(t, t_I^{(i)})} \ (t_I^{(i)}-t_{I_{neg}}), & g(t,t_I^{(i)}) > 0 \\[4mm] t_I^{(i)} + \dfrac{d(t_f - t)_{pos}}{d(t_f-t)_{pos}-g(t, t_I^{(i)})} \ (t_I^{(i)}-t_{I_{pos}}), & g(t,t_I^{(i)}) < 0 \end{cases}$$

$$(4.2.48)$$

where ( )pos = last positive quantity
( )neg = last negative quantity

This iterative technique replaces Step 3 and the linear interpolation of t_I in Step 4 of the TTGGA.

4.2.3 Time-To-Go Guidance as Applied to the EMRP

The Time-To-Go Guidance Algorithm used in the EMRP is the TTGGA presented in Subsection 4.2.1, modified to incorporate the enhancements described in Sub-subsections 4.2.2.4-7 and the variations of Time-To-Go Guidance outlined in Sub-subsections 4.2.2.1-3. Nominal Control

introduced in Sub-subsection 4.1.2.2, is also included in the algorithm as an option. It should be recalled that the two variations of Time-To-Go Guidance, Current Time Guidance and Manual Time-To-Go Guidance, and Nominal Control Guidance are degenerate or simplified versions of Time-To-Go Guidance. Their inclusion within the algorithm is therefore natural and easy. This modified TTGGA used in the EMRP is designated as Time-To-Go Guidance Algorithm-Enhanced (TTGGAE).

The EMRP has rendezvous as its objective. This is reflected in Equations (2.2.17-22). This objective, of course, does not change for the perturbed trajectory, and so the terminal constraint level $\underline{y}$ in Equation (4.2.20) remains unchanged at zero [Eqs. (2.2.17-22)].

$$\underline{y}_N = \underline{y} = 0 \tag{4.2.49}$$

Thus by Equation (4.2.5)

$$d\underline{y} = 0 \tag{4.2.50}$$

As mentioned previously, Equation (4.2.50) eliminates the need for calculating $D(t_I)$ in Equation (4.2.19) using Equation (4.2.17). Since Equation (4.2.17) is not necessary, $\underline{R}_*$ need not be stored on file for $t_o \leq t \leq t_1$. Recall from Sub-subsection 4.2.2.4 that $\underline{R}_*$ is calculated as intermediate product when $\underline{S}_*$ is computed for $t_1 < t < t_f$. Equation (4.2.50) also obviates the need for saving $\underline{\nu}$ [or $\underline{n}_*$, recalling Equation (4.2.23)] on file for use in Equation (4.2.19). Equations (4.2.14) and (4.2.19) become

$$d(\tau_f - \tau) = -\underline{m}_*^T (\tau) \ d\underline{x}(\tau) - [1 - \underline{m}_*^T (\tau) \ \underline{f}_N (\tau)] \ d\tau \tag{4.2.51}$$

$$d\underline{u} = C_1 (t_I) \ d\underline{x} + [\underline{\dot{u}}_N(t_I) - C_1 (t_I) \ \underline{f}_N (t_I)] \ dt \tag{4.2.52}$$

The Time-To-Go Guidance Algorithm-Enhanced (TTGGAE) used in this

study as applied to the EMRP is summarized below.

Integrate Equations (2.1.1-6) forward from t_o to t_f using

Equations (2.1.7-9), determining $\underline{u}(t)$ at each step in the following

manner:

1. TTGGA Step 1

2. Find $d\underline{x}$ and dt from Equations (4.2.3-4) and evaluate $d(t_f - t)$

from Equation (4.2.51) [and Equation (4.2.22)] using stored values

of $\underline{x}_N (\tau)$, $\underline{\lambda}_N (\tau)$, and $\underline{f}_N (\tau)$ obtained at t_I by the DODE interpolator.

3. To find t_I , use the technique, described in Sub-subsection 4.2.2.7,

of successive evaluations of Equation (4.2.51) and linear interpolations,

until $|d(t_f - t)|$ is less than a specified tolerance.

4. Use the DODE interpolator to evaluate stored values of $\underline{x}_N (t_I)$,

$\underline{f}_N (t_I)$, $\underline{\lambda} (t_I)$, and $\underset{\sim}{S}_* (t_I)$ as described in Sub-subsection 4.2.2.4.

If $t_1 < t_I < t_{\overline{\underline{\nu}}}$, instead of evaluating $\underset{\sim}{S}_* (t_I)$, evaluate $\underset{\sim}{S}(t_I)$, $\underset{\sim}{R}(t_I)$,

and $\underset{\sim}{Q}(t_I)$ and determine $\underset{\sim}{S}_*(t_I)$ from Equation (2.3.43). If $t_{\overline{\underline{\nu}}} \leq t_I$

evaluate $\underset{\sim}{S}(t_I)$ and $\underset{\sim}{R}(t_I)$.

5. The following values are calculated from the interpolated

quantities in Step 4. $\underline{u}_N(t_I)$ is determined by dividing Equations

(2.3.78-79) and (2.3.80-81).

$$u_1 = \text{arc tan}_2 \ (-\lambda_2 \ , \ \sqrt{\lambda_1{}^2 + \lambda_2{}^2} \ ) \tag{4.2.53}$$

$$u_2 = \text{arc tan}_2 \ (-\lambda_2 \ , \ -\lambda_1) \tag{4.2.54}$$

where (for arc tan defined between $-\pi/2$ and $\pi/2$)

$$\text{arc tan}_2 (a,b) \equiv \begin{cases} \text{arc tan} \ \dfrac{a}{b} & , \ a \geq 0 \\[2em] \text{arc tan} \ \dfrac{a}{b} \ + \ \pi & , \ a < 0 \end{cases} \tag{4.2.55}$$

Calculate $H_{\underline{u}\,\underline{u}}^{-1}(t_I)$, $H_{\underline{u}\,\underline{x}}(t_I)$, and $\underline{f}_{\underline{u}}(t_I)$ with Equations (2.3.85), (2.3.86) and (2.3.83) [and (2.3.78-80)] respectively. $C_1(t_I)$ is determined by Equation (4.2.16). $\dot{\underline{u}}_N(t_I)$ is found from Equations (2.3.111) and (2.3.113). If the Second Order Control Variation described in Sub-subsection 4.2.2.5 is implemented, compute $\underline{f}_{\underline{x}}(t_I)$ and $\ddot{\underline{x}}(t_I)$ from Equation (2.3.82) and Equations (2.3.104-109) [and (2.1.7-9)]. If $t_{\underline{d\nu}} \leq t_I \leq t_{\overline{\nu}}$, where $t_{\underline{d\nu}}$ and $t_{\overline{\nu}}$ are the input lower and upper time limits for calculating $\overline{d\nu}$ during at least one integration step, calculate $\overline{d\nu}$ with Equation (4.2.41) [and (4.2.8)]. The $\overline{d\nu}$ calculated on the last integration step within this time interval is the one actually used in Step 6.

6. Evaluate $d\underline{x}$ and dt from Equations (4.2.3-4). $d\underline{u}$, from Equations (4.2.19) and (4.2.48), is given by Equation (4.2.52). If the Second Order Control Variation technique described in Sub-subsection 4.2.2.5 is used, $d\underline{u}$, from Equations (4.2.36), (4.2.7), and (2.2.1), is given instead by

$$d\underline{u} = C_1(t_I) [I + \underline{f}_{\underline{x}}(t_I)dt + \underline{f}_{\underline{u}}(t_I) C_1(t_I) dt]^{-1} \qquad (4.2.56)$$

$$\cdot [d\underline{x} - \underline{f}_N(t_I) dt - \tfrac{1}{2} \ddot{\underline{x}}_N(t_I)(dt)^2] + \dot{\underline{u}}_N(t_I) dt$$

where $\underline{f}_{\underline{x}}(t_I)$ is found from Equation (2.3.82) and $\ddot{\underline{x}}(t_I)$ from Equation (2.3.104-109). When $t_I > t_{\overline{\nu}}$, $d\underline{u}$ is determined from Equation (4.2.45). The control on the perturbed trajectory is then given by Equation (4.2.2).

4.3 MINIMUM DISTANCE GUIDANCE DEVELOPMENT

In this section Minimum Distance Guidance is developed in detail for the free final time problem. The different variations of Minimum Distance Guidance are mentioned. Enhancements of Minimum Distance Guidance are identical with those of Time-To-Go Guidance, and so they will be listed, but not discussed in depth. The application of Minimum Distance Guidance and its variations to the EMRP are given. Since Minimum Distance Guidance is similar to Time-To-Go Guidance, this section is somewhat abbreviated.

4.3.1 Minimum Distance Guidance in General

As mentioned in Sub-subsection 4.1.2.6, the object of Minimum Distance Guidance is to compute the control correction based on gain information from a point on the nominal trajectory which in some sense is at a "minimum distance" from the current state on the perturbed trajectory. This "distance" is actually a metric of weighted position and velocity components and time given by

$$\rho = \sqrt{\sum_{i=1}^{6} a_i \left[x_i(t) - x_{N_i}(t_I) \right]^2 + a_0 (t - t_I)^2} \qquad (4.3.1)$$

where the a_i are positive weighting factors. The index time, t_I, is that time which minimizes ρ (see Fig. 7).

The development of the guidance is essentially identical to that for Time-To-Go Guidance given in Subsection 4.2.1, except that t_I is determined by minimizing ρ given by Equation (4.3.1) instead of by finding the zero of $d(t_f - t)$ given by Equation (4.2.14), and except for the corresponding changes to the TTGGA given below. Minimizing ρ in Equation (4.3.1) requires that
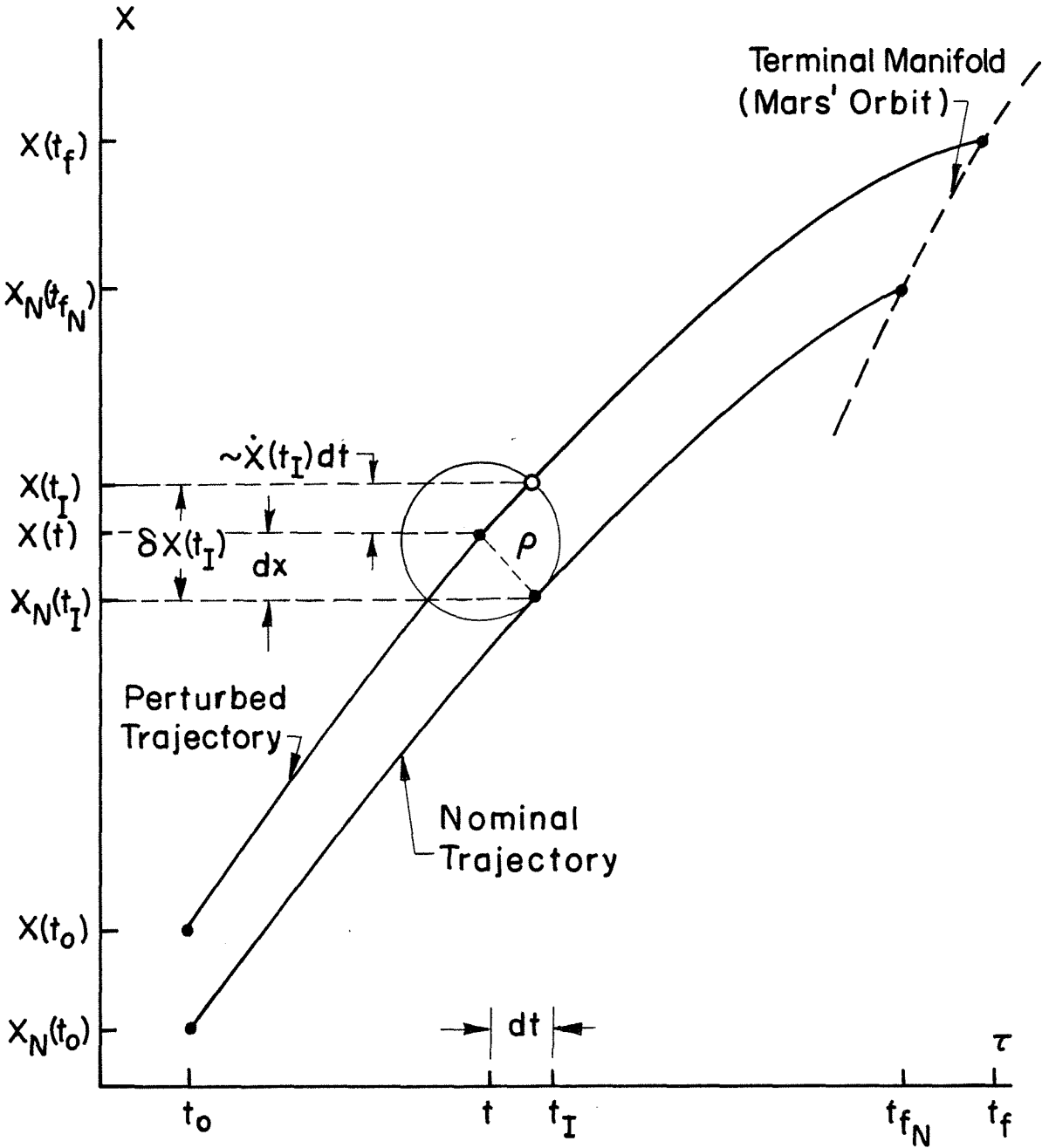
FIG. 7 ONE STATE COMPONENT REPRESENTATION
OF MINIMUM DISTANCE

$$\frac{d(\rho^2)}{dt_I} \equiv 2 \sum_{i=1}^{6} a_i \left[x_i(t) - x_{N_i}(t_I)\right] \dot{x}_{N_i}(t_I) \qquad (4.3.2)$$

$$+ 2 a_0 (t-t_I) = 0$$

The Minimum Distance Guidance Algorithm (MDGA) can be summarized as

follows:

During the integration of Equations (2.1.1-6) [and Eqs. (2.1.7-10)]

from t_o to t_f , with a_i specified:

    1.   Same as TTGGA Step 1.

    2.   Find $d\underline{x}$ and dt from Equations (4.2.3-4) and evaluate $\frac{d(\rho^2)}{dt_I}$ from

Equation (4.3.2) [and (2.2.1)] using stored values of $\underline{x}_N(\tau)$ and $\underline{f}_N(\tau)$

linearly interpolated to t_I.

    3.   Same as TTGGA Step 3, except replace $d(t_f-t)$ with $d(\rho^2)/dt_I$.

    4.   Same as TTGGA Step 4, except replace $d(t_f-t)$ with $d(\rho^2)/dt_I$.

    5.   Evaluate $d\underline{x}$ and dt from Equations (4.2.3-4), evaluate $d\underline{u}$ from

Equation (4.2.52), then find the control on the perturbed trajectory from

Equation (4.2.2).

Note that Equation (4.2.49) has been assumed here.

4.3.2 Variations and Enhancements of Minimum Distance Guidance

The two basic variations of Minimum Distance Guidance considered

here are Current Time Guidance and Minimum Distance Guidance itself. As

with Time-To-Go Guidance, Current Time Guidance is the degenerate vari-

ation of Minimum Distance Guidance, when the search for an index time is

eliminated and the index time is set equal to the current time. There-

fore, the development presented in Sub-subsection 4.2.2.1 still applies,

with appropriate substitutions of $\frac{d(\rho^2)}{dt_I}$ and MDGA for references to

$d(t_f - t)$ and TTGGA and use of Equation (4.2.50) to eliminate $d\underline{y}$.

Minimum Distance Guidance is the generic guidance discussed in Subsection 4.3.1, which in turn is essentially the same as Time-To-Go Guidance developed in Subsection 4.2.1, with the mentioned difference in techniques for index time determination. An infinite number of versions of Minimum Distance Guidance may be postulated, if one considers the disparate ways of specifying the a_i[24]. A few such variations may be considered of fundamental importance, namely those given in Table 6. Note that since a_i are relative weights, all of the a_i for a given variation may be multiplied by a constant, without changing the zero crossing of $\frac{d(\rho^2)}{dt_I}$, or t_I. Hart[1], Lattimore[2], and Stoker[3] all considered only Weight 3. This was done to allow for an explicit solution for t_I from Equation (4.3.2) and first order expansions of $\underline{x}_N(\tau)$ and $\underline{\dot{x}}_N(\tau)$. Variation 1, on the other hand, treats all the components and time equally and, therefore, is the most logical choice.

The enhancements covered in Subsection 4.2.4-7 apply identically to the Minimum Distance Guidance (with appropriate reference to $\frac{d(\rho^2)}{dt_I}$ and MDGA instead of $d(t_f - t)$ and TTGGA) and will also not be repeated here.

4.3.3 Minimum Distance Guidance as Applied to the EMRP

The minimum distance guidance algorithm used in the EMRP is the MDGA presented in Subsection 4.3.1, modified to incorporate the enhancements and variations of Minimum Distance Guidance described in Subsection 4.3.2. Nominal Control is also included in the algorithm as an option. Thus, the modified MDGA, MDGAE, is almost identical to the TTGGAE described in Subsection 4.2.3, and will not be repeated here. The only differences,

TABLE 6. FUNDAMENTAL MINIMUM DISTANCE GUIDANCE WEIGHTS

	a_0	a_1	a_2	a_3	a_4	a_5	a_6
1	t_c		v_c			r_c	
2	0		1			0	
3	0		0			1	
4	1		0			0	
5	0		v_c			r_c	
6	0	v_c	v_c	kv_c	r_c	r_c	kr_c

where

t_c = characteristic time

v_c = characteristic velocity

r_c = characteristic distance

k = constant to emphasize or de-emphasize out-of-plane components

other than names, are that $\dfrac{d(\rho^2)}{dt_I}$ and Equation (4.3.2) should be refer-

enced instead of $d(t_f - t)$ and Equation (4.2.51), and that the a_i must be

specified.

5. NUMERICAL COMPARISON OF THE GUIDANCE SCHEMES

As in the nominal trajectory optimization, the results of which were discussed in Chapter 3, only the highlights of the development of the guidance programs and the final results will be presented. The tedious "trial and error" incremental steps leading to the working programs are, therefore, omitted.

A Fortran V computer program that incorporates the same high fidelity integrator discussed in Subsection 3.1.1 was written for use again on the JPL Univac 1100/80 computer system. This program solves the Time-To-Go Guidance problem presented in Subsection 4.2.3. This program, with appropriate inputs, permits the use of the degenerate and simplified variations of Time-To-Go Guidance discussed in Subsection 4.2.2, Current Time Guidance and Manual Time-To-Go Guidance, as well as the Nominal Control technique presented in Sub-subsection 4.1.2.2. Double precision is again used throughout the program. Segmenting of major portions of the program is again used to save core space. A total of 34,600 words are overlayed into, at most, 26,900 words of space. Some of the sub-routines developed for the optimization program are utilized in the Time-To-Go Guidance program. These include subroutines for evaluating the spacecraft state derivative and Mars' state derivative, as well as for vector addition, matrix addition, vector multiplication, and file assignment. Also, in addition to the integrator, JPL program library routines used are the integrator's interpolator, the matrix inverter, the matrix multiplier, the Kepler's equation routine, a file input/output routine, a card-reading input routine, and other utility routines.

The cases considered are presented in the first section. Not only

was the DODE integrator used to integrate the equations of motion in the guidance program, but the DODE interpolator was used to interpolate the nominal state, Lagrange multipliers, and S_* (S, R, and Q for $t_I > t_1$), as discussed in Sub-subsection 4.2.2.4. This interpolation, as well as the selection of integrator error tolerances and the time of switchover to constant $\overline{dy}$ are discussed in the second section. Also discussed are the intermediate plot files used to graphically display and compare results and the use of limitation of control changes for one particular case. The third section contains a description of the plot comparison program, the guidance program results, and a comparison of the results with those of previous studies. The comparison shows that the present results are orders of magnitude better than the previous results.

Since Minimum Distance Guidance is identical to Time-To-Go Guidance except for the determination of the index time, the Minimum Distance Guidance program was created by modifying a copy of the Time-To-Go Guidance program, reflecting this difference and renaming a few sub-routines and variables. Therefore, the Minimum Distance Guidance program retains the same parameters and techniques (except index time determination) as Time-To-Go Guidance, and so the specification of these quantities will be presented but once.

5.1 CASES CONSIDERED

In order to compare the results of previous studies with the results of the current study, the cases considered must be the same.

Hart[1] states he examined the following cases (perturbations in one state variable at a time):

$$\delta x_i(t_j) = 5 \times 10^{-k} \qquad \left(\begin{array}{l} \text{AU/day, } i = 1, 2, 3 \\ \quad \text{AU} \quad , i = 4, 5, 6 \end{array} \right)$$

$t_1 = 0$ days

$t_2 = 65$ days

$t_3 = 165$ days

where for Modified Minimum Distance 1 Guidance (MMD1)

$$i = 1, \ldots, 6 ; \qquad \left\{ \begin{array}{ll} j = 1, 2 ; & k = 4, 5, 6 \\ j = 3 \quad ; & k = 6 \end{array} \right.$$

and where for Modified Minimum Distance 2 Guidance (MMD2) and Time-To-Go Guidance (TTG)

$$i = 1, \ldots, 6 ; \qquad j = 1,2 ; \qquad k = 4$$

Hart presents the change in terminal time for all cases considered for MMD1. However, he plots control and state deviations for only a few of the cases. These cases with additional data are the only ones for which meaningful comparisons can be made.

Lattimore[2], who examined a closed-loop version of Hart's Minimum Distance Guidance, considered the following cases with various loop closure rates:

$$\delta x_1 \ (0) \ = 5 \times 10^{-6} \ \text{AU/day}$$

$$\delta x_1 \ (65) = 5 \times 10^{-6} \ \text{AU/day}$$

$$\delta x_4 \ (0) \ = 5 \times 10^{-6} \ \text{AU}$$

$$\delta x_4 \ (65) = 5 \times 10^{-6} \ \text{AU}$$

Since Hart presented in detail only a subset of the cases he examined, because the others exhibited "the same characteristics," a similar philosophy is adopted here in that those perturbations at times other than t = 0 will not be examined. The remaining comparison cases of Hart and Lattimore, the cases studied by Stoker[3], and those presented in this study are tabulated in Tables 7-10. As can be seen in these tables, many of Stoker's intermediate sized perturbations were not examined here. These cases tend to duplicate the results of more extreme cases.

The notation used in Tables 7-10 is as follows:

$\delta x_i (0)$ - perturbation of x_i at t = 0

$$\left| \underline{x}_{o_V} \right| = \sqrt{x_{o_1}^2 + x_{o_2}^{\cdot 2} + x_{o_3}^2}$$

$$\left| \underline{x}_{o_r} \right| = \sqrt{x_{o_4}^2 + x_{o_5}^2 + x_{o_6}^2}$$

   C   - Hart's MMD1 Guidance

   T   - Time-To-Go Guidance

   M   - Minimum Distance Guidance (Weight 3)

   N   - Minimum Distance Guidance (Weight 1)

   O   - Other schemes such as Current Time or Manual

            Time-To-Go Guidance

TABLE 7. CASES STUDIED WITH INITIAL PERTURBATIONS IN x_1

$\delta x_1(0)$	$\dfrac{\delta x_1(0)}{x_{o_1}}$	$\dfrac{\left|\delta x_1(0)\right|}{\left|\underline{x}_{o_v}\right|}$	HART	LATTIMORE	STOKER	THIS STUDY
-.4-4	.002693	.002287			TM	TMN
-.3-4					TM	
-.2-4					TM	
-.15-4	.001	.0008574				TMN
-.1-4	.0006741	.0005716			TM	TMN
.5-5	-.000337	.0002858	C	M	TM	TMN
.1-4					TM	
.2-4					TM	
.3-4					TM	
.4-4					TM	
.5-4	-.00337	.002858	C		TM	TMN
.5-3	-.0337	.02858	CTM			OMN

TABLE 8. CASES STUDIED WITH INITIAL PERTURBATIONS IN x_4

$\delta x_4(0)$	$\dfrac{\delta x_4(0)}{x_{o_4}}$	$\dfrac{\|\delta x_4(0)\|}{\|\underline{x}_{o_r}\|}$	HART	LATTIMORE	STOKER	THIS STUDY
$-.21-2$	$-.004039$	$.002136$			TM	TMN
$-.15-2$					TM	
$-.9-3$					TM	
$-.3-3$	$-.000577$	$.0003051$			TM	TMN
$.5-5$	$.0000096166$	$.000005085$	C	M		TMN
$.5-4$	$.000096166$	$.00005085$	C			TMN
$.3-3$	$.000577$	$.0003051$			TM	TMN
$.5-3$	$.00096166$	$.0005085$	CTM			TMN
$.9-3$					TM	
$.15-2$					TM	
$.21-2$					TM	
$.27-2$					TM	
$.33-2$	$.006347$	$.003356$			TM	TMN

TABLE 9. CASES STUDIED WITH INITIAL PERTURBATIONS IN x_3

$\delta x_3(0)$	$\dfrac{\|\delta x_3(0)\|}{\|x_{o_v}\|}$	HART	LATTIMORE	STOKER	THIS STUDY
-.35-4	.002001			T	TM
-.25-4				T	
-.15-4				TM	
-.5-4				TM	
.5-5				TM	
.15-4				TM	
.25-4				TM	
.35-4	.002001			TM	TM

TABLE 10. CASES STUDIED WITH INITIAL PERTURBATIONS IN x_6

$\delta x_6(0)$	$\dfrac{\|\delta x_6(0)\|}{\|x_{o_r}\|}$	HART	LATTIMORE	STOKER	THIS STUDY
-.27-2	.002746			TM	TM
-.21-2				TM	
-.15-2				TM	
-.9-3				TM	
-.3-3				TM	
.3-3				TM	
.9-3				TM	
.15-2				TM	
.21-2				TM	
.27-2				TM	
.33-2	.003356			TM	TM

5.2 TECHNIQUES AND PARAMETER VALUES USED IN THE GUIDANCE RUNS

The parameter values used in the guidance programs were specified to correspond to those of the optimization program. Several techniques were employed in the guidance programs to enhance accuracy.

5.2.1 The DODE Integrator

For many of the reasons given in Subsection 3.1.1, the DODE integrator was chosen for the guidance programs.

5.2.1.1 Absolute Error Tolerances and Step Size

To correspond with the error tolerances selected for the state equations in the optimization program, an absolute error tolerance of 10^{-10} was selected for all six of the equations of motion. These state equations were the only equations integrated in the guidance programs and, again, are in the units of the previous authors, AU/day and AU.

Step size limits were also chosen for the same reasons as in the Sub-subsection 3.1.1.1.

5.2.1.2 Gain File Interpolation

As described in Sub-sections 3.1.1.3 and 4.2.2.4, the DODE integrator interpolator is used in the guidance programs to obtain gain-related and other information from the nominal trajectory. This use of the integrator's interpolator should not be confused with the use of the entire DODE integrator for integrating the equations of motion in the guidance programs. The two functions are totally separate, and the interpolator subroutine for the gain-related information is distinguished from the corresponding interpolation subroutine used in the integration of the state equations by the use of a different set of names.

The gain file occupies 42 storage tracks, which is equivalent to

about 75,000 36-bit words. The file is written in the JPL Type-66 format, which permits the file to be read by a standard reader.

5.2.1.3 Intermediate Plot File Output

For plotting purposes (to be discussed in Subsection 5.3.1), as in the case of the optimization program, two other features of the DODE integrator were used. The integrator output interval was specified not only for printed output but for the output to an intermediate plot file containing state and control related data. Output could also be generated at a set of specified times to be printed and plotted.

The output from the guidance program to the intermediate plot file consists of t, h (stepsize), t_{p_I} (time of last step), t_I, dt, $\underline{u}_N$, $\delta\underline{u}$, d$\underline{u}$, $\underline{u}$, $\underline{x}$, $\delta\underline{x}$, $\underline{\psi}$, $|\underline{\psi}_v|$, and $|\underline{\psi}_r|$. ($|\underline{\psi}_v|$ and $|\underline{\psi}_r|$ are terminal velocity and position errors). Since the control related variables are not integrated, they are obtainable only at the end of a step which, in general, will not coincide with a regular output point. Thus, the Plot Combination program, to be discussed in Subsection 5.3.1, needs t_{p_I} in order to interpolate these variables to the regular output time, t, in order to compare them to reoptimized values.

5.2.2 Time of Switchover to Constant $d\overline{\underline{v}}$

The choice of $t_{\overline{\underline{v}}}$, the time for which $d\overline{\underline{v}}$ is computed from (4.2.4c) and used in (4.2.4.4) to determine $\delta\underline{u}$, as described in Sub-subsection 4.2.2.6, is one of "trial and error." This time may be expressed as a fraction of t_{f_N}:

$$t_{\overline{\underline{v}}} = c_{t_{\overline{\underline{v}}}} \cdot t_{f_N} \qquad\qquad (5.2.1)$$

where $c_{t_{\overline{\underline{v}}}}$ lies between zero and one.

The performance of Time-To-Go Guidance and Minimum Distance Guidance, as measured by terminal error, was investigated for various values of $c_{\frac{t}{\underline{v}}}$ for all of the cases. $c_{\frac{t}{\underline{v}}}$ was found to exert quite an effect on performance for many of the cases.

Intuition might lead one to expect that the best choice of $c_{\frac{t}{\underline{v}}}$ should be as close to one as possible, e.g. .98 or .99, to ensure accurate representation of the closed loop process, but not so close to one to allow the gains to be computed with large roundoff errors. Accordingly, for each guidance type the value of $c_{\frac{t}{\underline{v}}}$ was varied, as necessary, in increments of .01 to minimize the sum of the non-dimension-alized terminal velocity error, $|\underline{\psi}_v|_{ND}$, plus the terminal position error, $|\underline{\psi}_r|$. This sum is thus given by

$$
\begin{aligned}
\Sigma_{ND} &= |\underline{\psi}_v|_{ND} + |\underline{\psi}_r| \\
&= \frac{|\underline{\psi}_v|}{v_c} + |\underline{\psi}_r| \\
&= \frac{\sqrt{\psi_1^2 + \psi_2^2 + \psi_3^2}}{v_c} + \sqrt{\psi_4^2 + \psi_5^2 + \psi_6^2}
\end{aligned}
\tag{5.2.2}
$$

where the characteristic velocity may be expressed as

$$
v_c = \sqrt{\frac{\mu}{R}}
\tag{5.2.3}
$$

and μ is the gravitational parameter of the Sun introduced in Chapter 2. R is the characteristic distance and is equal to 1 AU. The numerical value of v_c is .01720486954 AU/day. The results of these searches are tabulated in Tables 11-25. For the case of $\delta x_1(0) = .5 \times 10^{-3}$ AU/day, see the next subsection. These tables are filled in with respect to $c_{\frac{t}{\underline{v}}}$ only

as much as was necessary to find the minimum of Σ_{ND} . As can be seen

from the tables, the values of $c_{t_{\underline{\nu}}}$ yielding the best performance for

the different cases follow no readily apparent pattern.

It must be understood that for each entry shown, the final time, t_f,

indicates that time at which the velocity error, $|\underline{\psi}_v|$, reached a mini-

mum, since the position error, $|\underline{\psi}_r|$, remains relatively constant when

$|\underline{\psi}_v|$ is near zero. These times were determined manually by inputting

several specified output times or, in some cases, automatically by the

Time-To-Go Guidance program.

The notation in the following tables is abbreviated as follows:

for t_f

  .abc denotes 196.abc

  7.def denotes 197.def

  .ghijk. . . indicates that this automatically determined time

         is truncated.

.abc-m   denotes .abc $\times 10^{-m}$

*   indicates the run (value of $c_{t_{\underline{\nu}}}$) for which Σ_{ND} was minimized for

  this case and guidance type; only this run is made use of in sub-

  sequent sections .

$\sim$ indicates the approximate minimum of $|\underline{\psi}_v|$ (and hence Σ_{ND}) for this

  value of $c_{t_{\underline{\nu}}}$

$\simeq$ indicates a crude approximation to the minimum of $|\underline{\psi}_v|$ (and hence

  Σ_{ND}) for this value of $c_{t_{\underline{\nu}}}$

TTG Time-To-Go Guidance

MD1 Minimum Distance Guidance (Weight 1)

MD3 Minimum Distance Guidance (Weight 3)

TABLE 11. TERMINAL ERROR VS. $c_{t_{\underline{v}}}$, $\delta x_1(0) = -.4-4$ AU/DAY

	TTG			MD1			MD3		
$c_{t_{\underline{v}}}$	$t_f - 196.$	$\lvert\underline{\psi}_v\rvert_{ND}$	$\lvert\underline{\psi}_r\rvert$	$t_f - 196.$	$\lvert\underline{\psi}_v\rvert_{ND}$	$\lvert\underline{\psi}_r\rvert$	$t_f - 196.$	$\lvert\underline{\psi}_v\rvert_{ND}$	$\lvert\underline{\psi}_r\rvert$
.99	.383	∿.108-5	.420-5	.38292	*.999-6	.419-5	.38292	*.988-6	.419-5
.98	.38292	.841-6	.420-5	.3829	.105-5	.419-5	.38292	.102-5	.419-5
.96	.38292	.606-6	.420-5	.3829	.107-5	.419-5	.38292	.104-5	.420-5
.95	.38294	.486-6	.420-5	.3829	.108-5	.420-5			
.93	.38293	.246-6	.420-5	.3829	.110-5	.420-5			
.91	.38294	.115-6	.421-5						
.90	.38294	*103-6	.421-5	.3829	.113-5	.420-5			
.89	.38294	.160-6	.421-5						
.88	.38294	.216-6	.423-5						
.85	.38294	.397-6	.423-5						

TABLE 12. TERMINAL ERROR VS. c_{t-_ν}, $\delta x_1(0) = -.1-4$ AU/DAY

c_{t-_ν}	TTG			MD1			MD3		
	$t_f - 196.$	$|\underline{\psi}_v|_{ND}$	$|\underline{\psi}_r|$	$t_f - 196.$	$|\underline{\psi}_v|_{ND}$	$|\underline{\psi}_r|$	$t_f - 196.$	$|\underline{\psi}_v|_{ND}$	$|\underline{\psi}_r|$
.99	.657399	*.481-7	.268-6	.6574	.102-6	.268-6	.657398	.113-6	.268-6
.98	.657399	.492-7	.268-6	.6574	.716-7	.268-6			
							.657399	.602-7	.268-6
.96	.657399	.506-7	.268-6	.657399	.554-7	.268-6	.657399	*569-7	.268-6
.95				.657399	*524-7	.268-6	.657399	.572-7	.268-6
.94	.657399	.527-7	.268-6	.657399	.524-7	.268-6	.657399	.573-7	.268-6
.93				.657399	.527-7	.268-6			
.92				.657399	.527-7	.268-6			
.90				.657399	.546-7	.268-6			

TABLE 13. TERMINAL ERROR VS. c_{t-_ν}, $\delta x_1(0) = .5-5$ AU/DAY

c_{t-_ν}	TTG			MD1			MD3		
	$t_f - 196$	$|\underline{\psi}_v|_{ND}$	$|\underline{\psi}_r|$	$t_f - 196$	$|\underline{\psi}_v|_{ND}$	$|\underline{\psi}_r|$	$t_f - 196$	$|\underline{\psi}_v|_{ND}$	$|\underline{\psi}_r|$
.99	.796821	.256-7	.676-7	.796821	*141-7	.676-7	.796821	*142-7	.676-7
.98	.796821	.254-7	.676-7	.796821	.203-7	.676-7	.796821	.213-7	.676-7
.97	.796821	.248-7	.676-7						
.96	.796821	*241-7	.676-7	.796821	.261-7	.677-7			
.95	.796821	.255-7	.676-7						

TABLE 14.   TERMINAL ERROR VS. $c_{t_{\underline{\bar{v}}}}$, $\delta x_1(0) = .5\text{-}4$ AU/DAY

$c_{t_{\underline{\bar{v}}}}$	TTG			MD1			MD3		
	$t_{\bar{f}}$ 190	$|\underline{\psi}_v|_{ND}$	$|\underline{\psi}_r|$	$t_{\bar{f}}$ 190	$|\underline{\psi}_v|_{ND}$	$|\underline{\psi}_r|$	$t_{\bar{f}}$ 190	$|\underline{\psi}_v|_{ND}$	$|\underline{\psi}_r|$
.99									
.98				7.22315	.281-4	.698-5			
.97				7.22315	.139-4	.698-5			
.96	7.2232	.602-5	.697-5	7.2232	.489-5	.699-5	7.2231	.641-5	.699-5
.95				7.2232	.340-5	.700-5	7.2231	.319-5	.700-5
.94	7.22315	.546-5	.698-5	7.22315	*288-5	.701-5	7.22314	*288-5	.701-5
				7.22315	.296-5	.702-5	7.22314	.300-5	.702-5
.92	7.22315	.502-5	.700-5	7.22315	.331-5	.703-5			
.90				7.22315	.433-5	.706-5			
.89	7.22315	.451-5	.704-5						
.85	7.2231	.363-5	.710-5						
.81	7.2231	.190-5	.725-5						
.80	7.223	.146-5	.732-5						
.79	7.223	*108-5	.741-5						
.78	7.22295	.967-6	.754-5						
.77	7.2229	.197-5	.798-5						
.74	7.2429	~418-5	.896-5						

TABLE 15. TERMINAL ERROR VS. $c_{t_{\underline{v}}}$, $\delta x_4(0) = -.21-2$ AU

$c_{t_{\underline{v}}}$	TTG			MD1			MD3		
	$t_f-196.$	$|\psi_{\underline{v}}|_{ND}$	$|\psi_{\underline{r}}|$	$t_f-196.$	$|\psi_{\underline{v}}|_{ND}$	$|\psi_{\underline{r}}|$	$t_f-196.$	$|\psi_{\underline{v}}|_{ND}$	$|\psi_{\underline{r}}|$
.99	.853904	.277-5	.408-6	.853	.457-4	.395-6			
.98				.852	~158-4	.373-6			
.96				.852	~487-5	.393-6			
.94				.852	~197-5	.434-6			
.93	.851947...	.209-5	.476-6						
.92				.85184	.553-6	.499-6	.85184	.691-6	.491-6
.91	.8519159...	.202-5	.518-6	.85186	*340-6	.532-6	.85184	*343-6	.541-6
.90	.851869...	.196-5	.566-6	.85186	.412-6	.568-6	.85184	.405-6	.568-6
.89	.851852...	*193-5	.592-6	.85186	.588-6	.605-6			
.88	.8519038...	.188-5	.647-6						
.85	.851827...	.179-5	.768-6						
.80	.851813...	.165-5	.100-5						

TABLE 16. TERMINAL ERROR VS. $c_{t_{\underline{v}}}$, $\delta x_4(0) = -.3-3$ AU

$c_{t_{\underline{v}}}$	TTG			MD1			MD3		
	$t_f-196.$	$|\psi_{\underline{v}}|_{ND}$	$|\psi_{\underline{r}}|$	$t_f-196.$	$|\psi_{\underline{v}}|_{ND}$	$|\psi_{\underline{r}}|$	$t_f-196.$	$|\psi_{\underline{v}}|_{ND}$	$|\psi_{\underline{r}}|$
.99	.76451	.382-7	.643-8	.764506	.275-7	.642-8	.7645058	.293-7	.641-8
.98	.7645059	.362-7	.652-8	.7645058	*845-6	.652-8	.764506	*728-8	.652-8
.97	.7645059	*353-7	.667-8	.7645058	.138-7	.667-8	.7645058	.195-7	.670-8
.96	.764506	.356-7	.689-8	.7645058	.311-7	.690-8			
.94	.764506	.354-7	.762-8						

TABLE 17. TERMINAL ERROR VS. $c_{t_{\bar{v}}}$, $\delta x_4(0)= .5-5$ AU

$c_{t_{\bar{v}}}$	TTG			MD1			MD3		
	$t_f -196.$	$|\psi_v|_{ND}$	$|\psi_r|$	$t_f 196.$	$|\psi_v|_{ND}$	$|\psi_r|$	$t_f 196.$	$|\psi_v|_{ND}$	$|\psi_r|$
.99	.749969196	*565–10	.248–10	.7499692	*376–10	.242–10	.74996919	~167–8	.418–10
.98	.749969203	.580–10	.290–10				.74996923	~405–9	.168–10
.97							.74996926	~479–9	.194–10
.96	.74997	~27–8	.27–10				.74996926	~*575–10	.212–10
.95							.74996926	~706–10	.260–10
.94							.74996926	.112–8	.224–10

TABLE 18. TERMINAL ERROR VS. $c_{t_{\bar{v}}}$, $\delta x_4(0)= .5-4$ AU

$c_{t_{\bar{v}}}$	TTG			MD1			MD3		
	$t_f 196.$	$|\psi_v|_{ND}$	$|\psi_r|$	$t_f 196.$	$|\psi_v|_{ND}$	$|\psi_r|$	$t_f 196.$	$|\psi_v|_{ND}$	$|\psi_r|$
.99	.7478307	.931–9	.195–9	.747831	~165–8	.194–9	.74783073	*177–8	.196–9
.98	.74783071	.193–8	.213–9	.74783088	*107–8	.197–9	.74783085	.415–8	.197–9
.97	.74783071	*639–9	.202–9	.747831	~232–8	.200–9	.74783075	.249–8	.208–9
.96	.74783071	.874–9	.322–9	.747831	~342–8	.205–9			

TABLE 19. TERMINAL ERROR VS. $c_{t_{\underline{\nu}}}$, $\delta x_4(0)= .3-3$ AU

$c_{t_{\underline{\nu}}}$	TTG			MD1			MD3		
	$t_f - 196.$	$\|\psi_v\|_{ND}$	$\|\psi_r\|$	$t_f - 196.$	$\|\psi_v\|_{ND}$	$\|\psi_r\|$	$t_f - 196.$	$\|\psi_v\|_{ND}$	$\|\psi_r\|$
.99	.735979	≂325-7	.636-8				.73597985	.849-7	.635-8
.98	.7359785	.315-7	.644-8	.735979	.596-7	.643-8			
.97	.7359785	*257-7	.677-8	.735979	.526-7	.656-8	.73597985	.535-7	.660-8
.96	.7359785	.279-7	.686-8	.7359785	.461-7	.675-8	.73597985	.430-7	.678-8
.95				.735979	.523-7	.700-8	.73597985	.437-7	.713-8
.94	.7359785	.301-7	.749-8	.735979	.451-7	.731-8			
.92	.735979	.312-7	.804-8	.7359789	.390-7	.841-8			
.91	.735979	.246-7	.916-8	.7359787	.385-7	.891-8	.7359787	.360-7	.885-8
.90	.735979	.253-7	.952-8	.735979	*364-7	.923-8	.7359789	*336-7	.950-8
.89				.735979	.376-7	.994-8	.735979	.372-7	.989-8
.88	.735979	.277-7	.103-7						
.87				.7359795	.385-7	.112-7			

TABLE 20. TERMINAL ERROR VS. $c_{t_{\underline{\nu}}}$, $\delta x_4(0) = .5\text{-}3$ AU

$c_{t_{\underline{\nu}}}$	TTG			MD1			MD3		
	$t_{\bar{f}}$ 196.	$\|\psi_v\|_{ND}$	$\|\psi_r\|$	$t_{\bar{f}}$ 196.	$\|\psi_v\|_{ND}$	$\|\psi_r\|$	$t_{\bar{f}}$ 196.	$\|\psi_v\|_{ND}$	$\|\psi_r\|$
.99	.72649596...	.160-6	.176-7	.726533	.330-6	.175-7			
.97	.726532	.893-7	.182-7	.726532	.177-6	.181-7			
.96	.726532	*.735-7	.190-7	.726532	.150-6	.186-7			
.95	.726532	.836-7	.195-7	.726532	.144-6	.194-7			
.94	.726533	.103-6	.205-7	.726532	.143-6	.200-7	.726532	.134-6	.200-7
.93				.726532	.123-6	.211-7	.726532	.126-6	.210-7
.92				.726532	.123-6	.219-7	.726532	.124-6	.220-7
.91				.726533	.123-6	.238-7	.726532	.112-6	.240-7
.90				.726533	.116-6	.250-7	.726532	*.110-6	.250-7
.89				.726533	.116-6	.262-7	.726532	.118-6	.265-7
.88				.726534	.113-6	.275-7	.726534	.109-6	.280-7
.87				.726534	*.105-6	.305-7	.726534	.113-6	.294-7
.86				.726534	.109-6	.321-7	.726535	.105-6	.330-7
.85				.726536	.103-6	.338-7	.726535	.105-6	.350-7
.84				.726536	.107-6	.357-7	.726536	.102-6	.371-7
.83				.726536	.101-6	.386-7			
.81				.726538	.103-6	.437-7			

TABLE 21. TERMINAL ERROR VS. $c_{t_{\underline{\nu}}}$, $\delta x_4(0)= .33-2$ AU

$c_{t_{\underline{\nu}}}$	TTG t_f 196.	$\left|\underline{\psi}_v\right|_{ND}$	$\left|\underline{\psi}_r\right|$	MD1 t_f 196.	$\left|\underline{\psi}_v\right|_{ND}$	$\left|\underline{\psi}_r\right|$	MD 3 t_f 196.	$\left|\underline{\psi}_v\right|_{ND}$	$\left|\underline{\psi}_r\right|$
.99									
.96	.5978	.582-5	.801-6						
.94				.5975	$\sim$101-4	.850-6			
.92	.5978	.176-5	.116-5	.5975	$\sim$855-5	.900-6			
.91	.5978	.167-5	.119-5						
.90	.5978	*.165-5	.122-5	.5977	$\sim$844-5	.929-6			
.89	.5978	.172-5	.122-5						
.88	.5978	.198-5	.119-5	.5978	.818-5	.966-6			
.86				.5978	.790-5	.103-5			
.84	.59785	.310-5	.117-5	.5978	.761-5	.112-5			
.82				.5978	.721-5	.128-5			
.80				.5979	.663-5	.159-5			
.77				.5979	.590-5	.211-5			
.76				.598	$\sim$570-5	.229-5	.598	.513-5	.230-5
.75				.598	*.532-5	.267-5	.598	*.484-5	.259-5
.74				.598	.516-5	.284-5	.598	.457-5	.289-5
.73				.5981	.492-5	.312-5			
.72				.5981	.475-5	.333-5			

TABLE 22. TERMINAL ERROR VS. $c_{t_{\underline{\nu}}}$, $\delta x_3(0) = -\ .35\text{-}4$ AU/DAY

$c_{t_{\underline{\nu}}}$	TTG			MD3		
	t_f-196	$\|\underline{\psi}_v\|_{ND}$	$\|\underline{\psi}_r\|$	t_f-196	$\|\underline{\psi}_v\|_{ND}$	$\|\underline{\psi}_r\|$
.99	.773035	*.395-6	.371-7	.7730	.417-5	.227-7
.98	.77289	∿.404-6	.425-7	.7729	.229-5	.274-7
.97	.772835	.410-6	.484-7			
.96	.7728	.415-6	.565-7	.7728	.106-5	.504-7
.95	.77277	.424-6	.761-7			
.93				.77275	.645-6	.114-6
.92				.77274	*.557-6	.141-6
.91				.77274	.556-6	.161-6
.90				.77274	.530-6	.182-6
.89				.77274	.473-6	.229-6
.88				.77275	.447-6	.255-6
.87				.77275	.425-6	.297-6
.86				.77275	.414-6	.342-6

TABLE 23. TERMINAL ERROR VS. $c_{t\frac{-}{\nu}}$, $\delta x_3(0) = .35-4$ AU/DAY

$c_{t\frac{-}{\nu}}$	TTG			MD3		
	t_f-196	$\left|\underline{\psi}_v\right|_{ND}$	$\left|\underline{\psi}_r\right|$	t_f-196	$\left|\underline{\psi}_v\right|_{ND}$	$\left|\underline{\psi}_r\right|$
.99	.73971	.462-6	.330-7	.72976	.431-5	.219-7
.98	.72949	.412-6	.357-7			
.97	.72941	*.394-6	.418-7			
.96	.72938	.386-6	.504-7	.7294	.110-5	.434-7
.95	.72936	.377-6	.685-7			
.93	.72935	~.370-6	.103-6	.72934	.660-6	.104-6
.92				.72934	.609-6	.125-6
.91				.72934	*.571-6	.149-6
.90				.72934	.530-6	.169-6
.89				.72934	.551-6	.190-6
.88				.72935	.513-6	.213-6

TABLE 24. TERMINAL ERROR VS. $c_{t\underline{\nu}}$, $\delta x_6(0) = -.27\text{-}2$ AU

$c_{t\underline{\nu}}$	TTG			MD3		
	$t_f\text{-}196$	$\|\underline{\psi}_v\|_{ND}$	$\|\underline{\psi}_r\|$	$t_f\text{-}196$	$\|\underline{\psi}_v\|_{ND}$	$\|\underline{\psi}_r\|$
.99	.75254765	*.366-8	.199-9	.7525476	$\sim$.623-8	.208-9
.98	.75254765	$\simeq$.553-8	.789-9	.7525477	.555-8	.218.9
.97				.7525477	.134-8	.232-9
.96				.7525477	$\overset{*}{\sim}$.352-9	.241-9
.95				.7525477	.152-8	.247-9
.92				.7525475	.202-8	.129-8

TABLE 25. TERMINAL ERROR VS. $c_{t\underline{\nu}}$, $\delta x_6(0) = .33\text{-}2$ AU

$c_{t\underline{\nu}}$	TTG			MD3		
	$t_f\text{-}196$	$\|\underline{\psi}_v\|_{ND}$	$\|\underline{\psi}_r\|$	$t_f\text{-}196$	$\|\underline{\psi}_v\|_{ND}$	$\|\underline{\psi}_r\|$
.99	.744663	*.822-8	.985-9			
.98	.744663	$\sim$.889-8	.107-8	.7446631	.174-7	.101-8
.97				.744663	*.654-8	.124-8
.96				.7446631	.738-8	.133-8

5.2.3 Control Change Limiting

Stoker[3] found it necessary to place limits on the control change

for the case $\delta x_1(0) = .5 \times 10^{-4}$ AU/day. Accordingly, the guidance

programs have the capability, through input command du_{MAX} , to limit the

magnitude of the components of $\underline{du}$. This limiting was necessary here

only for the case $\delta x_1(0) = .5 \times 10^{-3}$ AU/day, a more demanding case than

those considered by Stoker.

Time-To-Go Guidance fails for $\delta x_1(0) = .5 \times 10^{-3}$ AU/day because at

early times there apparently is no value of t_I for which Equation (4.2.14)

is equal to zero. Minimum Distance Guidance displays poor performance

for this case. These problems are probably due to nonlinearities not

included in the expression for $\underline{du}$. Current Time guidance ($dt_{MAN} = 0$)

and Manual Time-To-Go guidance for various values of dt_{MAN}, the input

value of dt, were tried for this case. The results appear in Table 26.

Again the final time, t_f, indicates the minimum value of Σ_{ND}, the sum of

the position and non-dimensionalized velocity terminal errors, $|\underline{\psi}_r|$

and $|\underline{\psi}_v|_{ND}$. All runs were made with $c_{t_{\underline{\upsilon}}}$ equal to .99 .

TABLE 26. FINAL TIMES (t_f) AND TERMINAL ERRORS ($|\underline{\psi}_v|_{ND}$, $|\underline{\psi}_r|$)

FOR SELECTED VALUES OF dt_{MAN} AND $d\underline{u}_{MAX}$

USING MANUAL TIME-TO-GO GUIDANCE, $\delta x_1(0) = .5$-3 AU/DAY

dt_{MAN}	$d\underline{u}_{MAX}$					
	.025,.05	.05,.10	.10,.20	.15,.30	.20,.40	.30,.60
0		180	183.5	187.5	190	193
		$\cong$.104–1	$\cong$.206–1	$\cong$.408–1	$\cong$.656–1	$\cong$.111+0
		.107+0	.897–1	.740–1	.619–1	.615–1
4.5		188				
		~.419–2				
		.713–1				
4.75	186.5	188.5	192	196		
	~.106–1	~.477–2	~.125–1	~.217–1		
	.717–1	.689–1	.711–1	.788–1		
5		189	193			
		.534–2	~.121–1			
		.666–1	.692–1			
5.25		190				
		~.601–2				
		.642–1				
5.5		190				
		~.640–2				
		.612–1				
6		191				
		~.732–2				
		.569–1				
7		193				
		~.869–2				
		.469–1				

TABLE 26. (continued)

$$\frac{du}{}_{MAX}$$

dt_{MAN}	.025,.05	.05,.10	.10,.20	.15,.30	.20,.40	.30,.60
9		196 ~.129-1 .265-1				
10		200 ~.632-2 .165-1				
11		202 *.430-2 .767-2	203 .114-1 .224-1			
12		203 ~.117-1 .168-1				
14		207 ~.113-1 .368-1				

5.3 COMPARISON OF THE RESULTS OF THE VARIOUS GUIDANCE SCHEMES AMONG

THEMSELVES AND WITH PREVIOUS RESULTS

There are three forms in which results may be presented in writing:

prose, tables, and figures. All of these forms are used in this report.

The prose is used to make general statements or to amplify upon tables

or figures. Tables are used to convey sets of data at one time, such as

terminal errors. Figures are used to convey geometrical concepts or to

present time histories.

While the prose is necessary and the tables are adequate in a few

instances, the graphs are very compact, easily understood images of the

results. It is for this reason that emphasis is made on a graphical

presentation in lieu of reams of words or pages of tabular data. Thus a

detailed description of the plot combination and synthesis program is

presented before the results.

The purpose of this study is twofold: to compare the different

guidance schemes and reoptimization to each other -- and to compare

their performance, as determined here, with the results obtained in

previous studies. This study shows that reoptimization is, of course,

the most accurate technique, but that, for the smaller perturbations,

the other guidance schemes are clearly acceptable. Moreover, contrary

to what is indicated by the earlier research, the perturbation guidance

schemes do not diverge or perform ineffectively, but work rather well.

These results call into question the validity of the earlier comparisons.

5.3.1 The Plot Combination and Synthesis Program (PCSP)

This program takes as input, for a given case, the intermediate

plot files of the nominal and reoptimized trajectories from the

optimization program, the guided trajectory from the Time-To-Go Guidance

program, and the guided trajectory from the Minimum Distance Guidance

program. It produces a final plot file of at most 18 variables. These

variables may simply be those on the intermediate plot files (described in

Subsections 3.1.1.4 and 5.2.1.3), perhaps interpolated to appropriate

time points, or they may be differences of variables or vectors of vari-

ables from various intermediate plot files. These variables and differ-

ences are listed in Table 27.

The intermediate plot file records are typically written at one day

intervals. The PCSP can write records on the final plot file at any

common multiple of the intermediate plot file intervals. One day is

usually used. As mentioned in Subsection 5.2.1.3, the $\underline{u}$-related variables

are not available at the regular output points in the guidance programs

and so must be interpolated to these regular points for the final plot

file. A JPL variable order Lagrangian interpolation routine is used for

this purpose. For plots of $\underline{u}$ itself, linear interpolation provides ample

resolution -- higher order interpolations yield plots that are indiscern-

ible from the linear interpolation plots. For plots of differences in

values of $\underline{u}$ between the guidance schemes and reoptimization, higher order

interpolation is crucial to an accurate representation of the data. At a

minimum, order 5 is needed to smooth out "interpolation noise." In

general, the final times for the various techniques are slightly different

for a given case. The variables are, therefore, linearly interpolated to

the reoptimized final time for plotting purposes.

The need to combine information from several programs into the final

plot file adds complexity to the task of comparing guidance scheme

TABLE 27.   VARIABLES OBTAINABLE FROM THE PLOT

COMBINATION AND SYNTHESIS PROGRAM

NOMINAL TRAJECTORY $-$ t, h, u_1, u_1, x_1, x_2, x_3, x_4, x_5, x_6, x_{M_1}, x_{M_2},

x_{M_3}, x_{M_4}, x_{M_5}, x_{M_6}, ψ_1, ψ_2, ψ_3, ψ_4, ψ_5, ψ_5, $|\underline{\psi}_v|$, $|\underline{\psi}_r|$

REOPTIMIZED TRAJECTORY $-$ Same as nominal trajectory

TTG GUIDANCE $-$ t, h, t_{p_I}, t_I, dt, u_{N_1}, u_{N_2}, δu_1, δu_2, du_1, du_2,

u_1, u_2, x_1, x_2, x_3, x_4, x_5, x_6, δx_1, δx_2, δx_3, δx_4, δx_5,

δx_6, x_{M_1}, x_{M_2}, x_{M_3}, x_{M_4}, x_{M_5}, x_{M_6}, ψ_1, ψ_2, ψ_3, ψ_4,

ψ_5, ψ_6, $|\underline{\psi}_v|$, $|\underline{\psi}_r|$

MD GUIDANCE $-$ Same as TTG Guidance

DIFFERENCES BETWEEN TRAJECTORIES

$$\Delta u_i^{T,M} = u_i^{T,M} - u_i^R$$

$$\delta u_i = u_i^R - u_i^N$$

$$\Delta \delta u_i^{T,M} = \delta u_i^{T,M} - [u_i^R - u_i^N]$$

$$\Delta x_i^{T,M} = x_i^{T,M} - x_i^R$$

$$\delta x_i = x_i^R - x_i^N$$

$$\Delta \delta x_i^{T,M} = \delta x_i^{T,M} - [x_i^R - x_i^N]$$

TABLE 27. (continued)

DIFFERENCES BETWEEN TRAJECTORIES (continued)

$$\Delta \psi_i^{T,M} = \psi_i^{T,M} - \psi_i^R$$

$$\Delta |\underline{\psi}_{v,r}^{T,M}| = |\underline{\psi}_{v,r}^{T,M}| - |\underline{\psi}_{v,r}^R|$$

$$|(\underline{\Delta x})_{v,r}|^{T,M} = \sqrt{\sum_{v,r} (x_i^{T,M} - x_i^R)^2}$$

$$|(\underline{\Delta \psi})_{v,r}|^{T,M} = \sqrt{\sum_{v,r} (\psi_i^{T,M} - \psi_i^R)^2}$$

where

$(\ )^N$ — from the nominal trajectory

$(\ )^R$ — from the reoptimized trajectory

$(\ )^T$ — from the Time-To-Go trajectory

$(\ )^M$ — from the Minimum Distance trajectory

performance. The correct variables from the right records must be read

from the appropriate intermediate plot files at the proper time, perhaps

interpolated and/or differenced, and then written correctly on the appro-

priate record of the final plot file. Many such final plot files can be

generated for each case.

5.3.2 Time-To-Go Guidance vs. Minimum Distance Guidance vs. Reoptimization

Tables 28-30 present the terminal errors and final times of the

cases studied for Reoptimization (REO), Time-To-Go Guidance (TTG),

Minimum Distance Guidance with Weight 1 (MD1), and Minimum Distance

Guidance with Weight 3 (MD3). Recall that, for Reoptimization, the speci-

fied accuracy required for convergence is 1×10^{-9} in each normalized

component of $[\underline{x}(t_o)-\underline{x}_o],\underline{\psi}$, and Ω. For some cases, the last iteration in

the Reoptimization program produced a much more accurate solution than

specified. It is felt that for all the cases, a specified accuracy of

at least 10^{-11} in each normalized component is readily achievable by

Reoptimization.

The tables show that Reoptimization always produces the lowest final

time, i.e., it minimizes the performance the best. However, for the

smaller perturbations, the three guidance schemes differ from Reoptimiza-

tion by less than 1 second in final time and in no case (other than the

large perturbation case of $\delta x_1(0) = .5 \times 10^{-3}$ (AU/DAY)) is the difference

more than 2 minutes.

The perturbation guidance schemes also exhibit very good performance,

as measured by terminal error, especially for the smaller perturbations.

Time-To-Go Guidance exhibits no clear advantage over either Minimum

Distance Guidance scheme, and the two variations of Minimum Distance

TABLE 28. FINAL TIMES AND TERMINAL ERRORS FOR THE

DIFFERENT TECHNIQUES (REO, TTG, MD1, MD3) FOR PERTURBATIONS IN x_1

$$\delta x_1(0) \ (AU/day)$$

	$-.4-4$	$-.1-4$	$.5-5$	$.5-4$	$.5-3$
REO					
t_f(days)	196.381561	196.657348	196.796813	197.221634	202.077910
$\lvert\underline{\psi}_v\rvert$(AU/day)	.22-13	.16-10	.24-11	.26-13	.61-11
$\lvert\underline{\psi}_r\rvert$(AU)	.15-13	.91-11	.90-12	.15-13	.23-11
TTG					
t_f(days)	196.38294	196.65740	196.79682	197.2230	DID
$\lvert\underline{\psi}_v\rvert$(AU/day)	.18-8	.83-9	.41-9	.19-7	NOT
$\lvert\underline{\psi}_r\rvert$(AU)	.42-5	.27-6	.68-7	.74-5	WORK
MD1					
t_f(days)	196.38292	196.65740	196.79682	197.22315	
$\lvert\underline{\psi}_v\rvert$(AU/day)	.17-7	.90-9	.24-9	.50-7	POOR
$\lvert\underline{\psi}_r\rvert$(AU)	.42-5	.27-6	.68-7	.70-5	RESULTS
MD3					
t_f(days)	196.38292	196.65740	196.79682	197.22314	
$\lvert\underline{\psi}_v\rvert$(AU/day)	.17-7	.98-9	.24-9	.50-7	POOR
$\lvert\underline{\psi}_r\rvert$(AU)	.42-5	.27-6	.68-7	.70-5	RESULTS

TABLE 29. FINAL TIMES AND TERMINAL ERRORS FOR THE

DIFFERENT TECHNIQUES (REO, TTG, MD1, MD3) FOR PERTURBATIONS IN x_4

$$\delta x_4(0) \ (AU)$$

	-.21-2	-.3-3	.5-5	.5-4	.3-3	.5-3	.33-2
REO							
t_f-196(days)	.851708	.764504	.749969	.747831	.735977	.726528	.597396
$|\underline{\psi}_v|$ (AU/day)	.83-14	.21-11	.28-10	.35-12	.75-12	.33-11	.55-13
$|\underline{\psi}_r|$ (AU)	.35-14	.84-12	.74-11	.13-12	.25-12	.15-11	.21-13
TTG							
t_f-196(days)	.85185	.764506	.749969	.747831	.735979	.726532	.5978
$|\underline{\psi}_v|$ (AU/day)	.33-7	.61-9	.97-12	.11-10	.44-9	.13-8	.28-7
$|\underline{\psi}_r|$ (AU)	.59-6	.67-8	.25-10	.20-9	.68-8	.19-7	.12-5
MD1							
t_f-196(days)	.85186	.764506	.749969	.747831	.735979	.726534	.598
$|\underline{\psi}_v|$ (AU/day)	.58-6	.15-9	.65-12	.18-10	.63-9	.18-8	.91-7
$|\underline{\psi}_r|$ (AU)	.53-6	.65-8	.24-10	.20-9	.92-8	.31-7	.27-5
MD3							
t_f-196(days)	.85184	.764506	.749969	.747831	.735979	.726532	.598
$|\underline{\psi}_v|$ (AU/day)	.59-6	.13-9	.99-12	.20-10	.58-9	.19-8	.83-7
$|\underline{\psi}_r|$ (AU)	.54-6	.65-8	.21-10	.20-9	.95-8	.25-7	.26-5

TABLE 30. FINAL TIMES AND TERMINAL ERRORS FOR THE

DIFFERENT TECHNIQUES (REO, TTG, MD3) FOR PERTURBATIONS IN x_3 AND x_6

	$\delta x_3(0)$ (AU/day)		$\delta x_6(0)$ (AU)	
	$-.35-4$	$.35-4$	$-.27-2$	$.33-2$
REO				
t_f-196 (days)	.772654	.729269	.752546	.744660
$\left\|\underline{\psi}_v\right\|$ (AU/day)	.32-10	.24-10	.20-14	.76-14
$\left\|\underline{\psi}_r\right\|$ (AU)	.27-10	.23-10	.11-14	.22-14
TTG				
t_f-196 (days)	.773035	.72941	.752548	.744663
$\left\|\underline{\psi}_v\right\|$ (AU/day)	.68-8	.68-8	.63-10	.14-9
$\left\|\underline{\psi}_r\right\|$ (AU)	.37-7	.42-7	.20-9	.99-9
MD3				
t_f-196 (days)	.77274	.72934	.752548	.744663
$\left\|\underline{\psi}_v\right\|$ (AU/day)	.96-8	.98-8	.61-11	.11-9
$\left\|\underline{\psi}_r\right\|$ (AU)	.14-6	.15-6	.24-9	.12-8

Guidance are virtually identical in performance. Similarly, Minimum

Distance Guidance exhibits no clear advantage over Time-To-Go Guidance.

Figures 8-47 are plots of the deviations in velocity, $|(\underline{\Delta x})_v|$,

position $|(\underline{\Delta x})_r|$, out-of-plane control angle, Δu_1, and in-plane control

angle, Δu_2, for Time-To-Go Guidance (TTG) and Minimum Distance Guidance

with Weight 3 (MD3). The cases shown are all of those studied (those

with a * in Tables 11-25) with initial perturbations in x_1 and x_4, except

for $\delta x_4(0) = .3 \times 10^{-3}$ AU, which is similar to $\delta x_4(0) = .5 \times 10^{-3}$ AU,

and the case $\delta x_1(0) = .5 \times 10^{-3}$ AU/day, which is discussed later. The

deviations are with respect to the reoptimized solution, as defined in

Table 27. Deviations of Time-To-Go Guidance are depicted with a solid

line and the symbol TTG. Deviations of Minimum Distance Guidance with

Weight 3 are depicted by a line composed of short dashes and the symbol

MD3. On the abscissa is the time scale, which is the same for all the

plots. Along the ordinate is the deviation, scaled to provide maximum

resolution.

Very evident upon first inspection is the similarity in behavior

of the two perturbation guidance schemes. In fact, in most cases the

two plot symbols are superposed. The cases of small perturbations

$(\delta x_4(0) = .5 \times 10^{-5}, .5 \times 10^{-4}$ AU) show very small deviations from the

reoptimized trajectories, which, in fact, almost get lost in "integration

noise," especially near the final time.

All of the state deviation plots, except for the two sets of devi-

ations lost in "integration noise," exhibit two common characteristics:

the maximum excursion occurs after the thrust reversal, near the middle

of the flight, and the deviation at the final time is much less than the

maximum excursion. Moreover, all the plots in position and in velocity
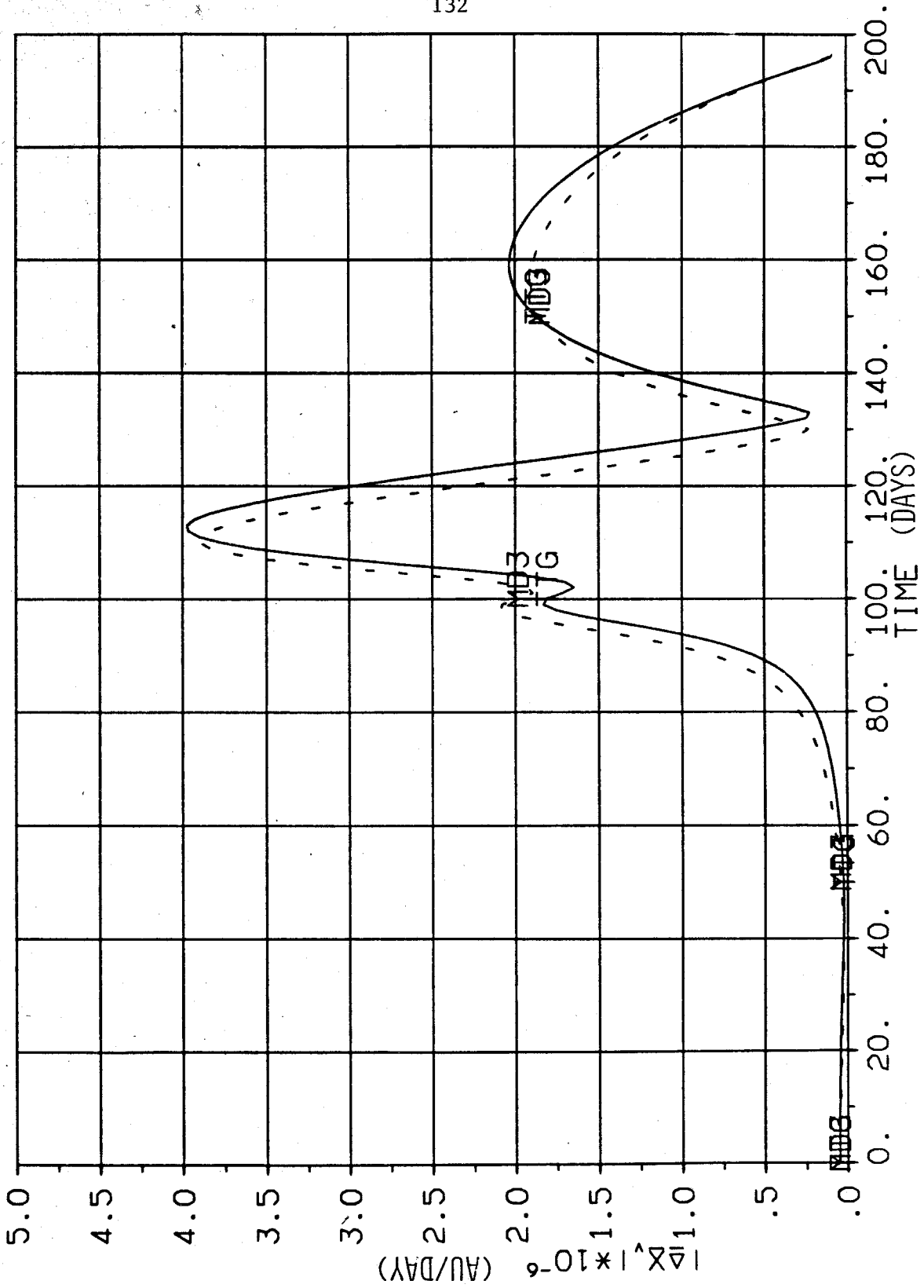
FIGURE 8. VELOCITY DEVIATIONS, $\delta x_1(0) = -.4-4$ AU/DAY
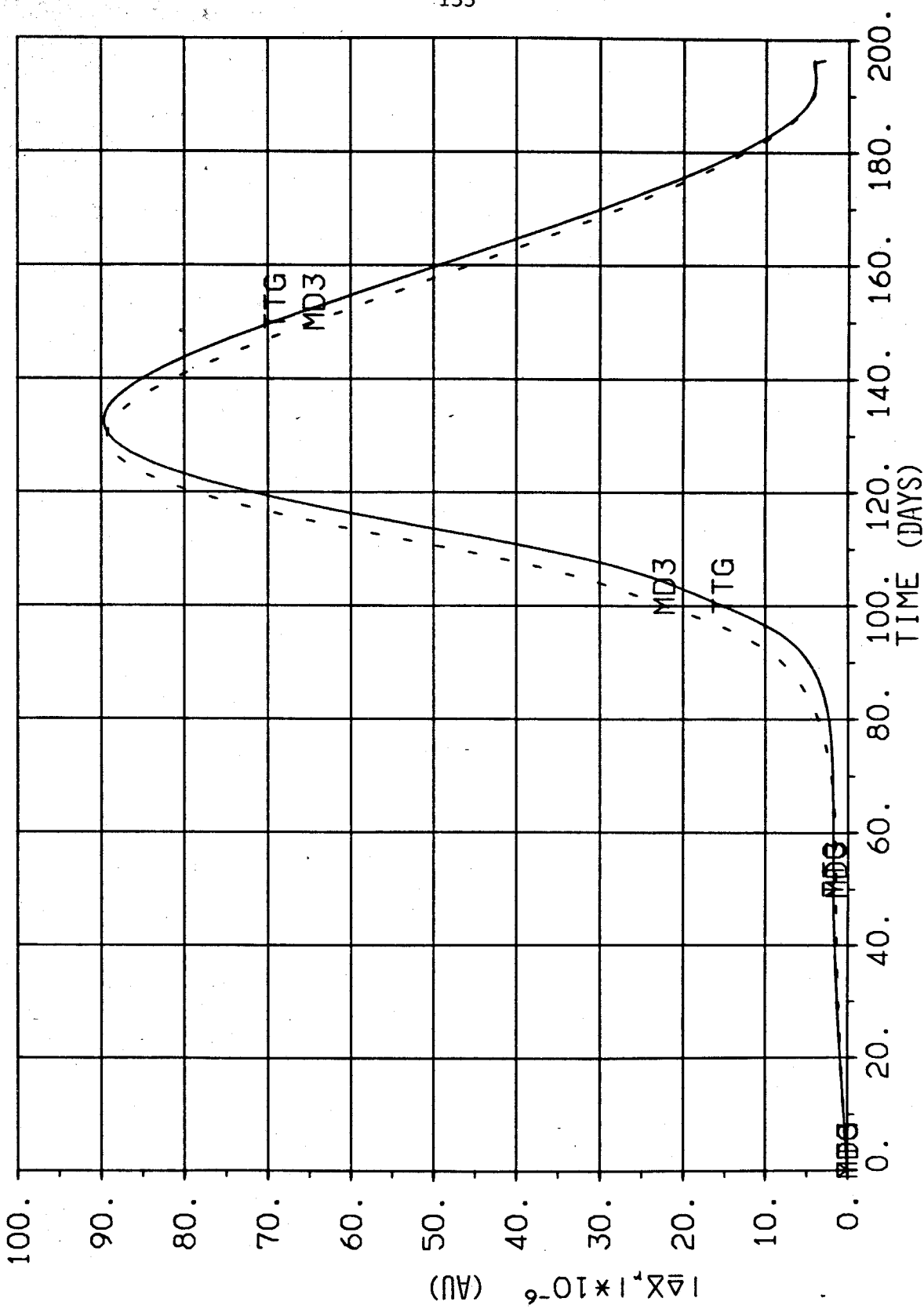
FIGURE 9, POSITION DEVIATIONS, $\delta x_1(J) = -.4\text{-}4$ AU/DAY
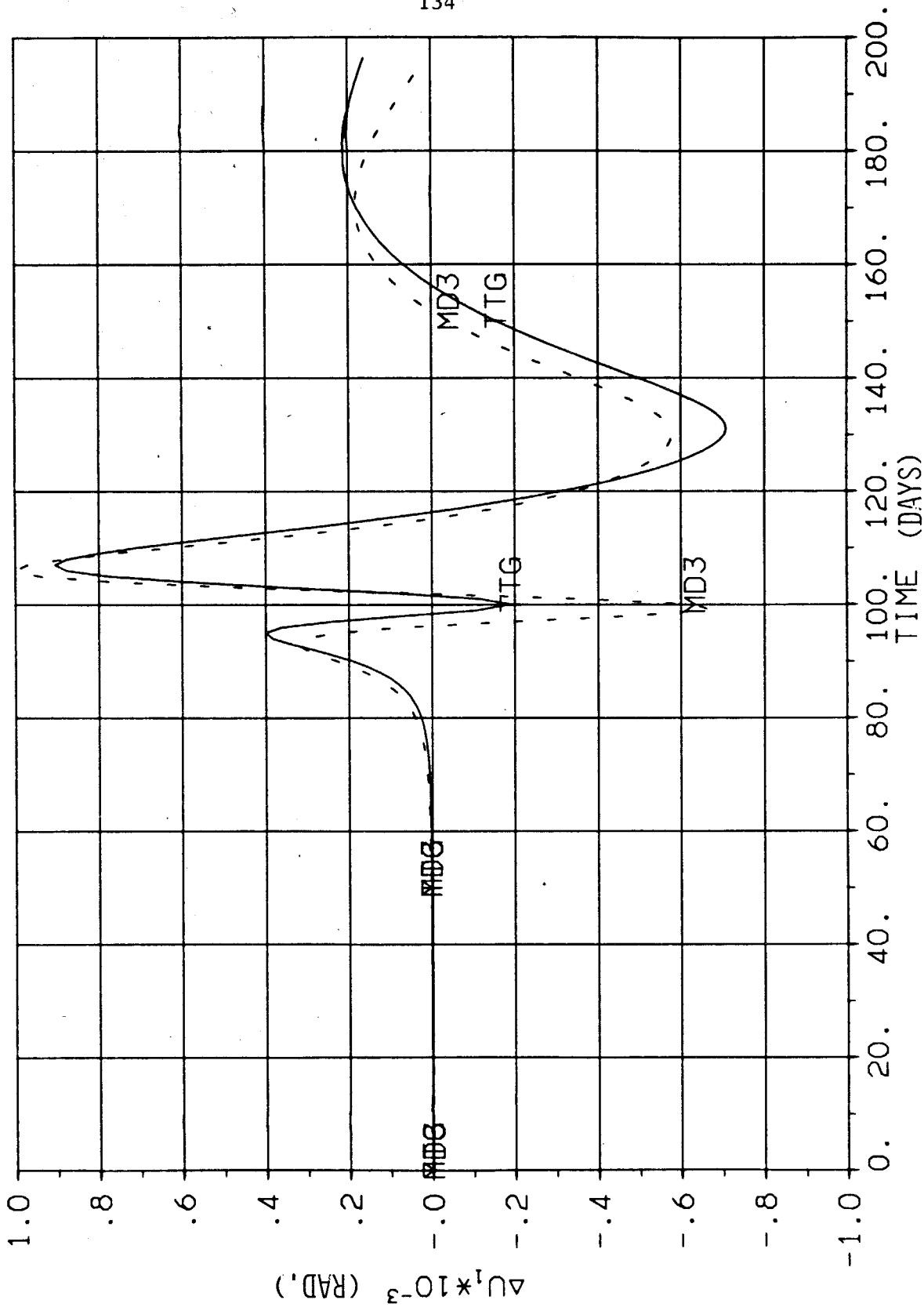
FIGURE 10. OUT-OF-PLANE CONTROL ANGLE DEVIATIONS, $\delta x_1(0) = -.4\text{-}4$ AU/DAY
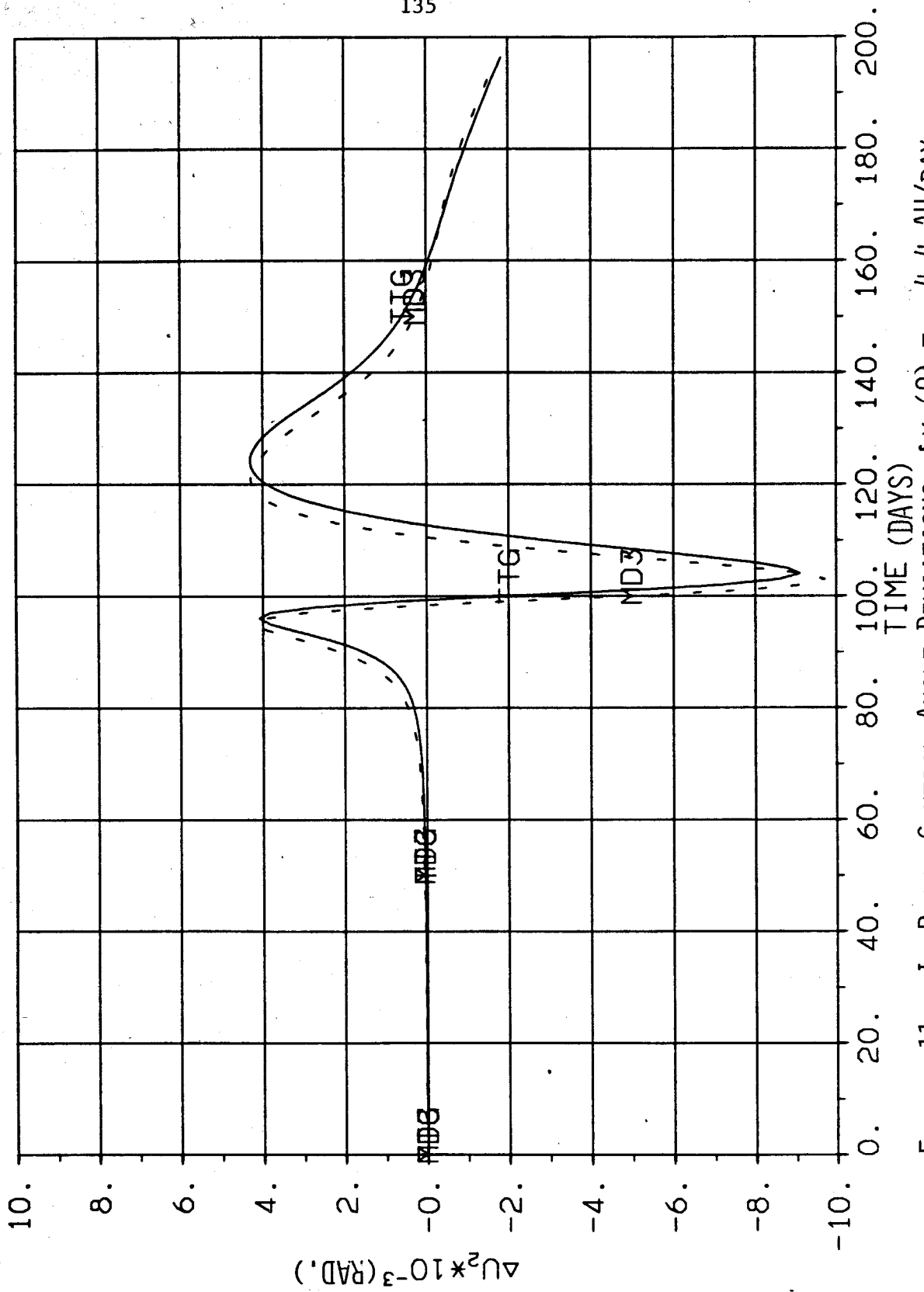
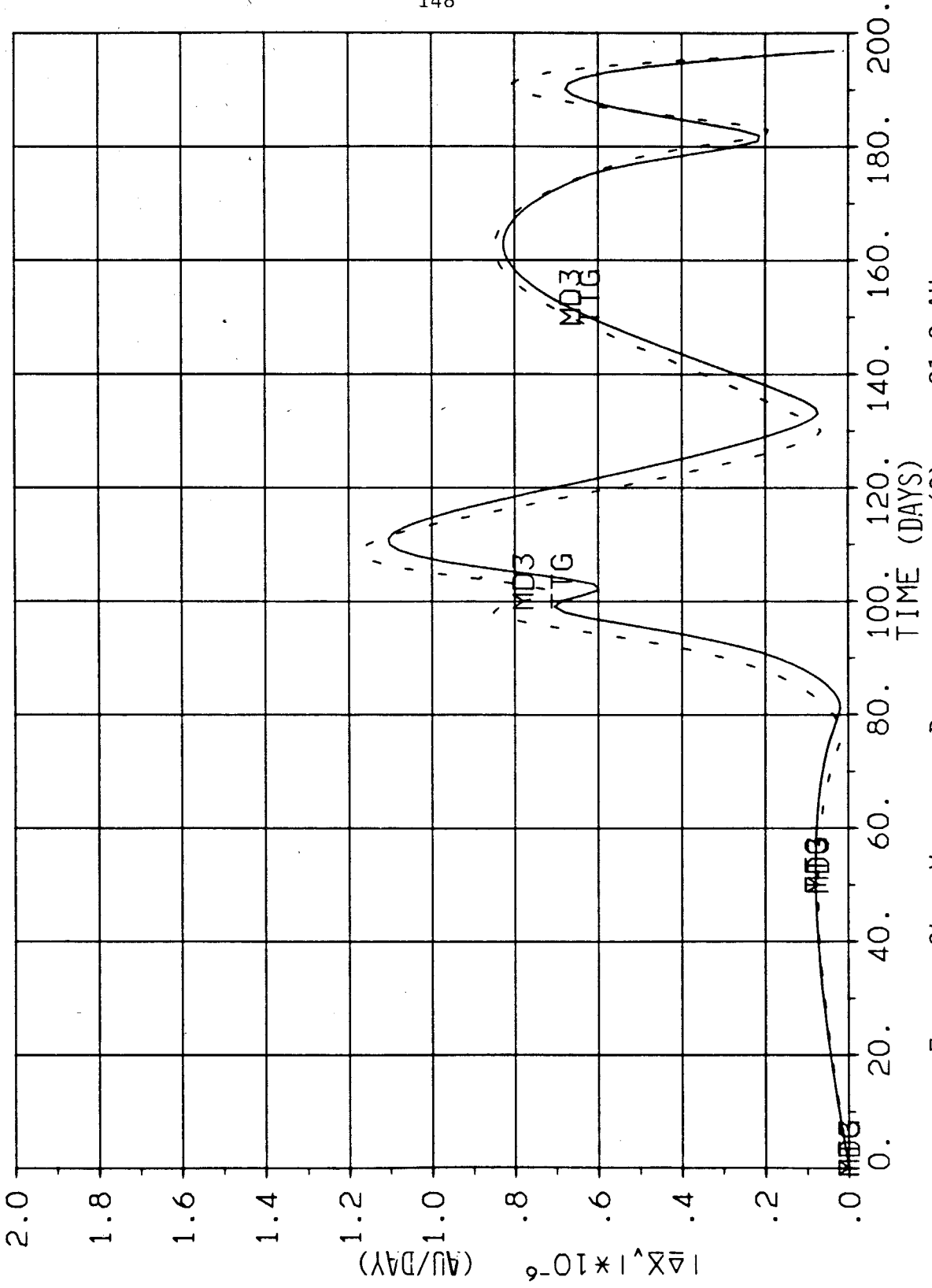FIGURE 11. IN-PLANE CONTROL ANGLE DEVIATIONS, $\delta x_1(0) = -.4-4$ AU/DAY
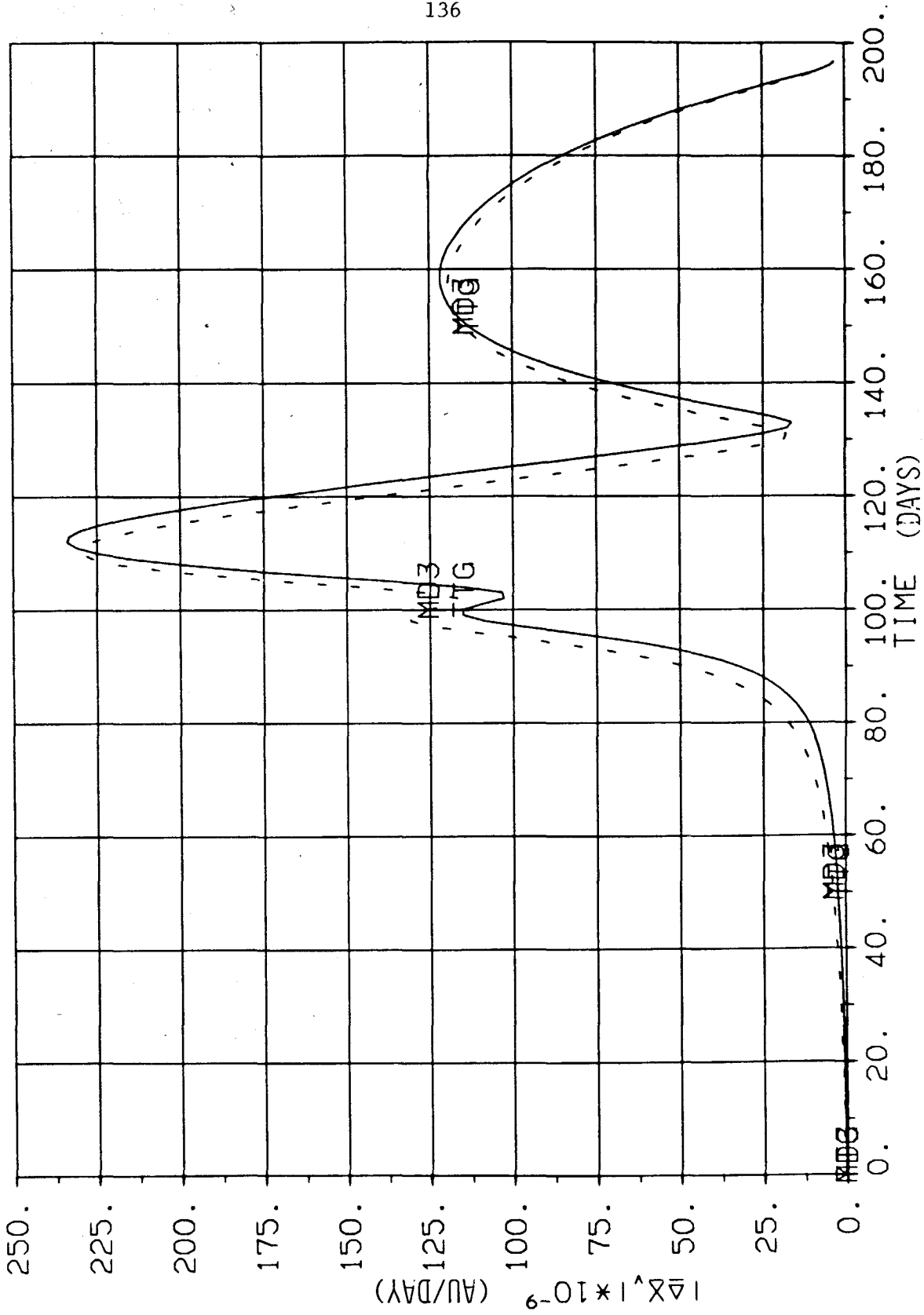
FIGURE 12. VELOCITY DEVIATIONS, $\delta x_1(0) = -.1\text{-}4$ AU/DAY
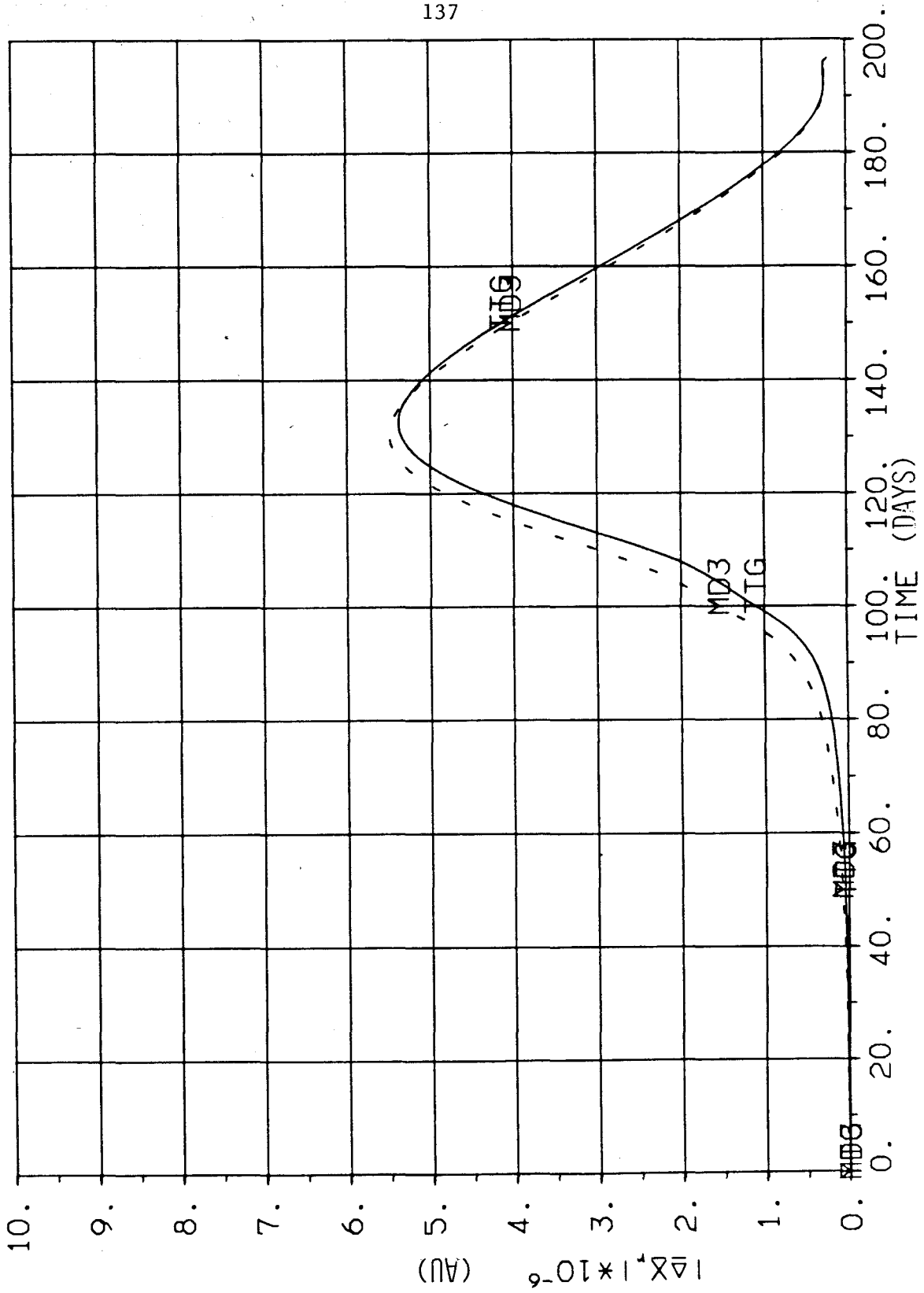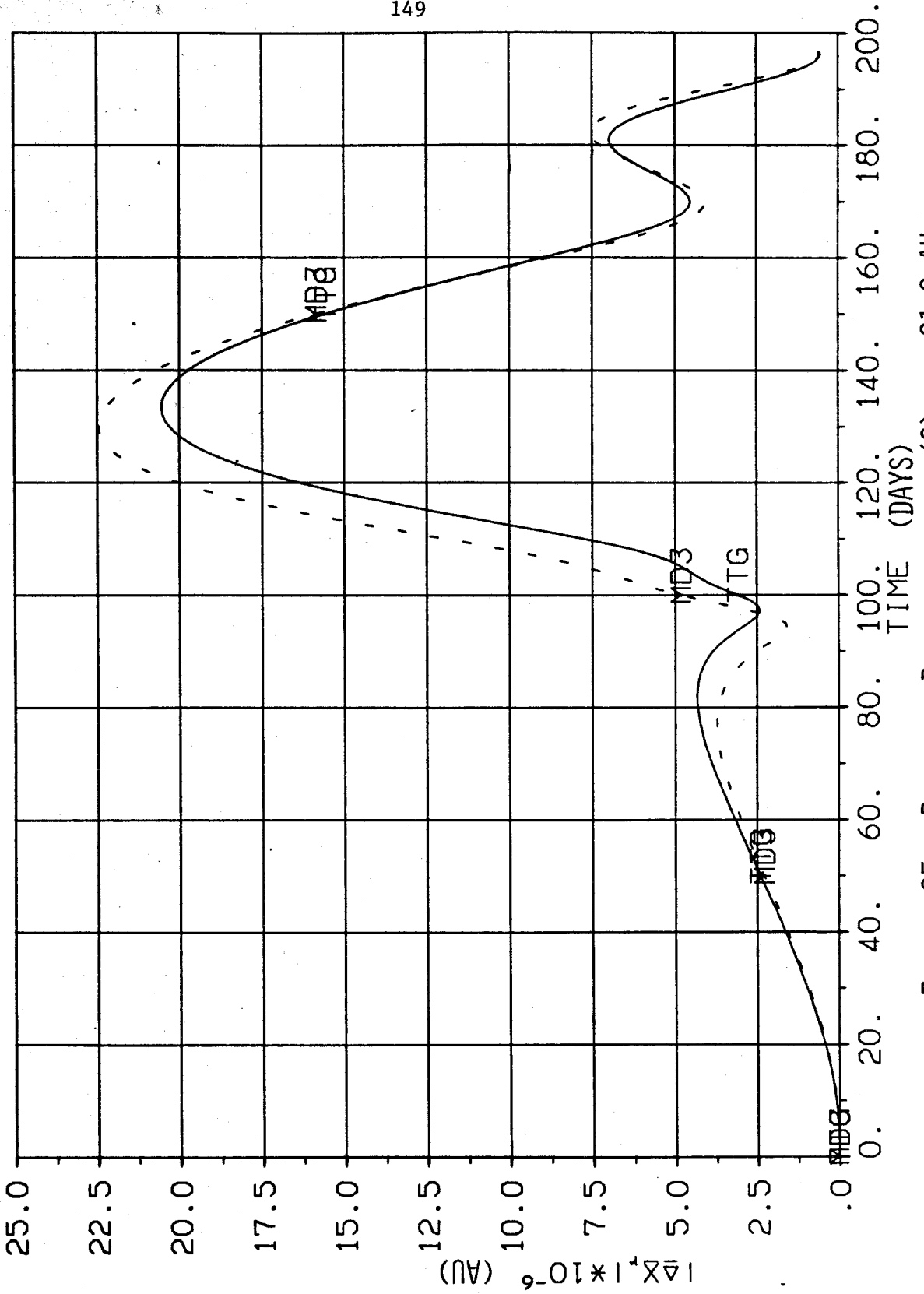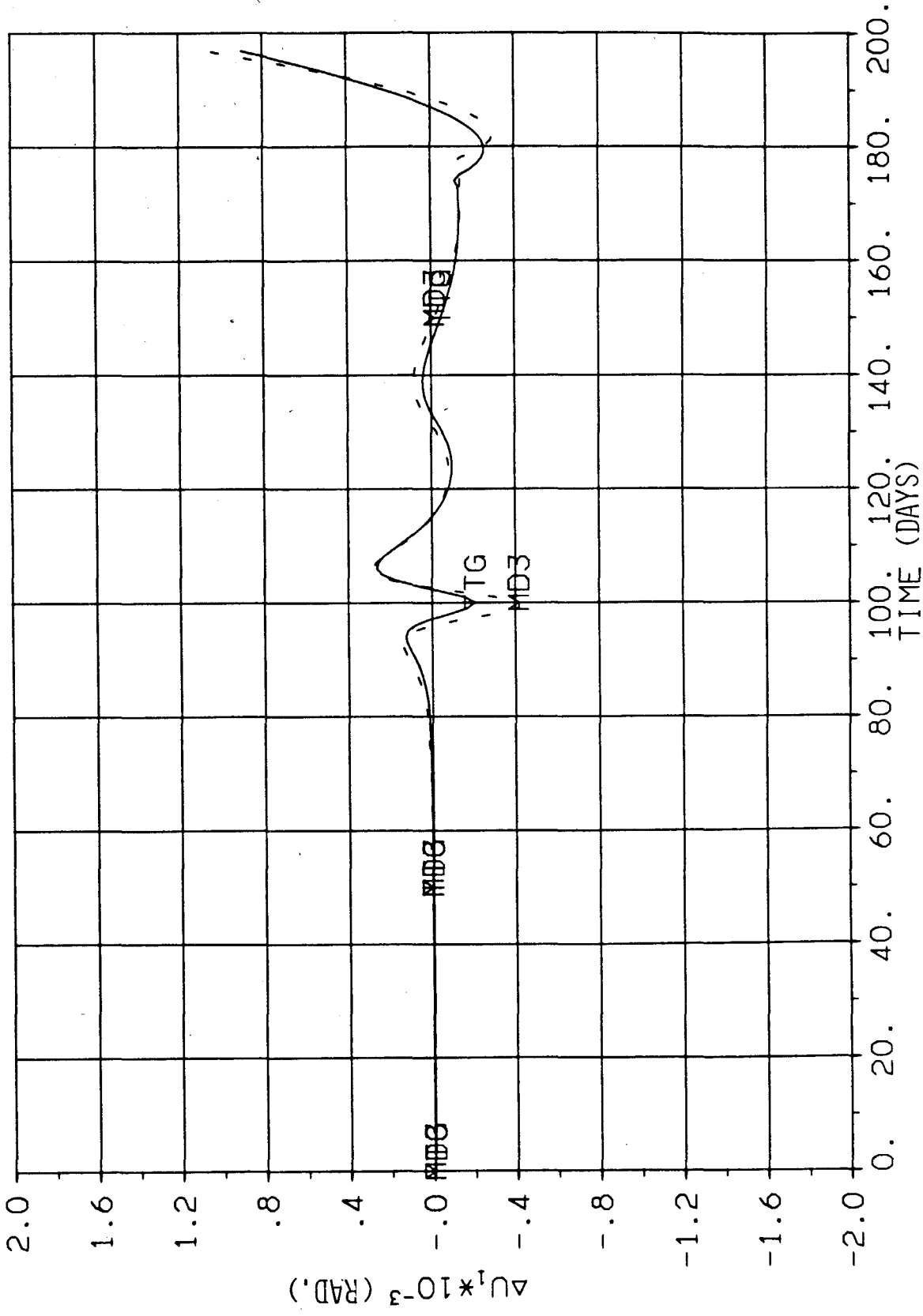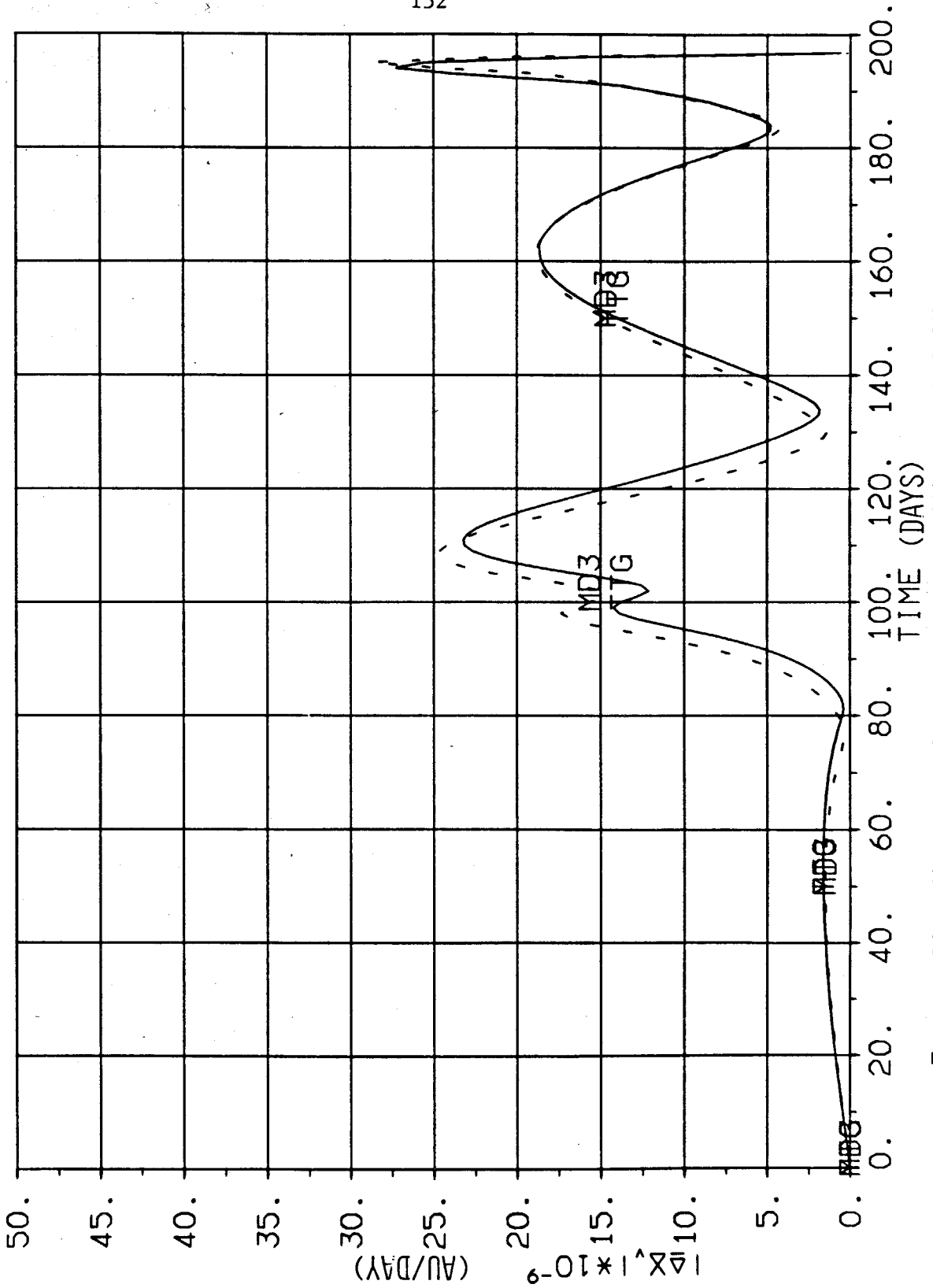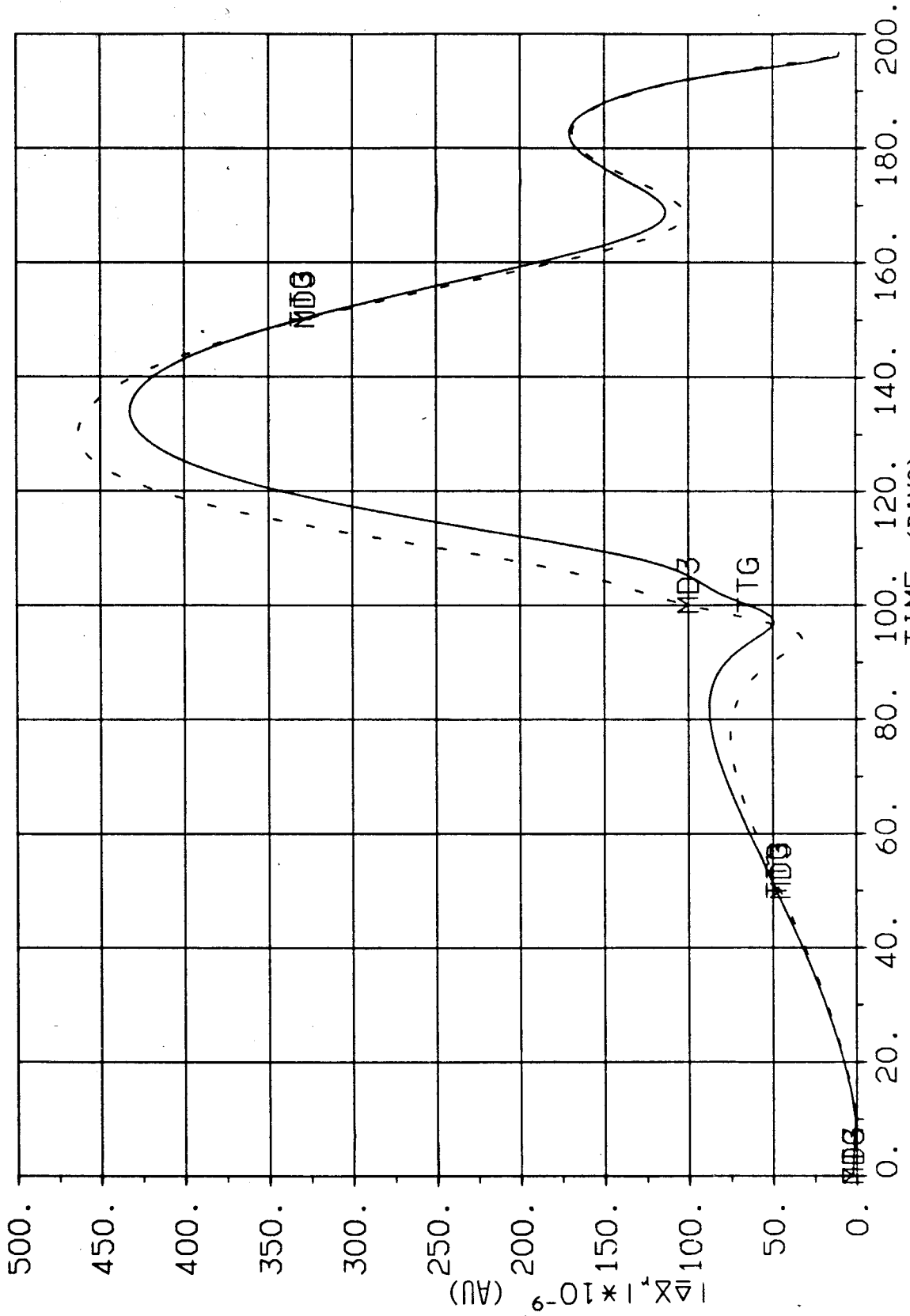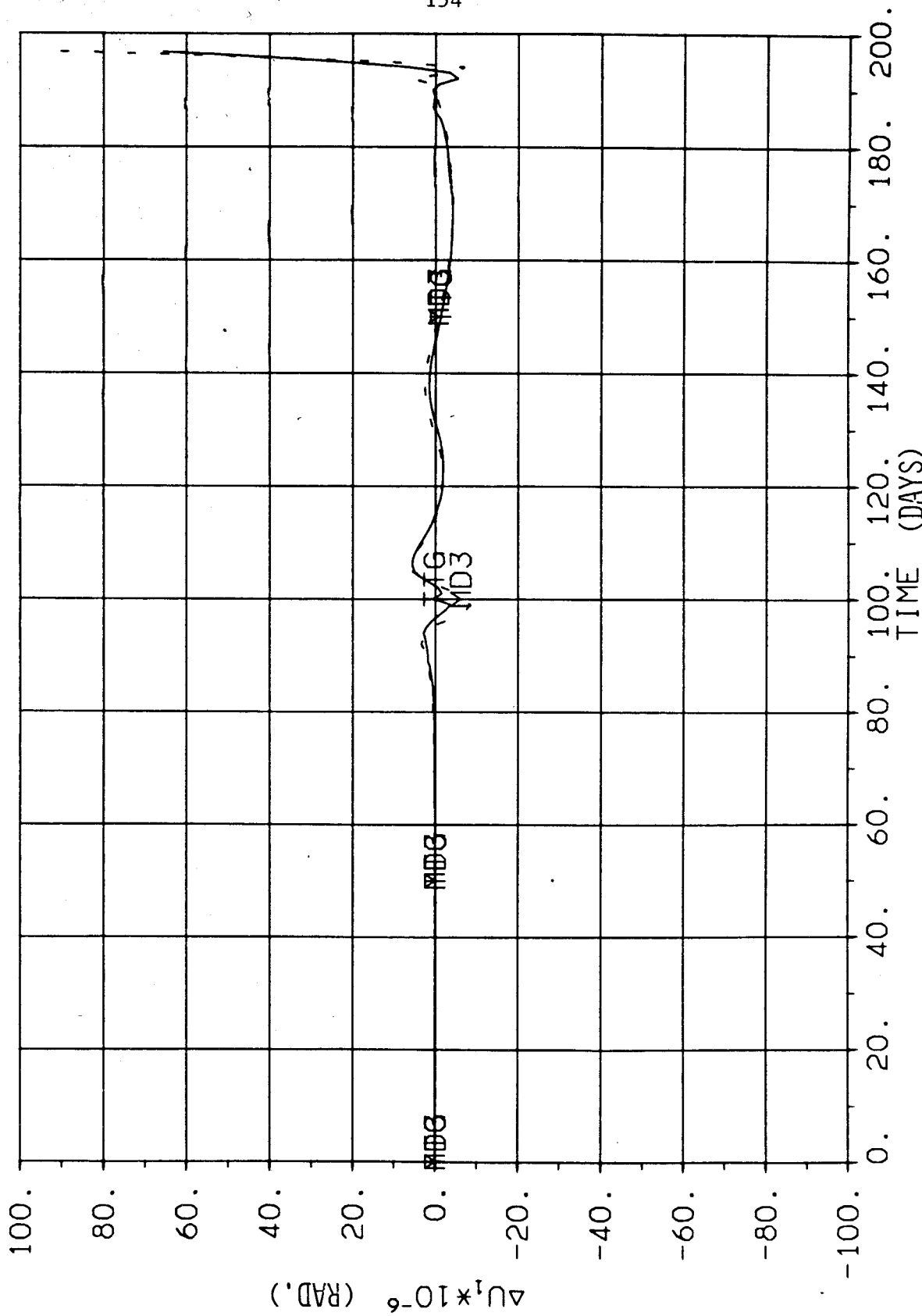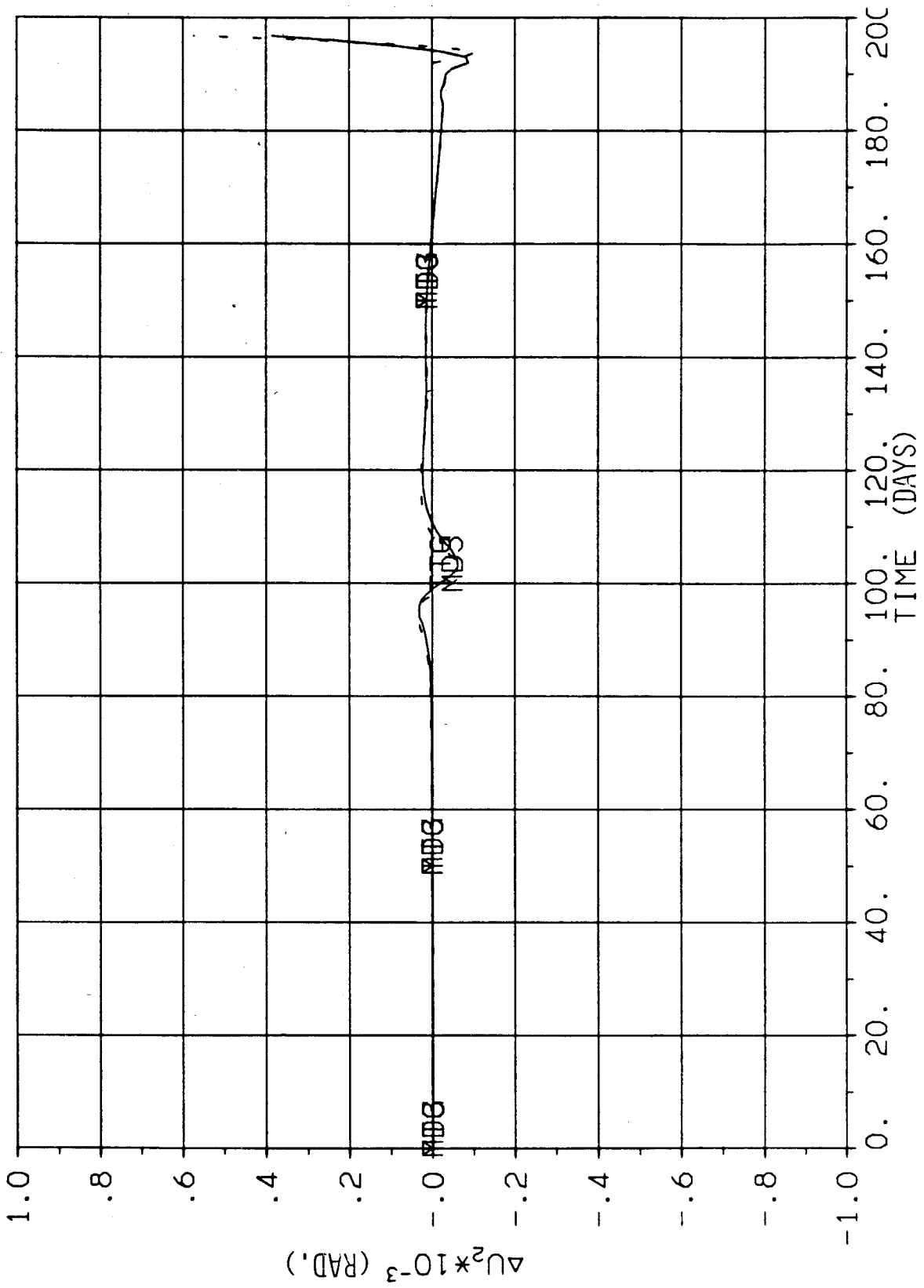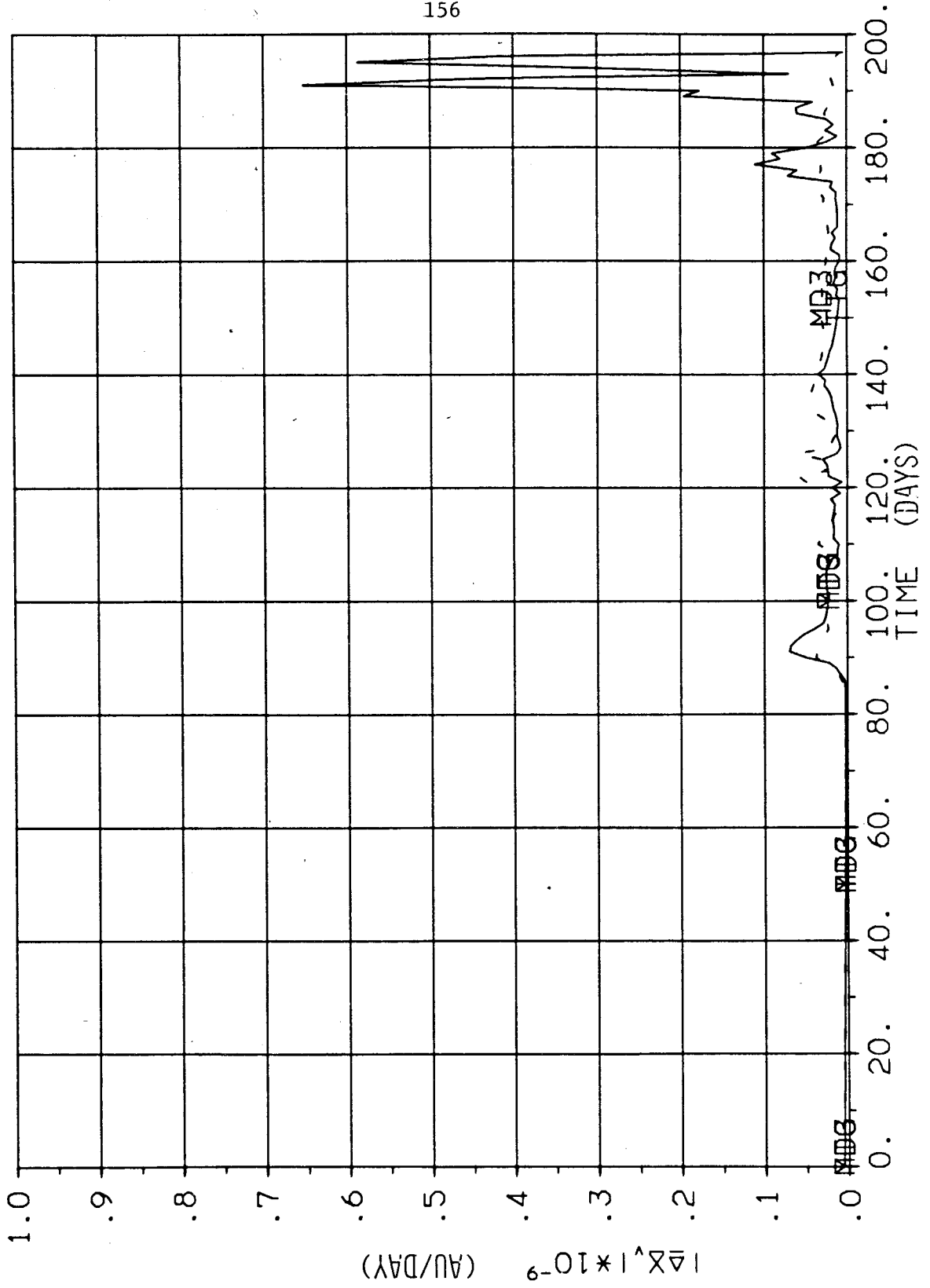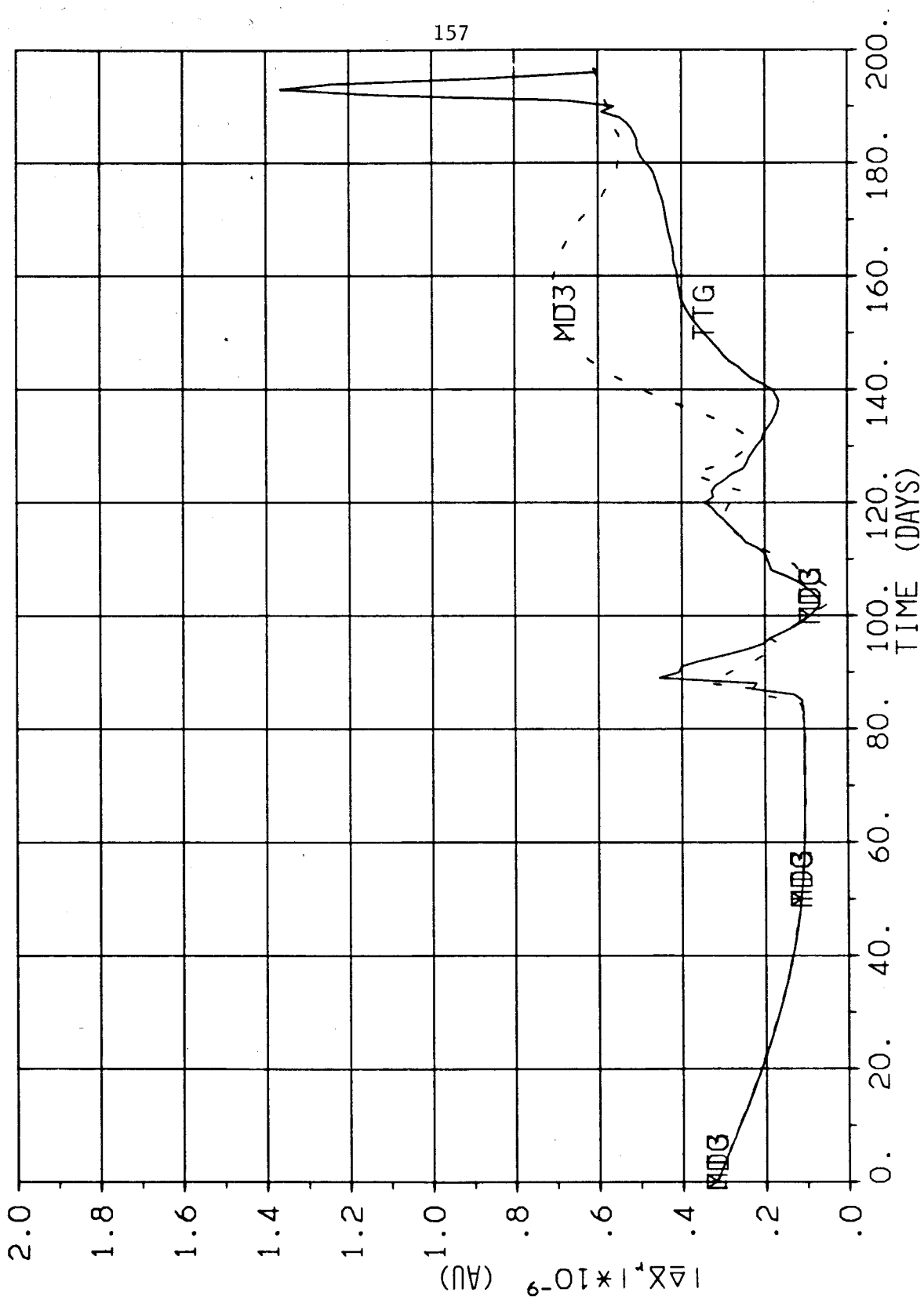
FIGURE 13. POSITION DEVIATIONS, $\delta x_1(0) = -.1-4$ AU/DAY
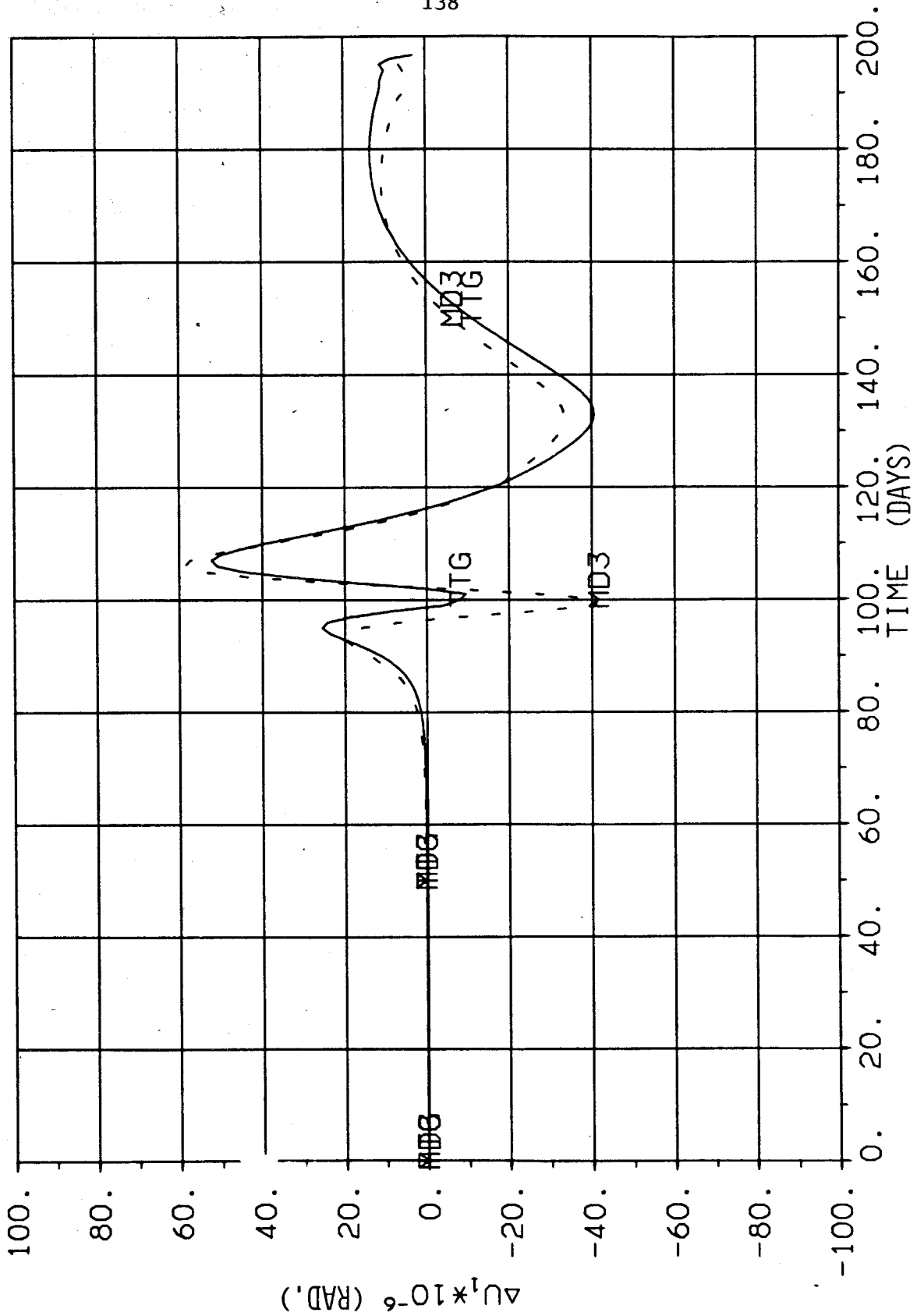
FIGURE 14. OUT-OF-PLANE CONTROL ANGLE DEVIATIONS, $\delta x_1('') = -.1 - 4$ AU/DAY
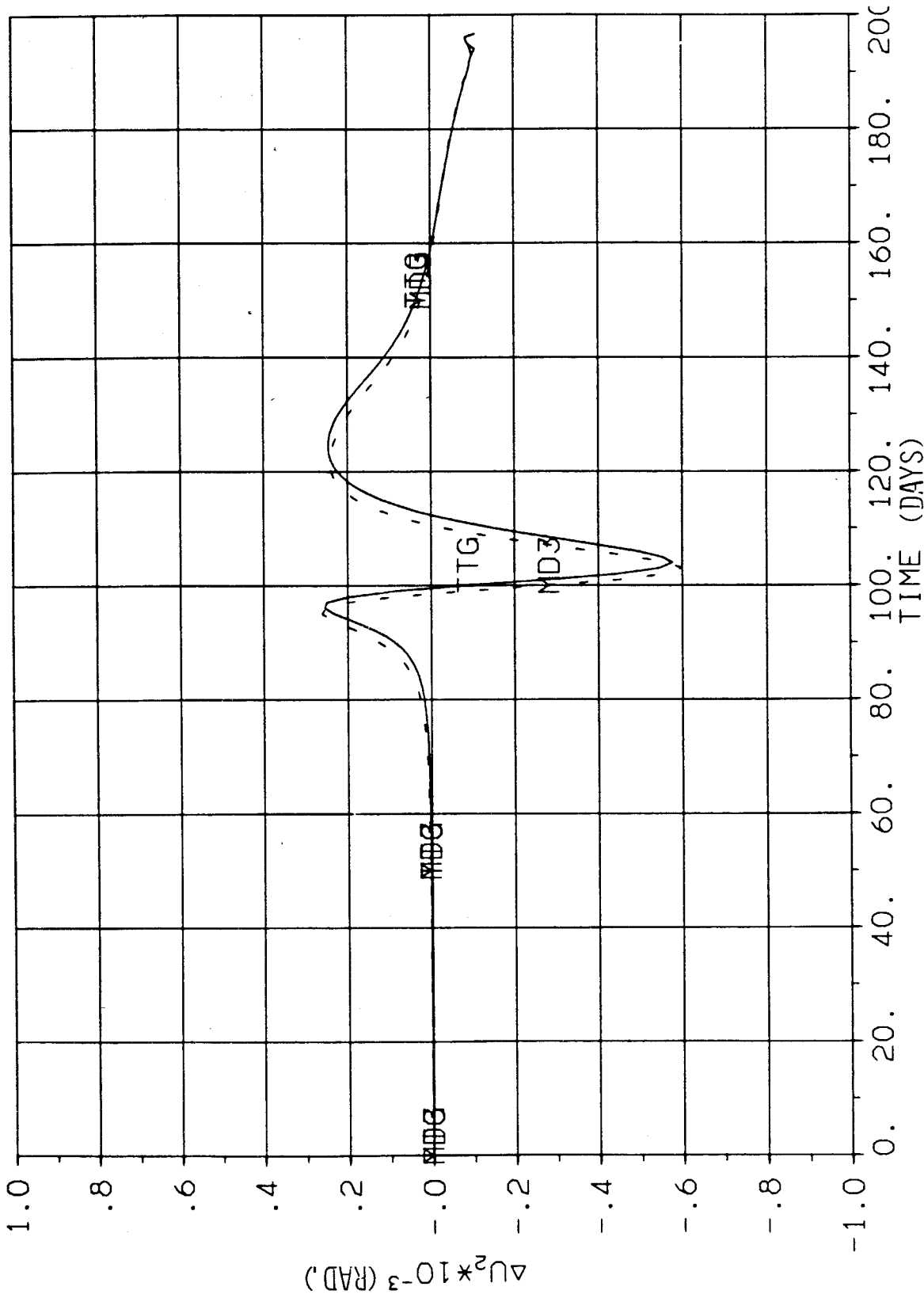
FIGURE 15. IN-PLANE CONTROL ANGLE DEVIATIONS, $\delta x_1(0) = -.1$-4 AU/DAY
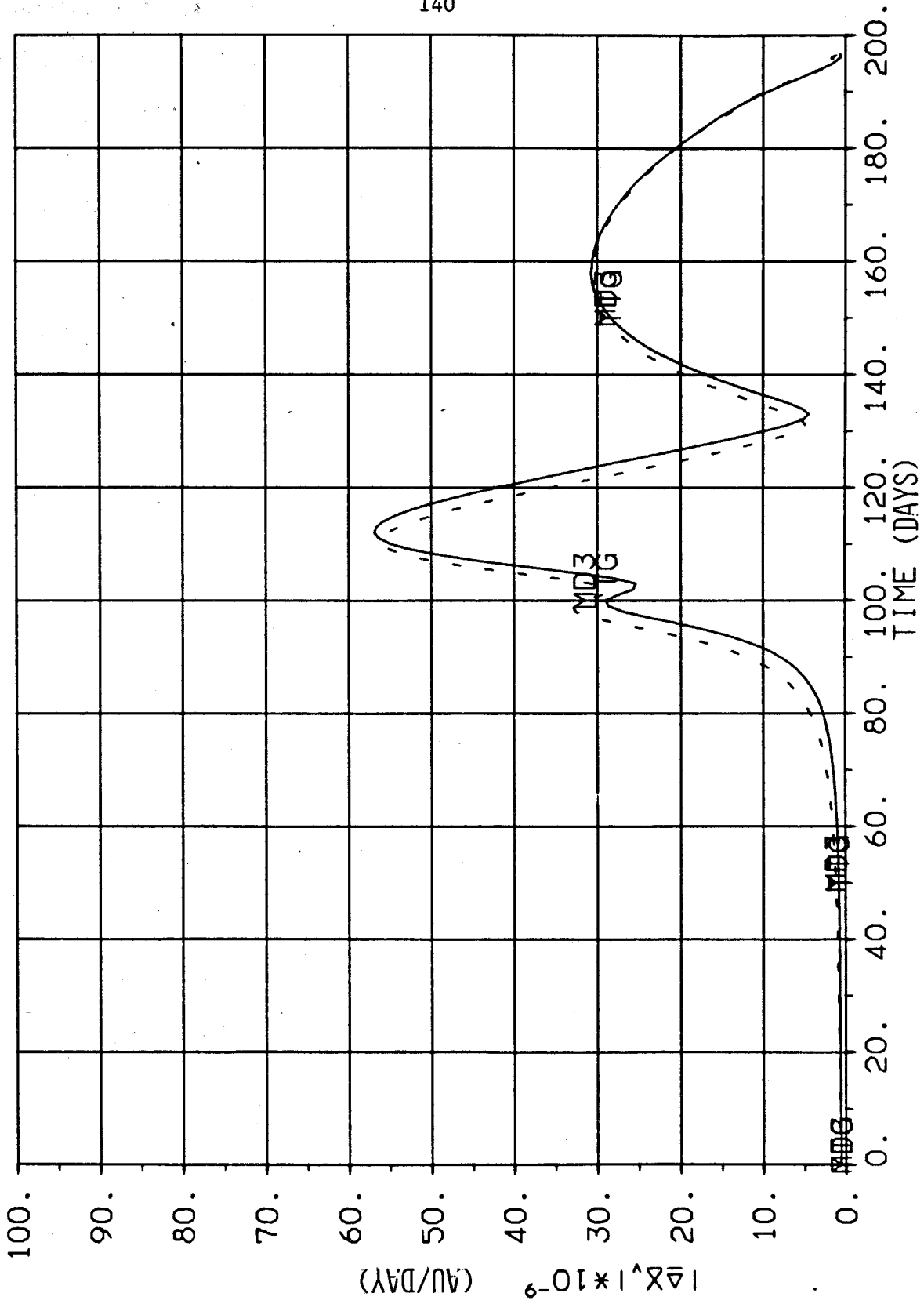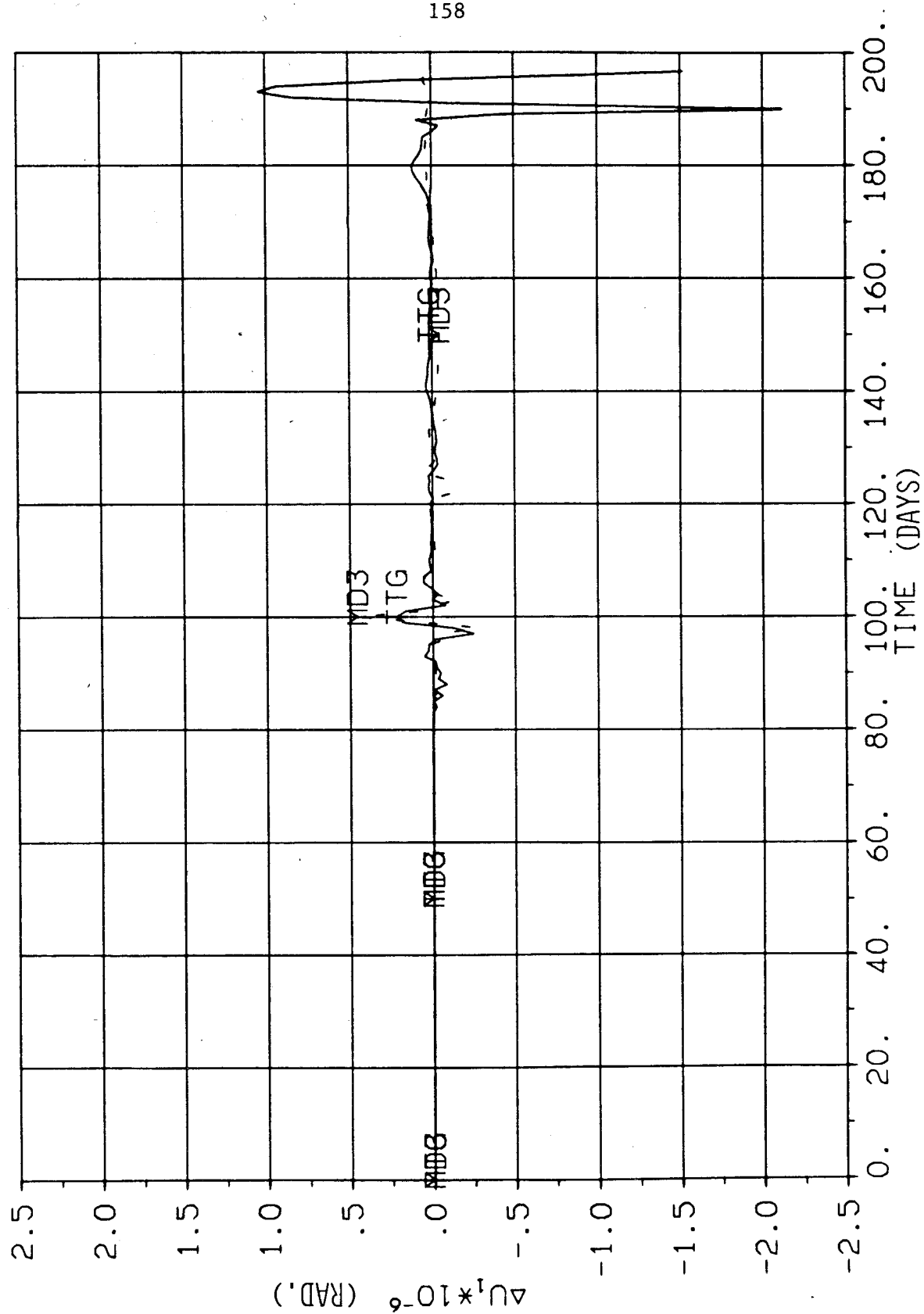
FIGURE 16. VELOCITY DEVIATIONS, $\delta x_1(0) = .5\text{-}5$ AU/DAY
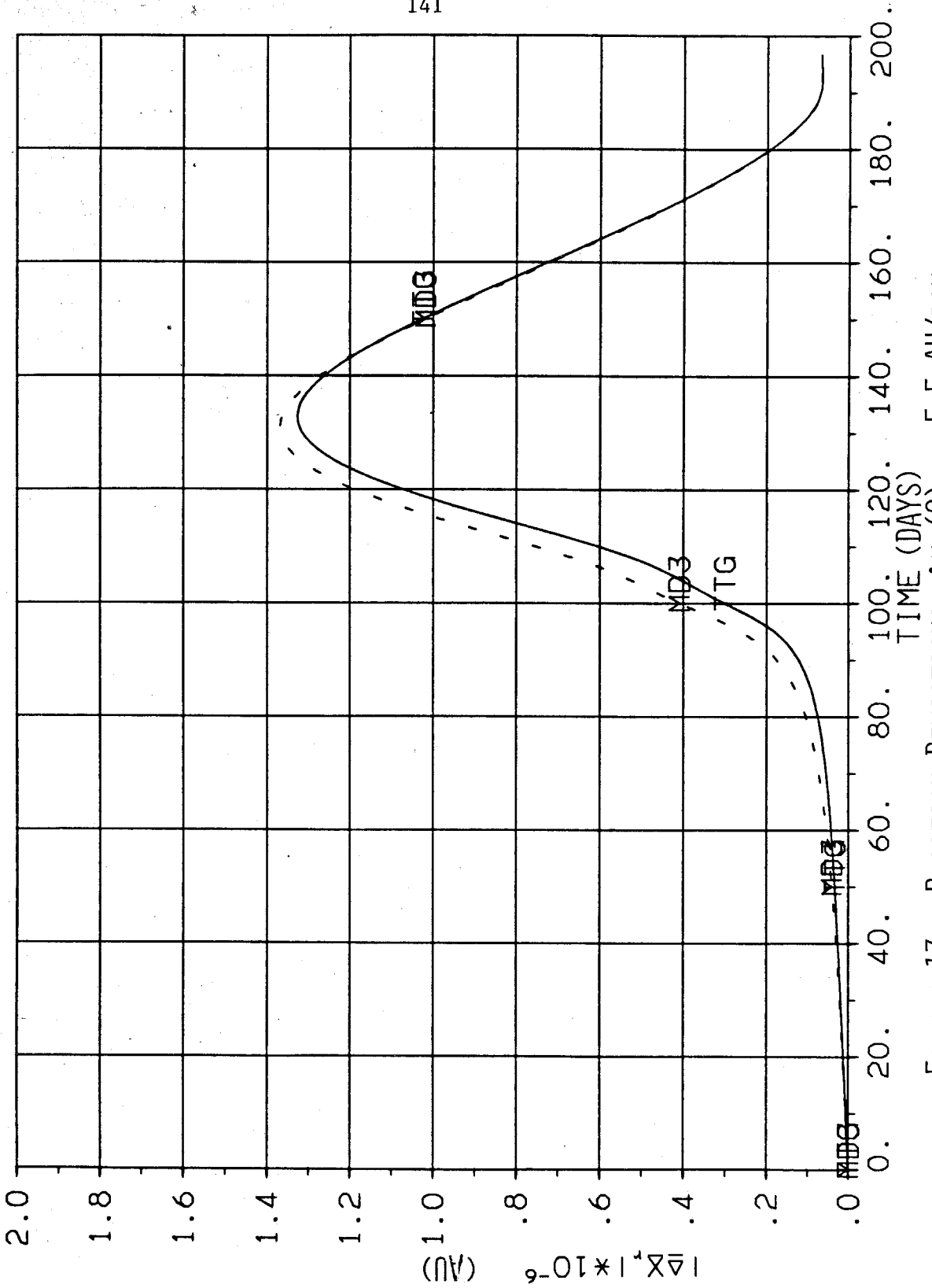
FIGURE 17. POSITION DEVIATIONS, $\delta x_1(0) = .5\text{-}5$ AU/DAY
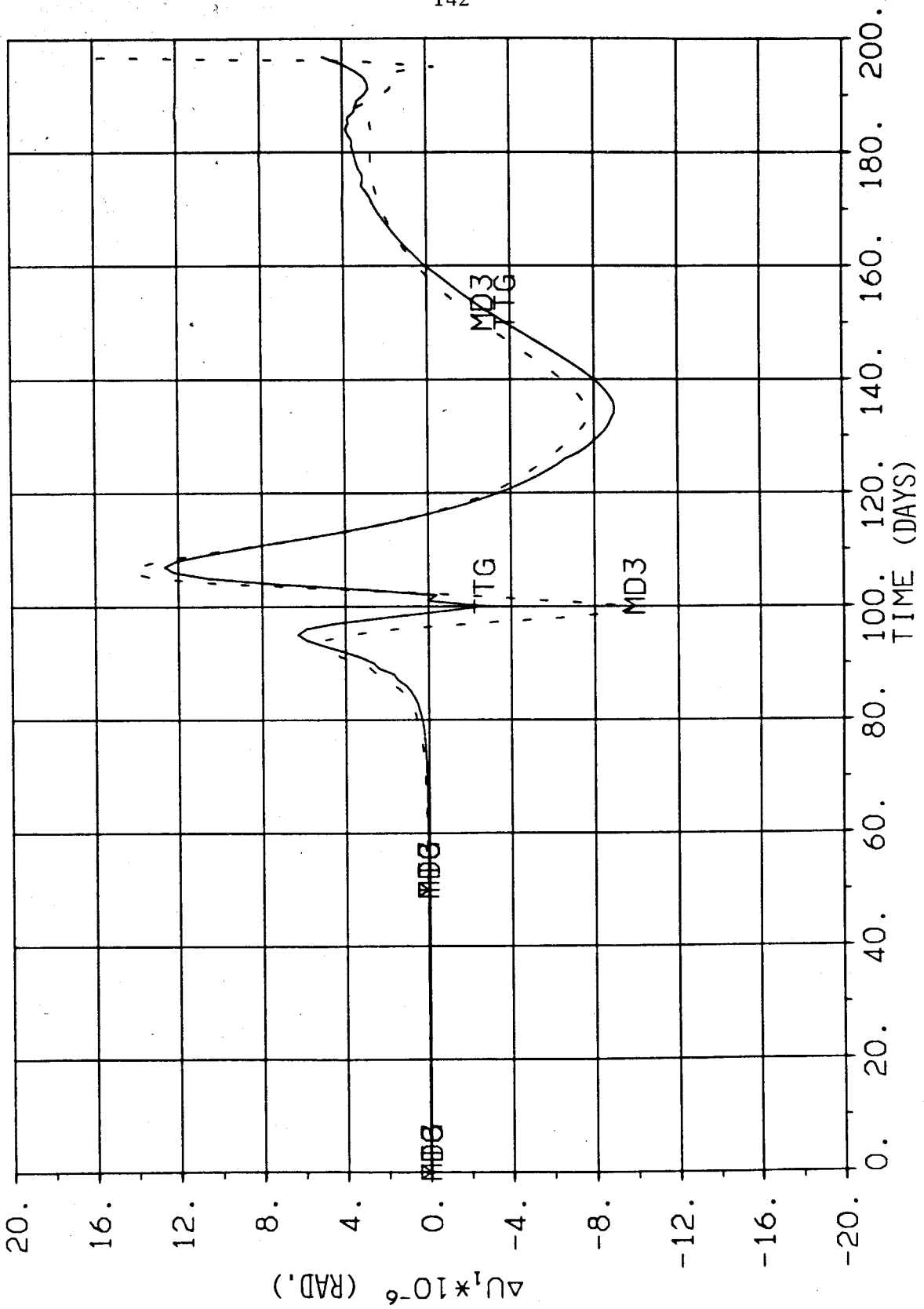
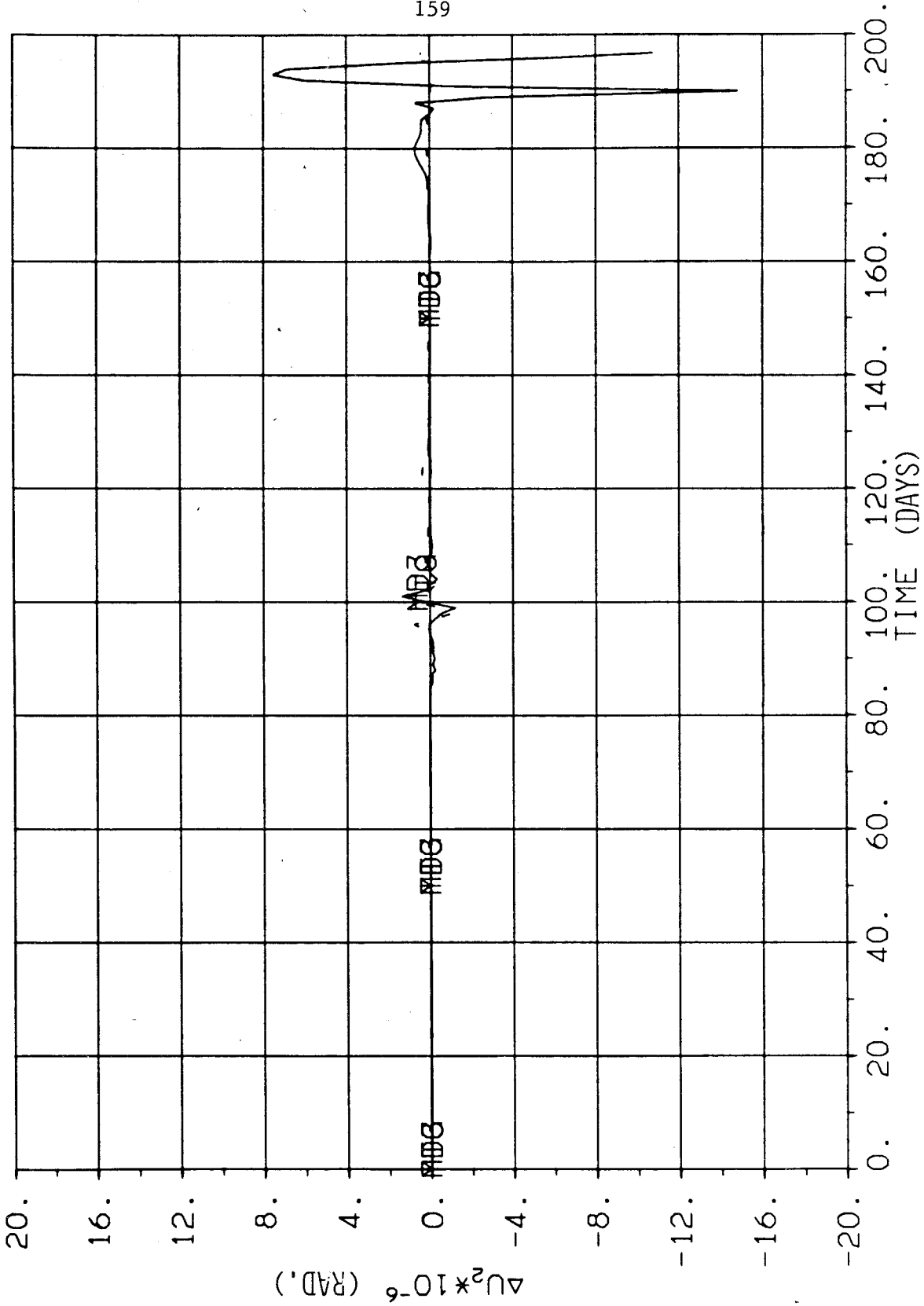FIGURE 18. OUT-OF-PLANE CONTROL ANGLE DEVIATIONS, $\delta x_1(0) = .5 \text{-} 5$ AU/DAY
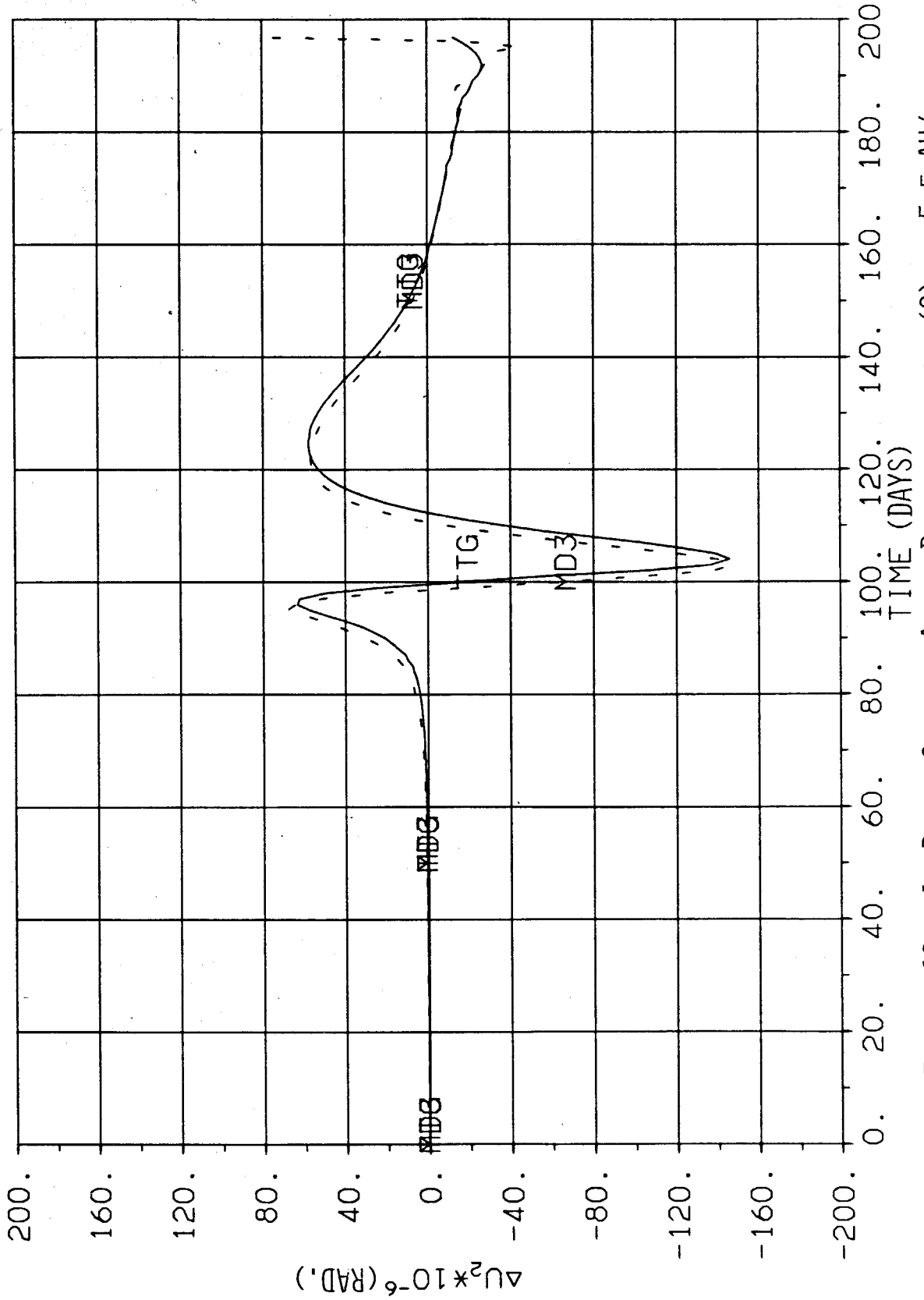
FIGURE 19. IN-PLANE CONTROL ANGLE DEVIATIONS, $\delta x_1(0) = .5\text{-}5$ AU/DAY
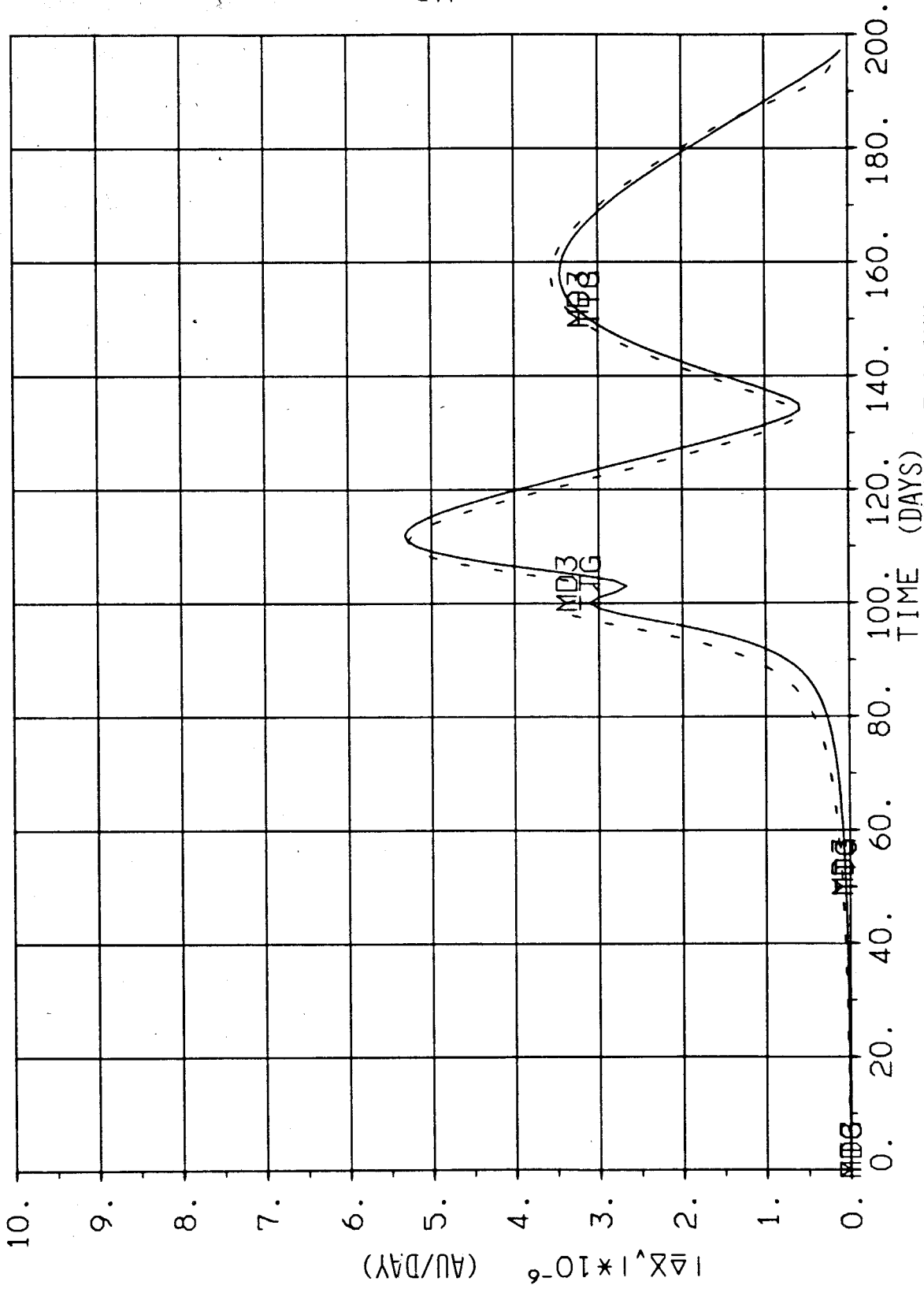
FIGURE 20. VELOCITY DEVIATIONS, $\delta x_1(0) = .5{-}4$ AU/DAY

145
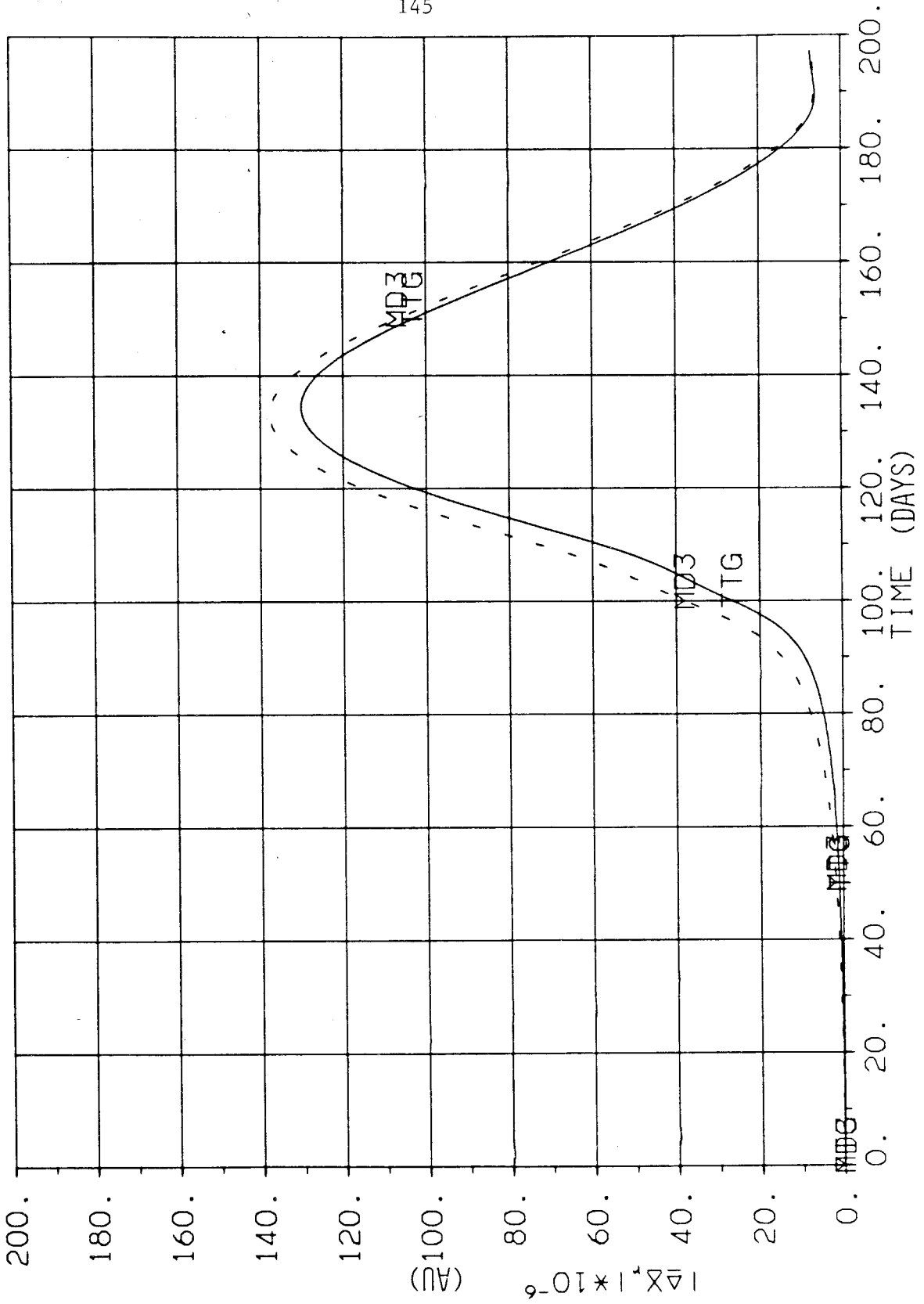
FIGURE 21. POSITION DEVIATIONS, $\delta x_1(0) = .5\text{-}4$ AU/DAY
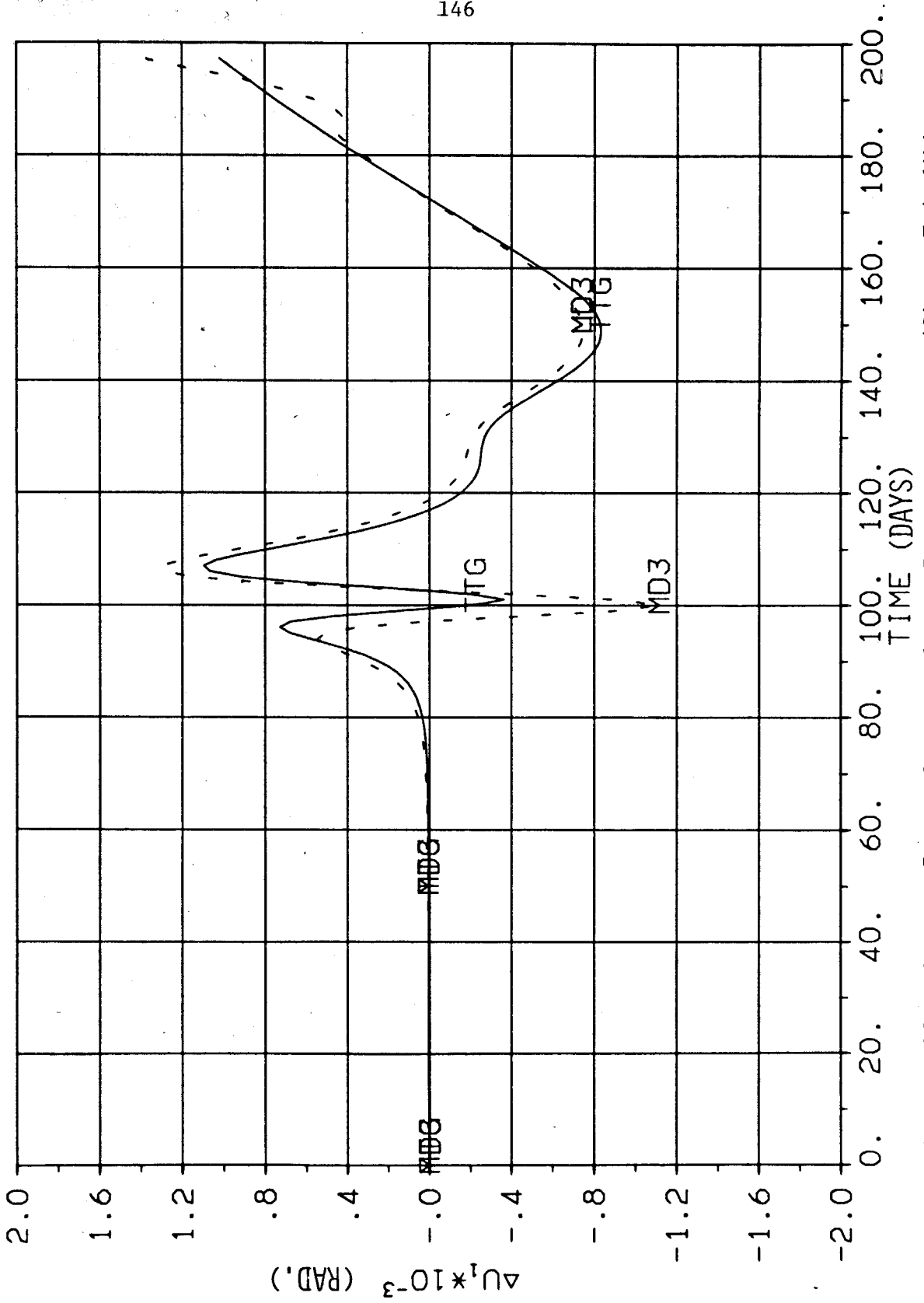
FIGURE 22. OUT-OF-PLANE CONTROL ANGLE DEVIATIONS, $\delta x_1(0) = .5\text{-}4$ AU/DAY
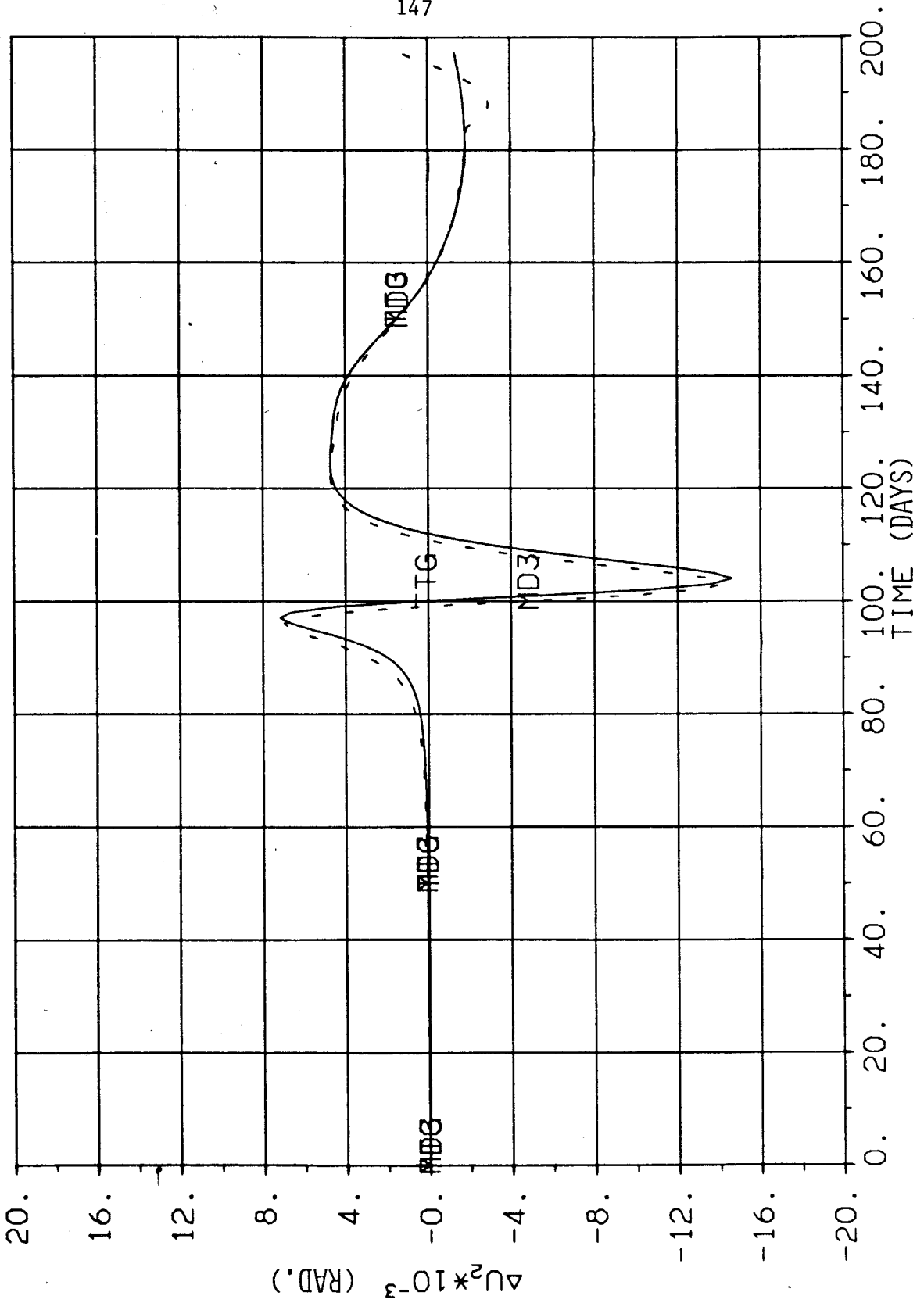
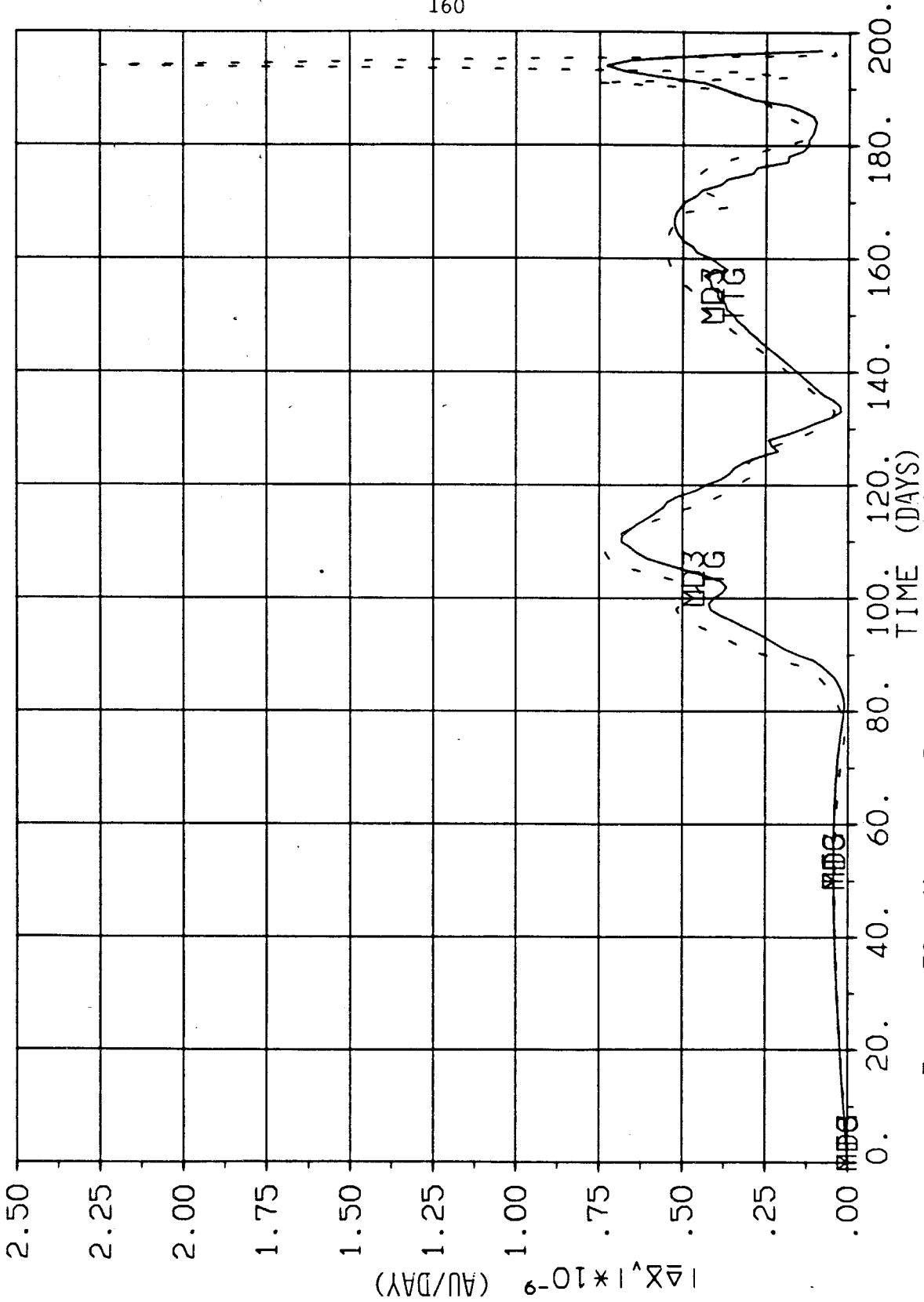FIGURE 23. IN-PLANE CONTROL ANGLE DEVIATIONS, $\delta x_1(0) = .5\text{-}4$ AU/DAY

FIGURE 24. VELOCITY DEVIATIONS, $\delta x_4(0) = -.21-2$ AU

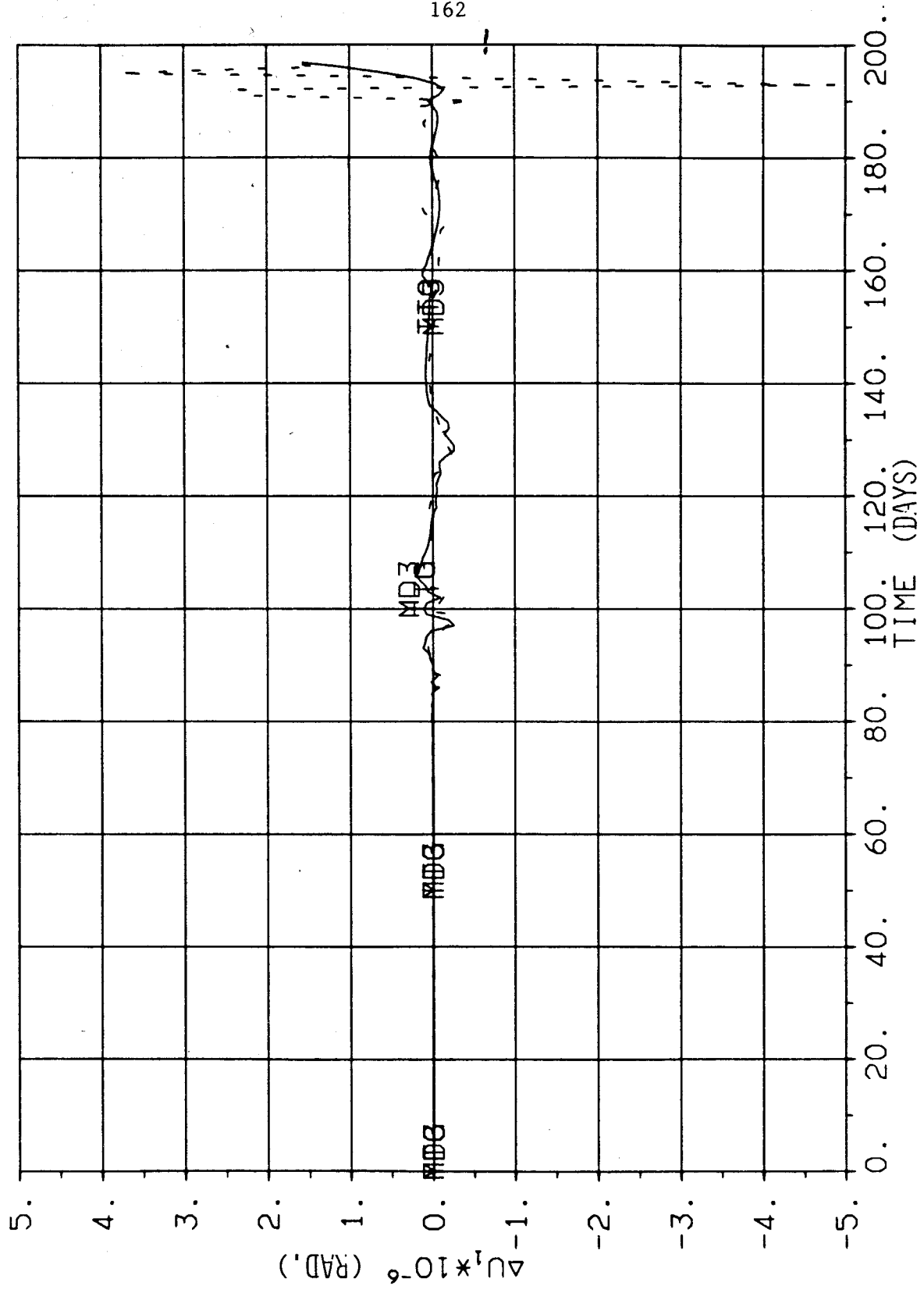FIGURE 25. POSITION DEVIATIONS, $\delta x_4(0) = -.21\text{-}2$ AU

FIGURE 26. OUT-OF-PLANE CONTROL ANGLE DEVIATIONS, $\delta x_4(0) = -.21\text{-}2$ AU
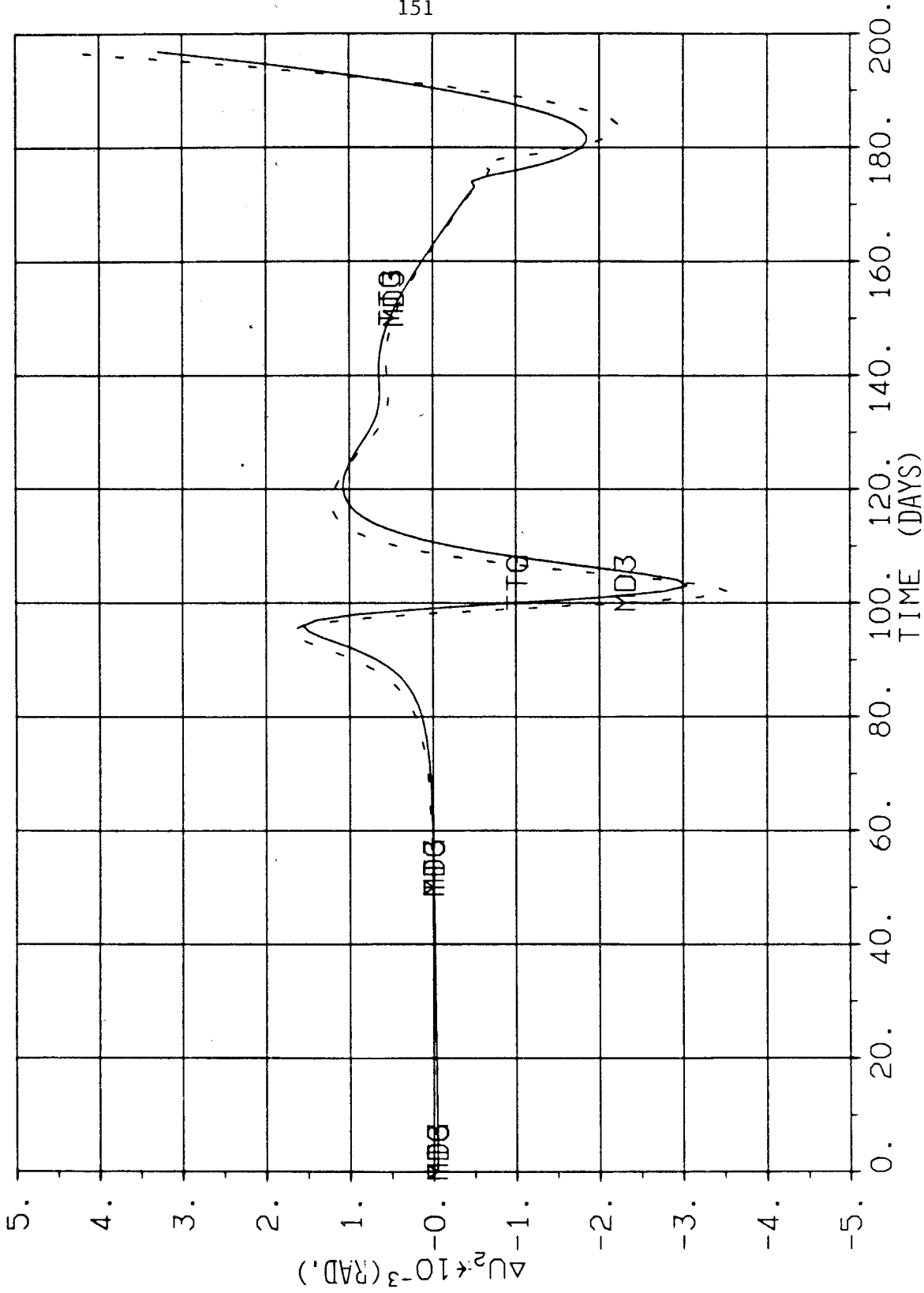
FIGURE 27. IN-PLANE CONTROL ANGLE DEVIATIONS, $\delta x_4(0) = -.21\text{-}2$ AU

152

FIGURE 28. VELOCITY DEVIATIONS, $\delta x_4(0) = -.3$-3 AU

FIGURE 29. POSITION DEVIATIONS, $\delta x_4(0) = -.3-3$ AU

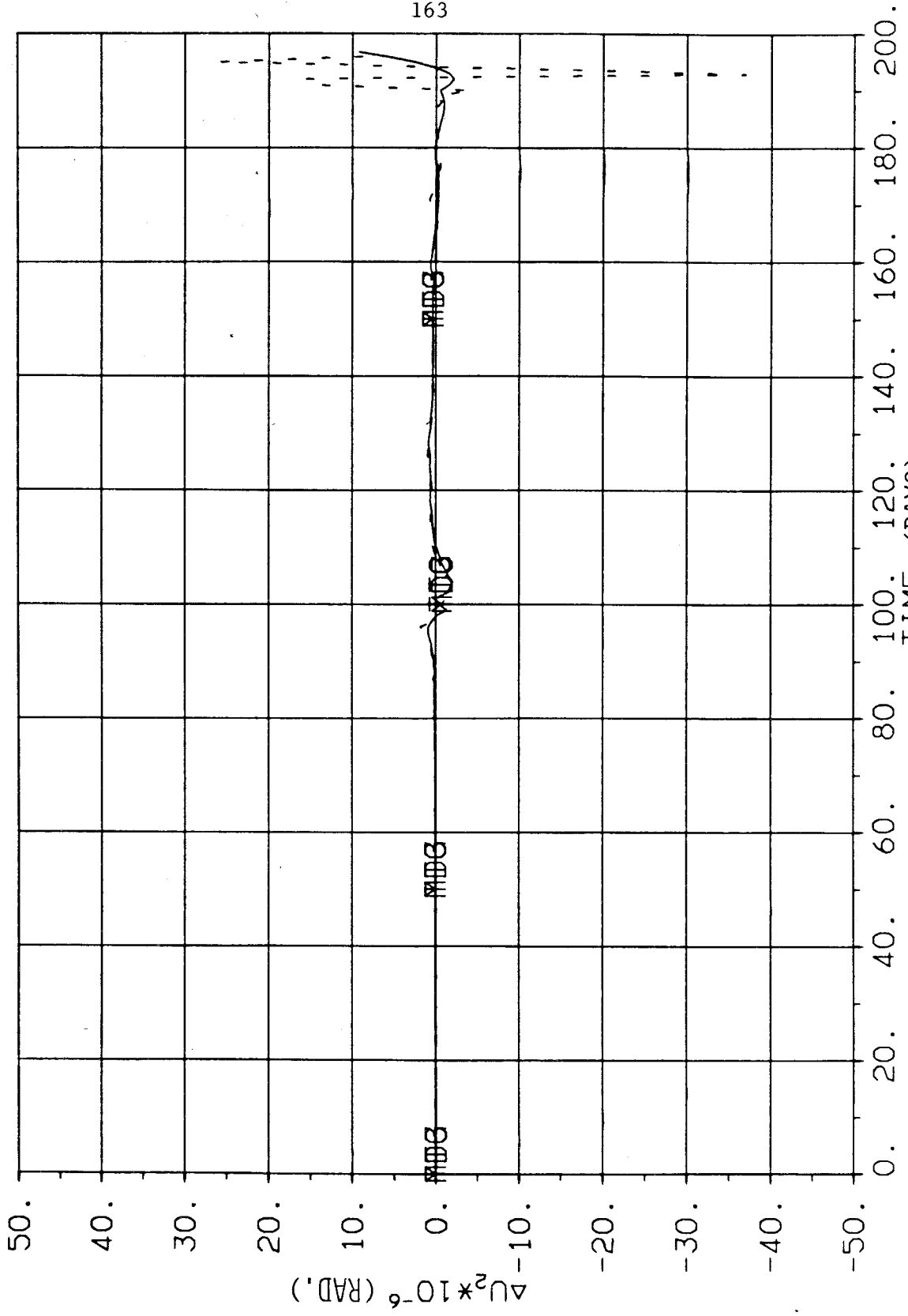FIGURE 30. OUT-OF-PLANE CONTROL ANGLE DEVIATIONS, $\delta x_4(0) = -.3\text{-}3$ AU

FIGURE 31. IN-PLANE CONTROL ANGLE DEVIATIONS, $\delta x_4(0) = -.3$-3 AU

FIGURE 32. VELOCITY DEVIATIONS, $\delta x_4(0) = .5\text{-}5$ AU

FIGURE 33. POSITION DEVIATIONS, $\delta x_4(0)$ = .5-5 AU

FIGURE 34. OUT-OF-PLANE CONTROL ANGLE DEVIATIONS, $\delta x_4 (0) = .5$-5 AU

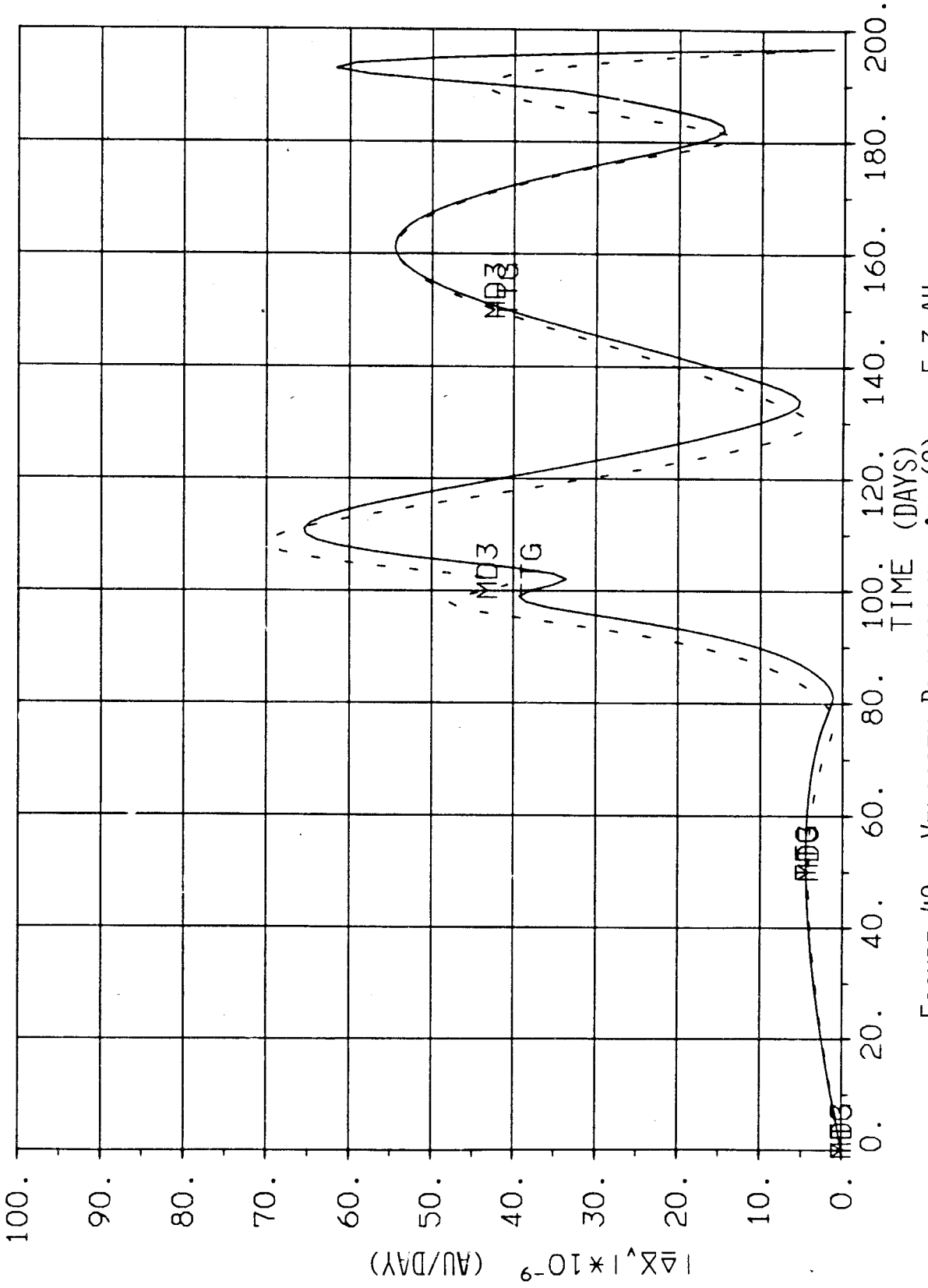FIGURE 35. IN-PLANE CONTROL ANGLE DEVIATIONS, $\delta x_4(0) = .5$-5 AU

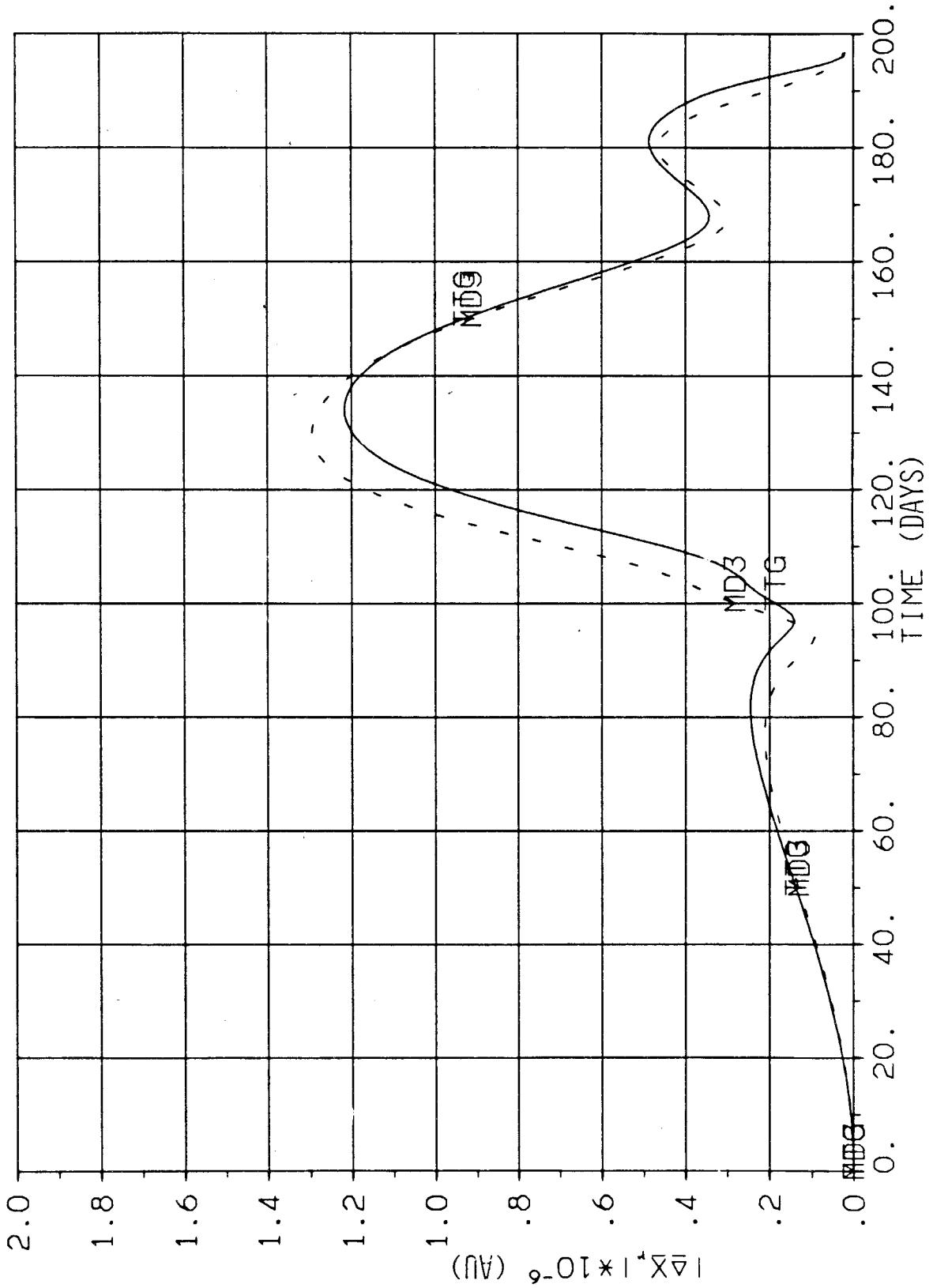FIGURE 36. VELOCITY DEVIATIONS, $\delta x_4(0) = .5$-4 AU
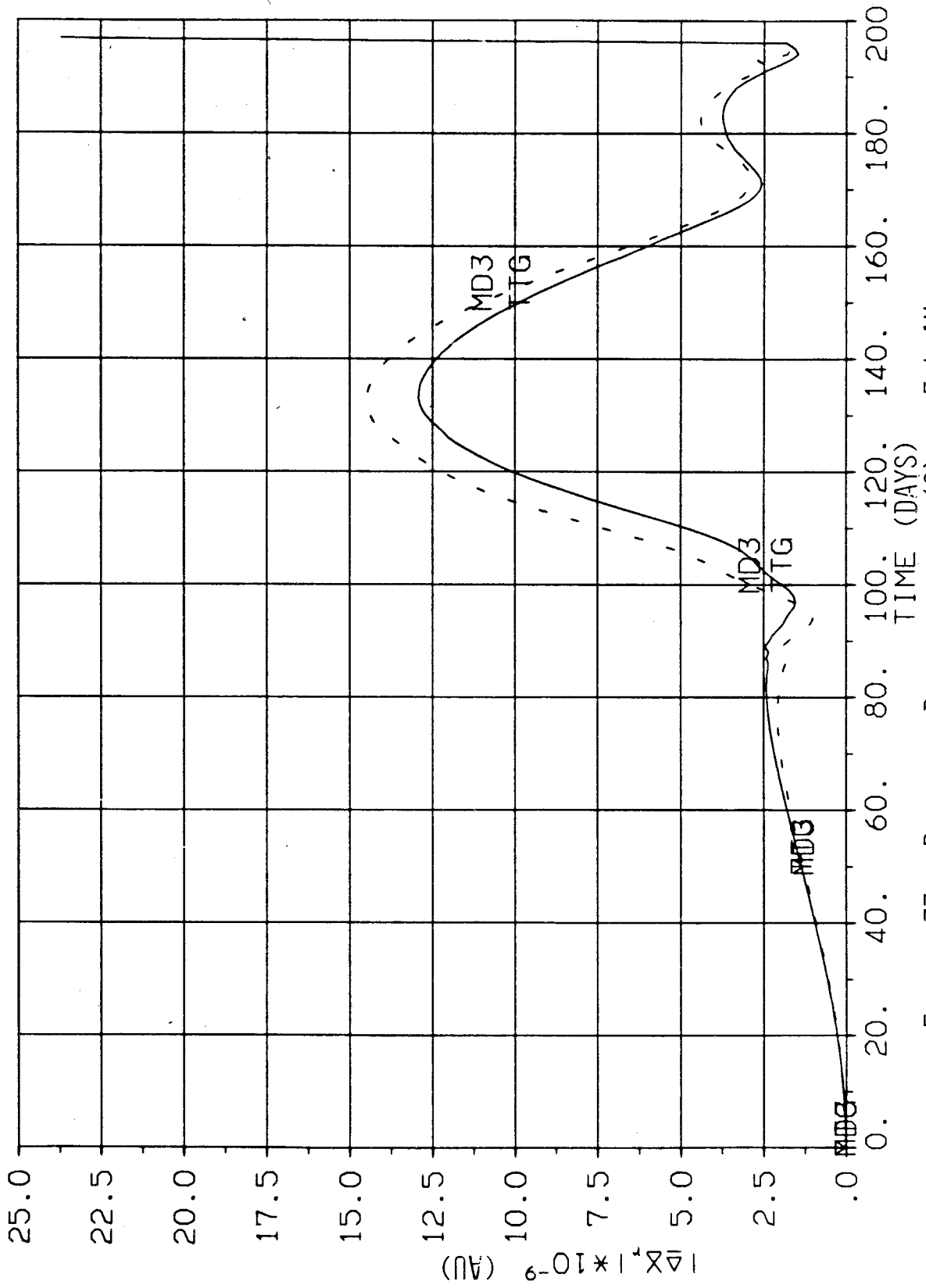
FIGURE 37. POSITION DEVIATIONS, $\delta x_4(0) = .5\text{-}4$ AU

FIGURE 38. OUT-OF-PLANE CONTROL ANGLE DEVIATIONS, $\delta x_4(0) = .5\text{-}4$ AU

FIGURE 39. IN-PLANE CONTROL DEVIATIONS, $\delta x_4(0) = .5\text{-}4$ AU

164

FIGURE 40. VELOCITY DEVIATIONS, $\delta x_4(0) = .5\text{-}3$ AU

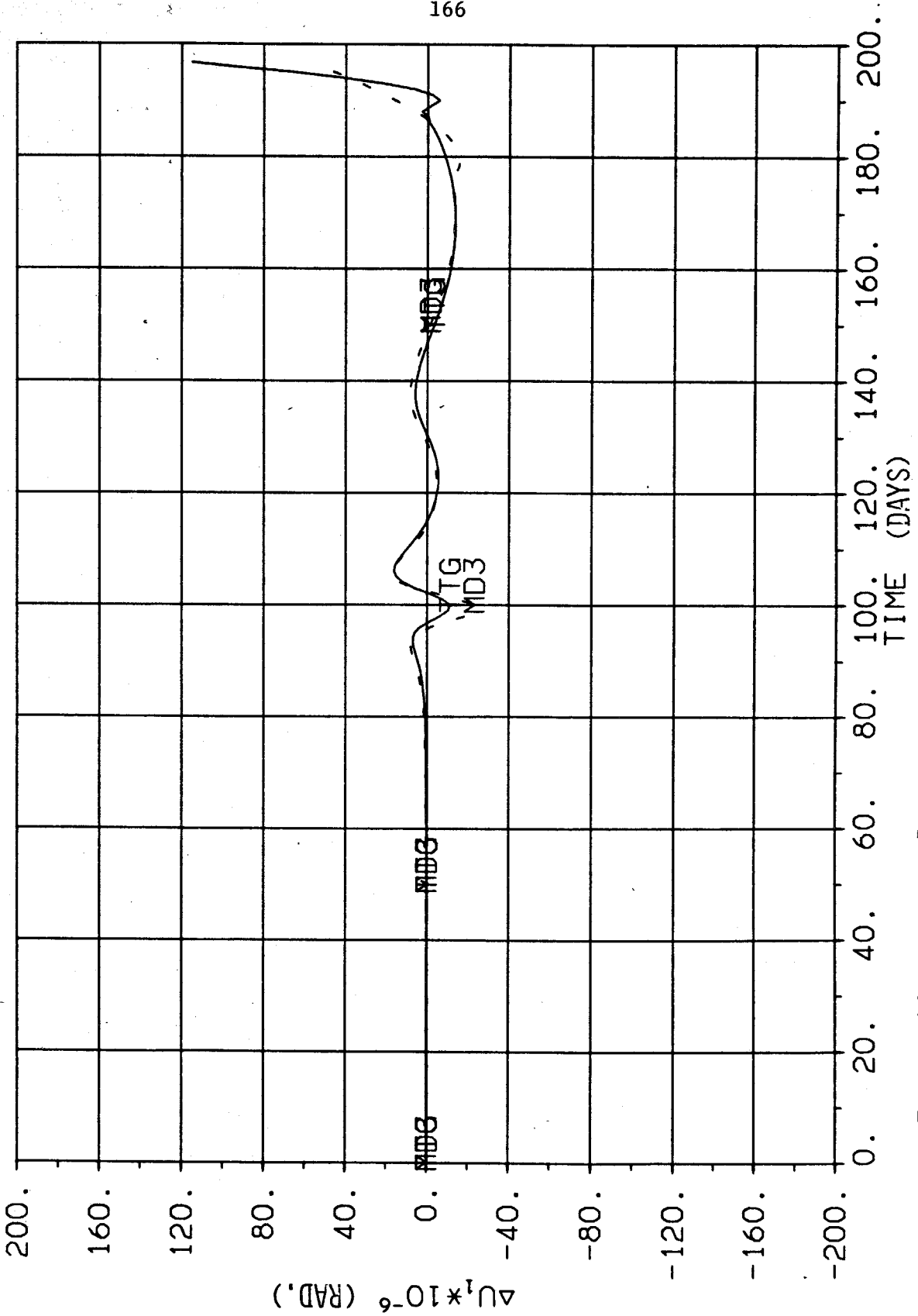FIGURE 41. POSITION DEVIATIONS, $\delta x_4(0) = .5\text{-}3$ AU

FIGURE 42. OUT-OF-PLANE CONTROL ANGLE DEVIATIONS, $\delta x_4(0) = .5\text{-}3$ AU
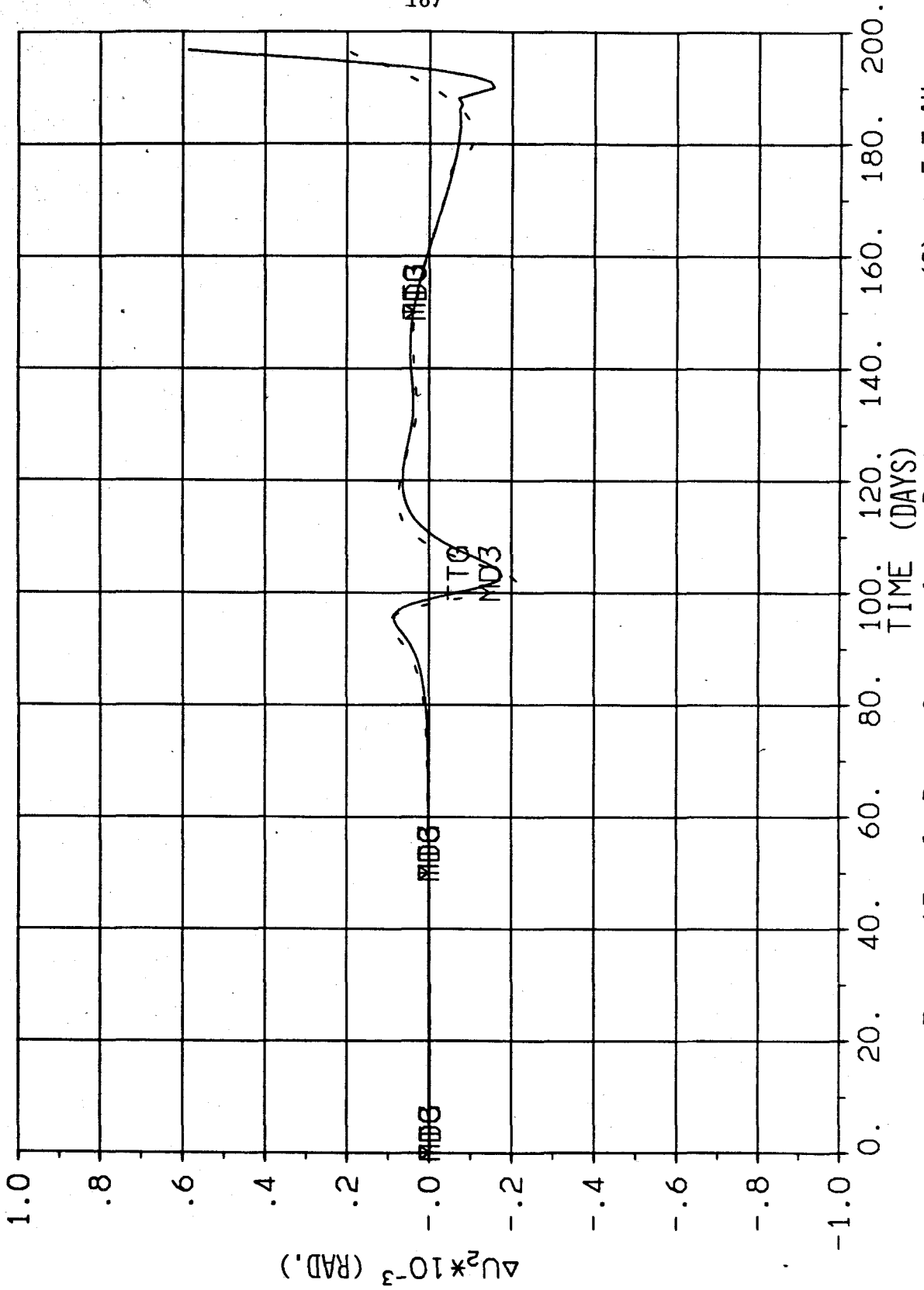
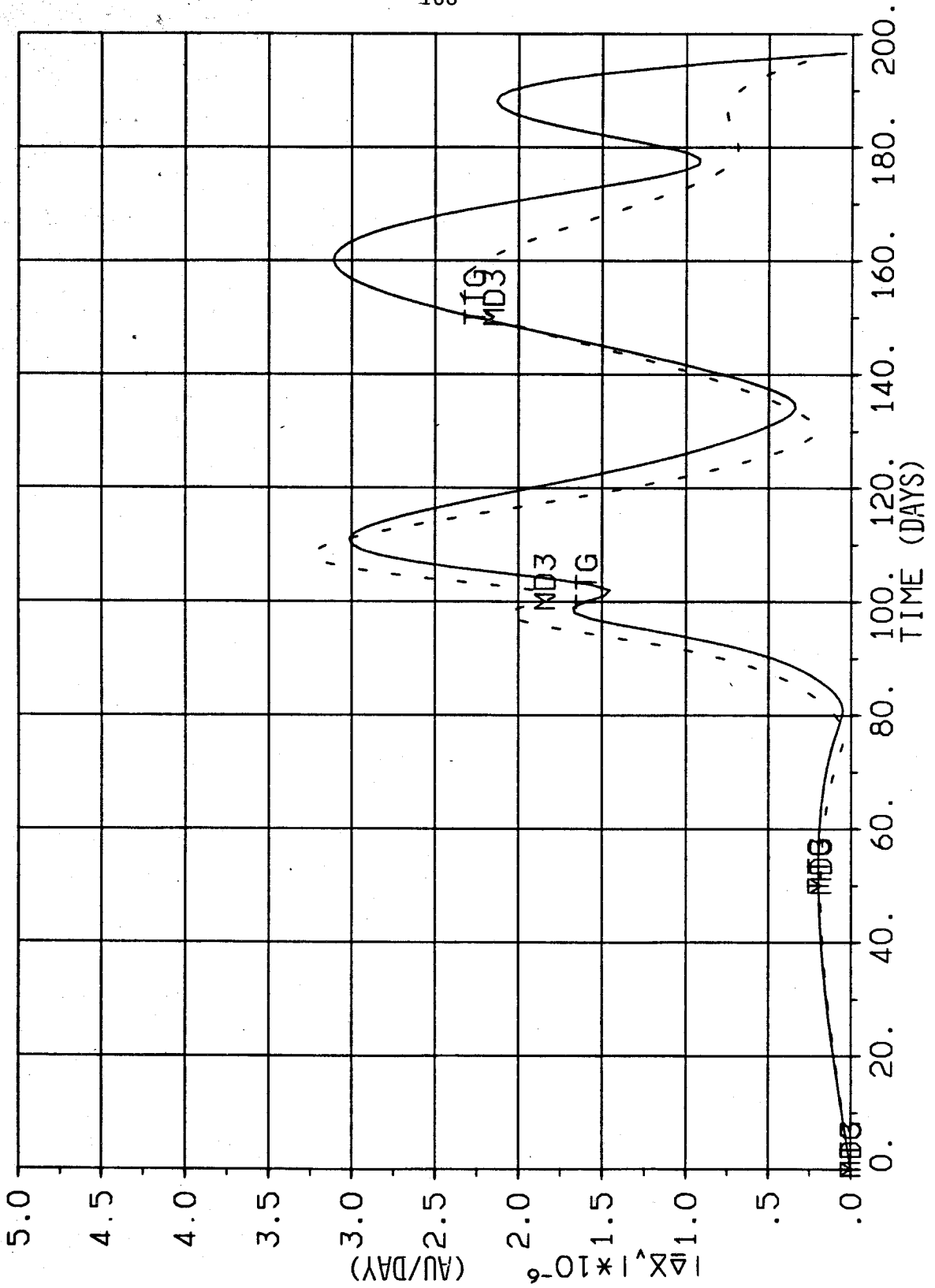FIGURE 43, IN-PLANE CONTROL ANGLE DEVIATIONS, $\delta x_4(0) = .5$-3 AU

FIGURE 44. VELOCITY DEVIATIONS, $\delta x_4(0) = .33\text{-}2$ AU
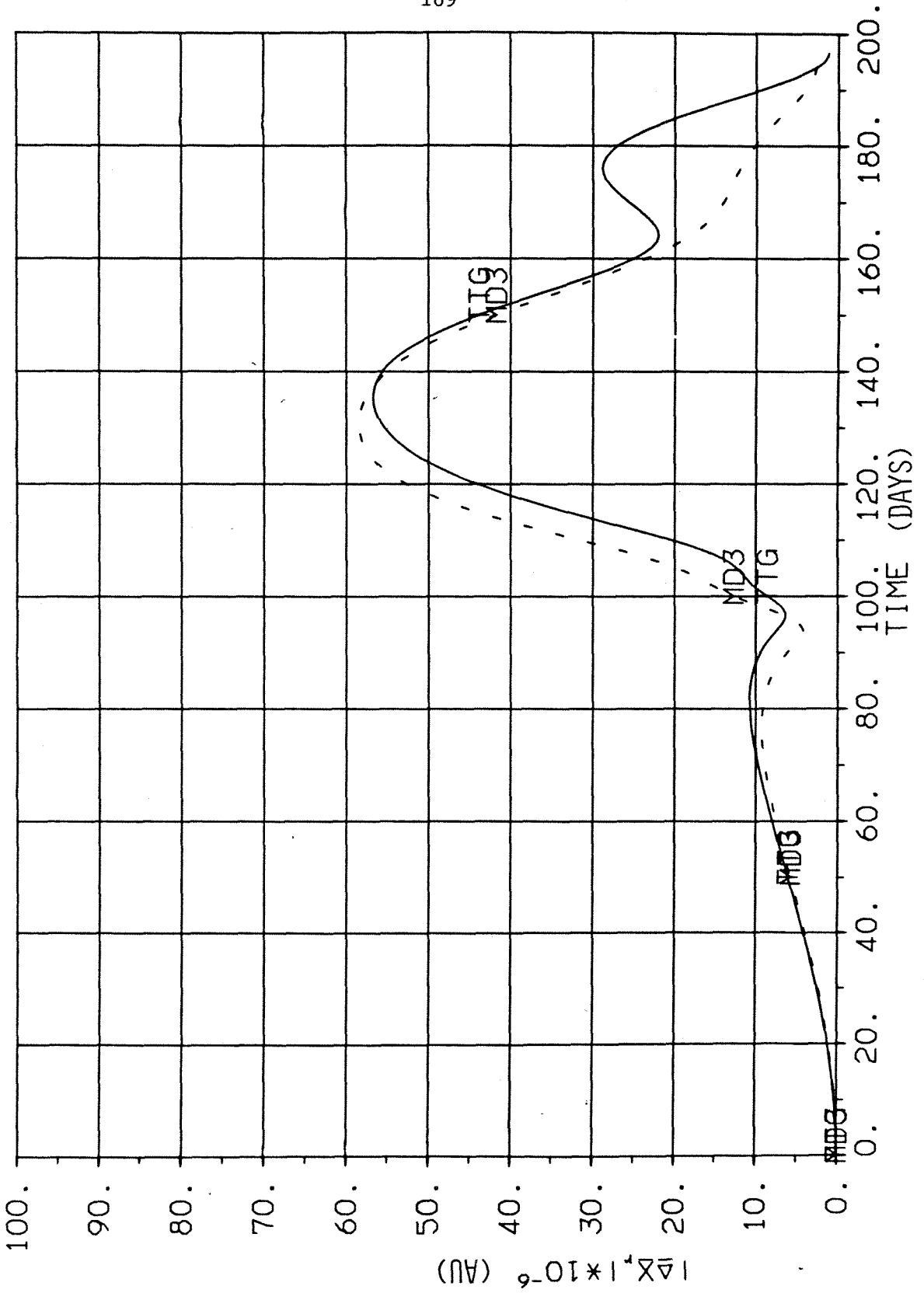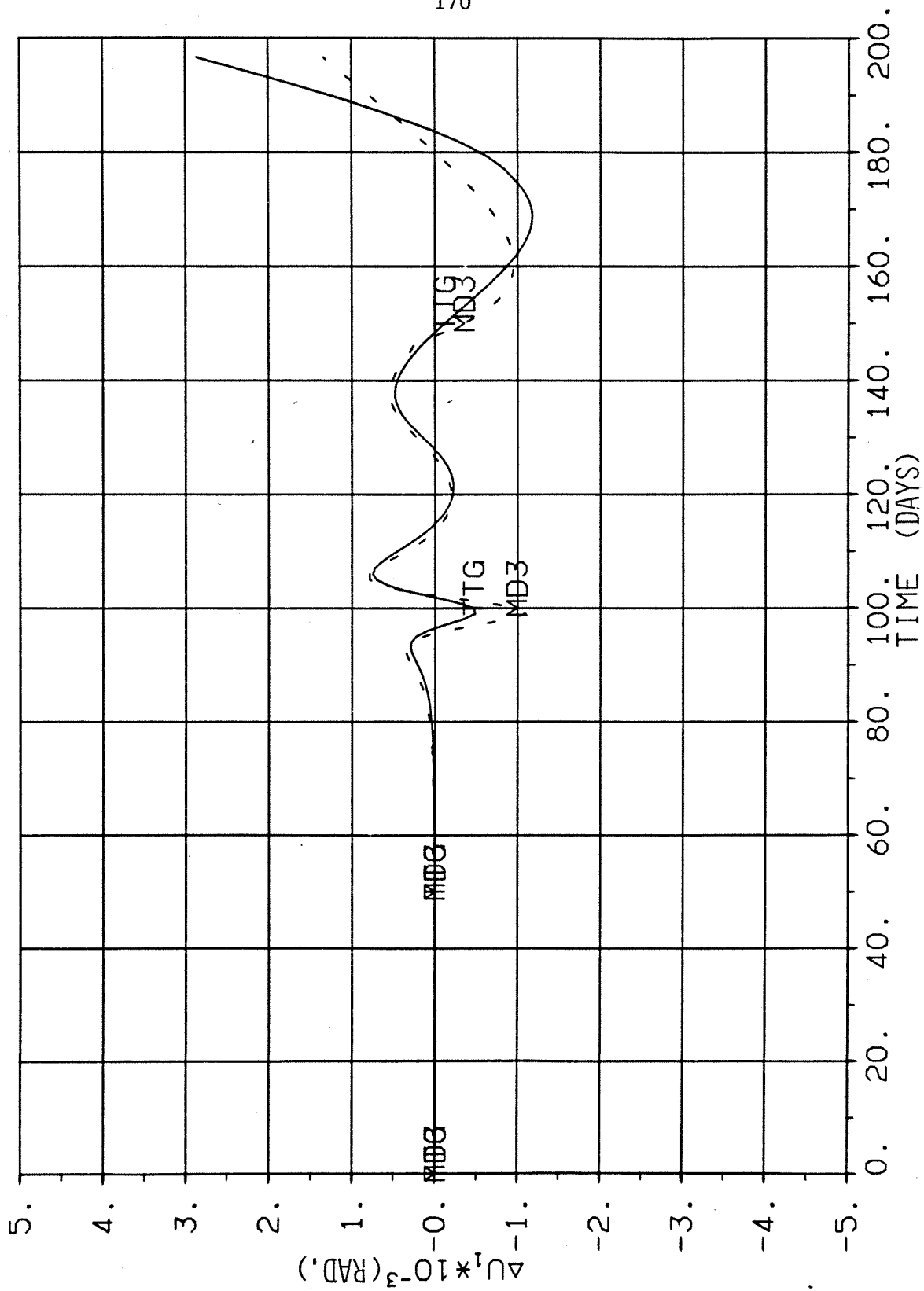
FIGURE 45. POSITION DEVIATIONS, $\delta x_4(0) = .33\text{-}2$ AU

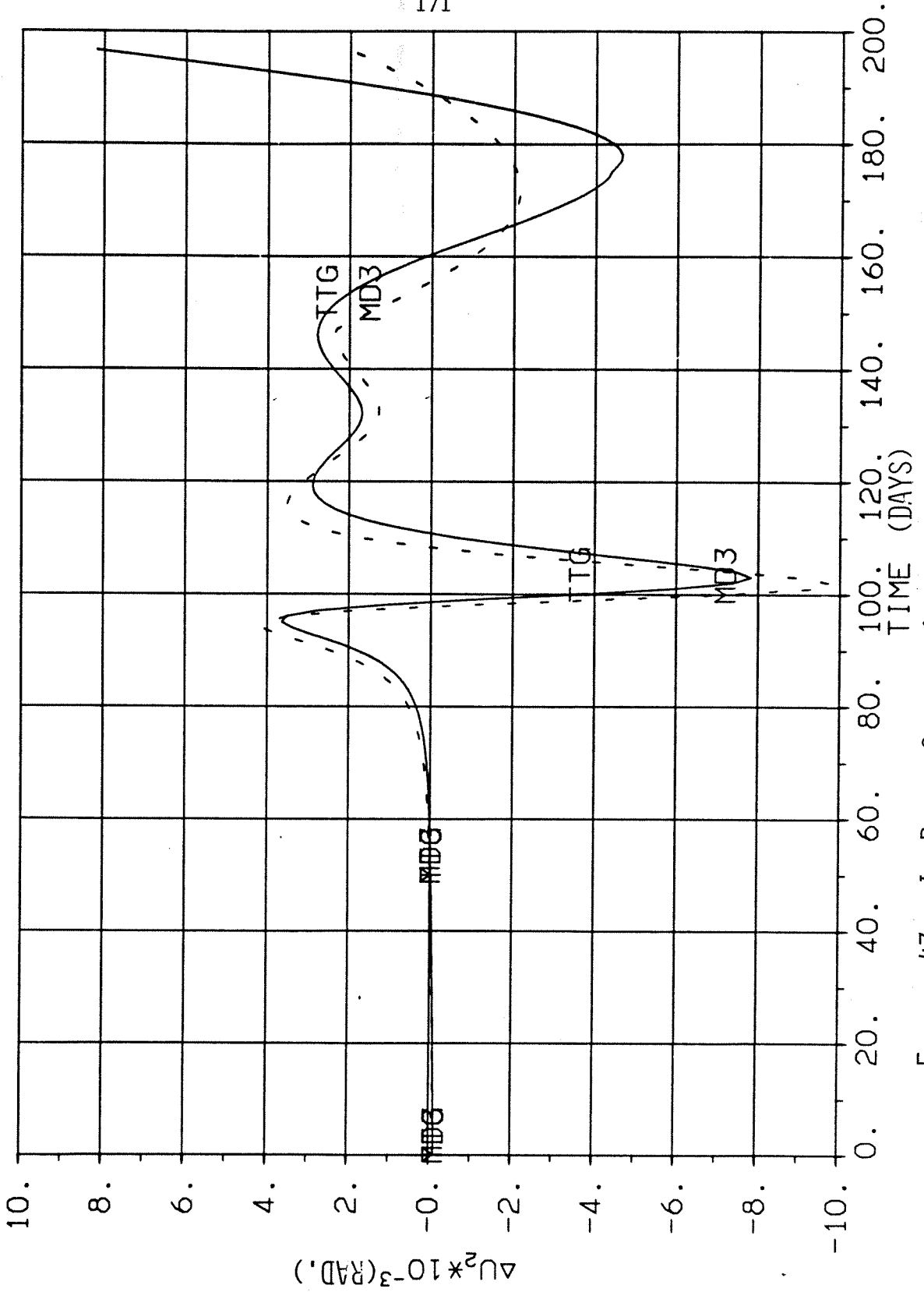FIGURE 46. OUT-OF-PLANE CONTROL ANGLE DEVIATIONS, $\delta x_4(0) = .33\text{-}2$ AU

FIGURE 47. IN-PLANE CONTROL ANGLE DEVIATIONS, $\delta \times_4 (0) = .33$-2 AU

for perturbations in x_1 have the same basic shape, two large (relative to the time-averaged value) excursions and one large excursion respectively. For perturbations in x_4, there are three large excursions and two large excursions in velocity and in position, respectively.

The deviations in control for the various cases also exhibit similarities. The largest excursions generally occur just after thrust reversal, although the deviations also tend to be large near the final time when the feedback gains are getting very large. Likewise, for each angle the shape of the curves for all the perturbations in a given component are similar. For three small perturbations ($\delta x_4(0) = .5 \times 10^{-5}$, $.5 \times 10^{-4}$, $.5 \times 10^{-3}$ AU) it was necessary to use 7th order Lagrangian interpolation to remove noise in the plots of the control deviations. Still, the curves get lost in the "integration noise."

Another comparison of Minimum Distance Guidance with Weight 1 (MD1), the weight that treats all the components of the metric equally in a non-dimensionalized sense, and Minimum Distance Guidance with Weight 3 (MD3), the weight used in the previous studies that neglects the velocity and time components of the metric, can be made by examining Figures 48-55. These plots show that state and control deviations for the two weights are very similar for the two cases presented. Deviations for Minimum Distance Guidance with Weight 1 are depicted with a line composed of long dashes and the symbol MD1.

Current Time Guidance (CT) performance, as measured by terminal state error, is compared with that of TTG, MD1, and MD3 for a selected value of $c_{t_{\overline{\nu}}}$, for cases with an initial perturbation in x_1 or x_4, in Tables 31-32. The terminal velocity errors for Current Time Guidance

FIGURE 48. VELOCITY DEVIATIONS, MD3 VS. MD1, $\delta x_1(0) = .5-5$ AU/DAY

FIGURE 49. POSITION DEVIATIONS, MD3 VS, MD1, $\delta x_1(0) = .5\text{-}5$ AU/DAY

FIGURE 50. OUT-OF-PLANE CONTROL ANGLE DEVIATIONS, MD3 VS. MD1, $\delta x_1(0) = .5$-5 AU/DAY

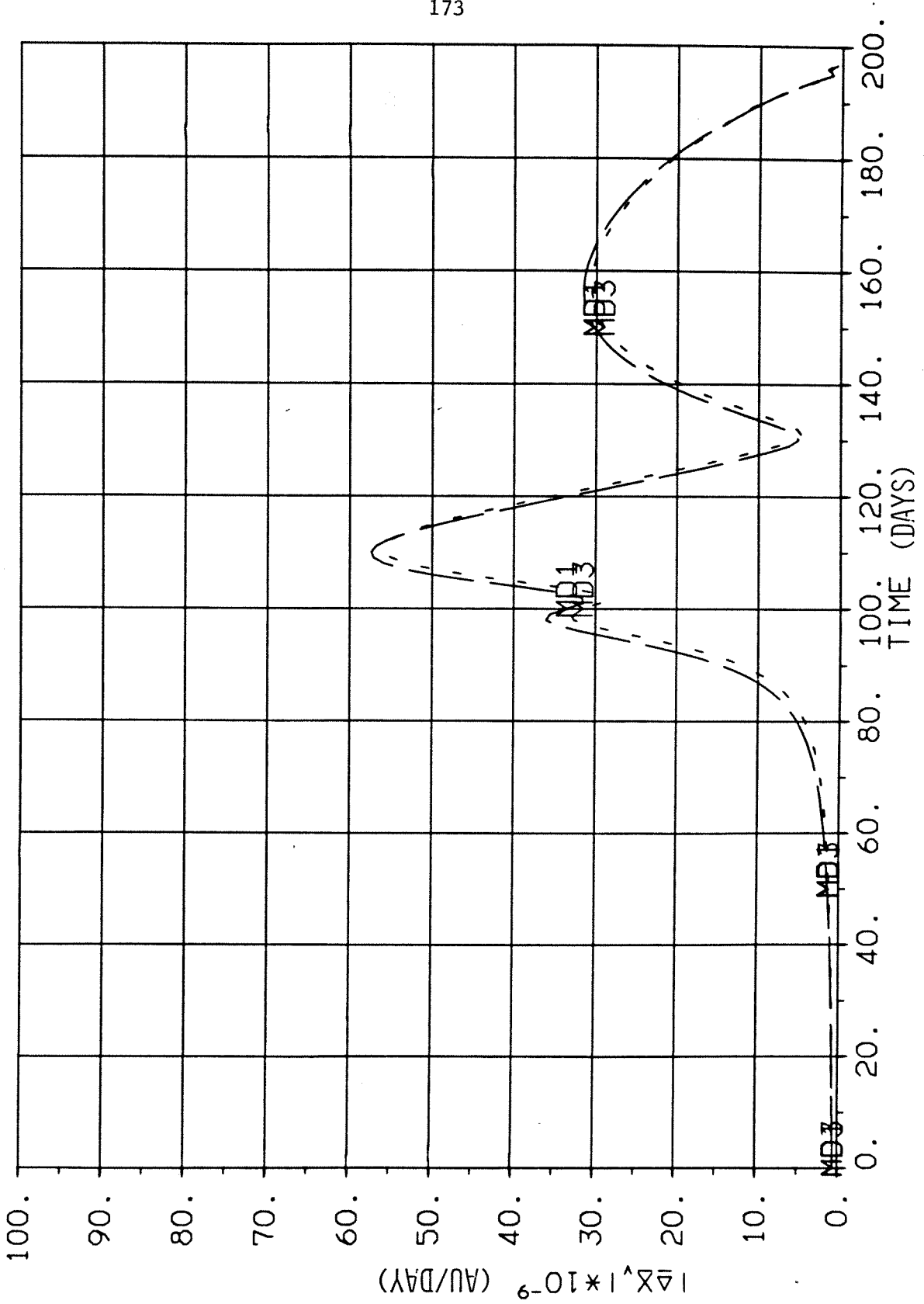FIGURE 51. IN-PLANE CONTROL ANGLE DEVIATIONS, MD3 VS. MD1, $\delta x_1(0) = .5$-5 AU/DAY
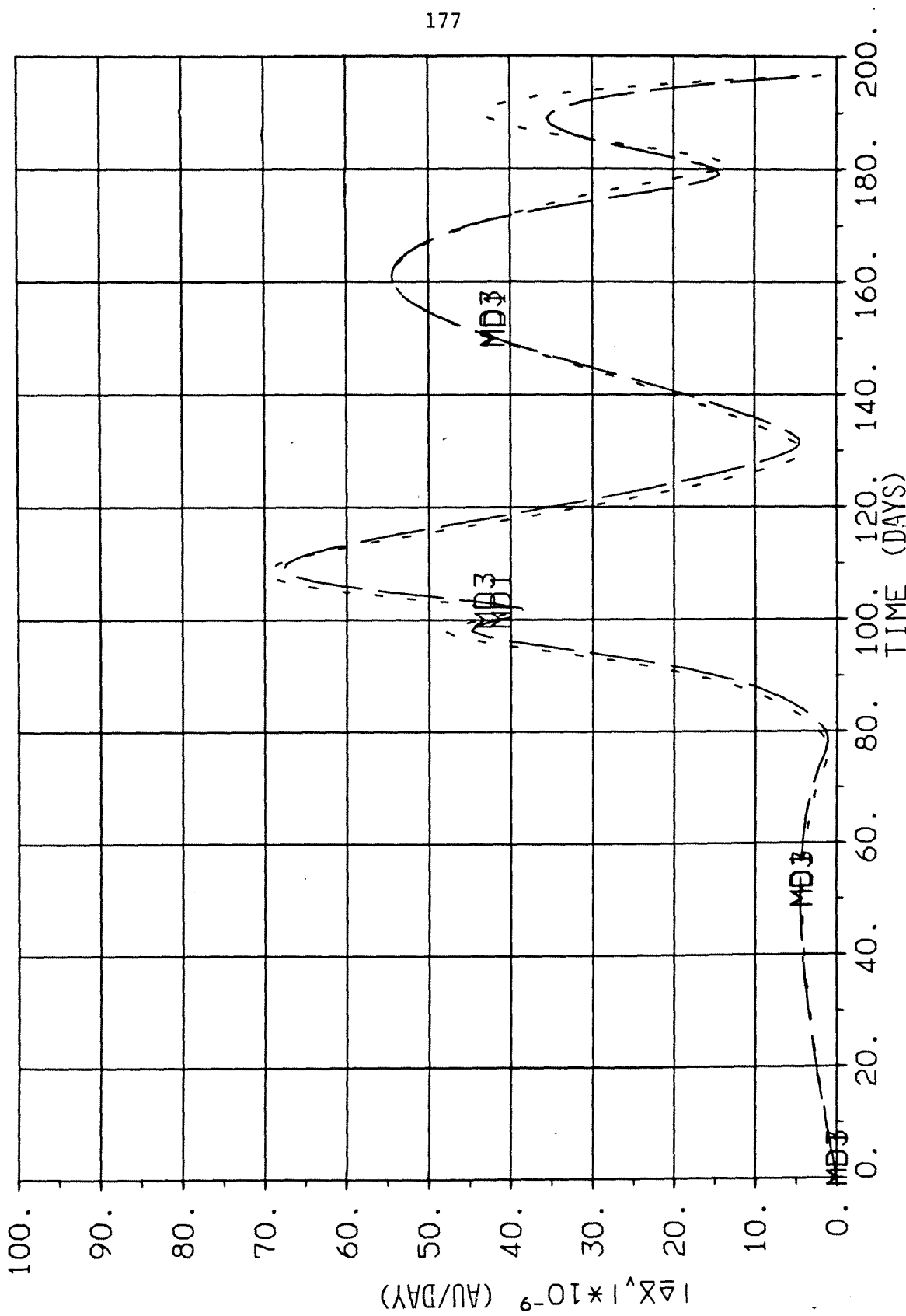
FIGURE 52. VELOCITY DEVIATIONS, MD3 VS. MD1, $\delta x_4(0) = .5$-3 AU

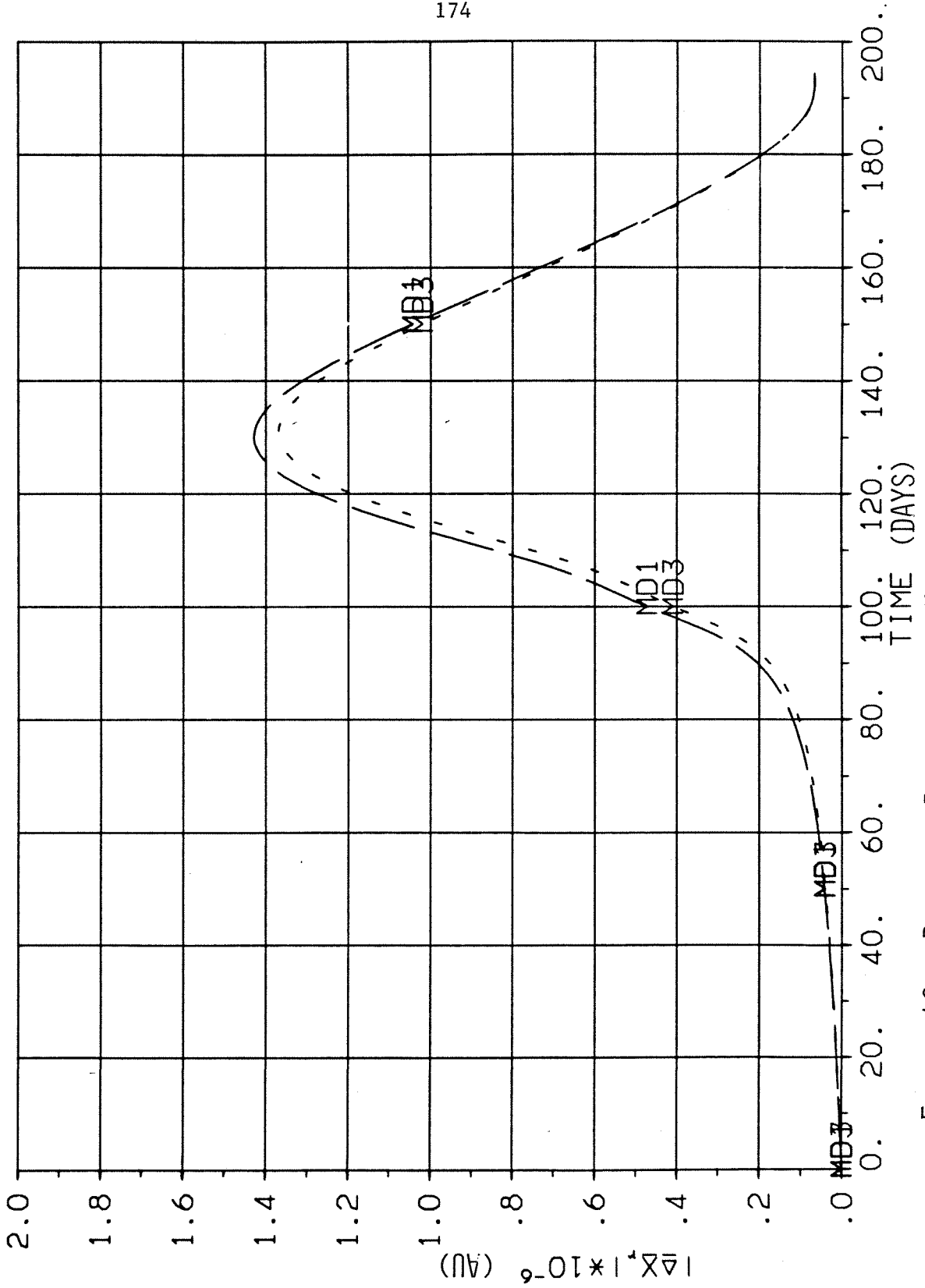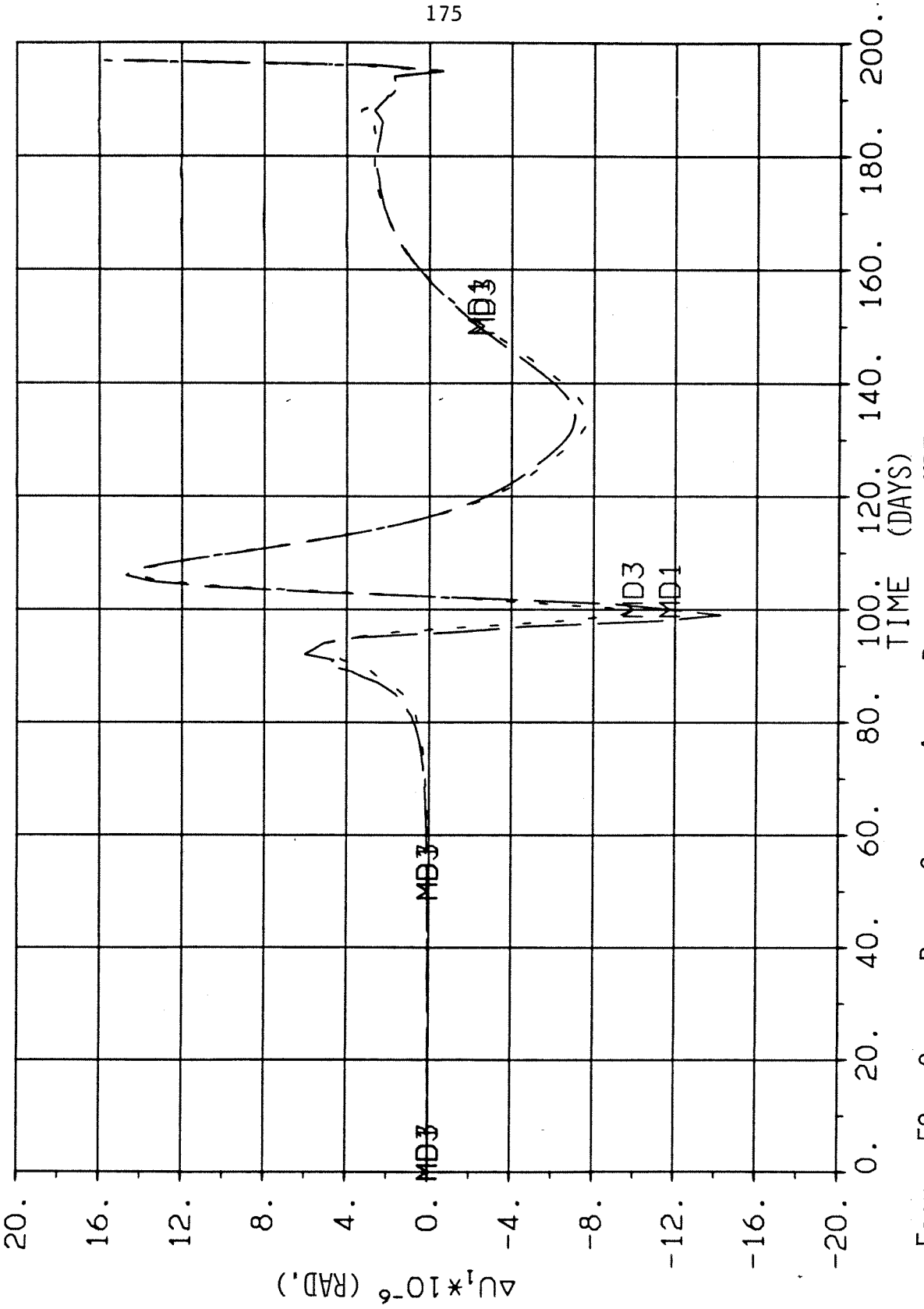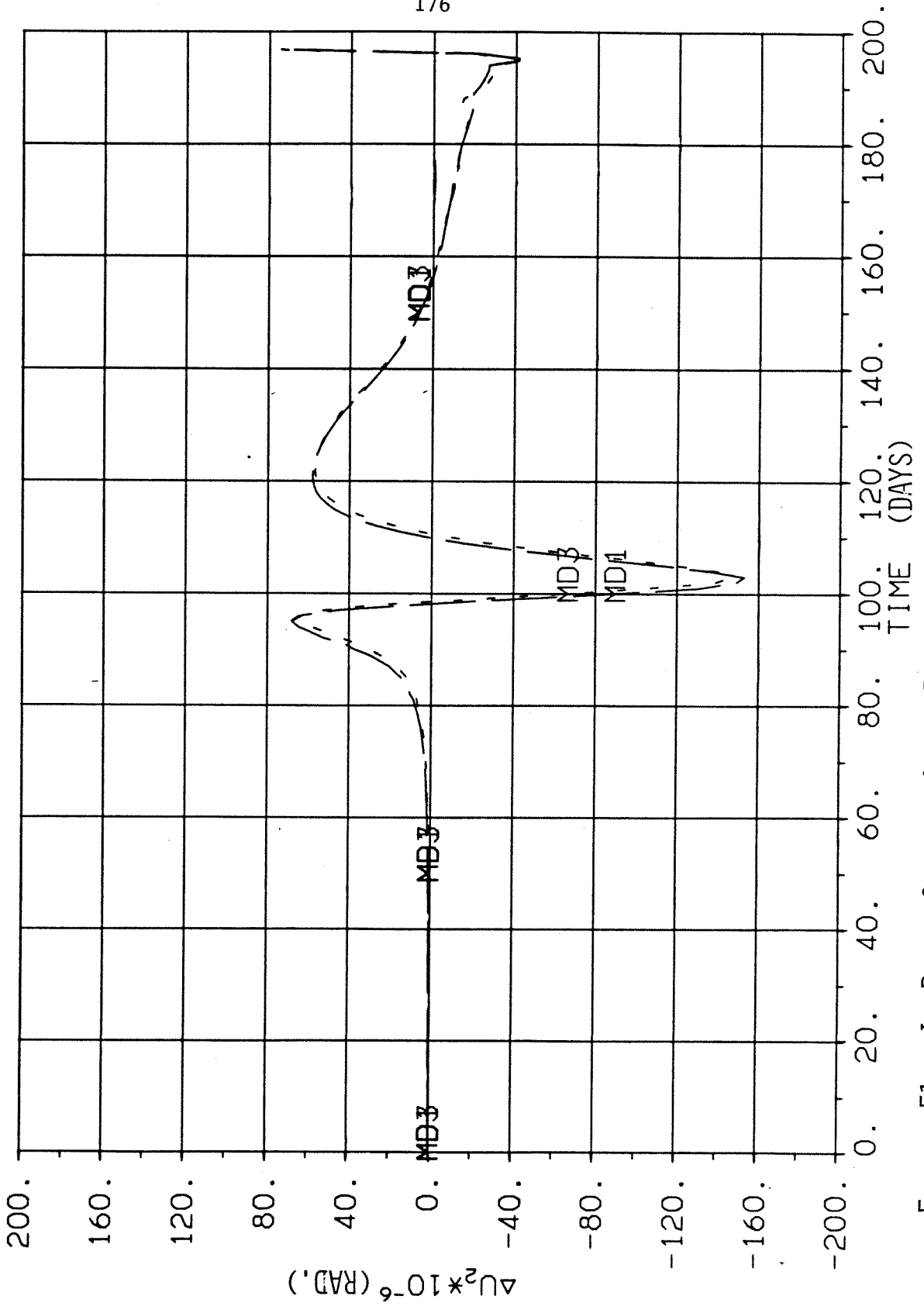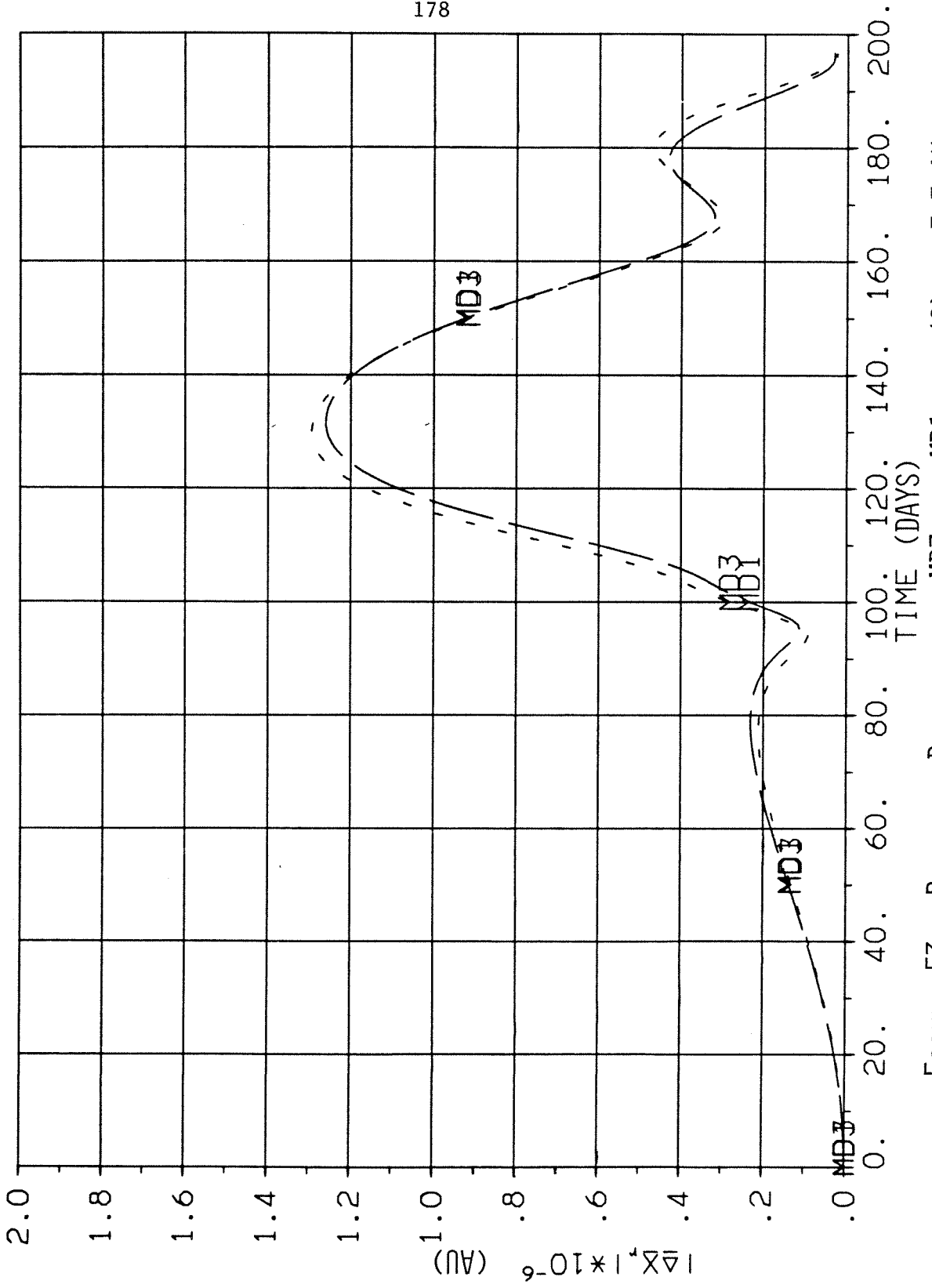FIGURE 53. POSITION DEVIATIONS, MD3 VS. MD1, $\delta x_4(0) = .5$-3 AU
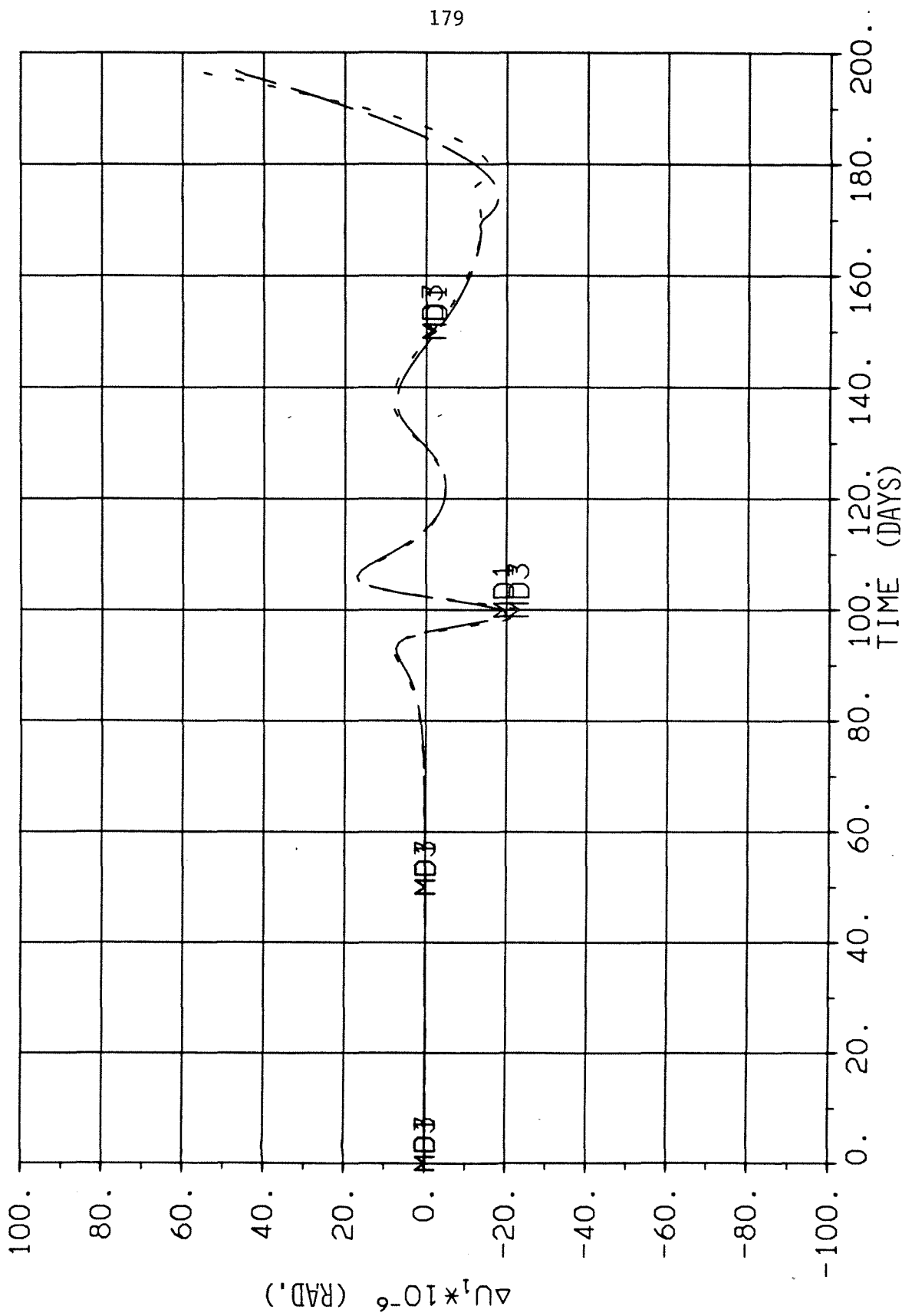
FIGURE 54. OUT-OF-PLANE CONTROL ANGLE DEVIATIONS, MD3 VS. MD1, $\delta x_4(0) = .5$-3 AU
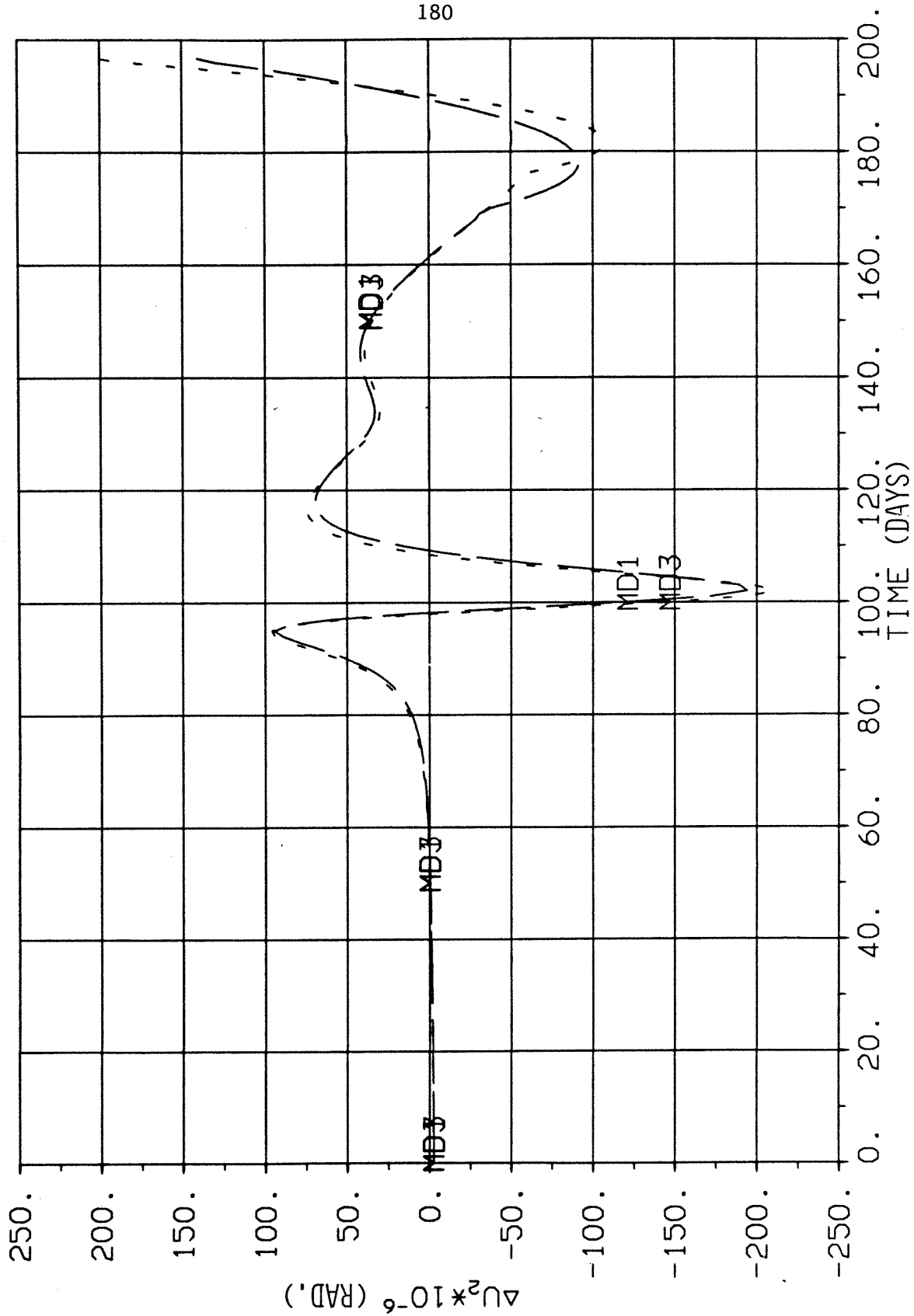
FIGURE 55. IN-PLANE CONTROL ANGLE DEVIATIONS, MD3 VS. MD1, $\delta x_4(0) = .5$-3 AU

TABLE 31. COMPARISON OF CURRENT TIME GUIDANCE TERMINAL ERRORS WITH THOSE OF TTG, MD1, AND MD3 FOR SELECTED VALUES OF $c_{t\underline{\nu}}$ AND PERTURBATIONS IN x_1

$\delta x_1(0)$ (AU/day)	$-.4-4$	$-.15-4$	$.5-5$	$.5-4$
$c_{t\underline{\nu}}$	.99	.99	.99	.96
CT				
$|\underline{\psi}_v|$ (AU/day)	.17−7	≃.34−8	.25−9	.10−6
$|\underline{\psi}_r|$ (AU)	.42−5	.59−6	.68−7	.70−5
TTG				
$|\underline{\psi}_v|$ (AU/day)	~.19−7	~.14−8	.44−9	.10−6
$|\underline{\psi}_r|$ (AU)	.42−5	.59−6	.68−7	.70−5
MD1				
$|\underline{\psi}_v|$ (AU/day)	.17−7	~.25−8	.24−9	.84−7
$|\underline{\psi}_r|$ (AU)	.42−5	.59−6	.68−7	.70−5
MD3				
$|\underline{\psi}_v|$ (AU/day)	.17−7	~.25−8	.24−9	.11−6
$|\underline{\psi}_r|$ (AU)	.42−5	.59−6	.68−7	.70−5

TABLE 32. COMPARISON OF CURRENT TIME GUIDANCE TERMINAL ERRORS WITH THOSE OF TTG, MD1, AND MD3 FOR SELECTED VALUES OF $c_{t_{\underline{\nu}}}$ AND PERTURBATIONS IN x_4

$\delta x_4(0)$ (AU)	$-.21-2$	$.5-5$	$.3-3$	$.33-2$
$c_{t_{\underline{\nu}}}$	$.99$	$.99$	$.99$	$.96$
CT				
$\left|\underline{\psi}_v\right|$ (AU/day)	$.77-6$	$\simeq.45-10$	$.15-8$	$.32-6$
$\left|\underline{\psi}_r\right|$ (AU)	$.39-6$	$.26-10$	$.63-8$	$.78-6$
TTG				
$\left|\underline{\psi}_v\right|$ (AU/day)	$.48-7$	$.97-11$	$.56-9$	$\sim.98-7$
$\left|\underline{\psi}_r\right|$ (AU)	$.41-6$	$.25-10$	$.64-8$	$.80-6$
MD1				
$\left|\underline{\psi}_v\right|$ (AU/day)	$.79-6$	$\simeq.65-12$		
$\left|\underline{\psi}_r\right|$ (AU)	$.40-6$	$.24-10$		
MD3				
$\left|\underline{\psi}_v\right|$ (AU/day)		$\sim.29-10$	$.15-8$	
$\left|\underline{\psi}_r\right|$ (AU)		$.42-10$	$.64-8$	

were found only crudely, in some cases, and the tables are incomplete and include a case that has not been presented before, $\delta x_1(0) = -.15 \times 10^{-4}$ AU/day. Nevertheless, the data show that Current Time Guidance produces the same terminal position errors as the other schemes and approximately the same terminal velocity errors. (Recall that $\sim$ indicates an approximation to (within a few percent of) the minimum, and that $\simeq$ indicates a crude approximation to (within thirty·or forty percent of) the minimum.)

The case of $\delta x_1(0) = .5 \times 10^{-3}$ AU/day is a case that presents difficulty to Time-To-Go Guidance. This perturbation is about 900 meters/ sec, or about 3%·of the initial velocity -- quite a large perturbation. It is believed that this case lies outside the range of linearity for linear perturbation guidance. Terminal errors for this case using Current Time Guidance and Manual Time-To-Go Guidance with limits placed on the control change were given in Subsection 5.2.3.

5.3.3 Results of This Study vs. Those of Hart, Lattimore, and Stoker

Tables 33-35 present the nondimensionalized terminal errors in velocity and position for the current study and for the previous studies of Hart[1], Lattimore[2], and Stoker[3]. The terminal errors were derived from Reference 1 by extracting the state deviations at the final time from plots of the state deviations, in accordance with the author's claim that these deviations at t_f represent the terminal state errors for the guidance schemes. The terminal errors from Reference 2 were obtained by reading a table and transposing the apparently mislabeled columns of position and velocity errors. The terminal errors from Reference 3 were obtained by taking the square root of the sum of the squares of the tabulated values of the components of velocity and position errors.

As mentioned, for presentation here, the velocity errors were then non-dimensionalized by dividing by Earth's characteristic velocity, v_c. The position errors, expressed in AU, are essentially already in non-dimensionalized units. The notation NOT GIVEN in Table 34 indicates that plots were made in Reference 1 only for deviations in control, not state.

TTG means Time-To-Go Guidance. MD is Minimum Distance Guidance, with MD1 and MD3 indicating Weights 1 and 3 respectively. MMD1 is Hart's Modified Minimum Distance Guidance #1, which apparently generates no guidance data after $t = t_{f_N}$. MMD2 is Hart's Modified Minimum Distance Guidance #2, which is identical to MMD1 until $t = t_{f_N}$. After t_{f_N} the feedback gain matrices for MMD2 are calculated from "an extended nominal trajectory," apparently with zero thrust. All of Hart's schemes are open-loop, in the sense that the control changes are determined from changes in the initial state, rather than the current state. The rest are closed-loop. Lattimore's scheme was intended to be the closed-loop version of Hart's Minimum Distance Guidance. The values shown for Lattimore's Minimum Distance Guidance are for a one day loop closure rate.

The performance of the perturbation guidance schemes, as determined in the previous studies, is clearly shown in Tables 33-35 to be inferior to the performance as determined in the current study. Except for the case $\delta x_1(0) = .5 \times 10^{-3}$ AU/day, the improvement in terminal state error ranges from almost 2 orders of magnitude to 5 orders of magnitude in the present study as compared with Hart's and Stoker's work, and up to 8 orders of magnitude compared with Lattimore's work. The exceptional case,

TABLE 33. TERMINAL STATE ERRORS FOR THE CURRENT AND PREVIOUS STUDIES WITH PERTURBATIONS IN x_1

$$\delta x_1(0) \quad (AU/day/v_c) \quad [(AU/day)]$$

		$-.23-2$ $[-.4-4]$	$-.58-3$ $[-.1-4]$	$.29-3$ $[.5-5]$	$.29-2$ $[.5-4]$	$.29-1$ $[.5-3]$
HART						
TTG	$\|\underline{\psi}_v\|_{ND}$					$.51-1$
	$\|\underline{\psi}_r\|$					$.52-1$
MMD2	$\|\underline{\psi}_v\|_{ND}$					$.20-1$
	$\|\underline{\psi}_r\|$					$.40-1$
MMD1	$\|\underline{\psi}_v\|_{ND}$			$.15-2$	$.93-2$	$.18-1$
	$\|\underline{\psi}_r\|$			$.15-2$	$.13-1$	$.39-1$
LATTIMORE						
MMD2	$\|\underline{\psi}_v\|_{ND}$			$.44-2$		
	$\|\underline{\psi}_r\|$			$.76-2$		
STOKER						
TTG	$\|\underline{\psi}_v\|_{ND}$	$.39-3$	$.27-3$	$.40-3$	$.26-1$	
	$\|\underline{\psi}_r\|$	$.34-3$	$.15-3$	$.13-3$	$.20-1$	
MD	$\|\underline{\psi}_v\|_{ND}$	$.93-3$	$.44-3$	$.58-3$	$.43-2$	
	$\|\underline{\psi}_r\|$	$.21-3$	$.18-3$	$.17-3$	$.25-2$	
THIS STUDY						
TTG	$\|\underline{\psi}_v\|_{ND}$	$.10-6$	$.48-7$	$.24-7$	$.11-5$	
	$\|\underline{\psi}_r\|$	$.42-5$	$.27-6$	$.68-7$	$.74-5$	
MD1	$\|\underline{\psi}_v\|_{ND}$	$.10-5$	$.52-7$	$.14-7$	$.29-5$	
	$\|\underline{\psi}_r\|$	$.42-5$	$.27-6$	$.68-7$	$.70-5$	

TABLE 33. (continued)

$$\delta x_1(0) \quad (\text{AU/day}/v_c) \quad [(\text{AU/day})]$$

		-.23-2 [-.4-4]	-.58-3 [-.1-4]	.29-3 [.5-5]	.29-2 [.5-4]	.29-1 [.5-3]
THIS STUDY						
MD3	$|\underline{\psi}_v|_{ND}$	.99-6	.57-7	.14-7	.29-5	
	$|\underline{\psi}_r|$	.42-5	.27-6	.68-7	.70-5	
OTHER	$|\underline{\psi}_v|_{ND}$					.43-2
	$|\underline{\psi}_r|$					.77-2

TABLE 34. TERMINAL STATE ERRORS FOR THE CURRENT AND
PREVIOUS STUDIES WITH PERTURBATIONS IN x_4

$\delta x_4(0)$ (AU)

		-.21-2	-.3-3	.5-5	.5-4	.3-3	.5-3	.33-2
HART								
TTG	$|\underline{\psi}_v|_{ND}$						.76-4	
	$|\underline{\psi}_r|$						.18-3	
MMD2	$|\underline{\psi}_v|_{ND}$						.38-4	
	$|\underline{\psi}_r|$						.78-4	
MMD1	$|\underline{\psi}_v|_{ND}$			NOT	NOT		.64-5	
	$|\underline{\psi}_r|$			GIVEN	GIVEN		.65-5	
LATTIMORE								
CLSD.	$|\underline{\psi}_v|_{ND}$			.41-2				
LOOP	$|\underline{\psi}_r|$			.68-2				
STOKER								
TTG	$|\underline{\psi}_v|_{ND}$	.24-3	.35-3			.42-3		.76-3
	$|\underline{\psi}_r|$	.15-3	.16-3			.13-3		.13-3
MD	$|\underline{\psi}_v|_{ND}$	.58-3	.35-3			.41-3		.81-3
	$|\underline{\psi}_r|$	.24-3	.10-3			.14-3		.15-3
THIS STUDY								
TTG	$|\underline{\psi}_v|_{ND}$	.19-5	.35-7	.57-10	.64-9	.26-7	.74-7	.17-5
	$|\underline{\psi}_r|$	.59-6	.67-8	.25-10	.20-9	.68-8	.19-7	.12-5
MD1	$|\underline{\psi}_v|_{ND}$	.34-6	.85-8	$\simeq$.38-10	.11-8	.36-7	.11-6	.53-5
	$|\underline{\psi}_r|$	.53-6	.65-8	.24-10	.20-9	.92-8	.31-7	.27-5
MD3	$|\underline{\psi}_v|_{ND}$	.34-6	.73-8	$\simeq$.58-10	.12-8	.34-7	.11-6	.48-5
	$|\underline{\psi}_r|$	.54-6	.65-8	.21-10	.20-9	.95-8	.25-7	.26-5

TABLE 35.   TERMINAL STATE ERRORS FOR THE CURRENT AND

PREVIOUS STUDIES WITH PERTURBATIONS IN x_3 OR x_6

| | | $\delta x_3(0)$ (AU/day/v_c) [(AU/day)] | | $\delta x_6(0)$ (AU) | |
		$-.20-2$ [$-.35-4$]	$.20-2$ [$.35-4$]	$-.27-2$	$.33-2$
STOKER					
TTG	$\|\underline{\psi}_v\|_{ND}$	.84-3	.28-3	.36-3	.34-3
	$\|\underline{\psi}_r\|$	.21-3	.25-3	.15-3	.16-3
MD	$\|\underline{\psi}_v\|_{ND}$		.53-3	.25-1	.37-3
	$\|\underline{\psi}_r\|$		.20-3	.18-1	.15-3
THIS STUDY					
TTG	$\|\underline{\psi}_v\|_{ND}$	.40-6	.39-6	.37-8	.82-8
	$\|\underline{\psi}_r\|$	.37-7	.42-7	.20-9	.99-9
MD3	$\|\underline{\psi}_v\|_{ND}$	.56-6	.57-6	.35-9	.65-8
	$\|\underline{\psi}_r\|$	.14-6	.15-6	.24-9	.12-8

as mentioned before, is believed to be beyond the range of linearity

of the guidance schemes, so that the improvement is not quite as dramatic

as in the other cases.

The tables also reinforce the observation that the different pertur-

bation guidance schemes are all roughly equivalent in performance, if

implemented correctly. In fact, Time-To-Go Guidance and Minimum Distance

Guidance frequently show identical terminal position errors. The

remaining slight differences are usually the result of the process of

minimizing $\sum_{ND}$, as described in Subsection 5.2.2.

Another way of characterizing the effectiveness of a guidance scheme

is to compute the ratio of the sum of the nondimensionalized terminal

velocity and position errors to the nondimensionalized initial perturba-

tion:

$$Z = \sum_{ND} / |\delta x(0)|_{ND} = (|\underline{\psi}_v|_{ND} + |\underline{\psi}_r|)/|\delta x(0)|_{ND} \qquad (5.3.1)$$

These ratios are given in Tables 36 and 37 for cases with initial per-

turbations in x_1 and x_4. The tables simply present the data from Tables

33 and 34 in an easily interpreted format. The poor showing of the

guidance schemes as found by the earlier studies can be described in

many cases as divergence, i.e., the state perturbations increase with

time rather than decrease. This divergence is plainly not evident in

the current study. Except for the case of the large perturbation

$\delta x_1(0) = .5 \times 10^{-3}$ AU/day, the current study shows that the guidance

schemes reduce the perturbation to a fraction of 1% of its initial value

at the end of the flight. For the smaller perturbations the reduction

TABLE 36. RATIOS OF TERMINAL ERRORS TO INITIAL PERTURBATIONS IN x_1

$$\delta x_1(0) \quad (AU/day/v_c) \quad [(AU/day)]$$

	-.23-2 [-.4-4]	-.58-3 [-.1-4]	.29-3 [.5-5]	.29-2 [.5-4]	.29-1 [.5-3]
HART					
TTG					3.6
MMD2					2.1
MMD1			10.	7.6	2.0
LATTIMORE			41.		
STOKER					
TTG	.32	.72	1.8	16	
MD	.50	1.1	2.6	2.3	
THIS STUDY					
TTG	.18-2	.55-3	.32-3	.29-2	
MD1	.23-2	.56-2	.28-3	.34-2	
MD3	.23-2	.56-3	.28-3	.34-2	
MANUAL TTG					.38

TABLE 37. RATIOS OF TERMINAL ERRORS TO INITIAL PERTURBATIONS IN x_4

$$\delta x_4(0) \quad (AU)$$

	-.21-2	-.3-3	.5-5	.5-4	.3-3	.5-3	.33-2
<u>HART</u>							
TTG						.51	
MMD2						.23	
MMD1						.26-1	
<u>LATTIMORE</u>			.22+5				
<u>STOKER</u>							
TTG	.19	1.7			1.8		.27
MD	.39	1.5			1.8		.29
<u>THIS STUDY</u>							
TTG	.12-2	.14-3	.16-4	.17-4	.11-3	.19-3	.88-3
MD1	.41-3	.50-4	≃.12-4	.26-4	.15-3	.28-3	.24-2
MD3	.42-3	.46-4	≃.16-4	.28-4	.15-3	.27-3	.22-2

is to about .01% or less. This performance is clearly quite good.

Tables 38 and 39 compare Hart's changes in final time for the different cases with those of the current study.

TABLE 38. CHANGES IN FINAL TIMES (dt_f) FOR THE

CURRENT STUDY AND THAT OF HART, PERTURBATIONS IN x_1

$\delta x_1(0)$ (AU/day)

	-.4-4	-.1-4	.5-5	.5-4	.5-3
HART					
REO			.4666-1	.472	5.334
SCHEMES			.4662-1	.4661	4.661
THIS STUDY					
REO	-.368648	-.928586-1	.46606-1	.471427	5.327703
TTG	-.36727	-.92807-1	.46613-1	.4728	
MD3	-.36729	-.92807-1	.46613-1	.47293	

TABLE 39. CHANGES IN FINAL TIMES (dt_f) FOR THE

CURRENT STUDY AND THAT OF HART, PERTURBATIONS IN x_4

$\delta x_4(0)$ (AU)

	-.21-2	-.3-3	.5-5	.5-4	.3-3	.5-3	.33-2
HART							
REO			-.2392-3	-.2391-2		-.2382-1	
SCHEMES			-.2393-3	-.2393-3		-.2393-1	
THIS STUDY							
REO	.101501	.142970-1	-.237960-3	-.237596-2	-.14230-1	-.236790-1	-.1524
TTG	.10164	.14299-1	-.237960-3	-.237596-2	-.14227-1	-.236750-1	-.152
MD3	.10163	.14299-1	-.237960-3	-.237596-2	-.14227-1	-.236750-1	-.152

6. THE SOLAR SAIL PROBLEM EXAMINED BY JAYARAMAN

This chapter, while not a part of the guidance study, is related to it in that an Earth to Mars orbit transfer using low-thrust propulsion is optimized and in that more careful work yields better results than an earlier study.

6.1 JAYARAMAN'S PAPER AND THE SOLAR SAIL PROBLEM

In Reference 25, Jayaraman presents the results of his optimizations of minimum-time heliocentric transfers between Earth's orbit and Mars' orbit using solar sail propulsion. This problem is the same as that of References 4-14 discussed in Chapter 2, except that the low-thrust propulsion system used is a solar sail instead of, e.g., a nuclear ion engine. (For a detailed description of the problem see Ref. 25 or 26.) This simply means that thrust magnitude is not constant, but is a function of heliocentric distance and the sun-relative sail pointing angle (hence, thrust direction), and that spacecraft mass is a constant. Jayaraman mentions that his results differ from those of earlier studies of the problem by Zhukov and Lebedev[27] and Kelley[28,5]. In particular, his performance index, final time, is 10% larger. He says further that by relaxing the terminal penalties he, too, can obtain a performance index closer to those of the earlier studies.

6.2   SOLUTION OF THE PROBLEM USING A TRANSITION MATRIX ALGORITHM

OF WOOD

In Reference 26, we present the results of our optimization of the
problem mentioned in the last section. The neighboring extremal method
used is of the transition matrix type and was developed by Wood[29] based
upon algorithms in Reference 16. This method, the Neighboring Extremal
Algorithm 1-VTF, consists of the following steps:

1. Guess $\bar{\underline{v}}$, t_f and $\underline{x}^{(2)}(t_f)$. Initialize ε ($0 < \varepsilon \leq 1$).

2. Determine $\underline{x}^{(1)}(t_f)$ from $\underline{\psi} = 0$. Determine $\underline{\lambda}(t_f)$, ν_{g+1} and $\underline{u}(t_f)$
from the simultaneous solution of

$$\underline{\lambda}(t_f) = \Phi^T \underline{x}(t_f) \qquad\qquad (6.2.1)$$

$$0 = \Omega \qquad\qquad (6.2.2)$$

$$0 = H_{\underline{u}}(t_f) \qquad\qquad (6.2.3)$$

3. Integrate the differential equations for $\underline{x}(\cdot)$ and $\underline{\lambda}(\cdot)$ backward
from t_f to t_o, determining $\underline{u}(\cdot)$ from $H_{\underline{u}}(\cdot) = 0$.

4. If $\underline{x}(t_o)$ equals the specified value $\underline{x}*(t_o)$ to the desired
accuracy, stop. Otherwise, compare the achieved change in $\underline{x}(t_o)$ from the
previous iteration with the predicted change. If the discrepancy is
large, reduce ε. If the discrepancy is very small, increase ε (subject
to $0 < \varepsilon \leq 1$). Then choose

$$\Delta\underline{x}(t_o) = -\varepsilon[\underline{x}(t_o) - \underline{x}*(t_o)] \qquad\qquad (6.2.4)$$

5. Repeat <u>steps 2 and 3</u> n additional times, with one component of
$\bar{\underline{v}}$, t_f, or $\underline{x}^{(2)}(t_f)$ perturbed slightly each time, the rest held constant.
Record the value of $\underline{x}(t_o)$ each time.

6. Construct the n x n matrix

$$\chi = \frac{\partial \underline{x}(t_o)}{\partial [\underline{\nu}, t_f, \underline{x}^{(2)}(t_f)]}$$

from the information obtained in <u>Step 5</u>.

7. Evaluate

$$\begin{bmatrix} \Delta \overline{\underline{\nu}} \\ \Delta t_f \\ \Delta \underline{x}^{(2)}(t_f) \end{bmatrix} = \chi^{-1} \Delta \underline{x}(t_o) \tag{6.2.6}$$

8. Replace $\overline{\underline{\nu}}$ with $\overline{\underline{\nu}} + \Delta \overline{\underline{\nu}}$, t_f with $t_f + \Delta t_f$, and $\underline{x}^{(2)}(t_f)$ with $\underline{x}^{(2)}(t_f) + \Delta \underline{x}^{(2)}(t_f)$, and go to <u>Step 2</u>.

The notation used in the above algorithm is similar to the notation used in the other chapters and

n   = number of state variables $\underline{x}$

g+1   = number of terminal constraints ψ

$\overline{\psi}, \overline{\underline{\nu}}$ = the first g components of ψ and $\underline{\nu}$, reordered if

       necessary, such that

$$\frac{d\psi_{g+1}}{dt_f}\left[\underline{x}^*(t_f^*), \underline{u}^*(t_f^*), t_f^*\right] \neq 0 \tag{6.2.7}$$

( )* - denotes optimal

The state vector is partitioned (and reordered) into a gx1 vector $\underline{x}^{(1)}$ and an (n-g)x1 vector $\underline{x}^{(2)}$ such that $\overline{\psi}_{\underline{x}^{(1)}}(t_f)$ is nonsingular.

6.3. RESULTS AND COMPARISON WITH THOSE OF JAYARAMAN

A computer program using the DODE integrator described in earlier chapters was implemented on the Jet Propulsion Laboratory's Univac 1100/80 computer system. The results of the computer runs are contained in Reference 26. Therein it is pointed out that the final time obtained, 7.02232 (408 days) and 5.57911 (324 days), for the characteristic accelerations of about 1 mm/s^2 and 2 mm/s^2 respectively, match those of References 27-29 and those of Sauer[30] to within about 1%. Moreover, the control histories match those of References 5 and 27 to within the error inherent in plotting and reading graphs. Jayaraman's final times, 7.66 and 6.11, thus disagree by about 10% with those just mentioned; and since his control history also differs substantially, his results are suspect. In Reference 26 we indicate that a possible source of error in the formulation of Jayaraman is his omission of the "1" in the transversality condition

$$H(t_f) + 1 = 0 \qquad\qquad (6.3.1)$$

This apparent omission further highlights the fact that the formulation and implementation of algorithms for solving optimal control problems must be done with great care.

7. CONCLUSIONS AND SUGGESTIONS FOR FURTHER STUDY

With reference to the nominal trajectory, the conclusions are:

1. The nominal trajectories determined by Hart, Lattimore, and Stoker apparently (as determined by an integration of their given values of initial state and multipliers, final time, and associated parameters) achieve rendezvous with Mars to an accuracy of 690 km/day in velocity and 75,000 km in position. The accuracy of the solution from the current study is 2×10^{-5} km/day in velocity and .004 km in position. The apparent inaccuracy of the previous solutions for the nominal trajectory may be a cause of the poor performance of the guidance schemes as found by the earlier studies, due to the resulting small inaccuracies of the feedback gains. More importantly, the faulty computed values of $\delta \underline{x}(t)$, derived in part from this inaccurate nominal trajectory, could corrupt the computation of the control changes, causing large terminal errors. Hart's reoptimized trajectories could also be presumed to be inaccurate, compounding the problem of determining the terminal errors of his guidance schemes.

2. The use of vector criteria in the ε adjustment process was essential to arriving at a solution of the TPBVP in a reasonable time. Also, the automation of this process greatly facilitated the quick determination of a solution of the TPBVP from an off-nominal initial guess.

3. Considerable care must be taken in selecting an algorithm for solving TPBVP's, an integrator, and the various associated parameters to obtain an accurate solution. Use of the Backward Sweep Algorithm (BSA), Krogh's variable order, variable step size, double precision

integrator, and relative error tolerances for integration of the $\dot{\underset{\sim}{S}}$, $\dot{\underset{\sim}{R}}$,

and $\dot{\underset{\sim}{Q}}$ matrix equations was demanding in implementation, but rewarding

in results.

With reference to the guidance schemes, the conclusions are:

1. Time-To-Go Guidance and Minimum Distance Guidance perform much

better, as measured by terminal state errors, than indicated by Hart,

Lattimore, and Stoker. In every case, except that of $\delta x_1(0) = .5 \times 10^{-3}$

AU/day, there is an improvement of roughly two to five orders of magni-

tude in performance, as determined by the present study. Possible

reasons for this improvement include more accurate guidance program

integration, use of high order feedback gain interpolation, finding

index time more accurately, the use of "partially" open-loop control

near the end of the flight by holding $\overline{d\underset{\sim}{v}}$ constant, and the second order

determination of $\delta\underset{\sim}{x}$. Also, conceptual and programming errors in the

earlier studies are suspected.

2. The reduction of the initial perturbation by factors of 100 to

10,000 over the flight means that the guidance schemes are acceptable

for use in real missions. They are not divergent as indicated by the

previous studies.

3. The two different weighting procedures tried, Weight 1, non-

dimensionalized equivalent weighting of all position, velocity, and time

components of the metric, and Weight 3, the equivalent weighting of

position components only, produced virtually identical performance for

the Minimum Distance Guidance technique.

4. The performance of Time-To-Go Guidance was essentially equiva-
lent to that of Minimum Distance Guidance. The terminal error in position
was the same for both schemes in many cases. This conclusion differs
from that in Reference 24 in which a stationary problem was examined for
very large initial perturbations.

5. A limited test of Current Time Guidance (with $d\bar{\underline{\nu}}$ fixed near the
end of the flight and using nominal final time gain information after the
nominal final time) revealed that its performance was almost as good as
that of Time-To-Go Guidance and Minimum Distance Guidance. This leads
to the observation that indexing the gains may not be necessary as
indicated in Reference 21. (The numerical examples of References 21
were a stationary problem and a first order problem with linear equations
and a very large initial perturbation.)

6. The time at which $d\bar{\underline{\nu}}$ is held constant, $t_{\overline{\underline{\nu}}}$, has an impact on the
performance. Variation of this parameter can yield improved performance.

7. A 3-dimensional rendezvous with Mars, assuming inclined, ellipti-
cal planetary orbits, is a much more complicated problem than a 2-
dimensional transfer to a circular orbit at the distance of Mars. Since
a degree of freedom is lost in that a rendezvous must be effected, the
guidance schemes cannot handle initial perturbations as easily as was
indicated by the simpler transfer problem. In particular, for the case
of the relatively large perturbation $\delta x_1(0) = .5 \times 10^{-3}$ AU/day, the
guidance schemes did not perform very well and control change limiting
was required. It is believed that this case lies outside the range of
linearity.

8. Plots of the deviations of the state and control with respect to a reoptimized trajectory reveal similar and interesting behavior for the different guidance schemes. The final state deviations are much smaller than the maximum excursions, which occur invariably after thrust reversal. The maximum excursions in control deviations occur, naturally enough, near thrust reversal and near the final time.

9. While cost comparisons were not a purpose of this study, it was observed that the computing cost of Reoptimization was a few times that of the perturbation guidance schemes. In a real, more complex problem it is conceivable that the guidance programs could be much less expensive in a relative sense, especially if a more efficient high order feedback gain interpolation is used.

With respect to the optimization of the nominal trajectory, suggestions for further study are:

1. Search for the value of t_1, the time at which transformation (2.3.43-45) is made, that provides the best accuracy of the feedback gains. Theoretically the choice of t_1 should make no difference. The accuracy depends on round-off errors.

2. Make a cost vs. accuracy tradeoff study by varying the tolerance level for the integration and step size limits.

3. Refine the determination of the proper relative error tolerance for each equation.

4. Implement an ε adjustment technique that permits "perfect guesses" of the final state.

With respect to the guidance schemes, suggestions for further study are:

1. Determine whether Current Time Guidance or Manual Time-To-Go Guidance is as good as Time-To-Go Guidance and Minimum Distance Guidance for all values of $t_{\overline{\nu}}$ in all cases.

2. Characterize and predict the performance as a function of $t_{\overline{\nu}}$. Theoretically, the value of $t_{\overline{\nu}}$ should make no difference. Any improvement in performance would be due to a reduction in round-off errors.

3. Determine the performance as a function of accuracy of the optimization of the nominal trajectory (accuracy of the feedback gains).

4. Make a cost vs. integration accuracy tradeoff by varying integration tolerances and step size limits.

5. Find another, more efficient technique to interpolate the feedback gains and determine the resulting performance.

6. Do more extensive research into the costs and benefits of not using a second order expression for $\delta \underline{x}$ and the partially open-loop technique of holding $d\overline{\nu}$ constant near the final time.

7. Study these guidance schemes as applied to other problems.

8. Consider different weights for Minimum Distance Guidance.

9. Explore the accuracy requirements for the determination of index time.

8. REFERENCES

1. Hart, J. D., "A Comparison of Low-Thrust Guidance Techniques," Ph.D. Dissertation, Univ. of Texas at Austin, 1971.

2. Lattimore, J. P., "A Comparison of Open and Closed Loop Applications of the Minimum Distance Guidance Technique," Engineer's Degree Dissertation, Univ. of Texas at Austin, 1972.

3. Stoker, P. W., "A Comparison of Linear Guidance Techniques, Applied to a Low-Thrust Orbit Transfer Problem," Engineer's Degree Dissertation, California Institute of Technology, Pasadena, Ca., 1975.

4. Wood, L. J., "Second Order Optimality Conditions and Optimal Feedback for Variable End Time Terminal Control Problems," Ph.D. Dissertation, Stanford Univ., Stanford, Ca., 1972.

5. Kelley, H. J., "Method of Gradients," in Optimization Techniques, edited by G. Leitmann, Chapter 6, Academic Press, New York, 1962, pp. 205-254.

6. Kenneth, P. and McGill, R., "Two Point Boundary Value Problem Techniques," in Advances in Control Systems, edited by C. T. Leondes, Vol. 3, Chapter 2, Academic Press, New York, 1966, pp. 69-109.

7. Kelley, H. J., Kopp, R. E., and Moyer, G. H., "A Trajectory Optimization Technique Based upon the Theory of the Second Variation," in Progress in Astronautics and Aeronautics, edited by V. G. Szebehely, Vol. 14, Chapter 5, Academic Press, New York, 1964, pp. 559-582.

8. Kopp, R. E., and Moyer, H. G., "Trajectory Optimization Techniques," in Advances in Control Systems, edited by C. T. Leondes, Vol. 4, Chapter 3, Academic Press, New York, 1966, pp. 104-155.

9. Moyer, G. H., and Pinkham, G., "Several Trajectory Optimization Techniques, Part II," in Computing Methods in Optimization Problems, edited by A. V. Balakrishnan and L. W. Neustadt, Chapter 3, Academic Press, New York, 1964, pp. 91-105.

10. McReynolds, S. R., "A successive Sweep Method for Solving Optimal Programming Problems," Ph.D. Thesis, Harvard Univ., 1965.

11. McReynolds, S. R., "The Successive Sweep Method and Dynamic Programming," _Journal of Mathematical Analysis and Applications_, Vol. 19, No. 3., 1967, pp. 565-598.

12. Tapley, B. D., and Lewallen, J. M., "Comparison of Several Numerical Optimization Methods," _Journal of Optimization Theory and Applications_, Vol. 1, No. 1, 1967, pp. 1-32.

13. Gershwin, S. B., and Jacobson, D. H., "A Discrete-Time Differential Dynamic Programming Algorithm with Application to Optimal Orbit Transfer," _AIAA Journal_, Vol. 8, No. 9, 1970, pp. 1616-1626.

14. Williamson, W. E., and Tapley, B. D., "Riccati Transformations for Control Optimization Using the Second Variation," AMRL 1035, University of Texas at Austin, 1971.

15. Battin, R. H., _Astronautical Guidance_, McGraw-Hill, New York, 1964.

16. Bryson, A. E., and Ho, Y. C., _Applied Optimal Control_, Hemisphere Publishing Corp., Washington, D.C., 1975.

17. Wood L. J., and Bryson, A.E., "Second Order Optimality Conditions for Variable End Time Terminal Control Problems," _AIAA Journal_, Vol. 11, No. 9, Sept. 1973, pp. 1241-1246.

18. Krogh, F. T., "Preliminary Usage Document for the Variable Order Integrators SODE and DODE," Computing Memorandum No. 399, Jet Propulsion Laboratory, Pasadena, Ca., 1982.

19. Krogh, F. T., "Changing Stepsize in the Integration of Differential Equations Using Modified Divided Differences," Technical Memorandum No. 312, Jet Propulsion Laboratory, Pasadena, Ca., 1973.

20. Krogh, F. T., "Variable Order Integrators for the Numerical Solution of Ordinary Differential Equations," Tech. Brief, NPO-11643, Jet Propulsion Laboratory, Pasadena, Ca., 1970.

21. Speyer, J. L., and Bryson, A. E., "A Neighboring Optimum Feedback Control Scheme Based on Estimated Time-To-Go with Application to Re-Entry Flight Paths," _AIAA Journal_, Vol. 6, No. 5, 1968, pp. 769-776.

22. Powers, W. F., "A Method for Comparing Trajectories in Optimum Linear Perturbation Guidance Schemes," _AIAA Journal_, Vol. 6, No. 12, 1968, pp. 2451-2452.

23. Wood, L. J., "Perturbation Guidance for Minimum Time Flight Paths of Spacecraft," AIAA Paper 72-915, AIAA/AAS Astrodynamics Conference, Palo Alto, Ca., Sept. 1972.

24. Powers, W. F., "Techniques for Improved Convergence in Neighboring Optimum Guidance," AIAA Journal, Vol. 8, No. 12, 1970, pp. 2235-2241.

25. Jayaraman, T. S., "Time-Optimal Orbit Transfer Trajectory for Solar Sail Spacecraft," Journal of Guidance and Control, Vol. 3, No. 6, 1980, pp. 536-542.

26. Wood, L. J., Bauer, T. P., and Zondervan, K. P., "Comment on 'Time-Optimal Orbit Transfer Trajectory for Solar Sail Spacecraft'," Journal of Guidance, Control and Dynamics, Vol. 5, No. 2, 1982, pp. 221-224.

27. Zhukov, A. N. and Lebedev, V. N., "Variational Problem of Transfer Between Heliocentric Circular Orbits by Means of a Solar Sail," Cosmic Research, Vol. 2, No. 1, 1964, pp. 41-44.

28. Kelley, H. J., "Gradient Theory of Optimal Flight Paths," ARS Journal, Vol. 30, No. 10, 1960, pp. 947-954.

29. Wood, L. J., "Lecture Notes on Deterministic Optimal Control Theory," Revision 2, California Institute of Technology, Pasadena, Ca., Autumn 1980.

30. Sauer, C. G., Jr., "Optimum Solar-Sail Interplanetary Trajectories," AIAA Paper 76-792, AIAA/AAS Astrodynamics Conference, San Diego, Ca., Aug. 1976.

31. Hull, D. G., "Applications of Parameter Optimization to Trajectory Optimization," AIAA Paper 74-825, Anaheim, Ca., Aug. 1974.

32. Powers, W. F. and Shieh, C. J., "Convergence of Gradient-Type Methods for Free Final Time Problems," AIAA Journal, Vol. 14, Nov. 1976, pp. 1598-1603.

9.   APPENDIX
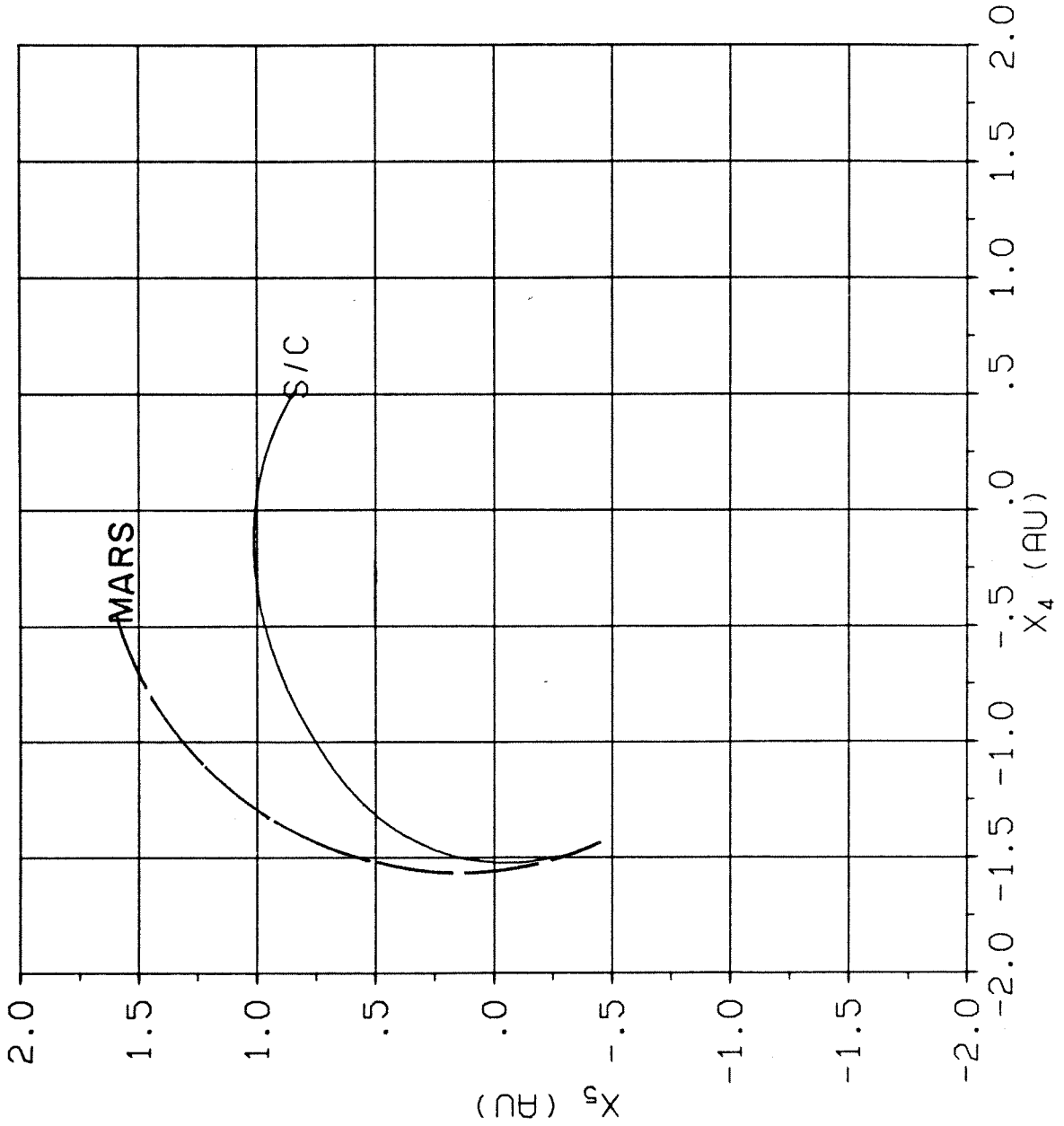
FIGURE 56.   ECLIPTIC PROJECTION OF NOMINAL TRAJECTORY
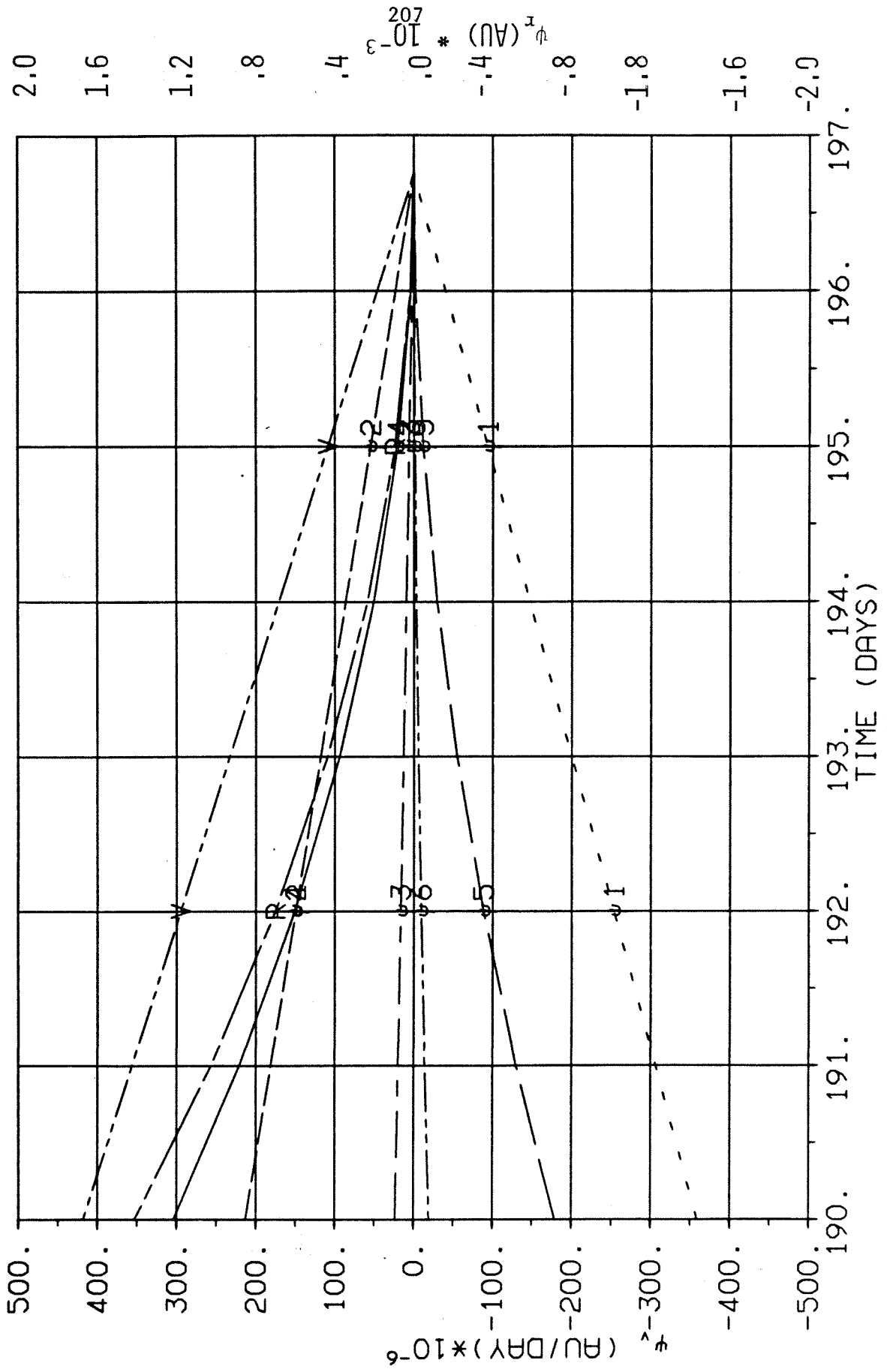
FIGURE 57. TERMINAL ERROR $(\psi_{1-6}, |\underline{\psi}_v|, |\underline{\psi}_r|)$ AS A FUNCTION OF TIME, NOMINAL TRAJECTORY

207
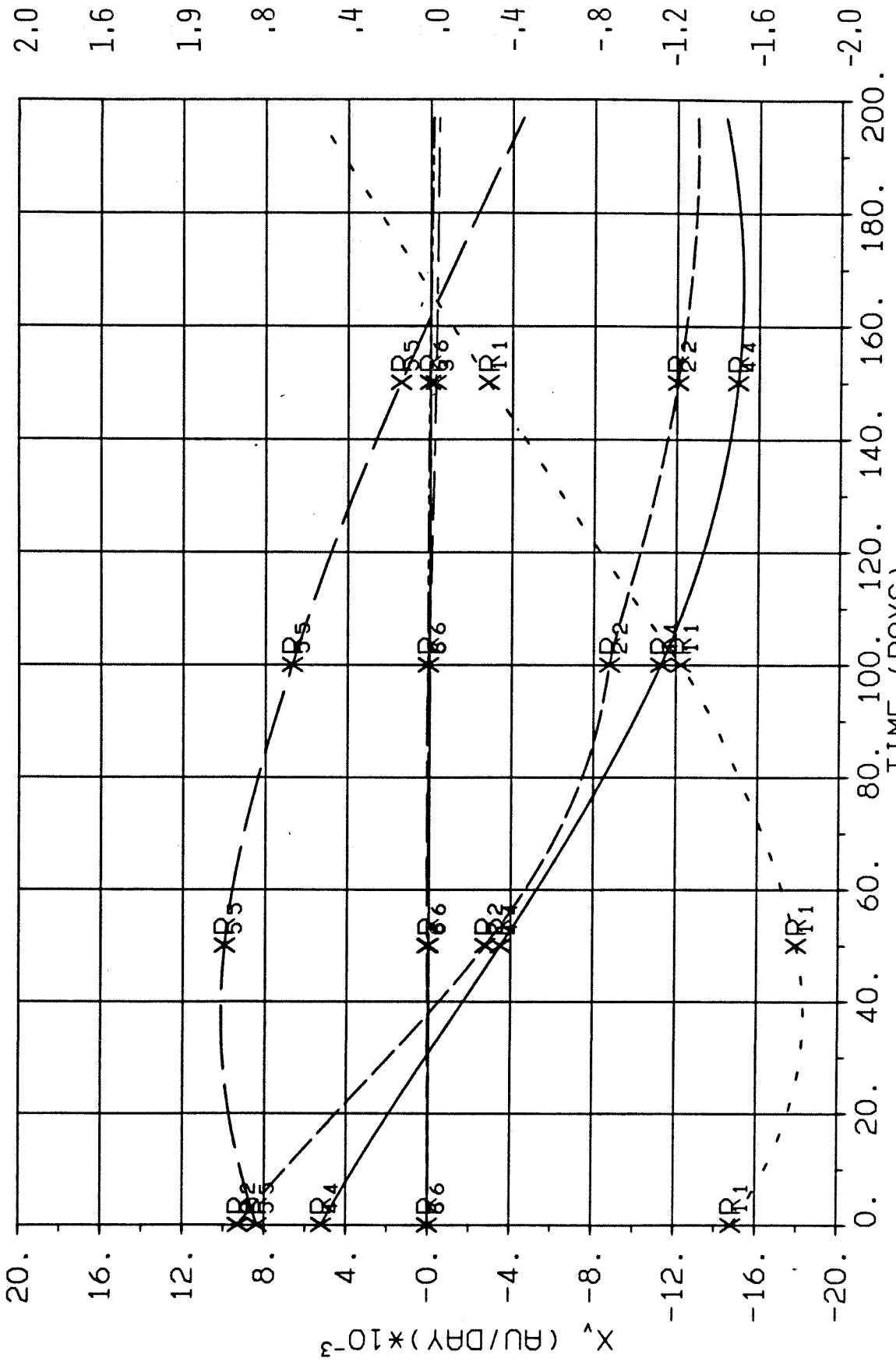
FIGURE 58. REO AND TTG STATE, $\delta x_1 (0) = .5\text{-}5$ AU/DAY
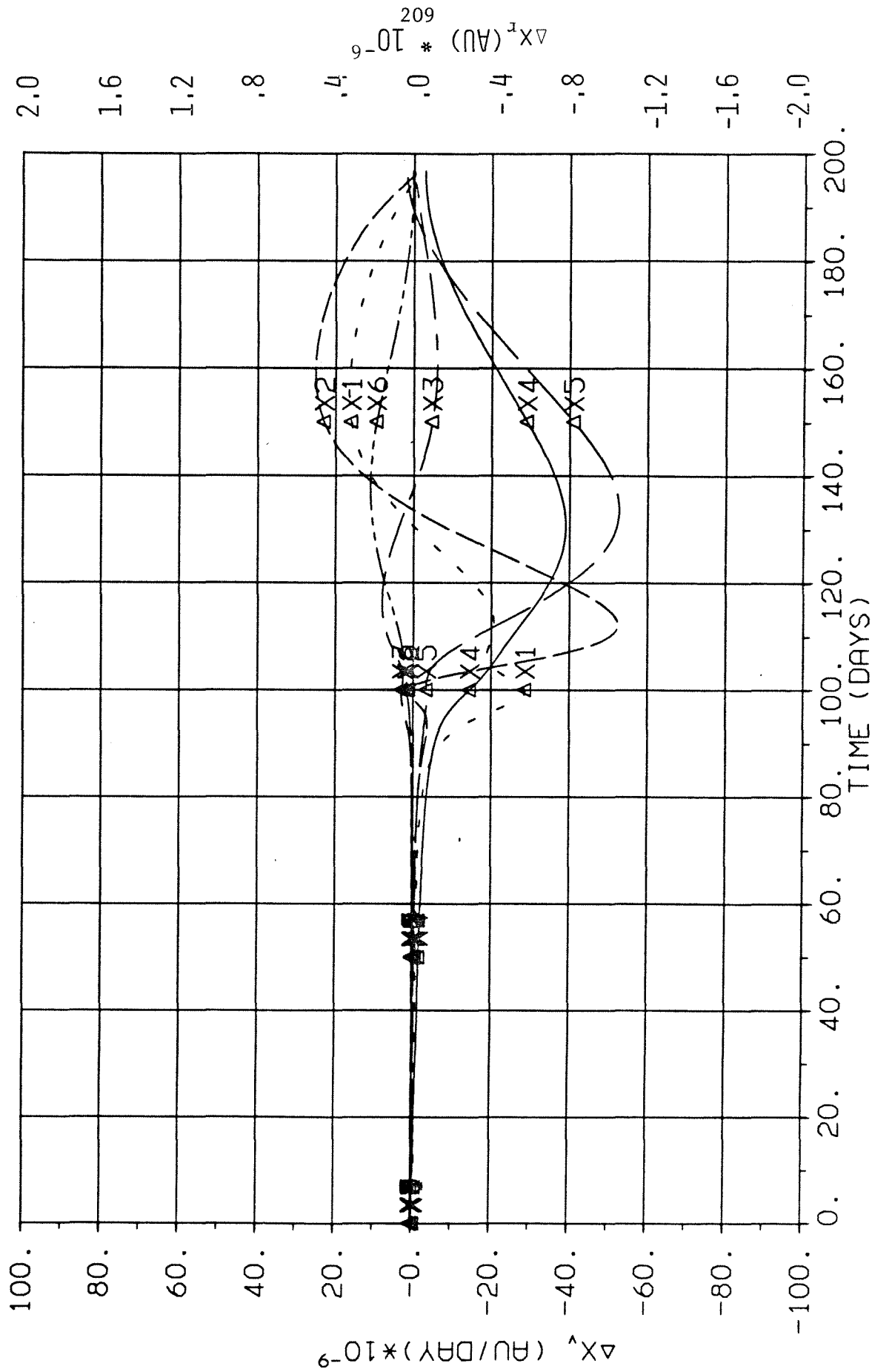
FIGURE 59. TTG State Component Deviations, $\delta x_1(0) = .5\text{-}5$ AU/DAY
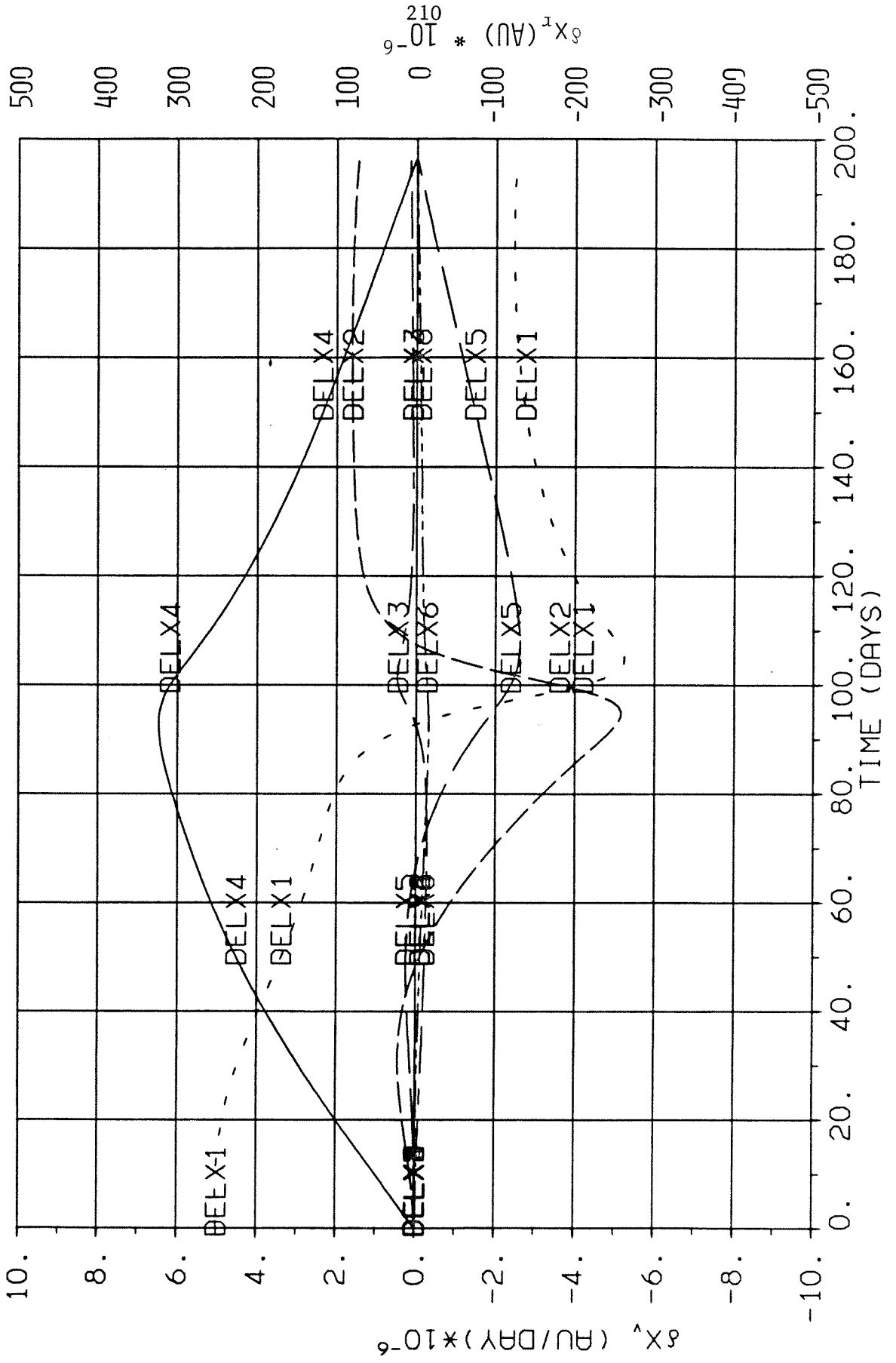
FIGURE 60. TTG $\delta x_{1-6}(T)$, $\delta x_1(0) = .5-5$ AU/DAY
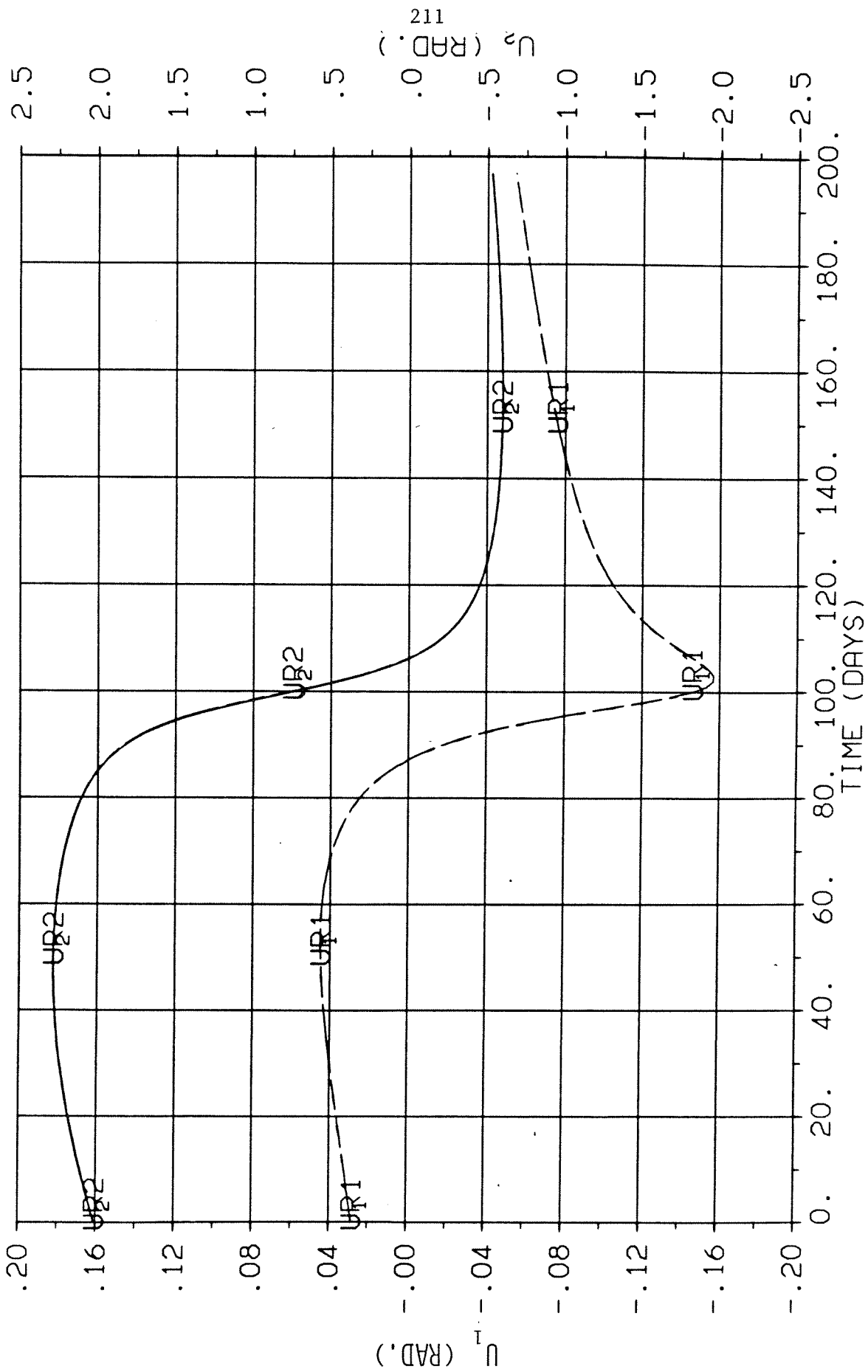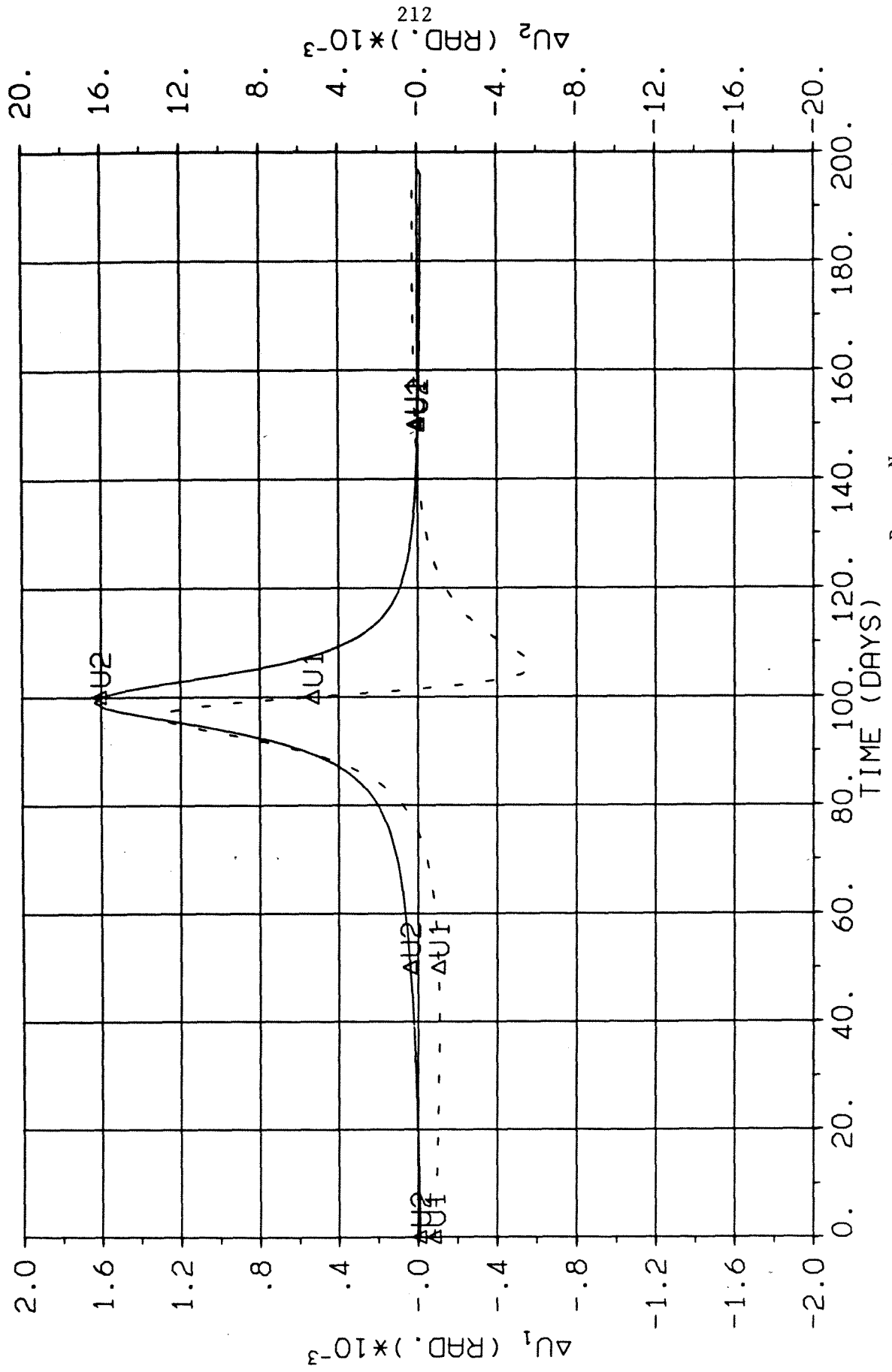
FIGURE 61. NOMINAL CONTROL AND REO CONTROL FOR $\delta x_1(0) = .5$-5 AU/DAY
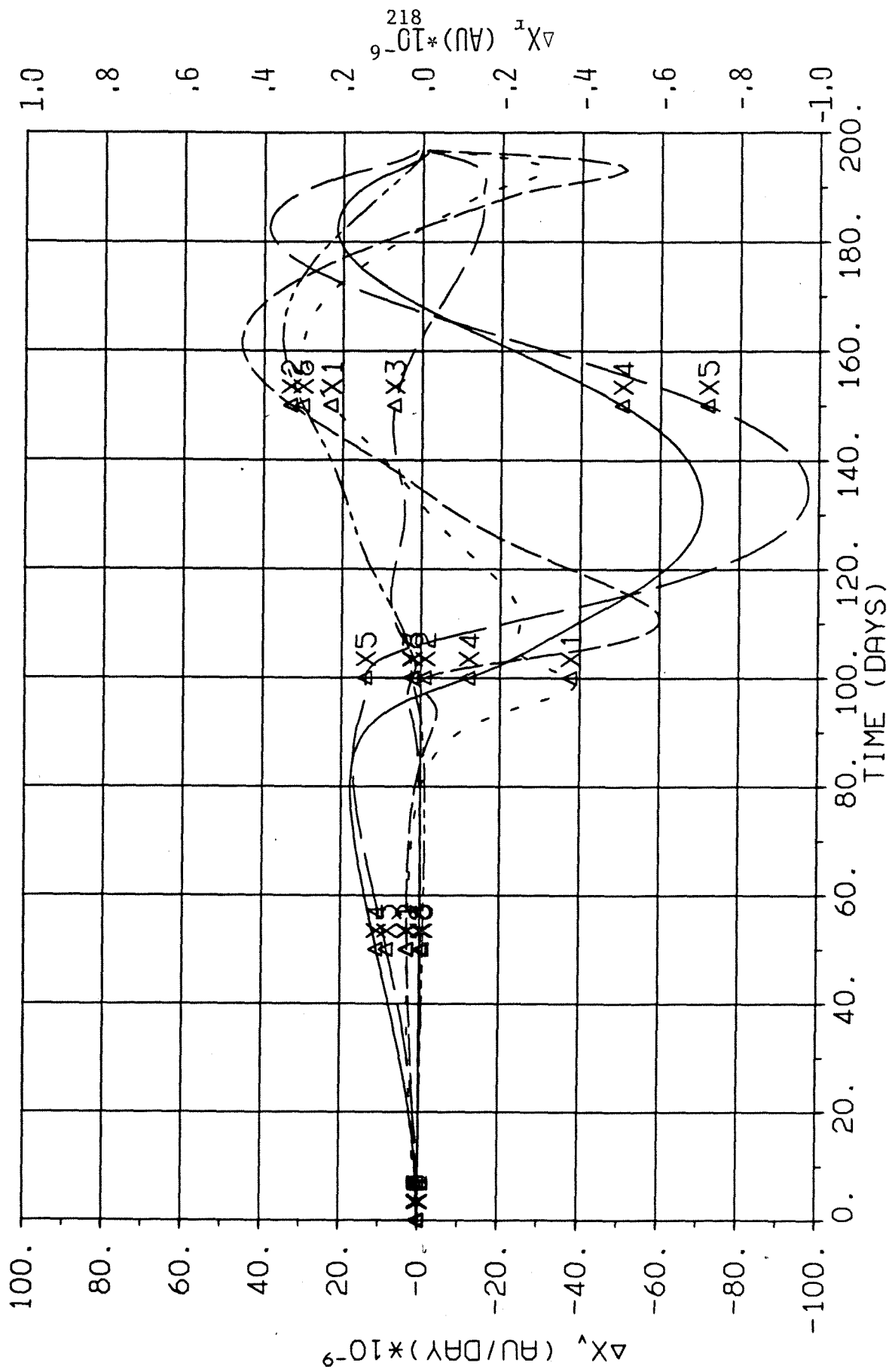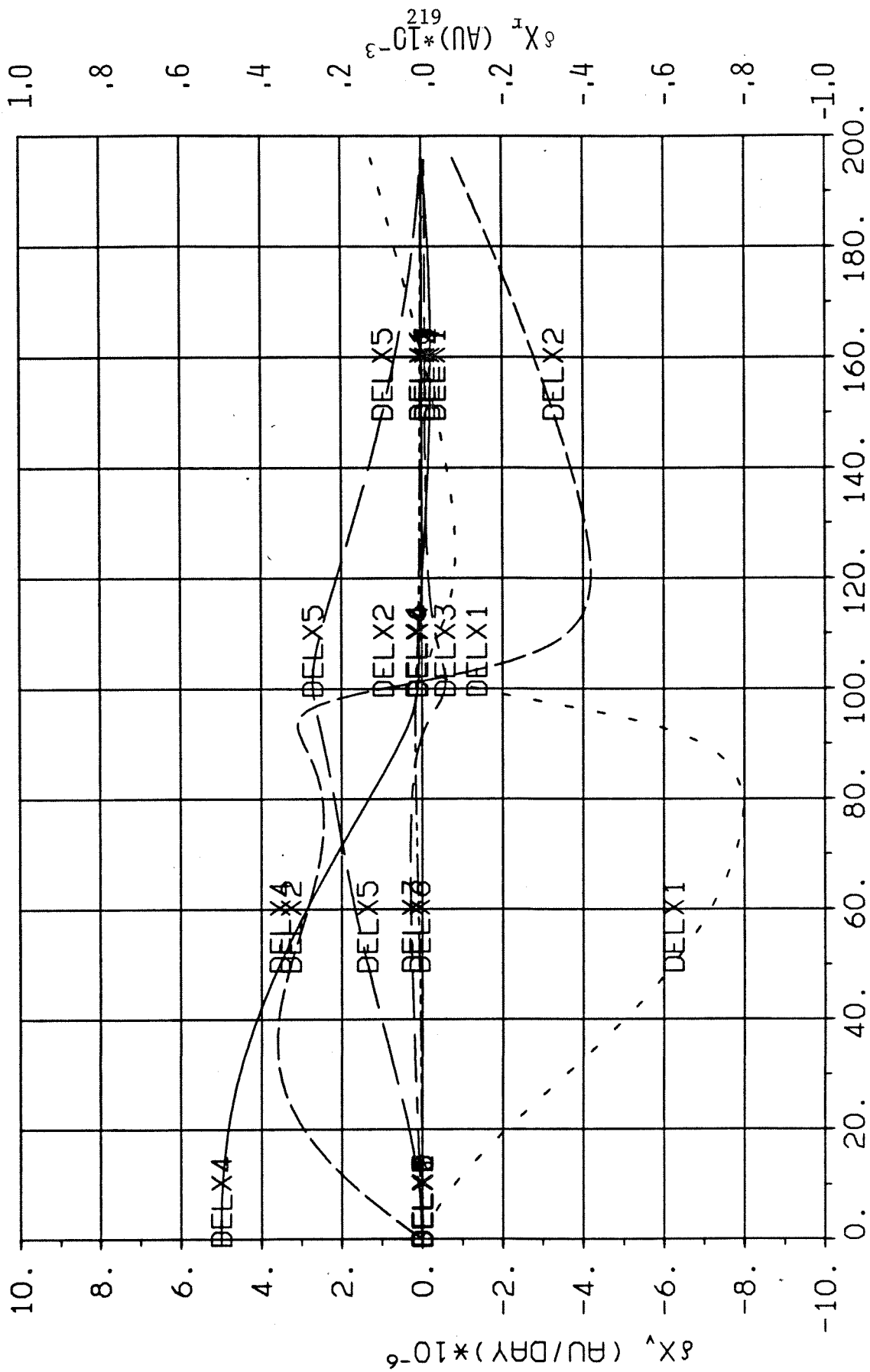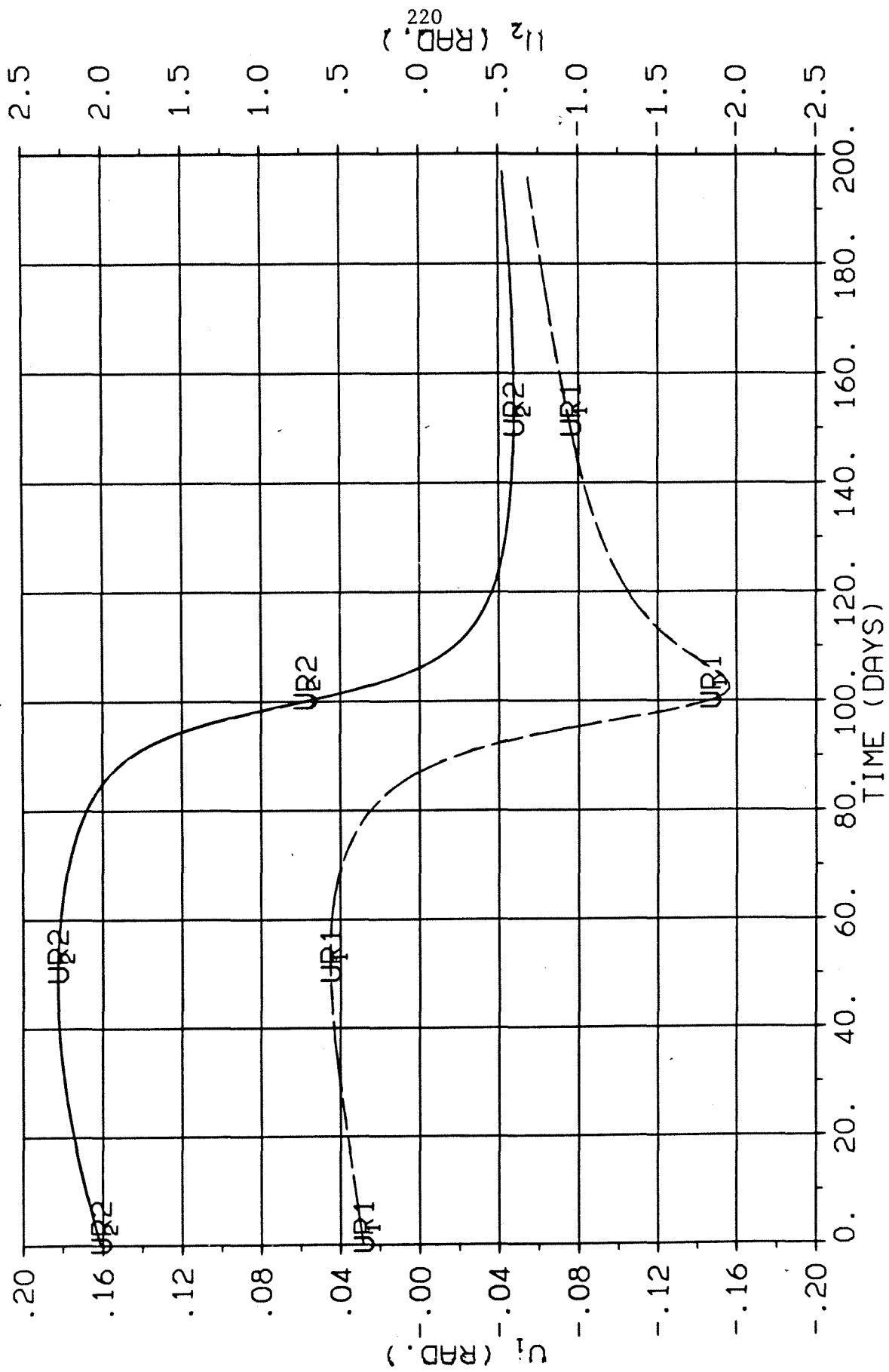
FIGURE 62. CONTROL DIFFERENCE ($\delta U_i = U_i^R - U_i^N$), $\delta X_1(0) = .5$-5 AU/DAY

212
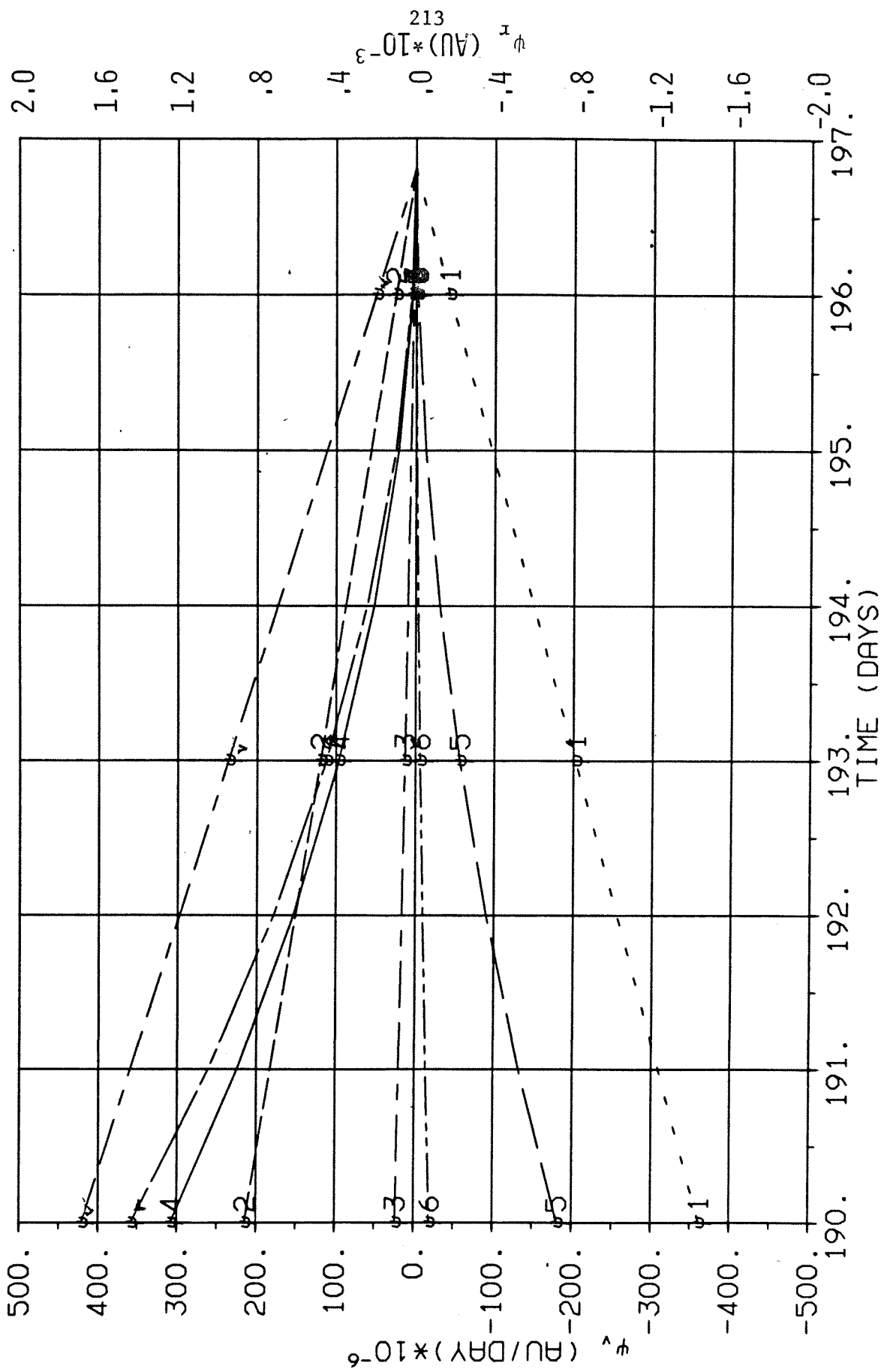
FIGURE 63. REO TERMINAL ERROR (ψ_{1-6}, $|\underline{\psi}_v|$, $|\underline{\psi}_r|$) AS A FUNCTION OF TIME, $\delta X_1(0)$ = .5-5 AU/DAY
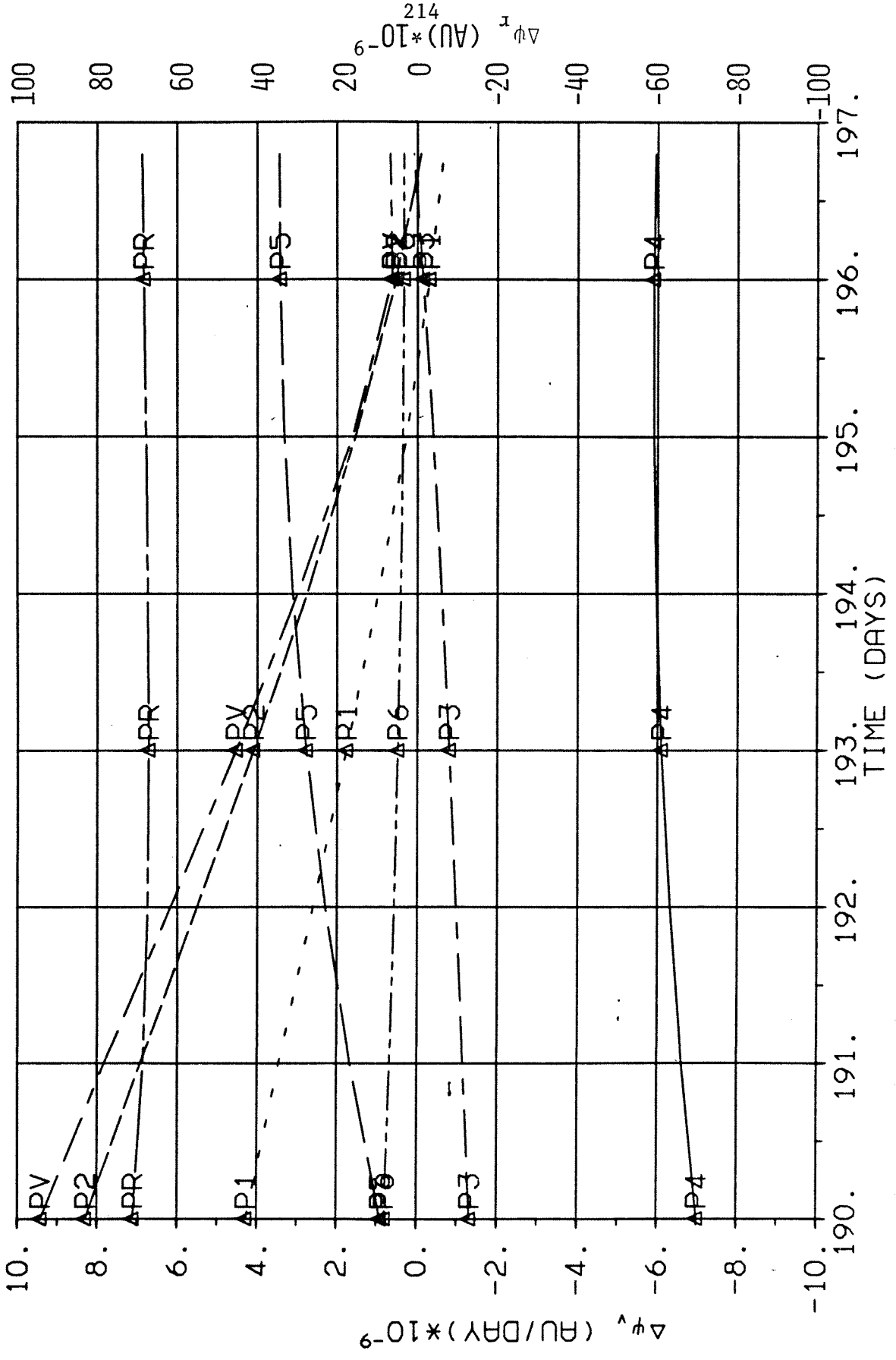
FIGURE 64. TTG TERMINAL ERROR DEVIATIONS $(\Delta\psi_{1-6}, |(\underline{\Delta\psi})_v|, |(\underline{\Delta\psi})_r|)$, $\delta x_1(0) = .5\text{-}5$ AU/DAY
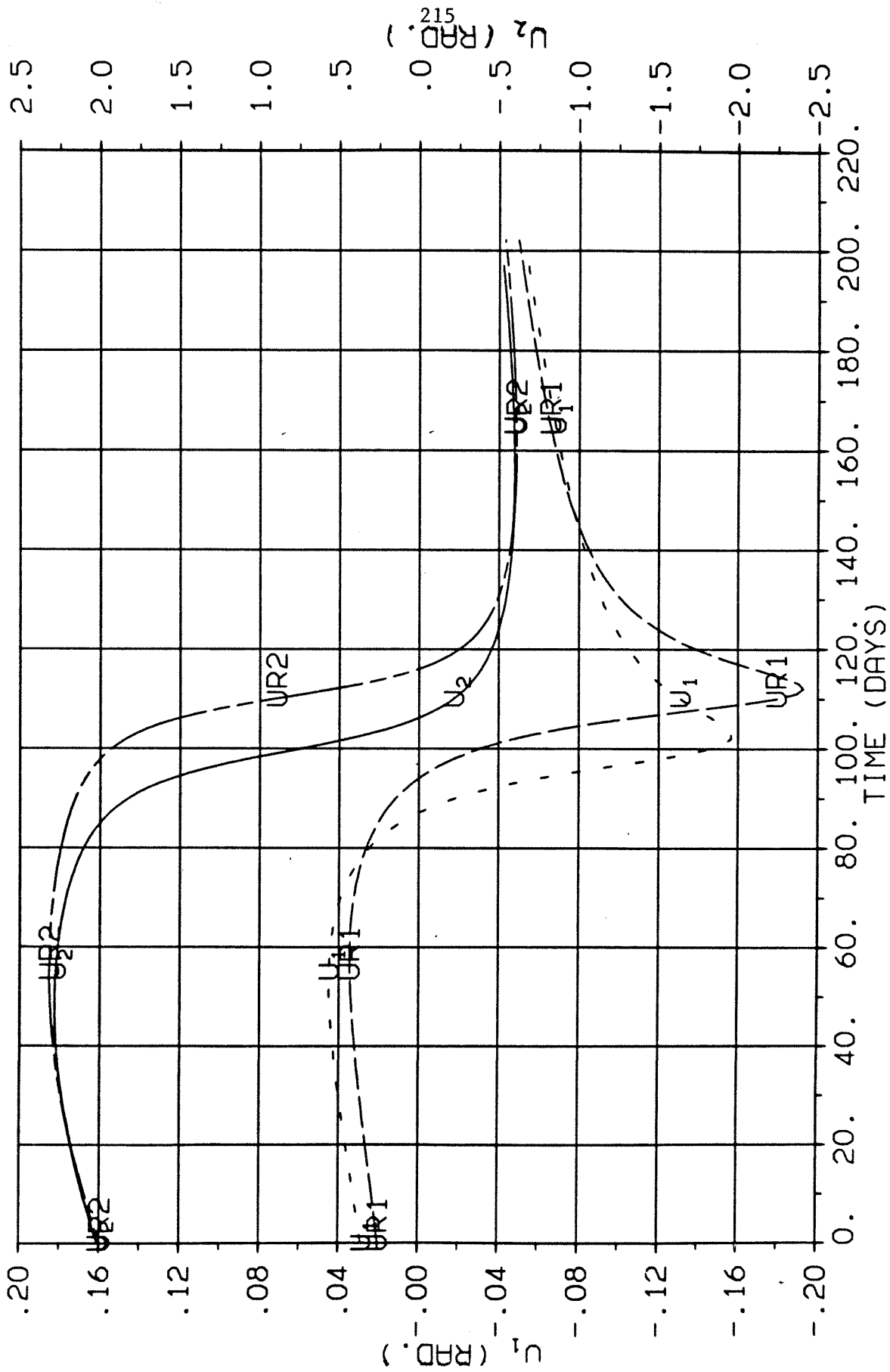
FIGURE 65. NOMINAL CONTROL AND REO CONTROL FOR $\delta X_1(0) = .5\text{-}3$ AU/DAY

216
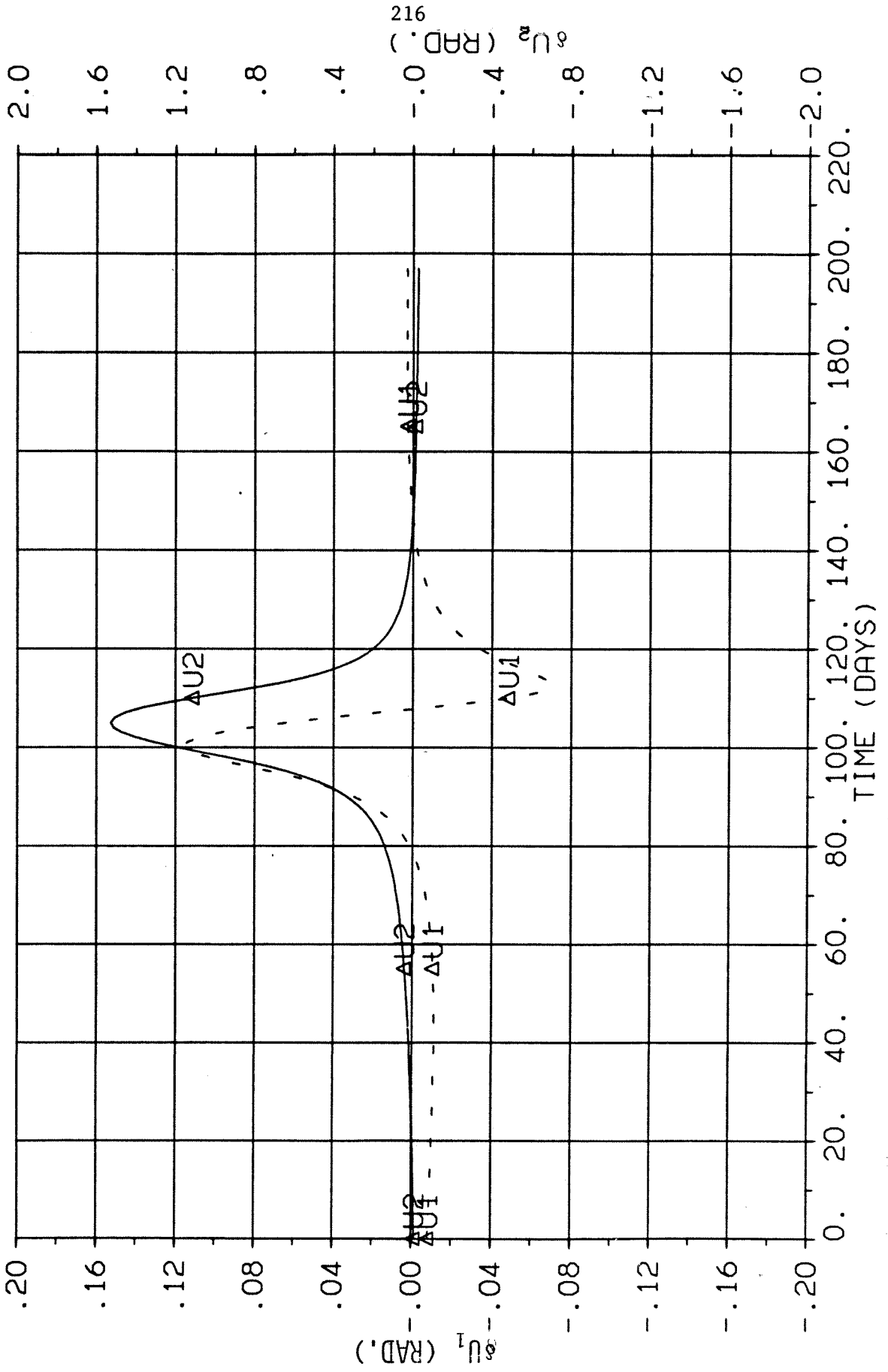
FIGURE 66. CONTROL DIFFERENCE ($\delta u_i = u_i^R - u_i^N$), $\delta x_1(0) = .5$–3 AU/DAY

217
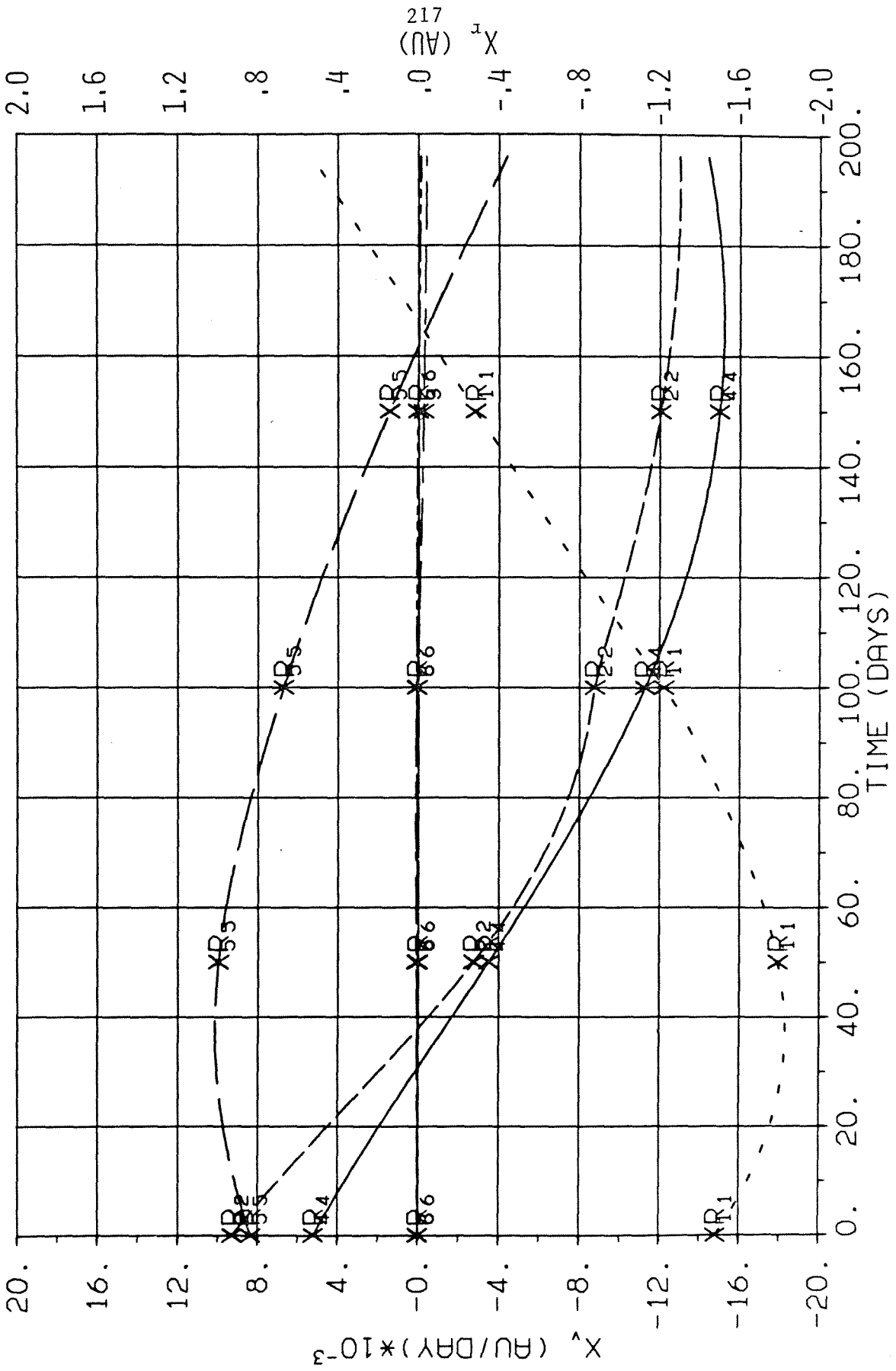
FIGURE 67. REO AND TTG STATE, $\delta x_4(0) = .5-3$ AU

FIGURE 68. TTG State Component Deviations, $\delta X_4(0) = .5\text{-}3$ AU

FIGURE 69. TTG $\delta x_{1-6}(\tau)$, $\delta x_4(0) = .5\text{-}3$ AU

FIGURE 70. NOMINAL CONTROL AND REO CONTROL FOR $\delta x_4(0) = .5\text{-}3$ AU
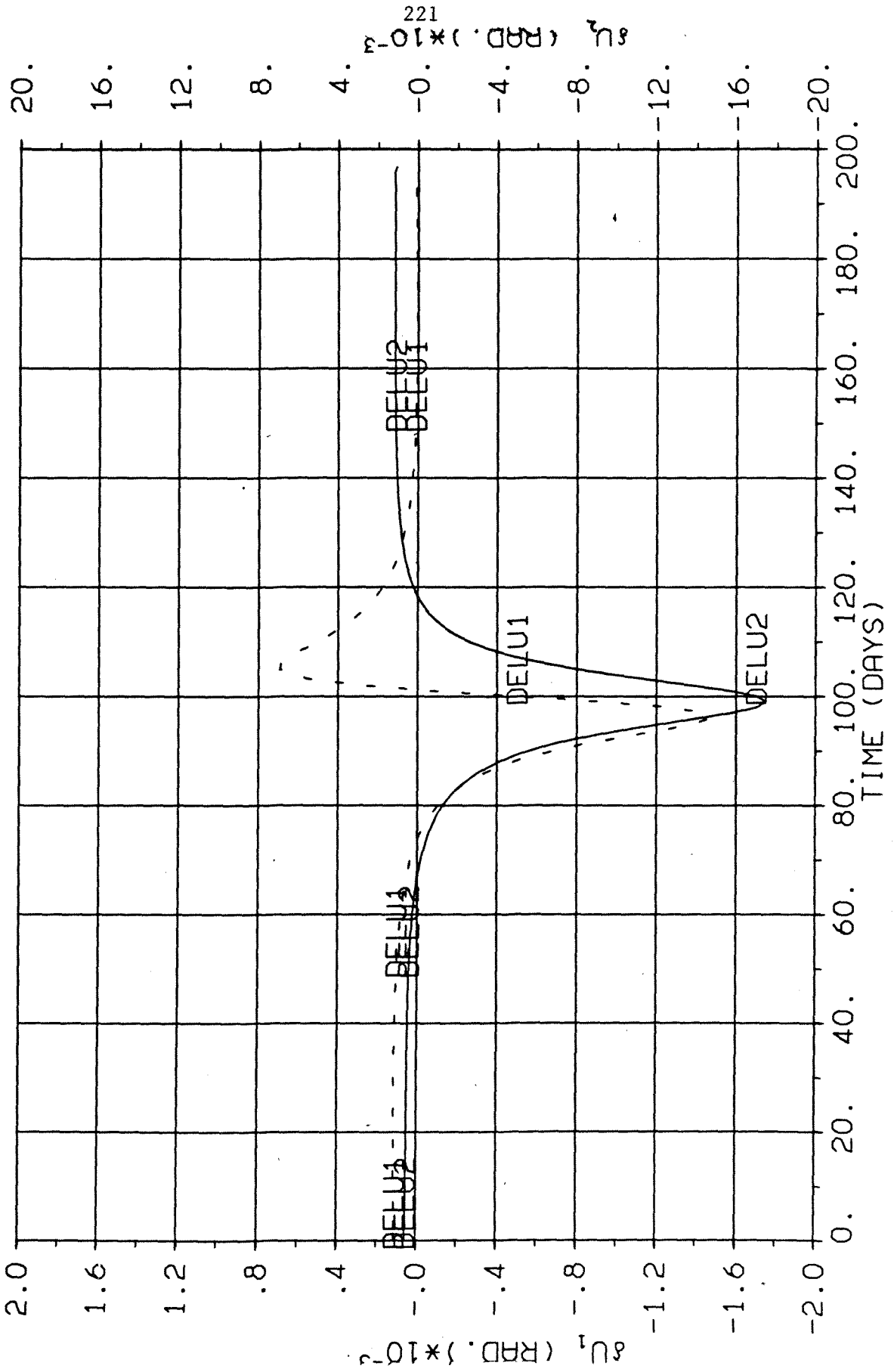
FIGURE 71. CONTROL DIFFERENCE $(\delta u_i = u_i^R - u_i^N)$, $\delta x_4(0) = .5\text{-}3$ AU
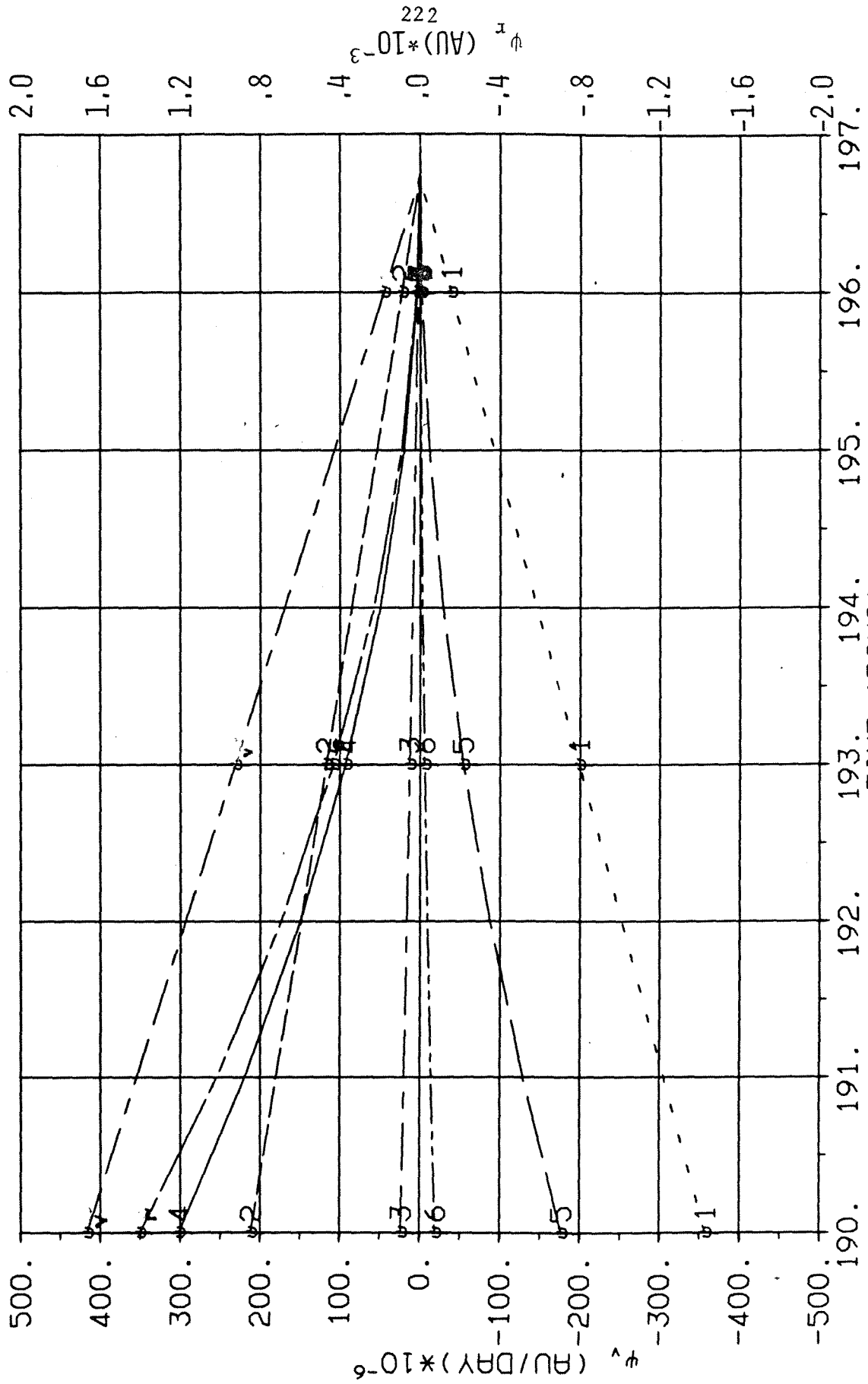
FIGURE 72. REO TERMINAL ERROR $(\psi_{1-6}, |\underline{\psi}_v|, |\underline{\psi}_r|)$ AS A FUNCTION OF TIME, $\delta X_4(0) = .5-3$ AU
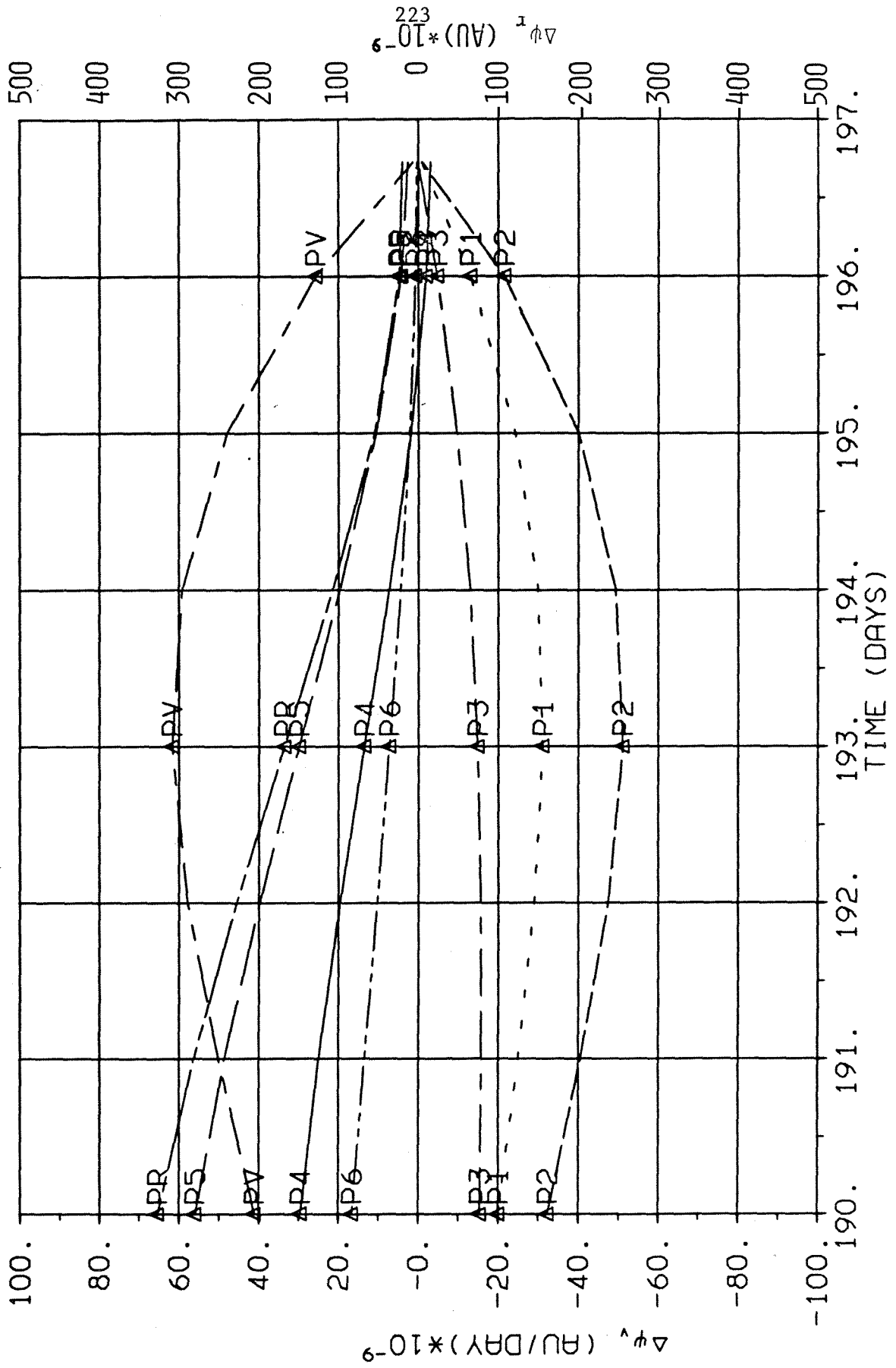
FIGURE 73. TTG TERMINAL ERROR DEVIATIONS $(\Delta\psi_{1-6}, |(\underline{\Delta\psi})_v|, |(\underline{\Delta\psi})_r|)$, $\delta x_4(0) = .5-3$ AU